ENTEC
214 Oxford Street / Fredericton, N.B. / Canada E3B 2W5
Energy Technology Consultants, Ltd.
Telephone (506) 455-4234

TITLE: MATHEMATICAL MODELLING (LENARD MODEL) OF THE FLAT ROLLING PROCESS UP-E-176

FINAL REPORT

BY

JOHN G. LENARD
SECRETARY - TREASURER
ENERGY TECHNOLOGY CONSULTANTS, LTD.
214 OXFORD STREET
FREDERICTON, N.B. E3B 2W5

Work on this project was conducted under the auspices of the Canada Centre for Mineral and Energy Technology, Energy Mines and Resources, Canada.

DSS FILE NUMBER: 07SQ.23440-4-9300

DSS CONTRACT SERIAL NUMBER : 1SQ84-00344

CANMET PROJECT NUMBER:

CANMET SCIENTIFIC AUTHORITY: Dr. D. Baragar

227 pp

MAY 03 1988

MICROMEDIA

TABLE OF CONTENTS

Acknowledgements IV

Executive Summary V

CHAPTER 1: METHODS OF ANALYSIS OF METALFORMING PROCESSES 1

- Introduction
- The slab method
- Upper bound/lower bound method
- Slip line field analysis
- Finite difference/finite element methods

CHAPTER 2: MATHEMATICAL MODELS OF FLAT ROLLING 5

- Introduction
- A mathematical model for flat rolling
- Orowan's theory
- Schey's method
- Sims' method
- Ford and Alexander's method
- Finite element method

CHAPTER 3: IDENTIFICATION OF VARIABLES AND PARAMETERS 18

- Introduction
- Friction in cold rolling
- Minimum rollable thickness
- Roll deformation
- Resistance to deformation: hot rolling
  cold rolling
- Mill dynamics and chatter
- Heat transfer

CHAPTER 4: COMPARISON OF MATHEMATICAL MODELS OF FLAT ROLLING ...44

- Introduction
- Discussion
- Roll-strip contour
- Interfacial friction
- Elastic entry and exit
- Simplifying assumptions
- Convergence
- Material properties
- Comparison of assumptions

CHAPTER 5: THE LENARD MODEL 51

- Introduction
- Derivation of the basic equations
  Plastic region
  Elastic regions
  Roll deformation
  Roll force and roll torque
  Computer program and flow chart

CHAPTER 6: CONSTITUTIVE EQUATIONS FOR HIGH TEMPERATURE DEFORMATION OF STEELS 69

- Introduction
- Results:
  Shida's formulation
  Ekelund's formulation
  Altan and Boulger's formulation
  Hajduk's formulation
  Gittins' formulation

CHAPTER 7: CALCULATIONS USING FLAT ROLLING MODELS 82

- Introduction
- Roll pressures, forces and torques - cold rolling
- Roll pressures, forces and torques - hot rolling
- Roll deformation

CHAPTER 8: EXPERIMENTAL SUBSTANTIATION OF VARIOUS FLAT ROLLING MODELS 122

- Introduction
- Statistical analysis of predictive capabilities of four mathematical models for hot, flat rolling
- Predictive abilities of flat rolling models:
  Laboratory data
  Hot rolling
  Cold rolling
- Conclusions

CHAPTER 9: DISCUSSION AND CONCLUSIONS 167

- Introduction
- Availability of the information for use in modelling
- Potential for on-line control
- Mathematical models in on-line control
- Directions for future research

REFERENCES 176

APPENDICES: COMPUTER PROGRAMS - Orowan 182

Sims

Bland & Ford

Lenard

ACKNOWLEDGEMENTS

Energy Technology Consultants, Ltd. is grateful for the funds received from The Department of Supply and Services under contract number 1SQ84-00344.

SOMMAIRE EXECUTIF

Ce rapport, intitulé "Modèle Mathématique des Processus de Laminoir Plat (Modèle Lenard)", considère les implications de l'utilisation de différents modèles mathématiques applicables aux laminoirs de bandes/ feuillards (chauds ou froids).

Plusieurs modèles mathématiques déjà publiés sont revisés d'une façon critique. Les paramètres et variables nécessaires pour les computations sont discutés; la disponibilité de ces variables est aussi examinée avec soin.

La friction entre les rouleaux et le feuillard/bande et la résistance des matériaux à la déformation sont deux des variables inclus dans les modèles mathématiques. Ces variables sont aussi les variables les moins connûts.

Suivant une comparaison évaluative des suppositions et des limitations de modèles traditionnellement acceptés, le modèle Lenard est décrit. Les différences sont soulignées en détail et l'accentuation est mise sur le fait que le modèle Lenard converge, quand tout les autres modèles faillissent.

Les modèles sont généralement très sensibles aux changements de paramètres, specifiquement la réduction et le coefficient de friction. Le rapport discute ce phénomène. Ensuite, les relations empiriques existantes sont données pour le comportement de l'acier sous l'effet de température élevée.

Pour mettre à l'épreuve les améliorations des capacités prévisibles du modèle Lenard, des expérimentations (chaud et froid) utilisant un laminoir ont été accomplis. Les forces et les couples de torsion agissant sur les rouleaux sont ensuite comparés a ceux qui ont été déterminés utilisant les données de force précises d'écoulement.

Même si la mécanique de laminer est bien comprise, il est sauf de mentionner que les conditions de limites (face commune rouleau/feuillard, région d'entrée/sortie) et le comportement du feuillard sous le processus du laminoir demande encore plus de recherche. L'utilisation de méthodes statistique pour évaluer les capacités prévisibles est aussi suggérée.

EXECUTIVE SUMMARY

The attached report, entitled "Mathematical Modelling (Lenard Model) of the Flat Rolling Process" considers the implications of the use of various mathematical models applicable to hot and cold plate/strip rolling. The objective of the writer has been to evaluate the predictive capabilities of the existing models with a view to industrial applications.

Several published mathematical models are critically reviewed in the report. The parameters and variables required for computations are discussed; the availability of those variables is also commented on.

Of the components that form a well-posed mathematical model of rolling, the interfacial friction and the resistance of the material to deformation are identified as being the least well known.

Following a comparative evaluation of the assumptions and limitations of the traditionally accepted models, the Lenard model is described. The differences are pointed out in detail and the fact that the model converges when all others fail is emphasized.

The sensitivity of the models to changes in process parameters, specifically the reduction and coefficient of friction, is then presented. As well, the available empirical relations for high temperature behaviour of steels are given.

To test the possible improvement of the predictive capabilities of the Lenard model, hot and cold rolling experiments were performed and the measured roll forces and torques compared to the calculated ones using accurate flow strength data.

It is concluded that while the mechanics of flat rolling is well understood, the boundary conditions (roll/strip interface, entry/exit regions) and the behaviour of the rolled strip require more detailed research. Further, it is suggested that the predictive capabilities of the models be evaluated in a statistical manner.

CHAPTER I

METHODS OF ANALYSIS OF METALFORMING PROCESSES

Introduction

Accurate knowledge of forces, pressures, torques, and powers is necessary for the efficient design and utilization of metalforming equipment. As well, understanding the mode of deformation and manner of plastic flow during forming would aid process planning since an improved estimate of the mechanical and metallurgical properties of the product may result from that knowledge.

Various techniques of analysis of more or less complexity and rigour are available to determine the above mentioned parameters. Included among them are the

Slab method;
Upper bound/lower bound method;
Slipline field analysis; and
Finite difference/finite element method.

In each of these the equations of motion, flow criteria, material properties/constitutive relations and initial/boundary conditions are treated, in addition to several assumptions, to allow calculation of the required unknowns. Use of these methods is documented in several textbooks in metalforming. See, for example, References [1] - [9].

After a brief discussion of the above mentioned approaches, applications to flat rolling will be presented.

Slab Method

In this technique a geometrically well-defined part, a "slab", of the plastically deforming material is isolated and Newton's law of equilibrium is used to express a balance of forces acting on it. The resulting differential equation(s) can then be combined with a criterion of plastic flow, constitutive relations and boundary conditions; the solution of the resulting family of equations is usually not prohibitively difficult. Examples of the application of slab method, which is often referred to as the equilibrium method, can be found in the texts of Hoffman and Sachs [4] and Rowe [5].

Upper Bound/Lower Bound Method

Both of these analyses involve the estimate of either the velocity field (for the upper bound method) or of the stress field (for the lower bound method). There are, of course, strict criteria to be followed in arriving at these estimates. However, once those are satisfied, calculation of the theoretically maximum power (by the upper bound method) or of the minimum possible power (by the lower bound method), is reasonably straightforward. A large number of applications of these techniques is presented by Avitzur [6].

Slip Line Field Analysis

Integrating the equations of equilibrium along lines, the directions of which coincide with the locations of maximum shearing stress allows the designer to calculate the variables associated with plastic flow. The technique can be used quickly and efficiently. See for example, Hill [7] or Johnson, Sowerby and Haddow [8]. Inherent limitations, however, do not allow for easy implementation when other than plane strain states are considered.

Finite Difference/Finite Element Methods

The equations governing the flow of material during finite straining are usually quite complex and highly nonlinear.

It is difficult to find exact, rigourous calculations of stresses, strains and strain rates that do not involve some simplifying assumptions that usually limit the usefulness of the result.

The finite difference technique attempts to overcome these difficulties by using sophisticated ways to transform the differential equations to a family of algebraic relations. Often, these are somewhat easier to handle, especially if access to computers is available.

The literature on the application of this technique is not excessive. In the opinion of the writer, more research is required before widespread application of the technique to the problems of metal flow is possible.

The finite element method--see for example, Owen and Hinton [9]--is an extremely powerful numerical technique that allows calculations of stresses, strains and strain rates in problems of solid mechanics. At a recent conference (First International Conference on the Technology of Plasticity, Tokyo, September, 1984), no less than fourteen presentations dealt with the use of the approach to problems of metal forming--see References [10] - [23]. However, in the opinion of this author, the technique, while an efficient research tool, is not yet ready for use in problems with large strains, finite deformations and time dependent variables.

CHAPTER 2

MATHEMATICAL MODELS OF FLAT ROLLING

Introduction

Mathematical models of the flat rolling process are numerous. In each of these, the equations of motion or equilibrium, material properties (flow curves and yield criteria), roll deformation and initial/boundary conditions are used to calculate - numerically or analytically - the roll pressure distribution, roll separating forces, roll torques and the deformed roll contour.

The consistency and accuracy of the predictive capabilities of these methods of computations depend largely on the quality of assumptions made either during the derivations or the solution of the basic equations. Almost without exception, researchers assume the existence of homogeneous compression of the strip, considered to be made of an isotropic and homogeneous material which remains incompressible during plastic deformation. Plane strain plastic flow is assumed to occur. As well, if upper bound analysis is considered a constant friction stress is usually assumed to exist; sticking friction is thought to occur in hot rolling while Coulomb friction conditions are most often assumed for cold rolling. Further, corrections for the contributions of the elastic entry and exit regions are also taken into account.

The success of a mathematical model is measured by its predictive ability. To establish that, a large number of measurements should be taken over a broad range of the experimental variables and the same variables sould be calculated--"predicted"--by the model. The average percentage difference of predictions and measurements will indicate the "accuracy" of the model and the standard deviation of those differences will indicate its "consistency". It is the latter that is of importance. A sometimes accurate predictive model is useless. However, an inaccurate but consistent model can always be used with appropriate "tuning parameters".

As far as rolling is concerned, a complete mathematical model should include:

i) Equations of motion of the deforming metal;
ii) Equations of equilibrium of the work roll;
iii) Description of the friction between the work roll and the metal;
iv) Description of material properties.

In the following, a mathematical model of flat rolling will be formulated and some of the currently used models will be discussed briefly.

A Mathematical Model for Flat Rolling

As the strip enters the roll gap it is first deformed elastically. It speeds up; the relative velocity between

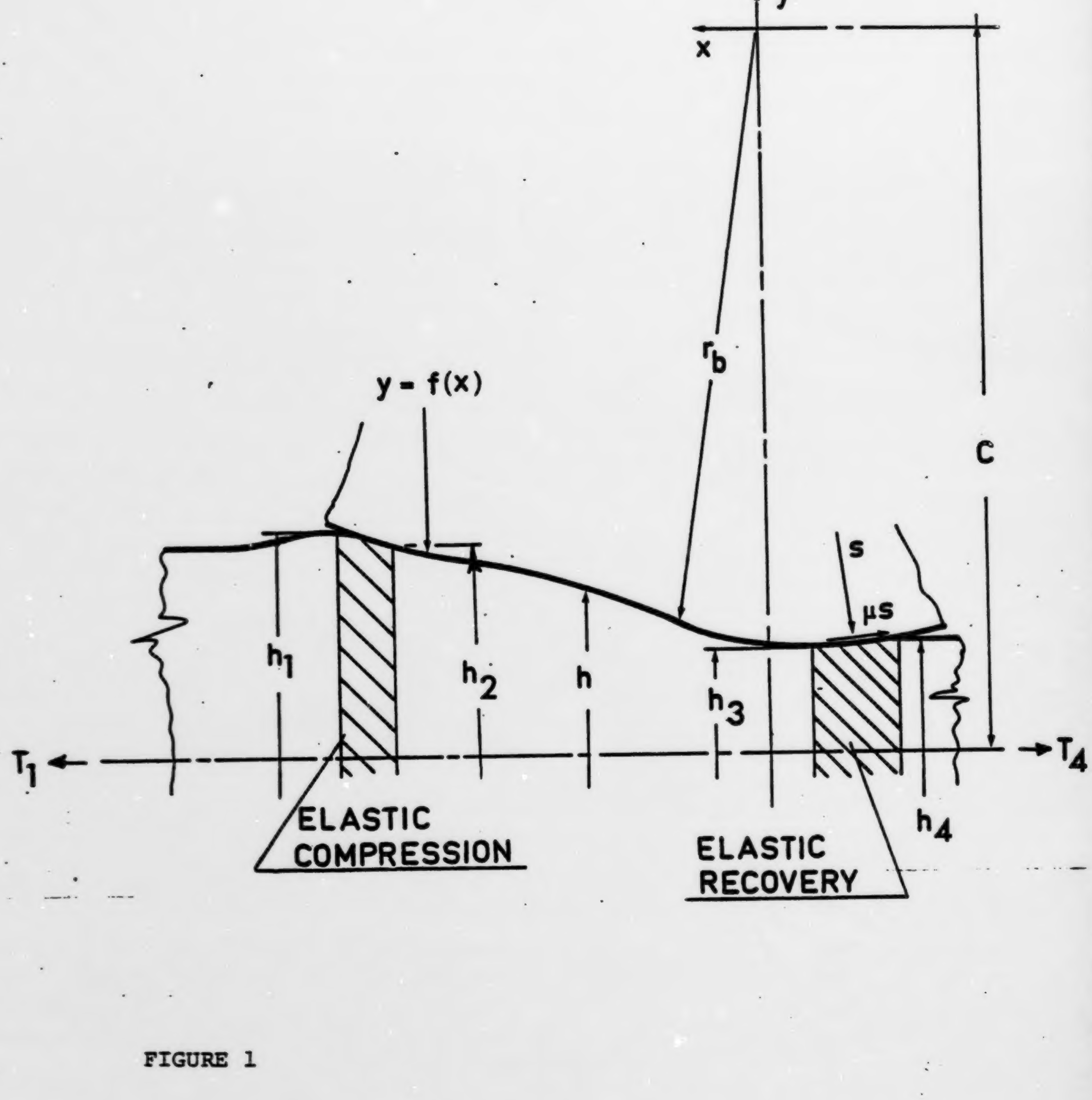
y
x
r_b
y = f(x)
C
s
µs
h_1
h_2
h
h_3
h_4
T_1
T_4
ELASTIC COMPRESSION
ELASTIC RECOVERY

FIGURE 1

the roll and the strip is such that friction "draws" the metal in. The criterion of plastic flow governs the manner in which the transformation from elastic to plastic states happens. As Figure 1 shows, the two states are separated by a surface called the "elastic-plastic interface". The strip proceeds through the roll gap; more plastic flow occurs until finally at exit the roll pressure is removed. The strip is unloaded and it returns, through an elastic state to the original, stress free condition. It is observed that during rolling, the relative velocities of the roll and the strip change; as the strip is accelerating forward it reaches the roll surface velocity at the "no-slip" or neutral point; from then on, as further compression occurs, the strip speeds up and the direction of friction changes in such a way that it now retards motion.

Several assumptions regarding material behaviour must be made to allow formulation of a model. The material is thus assumed to be, and to remain, isotropic and homogeneous; it is considered to be rigid-plastic; as gross plastic straining takes place, no elastic deformations need to be considered.* During forming the volume is taken to be constant; and finally, a plane state of strain is assumed to exist.

*The elastic regions are considered in detail in Chapter 5, "The Lenard Model".

The equations of motion can then be written as

$$\frac{\delta\sigma_x}{\delta x} + \frac{\delta\tau_{xy}}{\delta y} = \rho f_x \tag{1}$$

and

$$\frac{\delta\sigma_y}{\delta y} + \frac{\delta\tau_{xy}}{\delta x} = \rho f_y \tag{2}$$

where the acceleration in the x direction is given by

$$f_x = \frac{\delta u}{\delta t} + u\frac{\delta u}{\delta x} + v\frac{\delta u}{\delta y} \tag{3}$$

and in the y direction

$$f_y = \frac{\delta v}{\delta t} + u\frac{\delta v}{\delta x} + v\frac{\delta v}{\delta y} \quad . \tag{4}$$

The von Mises criterion of plastic flow, in terms of principal stresses is

$$(\sigma_1 - \sigma_2)^2 + (\sigma_1 - \sigma_3)^2 + (\sigma_2 - \sigma_3)^2 = 6k^2 \tag{5}$$

since for the plane strain case

$$d\varepsilon_z = 0 \tag{6}$$

the stress in the z direction becomes

$$\sigma_z = 0.5\ (\sigma_x + \sigma_y) \tag{7}$$

and the flow criterion simplifies to

$$(1/4)\ (\sigma_x - \sigma_y)^2 + \tau_{xy}^2 = k^2\ . \tag{8}$$

For the assumption of constant volume to be true, the trace of the strain rate tensor must vanish; this implies that

$$\frac{\delta u}{\delta x} + \frac{\delta v}{\delta y} = 0 \tag{9}$$

in the plastically deforming region. Finally, as isotropic behaviour is considered the slopesof the principal axes of strain-rates are taken to equal that of the stress components. Therefore,

$$\frac{2\tau_{xy}}{\sigma_x - \sigma_y} = \frac{\delta u/\delta y + \delta v/\delta x}{\delta u/\delta x - \delta v/\delta y}\ . \tag{10}$$

Equations (1), (2), (8), (9) and (10) contain five dependent variables; the three stress components σ_x, σ_y and τ_{xy} and the two velocity components u and v. If ideally plastic behaviour is assumed, that is k = constant, these equations form the basis of a mathematical model for flat rolling. If material properties are affected by parameters such as strain, strain-rate, temperature, chemical composition and past deformation history, an appropriate choice for an equation relating the flow strength, 2k, to those parameters must be made.

A solution of the above equations requires the definition of boundary conditions. These include conditions on the stresses as well as on the velocities. As far as the stresses are concerned an assumption regarding the frictional shear stresses at the roll-metal interface is usually made. One technique is to assume that Coulomb friction is present; hence the interfacial shear stress will equal the roll pressure multiplied by a constant coefficient of friction

$$\tau = \mu s \,. \tag{11}$$

Alexander [28] remarks that in hot rolling, the assumption of "sticking friction" is often very good; this mathematically would imply that

$$\tau = k \,. \tag{12}$$

It must be pointed out here that as the roll deforms during rolling the shape of the roll-metal interface is not known. For the present discussion it may be assumed that

$$y = f(x) \tag{13}$$

is a satisfactory relationship that describes the flattened roll cross-section. The function given in (13) must either be assumed or calculated.

The stresses in the longitudinal direction at exit and entry must equal the imposed front and back tensions

$$\sigma_x = \sigma_{xa} \quad @ \quad x=x_a \tag{14}$$

and

$$\sigma_x = \sigma_{xb} \quad @ \quad x=x_b \ . \tag{15}$$

Again, caution must be observed. It is not known where the distances "a" and "b" are located; nor can this writer offer any advice other than that arrived at by "educated guessing". Hence it is suggested that "a" be taken to coincide wit the exit and "b" be taken to coincide with the entry plane.*

---

* See Chapter 5.

Conditions on the velocities require that at entry

$$u = V_1 \tag{16}$$

and that at exit

$$u = V_2 \; . \tag{17}$$

There is no known rigorous solution of the above equations. Approximations are possible; these will be discussed in the following sections.

Orowan's Theory

The most comprehensive study of hot and cold flat rolling is due to Orowan [27], dating from 1943. The equations that he developed do not appear to yield analytical solutions for the roll pressure. Researchers--see References [24] to [26]--have therefore devised various approximate solutions. Alexander [28] in 1972 reviewed and critically evaluated some of these approximations. As well, he presented an essentially complete solution of the "Orowan equations" using a fourth order Runge-Kutta technique to integrate the differential equations.

Orowan's equations are based on a one dimensional equation of equilibrium which is combined with a yield criterion, frictional conditions, Hitchcock's formula and appropriate descriptions of the material's resistance. Numerical integration then allows computation of the roll separating forces, roll torques and roll pressures.

Corrections for the effects of elastic entry and exit are also included in Orowan's analysis as computerized by Alexander [28].

Schey's Method [24]

A rough estimate of the roll separating force is obtained from the formula

$$P_r = LwQ\,\sigma_{fm}$$

where P_r = roll separating force

$L = \sqrt{R(h_o - h_1)}$ = projected length of arc of contact

w = width of the strip

σ_{fm} = flow strength

h_o = entry thickness

h_1 = exit thickness

and Q, a pressure multiplying factor, is obtained from Figure 2 for $h/L>1$ and from Figure 3 for $h/L<1$. The roll torque M_t is calculated by

$$M_T = P_r L$$

It is observed that the reliability of the estimate will depend largely on the accuracy of the description of the material's flow strength.

Sims' Method [25] *

Sims estimates the magnitude of the roll separating force by a formula similar to Schey's. The exception is the multiplying factor, Q, which is now obtained from Figure 4, as a function of the percentage reduction in area and the roll radius/exit thickness ratio.

Ford and Alexander's Method [26]

In a paper published in 1963, Ford and Alexander [26] presented two formulas for the calculation of roll separating forces and roll torques in hot, flat rolling. They are

$$\frac{P}{kh_1} = 1.571\sqrt{\frac{Rr}{h_1}} + \left(\frac{R}{h_1}\right)\frac{r}{2-r}$$

and

$$\frac{G}{kh_1{}^2} = \frac{Rr}{h_1}\left[1.571 + \frac{3-2r}{(2-r)}\,2\sqrt{\frac{Rr}{h_1}}\right]$$

where P represents the separating force per unit width, G is the roll torque per unit width for both rolls and k is the average shear yield strength in the pass.

---

* In what follows, Sims' theory, as presented by Alexander [28], is used.

Finite Element Methods [20] - [23]

Several authors have written finite element codes to analyze flat and shape rolling as a three dimensional problem. While the technique is very promising, at present the following difficulties are observed:

i) The calculations take very long, require large computers, and are expensive;

ii) Several years of research are required to produce a workable program;

iii) No complete and rigourous code for flat rolling has yet been published; no comparison of their predictions has been done.

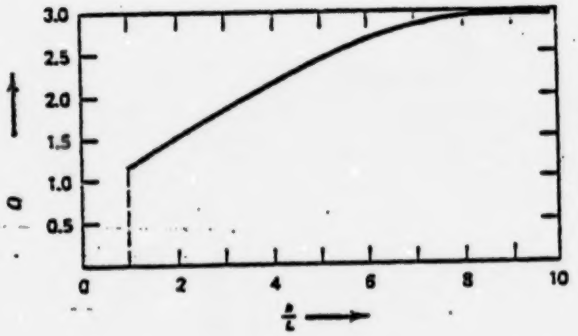

Figure 2

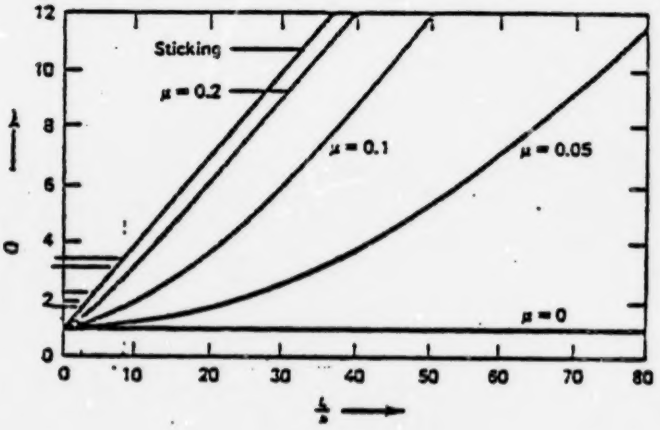

Figure. 3

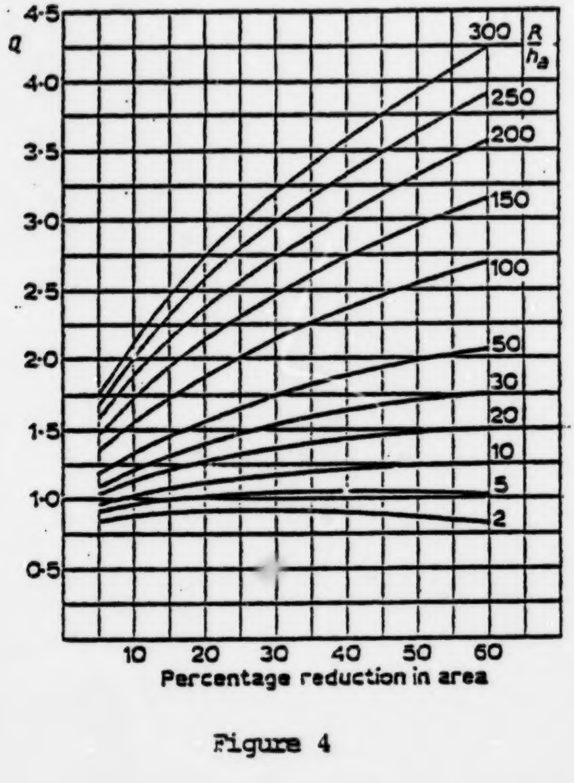

Figure 4

CHAPTER 3

IDENTIFICATION OF VARIABLES AND PARAMETERS

Introduction

The mathematical models described above are based on two assumptions. The first concerns plane strain flow while the other takes the distance in the direction of rolling as the only independent variable. All of the models treat the equilibrium equations; all account for roll flattening in a more or less rigourous manner; all make simplifying assumptions about the interfacial shear forces and all use some form of empirical constitutive relation to describe material strength.

Other phenomena not treated in the usual models of flat rolling include:

-Variability of the coefficient of friction in the roll gap;

-Development of anisotropy during rolling;

-Mill dynamics and chatter;

-Minimum rollable thickness;

-Material properties in the softening range;

-Looper dynamics

-Heat transfer from the hot strip to the cold rolls and air;

-Heat gain due to work done on the strip.

In what follows, a review of work done on friction in cold rolling, minimum rollable thickness, roll deformation and the material's resistance to deformation will be discussed. Mill dynamics, chatter and heat transfer problems, including controlled cooling, will also be referred to.

Friction in Cold Strip Rolling

The boundary condition between the work roll and the strip is the least well understood and probably the least researched phenomenon. The traditional approach here has been to assume that Amonton's law holds and that frictional forces in the roll gap are proportional to the normal forces, with the factor of proportionality--the coefficient of friction--remaining constant. This implies that an average frictional coefficient should be determined for each particular set of parameters, since, as pointed out by Rabinowicz [29] this coefficient depends critically on a large number of variables.

According to Reference [29] the "adhesion hypothesis", stating that friction is due to adhesive forces between the contacting surfaces, is almost universally accepted by the scientific community. Further, Rabinowicz lists and discusses the parameters that influence surface interactions. These include the interfacial velocity and volume properties, such as the yield strength, flow strength, penetration hardness, strain hardening sensitivity, Young's modulus, shear modulus, elastic energy, ductility and thermal properties. Further, surface properties, such as chemical reactivity, the tendency to absorb molecules from the environment, surface and interfacial energy must also be considered. The recent work of Mokhtar et al. [30] reinforces the dependence of the coefficient of friction on atomic volume, surface energy hardness, recrystallization temperature, melting point, boiling point, and coefficient of thermal expansion.

Tabor [31] in his Plenary Lecture at the 1980 ASME-ASLE International Lubrication Conference, entitled "Friction: The Present State of Our Understanding" emphasized that the three major elements of the frictional process are the true area of contact, the nature and strength of the interfacial bonds and the way in which the contacting materials are sheared and ruptured. In his conclusions he pointed out areas that need further research. Regarding sliding in deformation processes, work-hardening, which is a consequence of sliding, needs attention. As well, there appears to be no reliable experimental method of determining the true area of contact.

These and related concerns were studied and presented in References [32] to [48]. Their results lead to the conclusion that the frictional coefficient does not remain constant in the roll gap during rolling.

Experimental verification of the variation of μ in the roll gap can also be found in the technical literature. In one of the earlier projects, van Rooyen and Backofen [51] used two pin-type transducers imbedded in a work roll of 152.4 mm diameter to measure simultaneously normal pressures and interfacial shear stresses.

A cantilever-type transducer machined from the roll was employed by Banerji and Rice [52] and the results obtained during 12% reduction of aluminum strips were reported. Again, the friction coefficient varied widely throughout the roll gap but the location of the single pressure peak did not coincide with the location of the neutral point.

Al-Salehi, Firbank and Lancaster [49] presented results obtained by rolling aluminum, copper and mild steel strips and using a technique similar to that of van Rooyen and Backofen [51].

The experimentally determined distributions of frictional coefficients of Al-Salehi et al. [49] were incorporated in a model by Lenard [50]. In this study, roll deformation was analyzed by a finite element routine and it was shown that the technique reproduced roll pressure distributions, roll forces and roll torques substantially better than the traditional technique of Orowan [27].

Cole and Sansome [53] reviewed techniques used in measuring interfacial normal and tangential forces. As they point out, one of the major diffficulties in using any transducer imbedded in the work roll, is the possibility of the rolled strip extruding into the clearance between the transducer and the roll. The magnitude of this clearance is, of course, dependent on the magnitude and direction of the deformation of the transducer during the measuring cycle. MacGregor and Palme [54] used a pin-type transducer of 2.35 mm diameter and a radial clearance of 0.097 mm; van Rooyen and Backofen [51] used a precision fit and the radial clearance of their transducer was 0.005 mm. MacGregor and Palme [54] succeeded in measuring normal pressures only because back extrusion prevented recording of the tangential forces. In the "three component dynamometer" of Muzalevskii and Grishkov [55] a radial clearance of 0.041 mm was used but no mention of back extrusion is made. The cantilever-type transducer of Banerji and Rice [52] had a small clearance whose magnitude is not reported by the authors. However, no significant back extrusion was evident during testing.

Minimum Rollable Thickness

The existence of a lower limit on the thickness of a sheet that a particular rolling mill can produce has been the subject of many investigations. The majority of theoretical studies indicate that a limiting thickness does in fact exist; experience of rolling mill engineers -- including that of the present author--confirms this finding.

In conventional cold rolling practice, the minimum gauge is encountered as increasing screwdown produces progressively larger mill-frame stretch and roll flattening but no further plastic deformation. It is then reasonable to expect that a hydrostatic state of stress will exist in that portion of the rolled strip located in the roll gap. This consideration led to one of the earliest attempts to define a minimum thickness. Keller [56] presented a theoretical analysis, based on the existence of a hydrostatic state of stress, which can cause no permanent reduction.

Several formulas, predicting the minimum thickness, were presented by later researchers. The works of Stone [57], Tong and Sachs [58], Ford and Alexander [59], Hill and Longman [60], Roberts [61],Huggins [62] and Kuhn and Weinstein [63] have been reviewed by Roberts [64].

As he states, the parameters determining the limiting thickness are numerous. However, general similarity among the predictive type formulas is apparent. All include the same kind of parameters, along with a constant multiplier that differs in each.

Other parameters, especially those relating to mill and roll rigidity, are difficult to include in a rigorous mathematical model. An attempt to account for mill stretch in addition to roll flattening is presented by Horvath and Vero [65]. They use the theorem of Castigliano to analyze the response of the frame to roll forces. Their final formula, however, appears restricted to one type of mill and the constants required in the computation are given in graphical form.

There appears to be no investigation regarding the number of passes required to reach the minimum thickness nor the dependence of reduction rate on the process parameters.

Further, to decrease h the frictional coefficient should be reduced. The present author is not aware of experimental work, studying how roll surface quality affects the minimum gauge in dry rolling.

In a careful study of limiting thickness, Pawelski and Kading [66] measured the maximum plastic reduction obtainable in terms of the entry thickness of the strip, for various roll radii and lubricants. By extrapolating to zero these authors concluded that a zero reduction can only be obtained for a zero strip thickness. These experiments were carried out using an aluminum-killed steel. However, the validity of the extrapolation can be questioned since the smallest entry thickness employed was 0.05 mm, and it is possible that a limiting thickness may exist for smaller dimensions.

A detailed study of the production of aluminum foil was presented by Kokote and Nomura [67]. As they point out, rolling of aluminum foil is significantly different from that of steel; in apparent contradiction to theory, it can be rolled very easily. Thickness in the range of 0.018 mm on the second pass was reported. On the fifth pass, rolling two foils together, a minimum thickness of 0.008 mm was reached. The authors concluded that in the fourth and fifth passes the material may have softened considerably due to the heat generated in the roll gap.

As strip thickness decreases, material anisotropy tends to increase in the absence of interpass annealing [69], so that the rolls no longer reduce an isotropic solid. This matter has not been considered by other workers as it relates to minimum thickness, although Betten [69] has shown that the plastic compression in plane strain of an anisotropic metal obeys the same mathematical formulation as that of an elastically compressible viscoelastic material. It has been shown that plastic anisotropy assists plastic flow in the forming of sheet metal [70], but no similar results have been obtained for rolling. Theories relating mechanical anisotropy and crystallographic texture have been in existence for some time [70], but all existing theories of rolling assume the ingoing strip to be isotropic. Certainly there is no experimental evidence available concerning the dependence of minimum thickness on material anisotropy.

Roll Deformation

The other aspect of the analyses, mentioned above, is the manner in which roll deformation is described. Hitchcock's formula [71] is probably the most widely used technique to account for the deformation of the roll during rolling. It is not difficult to show, however, that in many practical cases the assumption that the deformed roll remains circular leads to misleading results. An improved method for calculating roll deformation was developed by Jortner et al. [72], based on Michell's [73] analysis, clearly showing that the deformed arc of contact is far from circular and that it depends on the nature of the distribution of the load. Golten [74] extended Jortner's work by including the effect of shear loading. He showed in the case of rolling materials with high co-efficients of friction, the radial deformation due to the shear loads can be as high as 8% of the radial deformation due to the normal loads. Grimble [75] combined the analyses presented in References [72] and [74] to study tin plate rolling. A two dimensional treatment of roll distortion was presented by Watanabe et al. [76].

Direct experimental substantiation of theories of roll deformation is scarce. The present author is not aware of publications other than the work of Kobasa and Shultz [77] and of Roychoudhuri and Lenard [132].

Resistance to Deformation

i. Hot rolling

Most of the difficulties in attempting to predict parameters in hot strip rolling are due to inaccurate determination or inadequate mathematical description of the material's resistance against plastic forming. Resistance of the material to deformation as well as the microstructures resulting from the thermal-mechanical treatments have to be established carefully.

Resistance to Deformation - Review of techniques to establish high temperature, high rate of strain behaviour of metals indicate that researchers often use a cam-plastometer to conduct constant strain rate compression tests. Alternatives, however, exist and these as well as the compression tests will be described below.

The tension test is the simplest to perform. The disadvantages it poses, however, limit its applicability. These include the magnitude of the attainable uniform strain which is significantly less than in other testing methods. As well, when necking develops, the initially uniaxial stress distribution becomes triaxial. Hence, interpretation of the results becomes difficult.

A modified tension test was developed by Thomsen et al. [78] for the purpose of overcoming the above mentioned difficulties. The testing was interrupted at several intervals and the speciments were remachined to remove the necked down sections and to remove triaxiality.

Marion [79] developed a testing facility for high temperature tensile testing of metals. The paper describes the measurement and control of temperature, temperature-gradient and strain. No mention of triaxiality of stress states is made.

A split Hopkinson bar was used for high rate tensile testing of aluminum by Nicholas [80]. Strain rates of 10^3 sec^{-1} were reached. All tests were conducted at room temperatures. One of the materials tested was 6061-T651 aluminum alloy which in previous compression tests showed no rate sensitivity at all. In Nicholas' tensile tests the material exhibited measurable rate sensitivity.

Several researchers use the hot torsion test to determine flow strength data. As McQueen and Jonas [81] mention, strains of the order of 20 can be reached. One of the difficulties inherent in the torsion test is the radial variation of the strain and strain rates.

Strains, significantly higher than in tension can be achieved in compression testing of solid or hollow cylindrical, conical or flat specimens. Constant strain-rate compression tests of solid cylindrical specimens are often performed using a cam-plastqmeter, the operation of which is described in detail by Stewart [82]. Modifications to produce constant strain-rates on an Instron testing machine, by using an analog function generator, were described by Luton et al. [83]. Drop tests, resulting in variable strain-rates during deformation, were conducted by Douglas and Altan [84]. Uniaxial compression testing was used by Suzuki et al. [85]. The report by Suzuki et al. is very comprehensive, comprising over 100 pages of data for both ferrous and non-ferrous metals. They used a cam-plastometer and also a drop hammer, measuring the flow stress of twenty-one non-ferrous metals and alloys and forty-nine steels (carbon, low alloy and stainless) in the hot-working range of temperature for each material and ranging over strain rates from $0.1s^{-1}$ up to $650s^{-1}$.

Results, obtained by the plane-strain compression test, which was developed by Watts and Ford [86], were discussed by Weinstein and Matsufuji [87]. They concluded that the mean deformation resistance of steel, obtained in plane-strain, variable strain rate tests is different from that obtained in uniaxial, constant strain rate compression. Further, better correspondence of predicted and measured rolling results was obtained by the use of plane-strain material strength data than by the use of uniaxial compression data.

One of the difficulties encountered during compression tests is caused by the friction present between the specimen and the compression platens. There are several ways of accounting for the friction losses. Among these is the one developed by Cook and Larke [88] who noticed that frictional effects are less on slender cylinders than on squat ones. By obtaining results for various height/diameter ratios and extrapolating, the zero-friction flow strength can be estimated. Alternatively, the analysis developed by Gelin et al. [89] may be used to calculate the true flow strength.

A split Hopkinson bar, including a "pulse-shaper" was developed by Ellwood et al. [90] for the purpose of conducting high, constant strain-rate compression experiments. Results obtained by that technique and a comparison to results obtained without the pulse-shaper (in which case no constant strain rate is possible) were presented at the International Conference on "Dynamical Mechanical Properties and Fracture Dynamics of Engineering Materials" in Valtice, Czechoslovakia in June of 1983.

Empirical Constitutive Relationships - A large number of empirical constitutive relations predicting the flow strength of materials and applicable for high temperature, rate dependent plastic flow, may be found in the technical literature.

One of the most complex equations was given by Ashby and Verall [91] in which the rate of straining was defined in terms of the flow strength, atomic volume, the Boltzman constant, absolute temperature, grain size, grain boundary surface energy, bulk diffusivity, grain boundary diffusivity, shear modulus, Burger's vector, activation energy and several material constants. Paton [92] replaced all of the above terms by simplified constants and obtained a simple form of the equation.

Altan and Boulger [93] have compiled a considerable amount of data on the behaviour of engineering materials. For high temperature flow they used the power law and presented the results in terms of the strength and strain rate hardening coefficients for specific temperature and strains. The chemical composition of the materials was also given.

One of the most comprehensive set of empirical equations was developed by Shida [94]. Using a constant strain rate camplastometer, the flow strength was determined in terms of strain, rate of strain, temperature and carbon content.

Gittins, Moller and Everett [95] used the hot torsion test to develop an empirical relation for the flow strength of six different steels. They also compared their results to those of Cook and McCrum [96]--conducted in compression and found good agreement. The differences in measurements were never more than 10%.

Cornfield and Johnson [97] presented a "...deformation law for steel in uniaxial tension, valid between 1000° and 1350°C"; it is suspected, however, that one of the constants in the equation is incorrect. The form of the relation is similar to that given by Sellars and Tegart [98]; it is the Arrhenius equation.

Wusatowski [99] gives two very useful formulae for the hot flow strength of steels; one is due to Ekelund, giving the strength as a function of temperature, carbon manganese and chromium content while the other, developed by Geleji, has temperature as the only independent variable.

High temperature, high rate behaviour of several steels was given in terms of material parameters by Hajduk [100]. A comprehensive review of constitutive relations applicable for high temperature, time dependent deformation of metals was presented by Alexander [101] in his keynote address at the conference "Plasticity Today" in Udine, Italy in June, 1983.

ii. Cold Rolling

For most materials, representing the room-temperature flow strength may be done simply and efficiently with the Swift equation:

$$\sigma = Y(1+B\varepsilon)^n$$

where Y, B and n are to be determined by non-linear regression analysis.

Mill dynamics and chatter

As Monaco [102] points out, recent mill drive-train component failures have indicated a need for a more thorough understanding of transient torsional vibrations in those drive systems. He describes the torque buildup on entry of the strip to the mill, the subsequent speed drop and the overspeed as the material leaves.

Chatter in cold rolling is discussed by Tlusty and Chandra [103], Roberts [104]; surface finish and torque effects are studied by Moller and Hoggart [105]. Their concern is the significant periodic thickness variation of the strip caused by 100-200 Hz vibrations, reported by the engineers in the cold rolling industry.

Heat transfer

Several aspects of the phenomenon of hot strip rolling are considered here. These include the various mechanisms by which the strip loses and/or gains heat during conventional or controlled rolling/cooling. Experimental work in controlled cooling, the resulting microstructures, experimental procedures and analytical studies will be considered. As well, heat gain due to plastic deformation will be mentioned briefly.

Controlled cooling experiments

As stated by Pickering [106] the essence of controlled rolling and cooling is that the structure of the austenite is conditioned to allow it to transform to ferrite with the finest possible grain size. Controlled cooling has been used by several workers in rolled plates, strips, bars, rods and rails. These reports include descriptions of analytical predictions of temperature distribution in the work roll [107], [108]; prediction of temperatuure distribution in the strip [109]; experimental measurements of temperature variations in aluminum slabs during rolling [110]; description of techniques for temperature measurements in rolling [111] in addition to articles on the effect of cooling during and/or after rolling to achieve certain desired mechanical and metallurgical properties.

Among these are the papers of Heedman and co-workers. It is worth reviewing their conclusions in some detail.

Heedman and Sjostrom [112] used forced water cooling during rolling of bars; this resulted in improved mechanical properties. With forced air cooling after finish rolling increased strength resulted. Two types of steels were considered; one containing V and Nb, the other V in addition to approximately 0.2% C, 1.4% Mn, some Cr and Ni. For the water sprays, spray nozzles with a total heat transfer coefficient of 10000 W/m^2°C were used; for the air, a tube with holes, placed on one side of the bar was employed.

Heedman, Rutqvist and Sjostrom [113] considered the possibility of reducing the processing time in plate rolling. They experimented with one heavy water cooling during a holding period; with three moderate water cooling periods during holding; with two holding periods and moderate cooling during both and with no water cooling at all. Nb, V and Nb-V steels were used. They concluded that water cooling during the roughing stage resulted in shorter process time. Cooling during the holding period had no significant effect on bulk material properties. A thin surface layer of fine grained structure was evident. Some possibility of creating residual stresses was also mentioned.

Lee, Sims and Wright [114] used a radiation pyrometer to record strip temperature between stands of the finishing mill. They also developed a simplified analysis and were able to predict the measured values to within 27°C.

Sigalla [115] conducted several experiments to study the cooling rate of a hot steel plate as a result of cooling by water jets or sprays. He used embedded thermocouples to monitor the drop of temperature. As he wrote, however, the response of his measuring system was too slow; his results can be taken as a means of comparison of the effectiveness of jets vs. sprays. He found that the water jets are much more effective in creating fast cooling conditions than the sprays. He also experimented with various nozzle diameters, number of jets and strip speed. As well, he derived a simple formula to predict the number of jets required to cause a certain temperature drop.

Sheppard and Wright [110] have conducted an analytical and experimental study of temperature effects during hot rolling of aluminum slabs. In their analysis they used a finite difference scheme to obtain predictions of the temperature distribution. In their experiments they employed embedded thermocouples to substantiate the predictions. Their results show that the temperature drop is a strong function of % reduction. Considering 10% reduction, a temperature drop of about 40 K was measured 1 mm away from the roll-slab interface. For 30% reduction they measured approximately 140 K. Their analytical predictions appear to be somewhat off; agreement is not unreasonable some distance from the interface, but near the interface predictions and measurements differ broadly.

Microstructures

Roberts [116], in his recent review of advances made by the steel industry in the last decade, identified controlled/accelerated cooling as one of the most significant developments. He listed the principal benefits as

i. grain refinement of polygonal ferrite;
ii. augmented precipitation strengthening;
iii. promotion of tough low carbon bainite;
iv. reduction of the carbon equivalent of the steel;
v. elimination of pearlite banding.

According to him, the main problem associated with cooling is the maintenance of flatness, resulting from the temperature distribution of the cooling product. He cites the experiences of Nippon-Kokan where levellers and straighteners are included in the on-line control of cooling.

In discussing grain refinement, he refers to the data of Ouchi et al. [117]. Using a 20 mm C-Mn steel plate, finish rolled at 800°C and subjected to accelerated cooling from 780°C-600°C, no significant refinement occurred beyond a rate of 4°C/second. The yield strength of a similar grade steel increased by approximately 12% when the cooling rate was 9.5°C/second.

One of the important aspects of controlled cooling is the "water-end-temperature" at which cooling in air is resumed.

Roberts also discusses the advantages and disadvantages of interpass cooling by reviewing the work of Fegredo [118] and Heedman et al. [119].

In mentioning advances in shape rolling, including the Temcore process, he writes about the various processes available for thermal-mechanical treatment of shapes. He identifies the difficulties as too high finishing temperatures, too high loads on equipment, roll wear and cooling arrangements. He concludes that this is an area where significant developments may be made.

Fegredo et al. [118] considered the effects of hold-period accelerated cooling on microalloyed plates. He concluded that water-spray cooling of V-Cb steels can decrease the hold period very significantly; however, a layer of hard, pancaked grains at the surface would result. These may be removed by using a compressed air-water mixture during interpass cooling. For the V steels no pancaked grains were found.

Fegredo et al. [120] considered the possibility of developing rails with $R_c \approx 43-45$ and yield strength in excess of 1000 MPa by controlled cooling methods. They used a steel containing 0.72% C, 0.81% Mn, 0.79% Cr, 0.21% Mo in addition to low levels of P and Si. They concluded that pearlitic structures of $R_c \approx 45$ can be produced by transformation at 575°C. To control the transformation conditions the cooling rail was placed, at a particular temperature, in an elevated temperature environment. Further, they hypothesized that high temperature straightening may be required for some, very high strength rails.

Direct quenching of six grades of steel plates after normal or controlled rolling was studied by Heedman et al [119]. They found that high yield strength and low transition temperatures can be achieved in low carbon steels. A potential problem with hardness differences between the centres and surfaces was identified.

Production of three types of dual phase sheet steels by controlled cooling was discussed by Mano et al. [121]. By water or air cooling the strips on the runout table, the authors established an optimum cooling to about 700°C; holding at that temperature to enhance ferrite transformation and then rapid cooling to the coiling temperature.

Experimental procedures

The difficulties inherent in the above described experiments are worth considering in some detail. These are described in the papers of Carney [122] and Farren and Taylor [123].

Carney [122] in an interesting paper considered cooling rates of eight low carbon steels for the purpose of hardenability. In order to determine the quenching constant for the materials he used embedded k-type thermocouples with which he monitored the temperature distribution in rods. He described the method of embedding the thermocouples within the bars and the measures taken to ensure metal-metal contact at the thermocouple tips.

In one of the earliest studies of heat generation by plastic deformation, Farren and Taylor [123] measured the temperature rise of metals subjected to tension. They used steel, copper, plain aluminum and single crystals of aluminum. They found that adiabatic heating is proportional to the change of stress and that it does not depend on the hardness of the metal. Further, they estimated the increase of internal energy of each material as a percentage of the total work done. For steel they found 13.5%; for copper, 8 - 9.5%; and for plain aluminum, they found 7 - 8%. For single crystals of aluminum 4.5~5% was found.

Analysis

Analytical work attempting to predict temperature distribution in the work rolls as well as in the product (sheet, plate, strip and bar) can also be found in the technical literature.

Cerni et al. [124] have listed the aspects to be considered by analysts, attempting to study the "combined strip and roll temperature problem". According to them, account must be taken of the

i. heat content of the strip prior to rolling;
ii. heat generated in the strip in the arc of contact due to the work of deformation;

iii. heat generated by friction;
iv. heat carried away by the strip;
v. heat conducted into the roll;
vi. heat removed by coolant.

In their paper, the authors describe the method followed to derive expressions for the temperature distribution in the work roll and strip. They do not give these expressions; instead they state that they are available in Cerni's Ph.D. dissertation. In one example, the authors present the temperature rise in a strip, subjected to cold rolling. From entry to exit they predict a temperature rise of approximately 200°F.

Wilmotte et al. [125] derived a mathematical model to evaluate the temperature distribution within a strip during its passage through the finishing train. They also compared their predictions to actual experiments. In their analysis they considered heat loss of the strip in air, heat gain because of plastic work done during rolling and some more loss because of conduction into the work rolls. Their calculations predicted a temperature drop of approximately 150°C between the strip surface and centre during a pass. The deviations of measured and calculated temperatures was found to be approximately + 15°C.

The work in Reference [125] is among the most thorough in that the authors made use of a minimum number of assumptions.

Pavlassoglou [126] has presented mathematical models for the temperature distribution in the rolls and the strip during hot rolling. He considered the effect of a protective atmosphere as well.

Bishop [127] used difference equations to analyze the problem of time dependent heat flow in an incompressible, moving medium, with heat generation in the medium.

Lahoti, Shah and Altan [128] considered heat generation transport and transfer during rolling by using finite difference techniques. In hot rolling they predicted significant cooling of the strip even when the centre line temperature rises somewhat.

Hollander [128] considered the passage of the strip from the reheating furnance to the runout table and developed a mathematical model to estimate the distribution of temperature. He used a finite difference technique and in his model he included the temperature dependency of the physical parameters as well as the screening influence of the oxide layer. Water cooling was assumed to be by laminar jets; the number of jets was established by Sigalla's formula [115] . He also compared his predictions to measurements and found good agreement.

Seredynski [130] identified the factors affecting heat balance of the workpiece during hot plate rolling as the

i. heat conduction inside the workpiece;
ii. radiation loss to the surrounding medium;
iii. heat conduction to the rolls;
iv. heat gained by work done;
v. heat loss due to descaling jets.

He estimated the cooling rate to be approximately 3°C/ second.

CHAPTER 4

COMPARISON OF MATHEMATICAL MODELS OF FLAT ROLLING

Introduction

Five mathematical models are reviewed in this chapter in terms of the assumptions and simplicifications made either during their development and derivation, or when roll pressures, forces and torques are calculated. The models are due to Orowan [27], Bland and Ford [131], Sims [25], Ford and Alexander [26] and Roychoudhuri and Lenard [132], the "Lenard model".

The components of any model, as pointed out in Chapters 2 and 5, should include a mathematical description of the

i. equations of motion of the deforming metal;
ii. equation of equilibrium of the work rolls;
iii. boundary/initial conditions;
iv. material's resistance to deformation.

In what follows the manner in which the above mentioned models account for these four components will be discussed.

Discussion

All five models treat flat rolling as if it were a one dimensional problem. All assume that the only independent variable is the coordinate in the direction of rolling. All assume the problem to be quasi-static; none includes inertia terms. As well, most assume that homogeneous compression of the strip occurs and that the flow of the strip is occurring in the plane of rolling, i.e. plane strain flow is present and that there is no spread. The differences become apparent when one examines the way boundary conditions are applied by each model. These boundaries involve the roll-strip interface, the entry and the exit regions.

Considering the roll-strip interface, two aspects are to be noted. One is the contour of the interface, the other is friction. At the entry and exit regions, elastic compression and recovery need to be analyzed.

Roll-strip contour

The traditional approach here is to assume that the roll contour remains circular and that the radius of curvature becomes larger than the original roll radius. Hitchcock's formula [138] is then used to calculate the deformed roll radius. References [25], [26], [27], and [131] all recommend that method of calculations.

It was pointed out in some detail in Chapter 3, however, that Hitchcock's formula and its use do not predict the deformed roll shape very well. To overcome this, Reference [132] determines the shape of the roll-strip interface by going back to first principles.

The theory of elasticity is used to determine the flattening of an originally circular, solid steel cylinder due to the action of normal and shearing forces over a portion of its cylindrical surface. The resulting formulae then are matched to the analysis of the deforming strip.

Interfacial friction

References [25],[26],[27] and [131] assume that either of the following frictional conditions exist between the roll and the strip:

i. The coefficient of friction is constant

ii. Sticking friction is present

Evidence can be found in the technical literature that neither condition is correct--see References [136] and [137]. It is the model of Reference [132] that can be easily modified to include realistic frictional conditions. As pointed out in Chapter 3, the coefficient of friction does not remain constant in the roll gap. In Reference [132] digitally or functionally supplied forms of the variation of the frictional coefficient may be used. (See Chapter 7 where some of these calculations are performed.)

Elastic entry and exit

The four models mentioned above consider that the point of entry to the roll gap is at the intersection of the undeformed strip and roll. Exit is assumed to occur at a line connecting the roll centres. It is, of course, recognized that these assumptions are untrue. Researchers then use the correction formulae, discussed by Alexander [28] to include the effects of elastic entry and exit in the predicted roll forces and torques.

Reference [132] again makes use of first principles to include the entry and exit regions in the model. Elasticity theory and Hooke's law are employed and the resulting elastic stress distributions are coupled with the plastic regions by using the von Mises criterion of plastic flow.

Simplifying assumptions

The Orowan model claims to include as few simplifying assumptions as possible to yield an accurate but still usable form. The price one must pay for using that method is the need for a numerical solution. Since all five calculations are, by necessity, iterative, numerical solutions require long computer times. To overcome the need for numerical solution, Sims introduced the following simplifications, all based onthe fact that roll gap angles are small compared to unity:

$$\tan\phi = \sin\phi = \phi;$$

$$\cos\phi = 1;$$

$$1 - \cos\phi = 1/2\ \phi^2;$$

$$h = h_2 + R'\ \phi^2;$$

$$\tau\phi << 1;$$

$$\tau = k = \text{constant.}$$

Bland and Ford, in addition to the above, assumed that the roll pressure equals the stress in the vertical direction. Ford and Alexander introduced two empirical formulae for the computation of the roll forces and torques.

Convergence

In the traditional models of flat rolling, the differential equation of equilibrium is integrated for the roll pressure from the entry; then, with appropriate changes, from the exit and the neutral point is taken to coincide with the location of the intersection of the two curves. The roll pressure, thus obtained, is referred to as the "friction-hill"--see Figure 22 of Chapter 7, for example. It is known that the friction hill is an unrealistic representation of actual roll pressures. As well, when reduction of hard, thin strips is considered, using large roll diameter/strip thickness ratios, the models of Orowan, Bland and Ford, and Sims fail to converge.

In Reference [132], this problem is solved by using a coefficient of friction in either of two ways. If the actual variation of the coefficient is known, it is supplied to the model, slab by slab. If that is not available, a smooth changeover at the "no slip point" is assumed. Both methods cause Reference [132] to yield converging solutions when all other models fail.

Material properties

The manner of representation of the material's resistance to deformation is at the discretion of the analyst in all five models.

Comparison of assumptions

A table comparing the assumptions made by each of the models discussed above is presented on the next page.

	ROLL DEFORMATION	ENTRY/EXIT	FRICTION	SMALL ANGLES (see p.47/48)	CONVERGENCE $R/h \gg 1$
OROWAN	HITCHCOCK	CORRECTION	μ = CONST.	YES	NO
BLAND & FORD	"	"	"	"	"
SIMS	"	"	"	"	"
FORD & ALEXANDER	"	"	"	"	"
LENARD	MICHELL	ELASTICITY	$\mu = \mu(\phi)$	NO	YES

Assumptions common to all:

- homogeneous compression (Note: Sims uses Orowan's corrections for flow in inclined planes. This correction was not used in the present work)
- no inertia forces
- one dimensional treatment
- plane strain flow

COMPARISON OF ASSUMPTIONS

CHAPTER 5

THE LENARD MODEL

Introduction

In this chapter the "Lenard Model" for flat rolling is described in detail - see References [141], [142] and [132]. The underlying philosophy guiding the development of this method of computation is to achieve maximum computational accuracy and consistency while using a minimum of arbitrary assumptions.

The model consists of several parts. These include:

i. Plastic flow of the rolled strip in the roll gap;
ii. Elastic compression and unloading of the strip at entry and exit;
iii. Flattening of the work roll;
iv. Frictional conditions at the roll-material interface;
v. Material's resistance to deformation.

The assumptions, limiting the validity of the technique, are listed below:

i. No spread of the strip is considered. Plane strain plastic flow is present;
ii. The compression of the strip is homogeneous;
iii. The rolled material is isotropic, homogeneous and in the plastic state, incompressible. It obeys the von Mises criterion of plastic flow;

iv. There is no mill stretch and the problem is quasistatic.

Derivation of the basic equations

A schematic diagram of the flat rolling process is shown in Figure 1 with the various regions of concern clearly indicated. These include the plastically flowing zone of the strip, bounded by the elastic compression and elastic recovery regions. As well, the deformed roll contour, whose exact shape is to be determined as part of these computations, is shown. The task is then described as the derivation of a mathematical model that describes the mechanics of the process, accounting for the pressure distribution on the walls of an arbitrarily shaped die whose shape itself depends on the pressure distribution. The technique therefore, has to be iterative.

1. Plastic region

The equation of equilibrium in the longitudinal direction is obtained as:

$$[h(s-2k \mp \tau y')]' = 2(sy' \pm \tau) \qquad (1)$$

where h designates the current strip thickness, s is the roll pressure, k is the flow strength of the strip in shear and τ is the interfacial shear stress.

The deformed roll shape is given by

$$y = f(x) \qquad (2)$$

and the prime denotes differentiation with respect to the independent variable. The upper sign holds for the exit and the lower sign for the entry conditions; this convention will be adhered to in all subsequent developments.

The strip thickness at an arbitrary location is expressed by

$$h = 2(y + C) \tag{3}$$

where C is half of the centre to centre distance of the rolls.

The two frictional conditions at the strip-roll contact usually considered are:

$$\tau = \mu s \tag{4}$$

where μ is the coefficient of Coulomb friction and

$$\tau = k \tag{5}$$

where k is the yield strength in shear.

If the original Amonton-Coulomb theory is assumed to hold, the coefficient of friction is taken to remain constant. If the adhesion theory of friction is assumed to be valid the frictional coefficient should be related to material and process parameters - see Lim and Lenard [136] & Karagiozis and Lenard [137] - and a functional relationship where

$$\mu = \mu \text{ (material and process parameters, independent variables)}$$

should be used. This relation may be an empirical equation or values of μ may be supplied directly in a digital form.

Using the first condition as well as equations (2) and (3), equation (1) becomes

$$s' = sg_1(x,y) + g_2(x,y) \tag{6}$$

where

$$g_1(x,y) = \pm\mu[y''(y + C) + (y')^2 + 1]/ \\ [(y + C)\ (1 \mp \mu y')] \ ;$$

$$g_2(x,y) = [2k'(y + C) + 2ky']/[(y + C) \\ (1 \mp \mu y')]$$

while if equation (5) is valid the equation of equilibrium takes the form

$$s' = k\{2y'\pm[(y')^2 + 1)]\}/(y+C) + 2k'(1\pm y'/2) \pm ky''. \tag{7}$$

The boundary conditions prescribe the roll pressure at entry to the plastic zone as

$$s_2 = 2k_2 + p_2 - \mu s_2 y' \tag{8}$$

and at exit from the plastic zone

$$s_3 = 2k_3 + p_3 \quad . \tag{9}$$

In equations (8) and (9) p_2 and p_3 designate the stresses, at entry to and exit from the plastic zone respectively.

Considering now a slab of the strip, of finite thickness, the shape of its contact with the roll may be approximated by

$$y = a + bx \ ; \tag{10}$$

then, letting k = constant for a particular slab, equation (6) reduces to

$$s' = [\pm s\mu(1+b^2) + 2kb]/[(a+bx+C)(1 \mp \mu b)] \tag{11}$$

integration of which gives the roll pressure as

$$s = c_1(a+bx+C)^{\pm\frac{\mu(1+b^2)}{b(1\mp\mu b)}} \mp 2kb/[\mu(1+b^2)] \tag{12}$$

where c_1 = constant of integration.

The yield criterion of von Mises relates the stresses in the x direction (p) and in the y direction (q) to the flow strength in shear:

$$q-p = 2k\ ; \tag{13}$$

from the vertical equilibrium at the roll-strip interface

$$q = s \mp \mu s y'\ ; \tag{14}$$

combination of equations (10), (13) and (14) then yields another relationship for s and p in the form

$$s = (p+2k)/(1\mp\mu b). \tag{15}$$

Eliminating the roll pressure between (12) and (15) gives a relationship for the stress in the direction of rolling as

$$p = 2k[-1\mp b(1\mp\mu b)/\mu(1+b^2)] + c_1(1\mp\mu b)\,(a+bx+C)^{\pm\frac{\mu(1+b^2)}{b(1\mp\mu b)}} \tag{16}$$

Knowing p_i at the boundary of i^{th} slab, the constant c_1 may be found. Thus p_{i+1} is calculated for the next slab by ensuring horizontal equilibrium in between slabs:

$$p_{i+1} = 2k_i\left[-1\mp\frac{b_i(1\mp\mu b_i)}{\mu(1+b_i^2)}\right] + \left[p_i+2k_i\pm\frac{2k_i b_i(1\mp\mu b_i)}{\mu(1+b_i^2)}\right]\left[\frac{a_i+b_i x_{i+1}+C}{a_i+b_i x_i+C}\right]^{\pm\frac{\mu(1+b_i^2)}{b_i(1\mp\mu b_i)}} \tag{17}$$

and the roll pressure on slab i is calculated from equation (15) as

$$s_i = (p_i + k_i) / (1 \mp \mu b_i). \tag{18}$$

When a straight line segment approximating the roll shape becomes horizontal, i.e. b=0, equation (12) is no longer valid. This condition exists near the exit region and may also occur if the roll gets indented. Thus equation (11) for this case reduces to

$$s' = \pm\mu s/(a+C) \tag{19}$$

and a derivation similar to the one above gives the two equations for the stress in the x direction and the roll pressure respectively as

$$s_i = p_i + k_i \tag{20}$$

and

$$p_{i+1} = (p_i+2k_i) \exp[\pm\mu(x_{i+1}-x_i)/(a_i+C)] - 2k_i . \tag{21}$$

The second frictional condition given by equation (5) is not considered here as it is not believed to be realistic.

2. Elastic regions

The following derivation is to determine the surface pressure distribution as a function of the gauge profile in the elastic zones. In Figure 1 the elastic entry (compression) and elastic exit (recovery) zones are shown along with the plastic zone. It is assumed that if the vertical pressure loading in the elastic exit zone were removed, the strip would recover elastically to a uniform height h_4 from h_3.

Here the elastic exit is analysed. The elastic entry is a mirror image i.e. the terms multiplied by the coefficient of friction should be multiplied by -1.

The derivation now makes use of the equation of equilibrium in the y direction

$$\sigma_y = s(\mu y'-1) \tag{22}$$

and in the x direction

$$\frac{dp}{dx} = - \frac{py'}{(y+C)} + \frac{s}{(y+C)} (y'+\mu)$$

Hooke's law for the plane strain case is now used to express the strain in the y direction, integration of which defines the change of thickness, $v = h-h_u$, as

$$v= \int_0^h \varepsilon y \, dy = \frac{(1-\nu^2)}{E} \sigma_y h - \frac{\nu(1+\nu)}{E} \sigma_x h \ ; \tag{23}$$

here use was made of the fact that the only independent variable is x. The term h_u designates the undeformed strip thickness. It is equal to h_1 at entry and h_3 at exit.

At the end of the region $h = h_4$ and since no more contact with the roll exists

$$\sigma_y = 0 \; . \tag{24}$$

As well, the stress in the x direction must equal the back tension, so at that location

$$\sigma_x h_4 = T_4 \tag{25}$$

where T_4 designates the back tension stress per unit width. Since the total change of thickness at the recovery region is

$$v = h_4 - h_u \tag{26}$$

where h_4 is the thickness after elastic unloading, the exit thickness is obtained as

$$h_4 = [h_u - \frac{\nu(1+\nu)}{E} T_4] \; . \tag{27}$$

Combining equations (3) and (23) with the fact that $\sigma_x = -p$, the stress in the y direction is obtained:

$$\sigma_y = [2(y+C) - h_u - \frac{2\nu(1+\nu)(y+C)}{E} p] \; / \; [\frac{2(1-\nu^2)(y+C)}{E}] ; \tag{28}$$

substituting (28) in (22) and eliminating the roll pressure between that result and equation (23) gives

$$\frac{dp}{dx} = -p[\frac{y'}{(y+C)} + \frac{\nu(y'+\mu)}{(1-\nu)(y+C)(\mu y'-1)}] + \frac{E[2(y+C)-h_u](y'+\mu)}{2(1-\nu^2)(y+C)^2(\mu y'-1)} \tag{29}$$

integration of which, with (10) gives the stress in the elastic recovery zone, in the x direction as

$$p(x)=\frac{E(b+\mu)}{(1-\nu^2)(\mu b-1)b\omega}-\frac{Eh_u(b+\mu)(a+bx+C)^{-1}}{2(1-\nu^2)(\mu b-1)b(\omega-1)}+c_1(a+bx+C)^{-\omega} \qquad (30)$$

where

$$\omega = [1 + \frac{\nu(b+\nu)}{b(1-\nu)(\mu b-1)}]$$

and c_1 is a constant of integration.

Knowing p_i at the boundary of i^{th} slab, the constant c_1 can be found. This determines the pressure p_{i+1} at the other side of that slab, which in tern defines the boundary condition for the $i+1^{th}$ slab. Hence,

$$\begin{aligned} p_{i+1} = {} & \frac{E(b_i+\mu)}{(1-\nu^2)(\mu b_i-1)b_i\omega_i} - \frac{Eh_u(b_i+\mu)(a_i+b_ix_{i+1}+C)^{-1}}{2(1-\nu^2)(\mu b_i-1)b_i(\omega_i-1)} \\ & + [p_i - \frac{E(b_i+\mu)}{(1-\nu^2)(\mu b_i-1)b_i\omega_i}]\,[\frac{(a_i+b_ix_i+C)^{\omega_i}}{(a_i+b_ix_{i+1}+C)^{\omega_i}}] \\ & + \frac{Eh_u(b_i+\mu)(a_i+b_ix_i+C)^{(\omega_i-1)}}{2(1-\nu^2)(\mu b_i-1)b_i(\omega_i-1)(a_i+b_ix_{i+1}+C)^{\omega_i}} \end{aligned} \qquad (31)$$

Once p_i is solved for at the slab boundaries, s_i can be calculated from equation (22) as

$$s_i = \frac{E[2(a_i+b_ix_i+C)-h_u]}{2(1-\nu^2)(a_i+b_ix_i+C)(\mu b_i-1)} - \frac{\nu}{(1-\nu)(\mu b_i-1)}p_i. \qquad (32)$$

For the entry region the expressions for p and s remain the same except for the following changes

(1) $\mu = -\mu$

(2) $h_4 = h_1$

(3) $T_4 = T_1$.

The interface between the elastic and plastic zones is determined by checking where and when the yield criterion of von Mises is satisfied - see equations (8) and (9).

3. Roll deformation

The schematic loading diagram of a work roll is shown in Figure 5. The loading consists of the roll pressure, designated by $p_b(\theta)$ and the interfacial friction stress, $q_b(\theta)$. These loads must be balanced by a statically equivalent force system, the location of which would depend on the type of mill considered. For four or six high mills the backup rolls would supply the necessary balance while for two high mills the reaction forces would be applied through the bearings to the roll journals. As the present analysis is concerned with a two dimensional treatment of the work rolls of a two-high mill and roll bending is neglected, the balancing loads are taken to be distributed

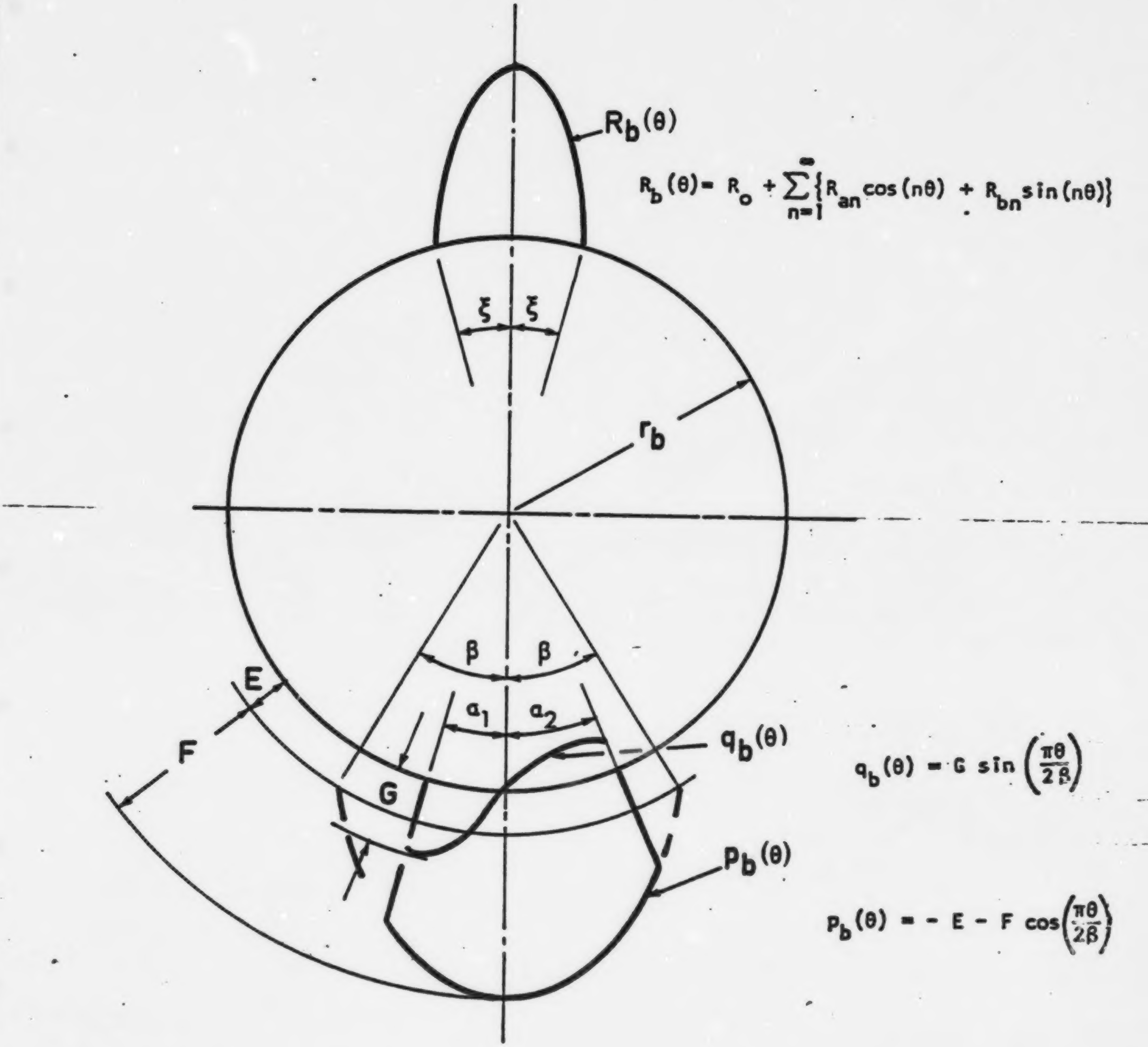
$R_b(\theta)$
ξ
ξ
r_b
β
β
E
a_1
a_2
$q_b(\theta)$
F
G
$p_b(\theta)$

$$R_b(\theta) = R_o + \sum_{n=1}^{\infty}\left\{R_{an}\cos(n\theta) + R_{bn}\sin(n\theta)\right\}$$

$$q_b(\theta) = G\sin\left(\frac{\pi\theta}{2\beta}\right)$$

$$p_b(\theta) = -E - F\cos\left(\frac{\pi\theta}{2\beta}\right)$$

FIGURE 5

over the rolls with $\xi = \pi/2$. This condition ensures that the midplane of the roll remains undeformed and stationary.

Following Michell [6], the stress and strain distribution in the cylinder in a state of plane strain may calculated from a stress function, given by

$$\phi = c_o r^2 + d_1 r^3 \sin\theta + d_2 r^3 \cos\theta + \sum_{n=2}^{\infty} \{a_{1n} r^n + b_{1n} r^{n+2}) \sin(n\theta) + (a_{2n} r^n + b_{2n} r^{n+2}) \cos(n\theta)\} \qquad (33)$$

where the coefficients of terms singular at the origin were taken to equal zero. The radial and shear stresses are then obtained from

$$\sigma_r = \frac{1}{r}\frac{\partial\phi}{\partial r} + \frac{1}{r^2}\frac{\partial^2\phi}{\partial\theta^2} \qquad (34)$$

and

$$\tau_{r\theta} = -\frac{\partial}{\partial r}\left(\frac{1}{r}\frac{\partial\phi}{\partial\theta}\right) \qquad (35)$$

respectively, subject to boundary conditions, given by

$$\sigma_r = p_b(\theta) \;\&\; \tau_{r\theta} = q_b(\theta) \text{ at } r = r_b \qquad (36)$$

for the contact region and similar expressions at the locations of the forces providing the reactions required for balance.

The coefficients in equation (33) are determined next by representing the normal and shear loading on the roll - $p(\theta)$ and $q_b(\theta)$- in terms of Fourier series

$$p(\theta) = p_{ao} + \sum_{n=1}^{\infty} \{p_{an}\cos(n\theta) + p_{bn}\sin(n\theta)\} \tag{37}$$

$$q_b(\theta) = q_{ao} + \sum_{n=1}^{\infty} \{q_{an}\cos(n\theta) + q_{bn}\sin(n\theta)\} \tag{38}$$

where the coefficients are obtained from the Euler formulas. For the normal pressure distribution then

$$p_{ao} = \frac{1}{2\pi}\left\{\int_{\alpha_1}^{\alpha_2} p_b(\theta)\,d\theta + \int_{-\pi/2}^{\pi/2} R_b(\theta)\,d\theta\right\}, \tag{39}$$

$$p_{an} = \frac{1}{\pi}\left\{\int_{\alpha_1}^{\alpha_2} p_b(\theta)\cos(n\theta)\,d\theta + \right.$$

$$\left.\int_{-\pi/2}^{\pi/2} R_b(\theta)\cos(n\theta)\,d\theta\right\} \tag{40}$$

and

$$p_{bn} = \frac{1}{\pi}\left\{\int_{\alpha_1}^{\alpha_2} p_b(\theta)\sin(n\theta)\,d\theta + \int_{-\pi/2}^{\pi/2} R_b(\theta)\sin(n\theta)\,d\theta\right\}; \tag{41}$$

and for the shear stress distribution

$$q_{ao} = \frac{1}{2\pi}\int_{\alpha_1}^{\alpha_2} q_b(\theta)\,d\theta \tag{42}$$

$$q_{an} = \frac{1}{\pi}\int_{\alpha_1}^{\alpha_2} q_b(\theta)\cos(n\theta)\,d\theta \tag{43}$$

and

$$q_{bn} = \frac{1}{\pi}\int_{\alpha_1}^{\alpha_2} q_b(\theta)\sin(n\theta)\,d\theta\,. \tag{44}$$

In equations (39), (40) and (41) $p_b(\theta)$ designates the roll pressure distribution in the roll gap. It may be expressed as a cosine-function in the form

$$p_b(\theta) = - E - F \cos \frac{\pi\theta}{2\beta}, \qquad (45)$$

shown in Figure 5, or alternatively, it may be given as a set of calculated points. The function R_b in equations (39), (40) and (41) represents the reactions required to keep the work roll in equilibrium. This can be done by expressing the reaction in terms of Fourier series

$$R_b(\theta)=R_o + \sum_{n=1}^{\infty}\{R_{an}\cos(n\theta) + R_{bn}\sin(n\theta)\} \qquad (46)$$

where again, the coefficients are obtained by the Euler formulas. It is noted that for a 4 high mill the value of ξ may be determined from the Hertz contact stresses. For a two high mill the reactions are represented by letting $\xi=\pi/2$ which in fact indicates distribution of those forces across a diametral plane of the roll.

In equations (42)-(44) the shear stress distribution is represented by

$$q_b(\theta) = G \sin \frac{\pi\theta}{2\beta} \ . \qquad (47)$$

The values E, F and G are indicated on Figure 5. As shown, the maximum value of the roll pressure is given by E+F; the period is 2β; entry and exit locations are designated by α_1 and α_2 respectively. G stands for the maximum value of the friction stress. Finally, the coefficients of the stress function expansion - and hence, those for the stresses and strains - are obtained as

$$c_o = p_{ao}/2;$$

$$d_1 = p_{b1}/2r_b = -q_{a1}/2r_b;$$

$$d_2 = p_{a1}/2r_b = q_{b1}/2r_b\ ;$$

$$a_{1n} = [np_{bn}-(n-2)q_{an}]/[2n(n-1)r_b{}^{n-2}]\ ; \qquad (48)$$

$$b_{1n} = [p_{bn}-q_{an}]/[2(n+1)r_b{}^{n}]\ ;$$

$$a_{2n} = -[np_{an}+(n-2)q_{bn}]/[2n(n-1)r_b{}^{n-2}]\ ;$$

$$b_{2n} = [p_{an} + q_{bn}]/[2(n+1)r_b{}^{n}]\ ;$$

and the plane strain form of Hooke's law is used to determine the strain components.

4. Roll force and roll torque

The roll separating force is obtained by integrating the roll pressure distribution over the arc of contact which includes the elastic compression and recovery zones. The expression

$$P^2 = \left[\int_{x_1}^{x_N} (s + \tau y')dx + \int_{x_N}^{x_4} (s - \tau y')dx\right]^2 + \left[\int_{x_1}^{x_N} (\tau - sy')dx + \int_{x_N}^{x_4} (\tau + sy')dx\right]^2 \qquad (49)$$

is used where x_1 and x_4 define the boundaries of the roll gap. The roll torque is computed by

$$T = s\left\{\int_{x_1}^{x_N} [x-yy' + \mu(y+xy')]dx - \int_{x_N}^{x_4}[x-yy' - \mu(y+xy')]dx\right\} \quad (50)$$

When a constant coefficient of friction is used, the location of the neutral plane is determined in the usual way i.e. by integrating the relevant equations from the exit and entry and searching for the place where $s_{exit} = s_{entry}$. If $\mu = \mu(x)$, obtained from experiments is used, the location of zero interfacial shear is supplied with the information. The calculations then begin at entry and the validity of the solution is proven by satisfying the prescribed boundary condition at exit without actually enforcing it.

5. Computer Program

The computer program calculates the following:

1. Roll pressure distribution including the elastic-plastic boundaries.
2. Roll deformation in the arc of contact and the gauge profile.
3. Angles of contact.
4. Arc length of contact.
5. Roll centre distance.
6. Roll separating force per unit length of the strip.

Figure 6 gives the flow chart of the computer program. It consist of two parts.

1. The calculation of the pressure distribution on the surface of the strip from a known gauge profile.
2. The calculation of the roll deformation to get the gauge profile.

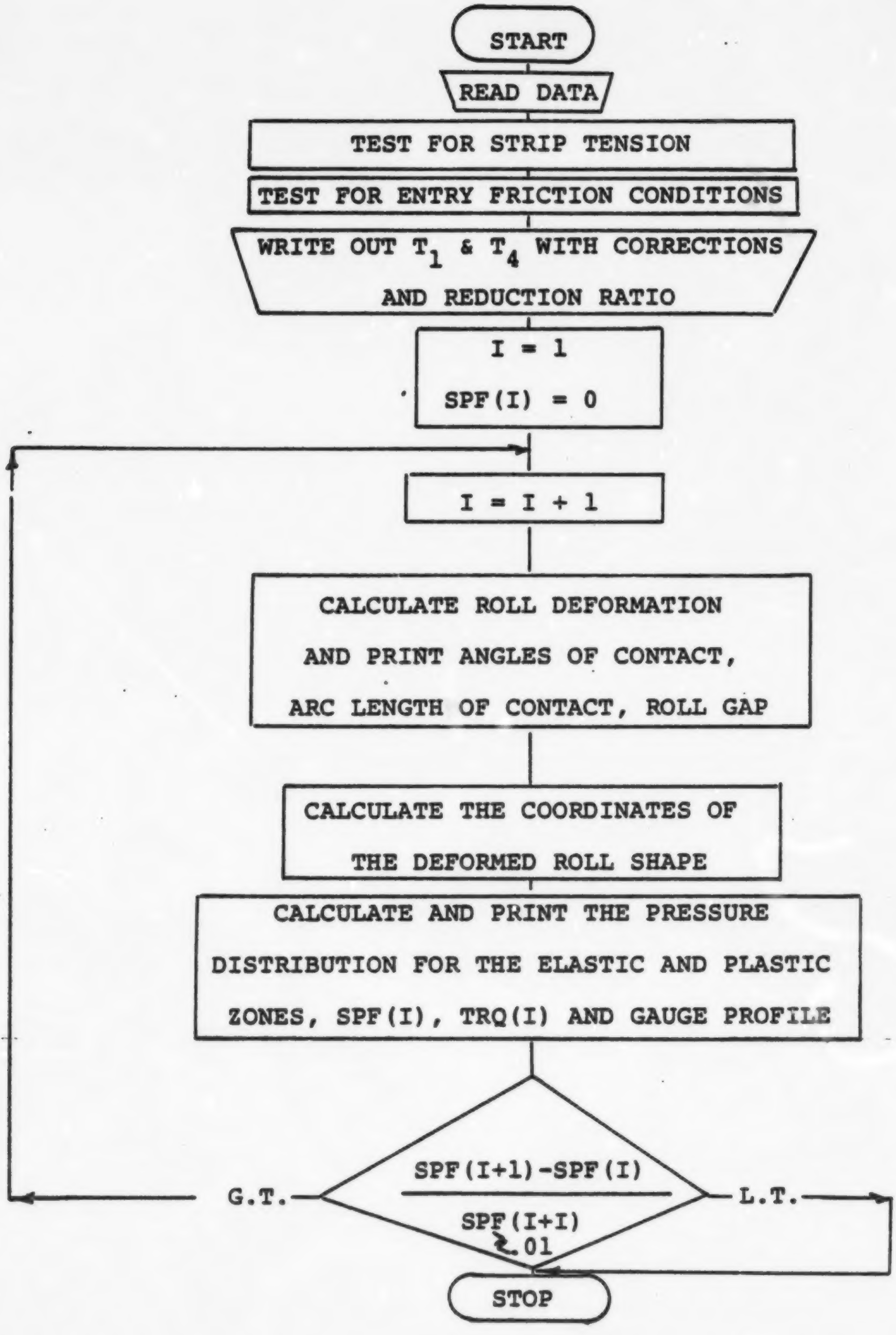
START
READ DATA
TEST FOR STRIP TENSION
TEST FOR ENTRY FRICTION CONDITIONS
WRITE OUT T_1 & T_4 WITH CORRECTIONS AND REDUCTION RATIO
I = 1
SPF(I) = 0
I = I + 1
CALCULATE ROLL DEFORMATION AND PRINT ANGLES OF CONTACT, ARC LENGTH OF CONTACT, ROLL GAP
CALCULATE THE COORDINATES OF THE DEFORMED ROLL SHAPE
CALCULATE AND PRINT THE PRESSURE DISTRIBUTION FOR THE ELASTIC AND PLASTIC ZONES, SPF(I), TRQ(I) AND GAUGE PROFILE
SPF(I+1)-SPF(I)
SPF(I+I)
≥.01
G.T.
L.T.
STOP

Figure 6: Flow chart of the computer program.

CHAPTER 6

CONSTITUTIVE EQUATIONS FOR HIGH TEMPERATURE DEFORMATION OF STEELS

Introduction

This chapter describes the calculations performed in order to analyze and compare the predictions of published empirical constitutive relations for high temperature deformation of low carbon steels. The equations used are due to Shida [94], Ekelund [99], Altan and Boulger [93], Hajduk [100] and Gittins et al. [95].

Results

Figures 7 - 14 show the flow curves obtained from the above references. The equations used are listed below.

(a) Shida's Formulation [94]

The flow strengths of low carbon steel are given in terms of strains, rates of strain, temperature and carbon content. The flow strength, in Kg/mm^2 is then

$$\sigma = \sigma_f \, f \, (\dot{\varepsilon}/10)^m$$

where for

$$t \geq t_d = 0.95 \, (C + 0.41)/(C + 0.32)$$

$$\sigma_f = 0.28 \exp[5/t - 0.01/(C + 0.05)]$$

and

$$m = (-0.019C + 0.126)t + (0.075C - 0.05).$$

For $t < t_d$

$$\sigma_f = 0.28\, q(C,t) \exp\,[5/t_d - 0.01/(C + 0.05)],$$

$$q(C,t) = 30\ (C + 0.9)[t - 0.95(C + 0.49)/(C + 0.42)]^2$$
$$+ (C + 0.06)/(C + 0.09)$$

and

$$m = (0.081C - 0.154)t + (-0.019C + 0.207) + 0.027/(C + 0.320).$$

The other parameters are defined as given below:

$$f = 1.3\ (\varepsilon/0.2)^n - 0.3\ (\varepsilon/0.2);$$
$$n = 0.41 - 0.07C;$$
$$\varepsilon = \ln\ (h_2/h_1)$$

and $\dot{\varepsilon}$ is the rate of strain. In flat rolling, Shida gives

$$\dot{\varepsilon} = [2\pi N/60 \sqrt{1 - h_2/h_1})] \sqrt{R'/h_1}\ \varepsilon\ .$$

In the above formulae t is the dimensionless temperature defined as

$$t = T\ (°K)/1000$$

where T is the absolute temperature of the strip. C is the carbon content in %; h_2 and h_1 are the exit and entry thicknesses respectively in mm; N is the roll rpm and R' is the flattened roll radius, as computed by Hitchcock's formula.

The range of applicability of these equations is also given by Shida; they are valid for

Carbon content: $<1.2\%$
Temperature: 700°C - 1200° C
Strain rate: $0.1 - 100 \text{ sec}^{-1}$
Strain: $< 70\%$

(b) Ekelund's Formulation [99]

$$K_f = (14 - 0.01t) \quad (1.4 + C + Mn + 0.3Cr)$$

where K_f is the flow strength, given in Kg/mm^2, t is the strip temperature in °C and C, Mn and Cr are the carbon, manganese and chromium contents respectively in %.

(c) Altan and Boulger's Formulation [93]

The equation used is

$$\sigma = C\dot{\varepsilon}^m;$$

C and m are given by Altan and Boulger as functions of temperature and strain for a large number of ferrous and nonferrous metals.

(d) Hajduk's Formulation [100]

Hajduk's equation is given in the form

$$\sigma_S = \sigma_O K_T K_\varepsilon K_U$$

where σ_0, K_T, K_ε , and K_U are functions of the material, temperature, strain and strain rate. Hajduk gives those values for 25 different low and medium carbon steels.

(e) Gittins' Formulation [95]

Gittins, Moller and Everett [95] derived the coefficients of an equation giving the mean yield strength

$$K_p = A'_o + r^{0.2} [A'_1 + A'_2 \ln\lambda + A'_3/(T/1000)]$$

for mild steel, and several other steels. The parameters in the above equation are given for several steels in Reference [95].

Discussion:

Figures 7 to 10 show the stress-strain rate curves for AISI 1015 steel, at 800°C and 1000°C, subjected to strains of 0.25 and 0.50 respectively. Wide variations in predicted behaviour are noticed.

The behaviour of the AISI 1045 steel is shown in Figures 11 to 14. As for the 1015 steel, it is impossible to decide which empirical relation is reliable.

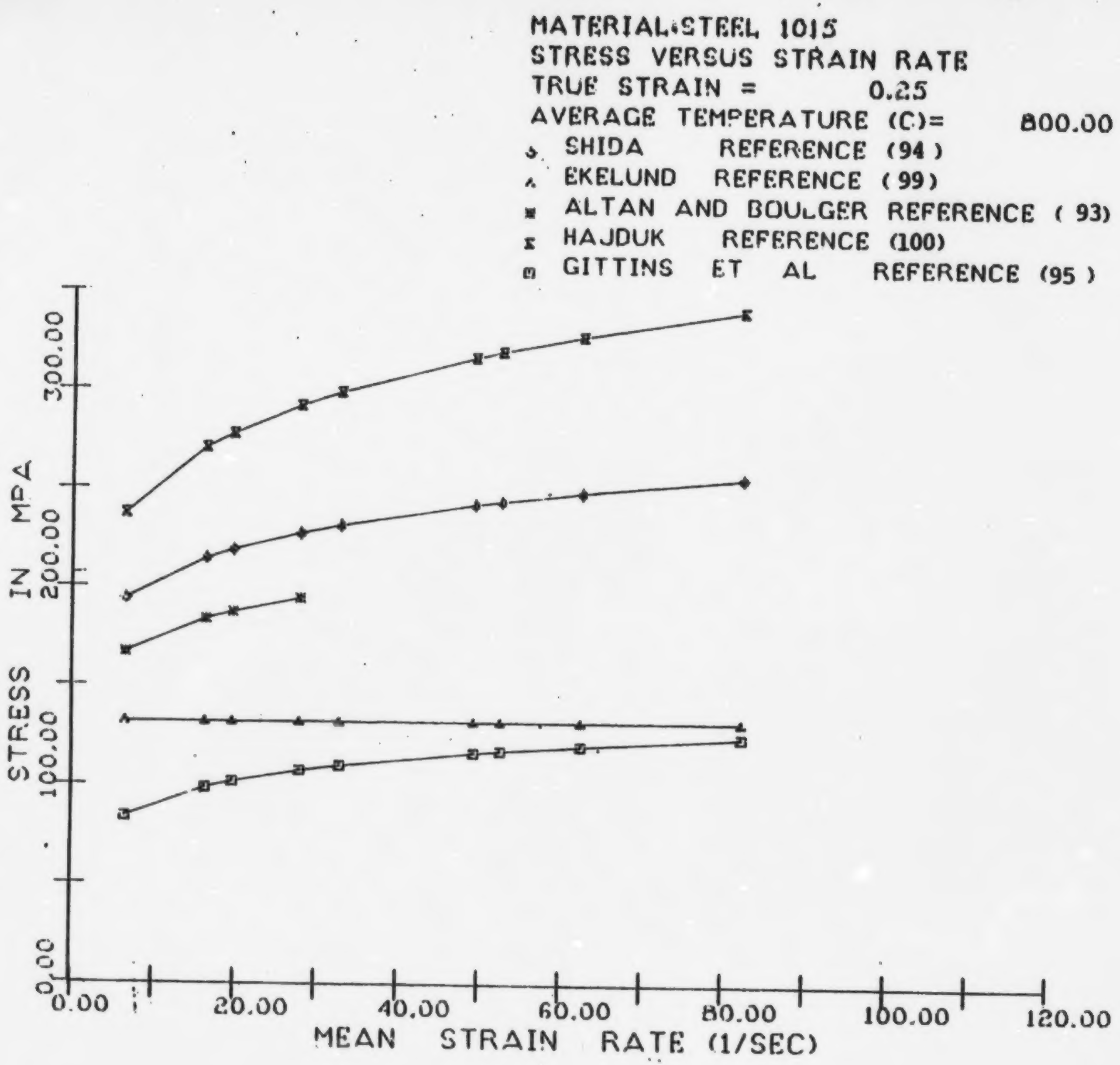
MATERIAL:STEEL 1015
STRESS VERSUS STRAIN RATE
TRUE STRAIN = 0.25
AVERAGE TEMPERATURE (C)= 800.00
SHIDA REFERENCE (94)
EKELUND REFERENCE (99)
ALTAN AND BOULGER REFERENCE (93)
HAJDUK REFERENCE (100)
GITTINS ET AL REFERENCE (95)
STRESS IN MPA
0.00
100.00
200.00
300.00
0.00
20.00
40.00
60.00
80.00
100.00
120.00
MEAN STRAIN RATE (1/SEC)

FIGURE 7

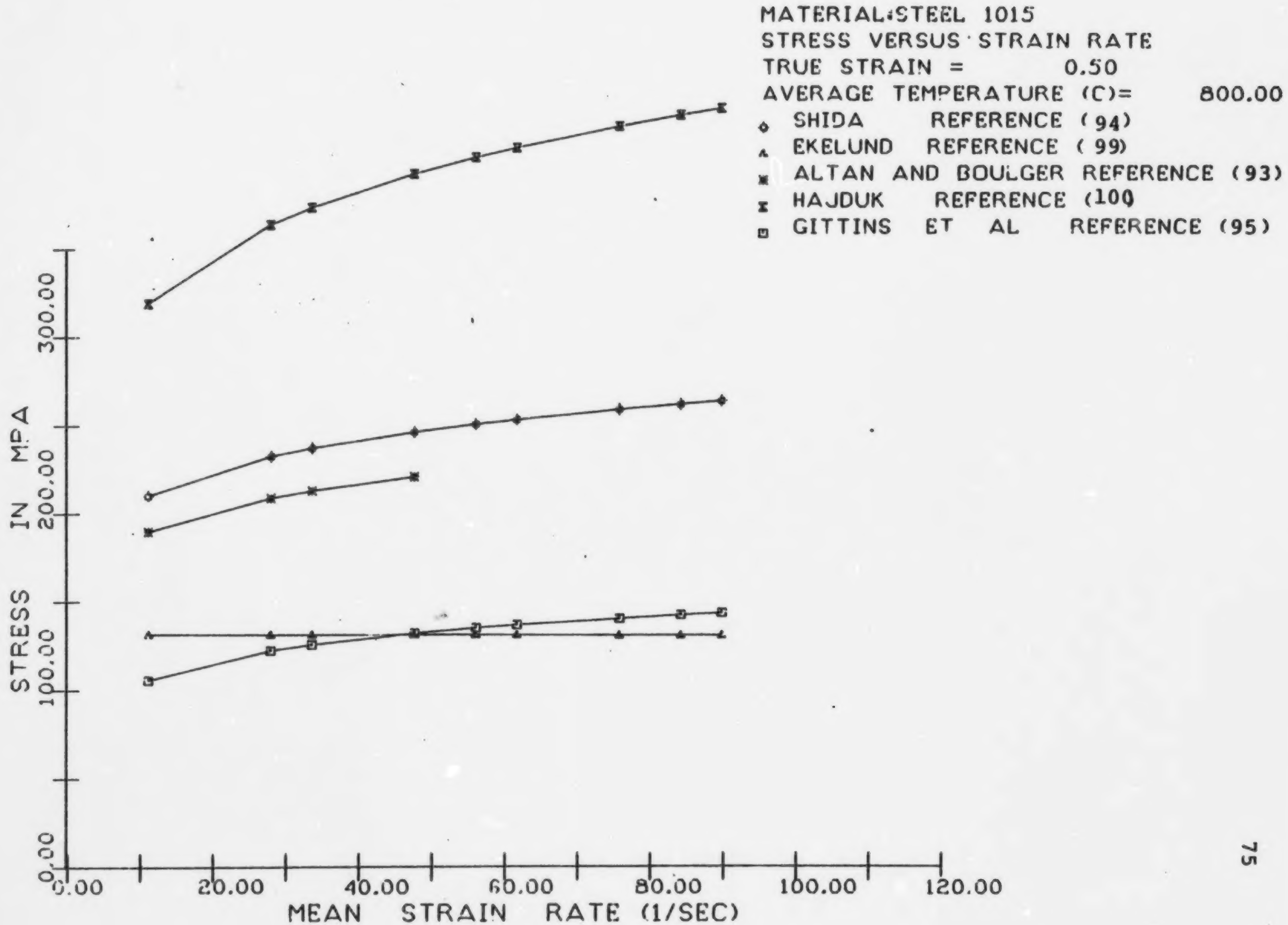
MATERIAL:STEEL 1015
STRESS VERSUS STRAIN RATE
TRUE STRAIN = 0.50
AVERAGE TEMPERATURE (C)= 800.00
◇ SHIDA REFERENCE (94)
▵ EKELUND REFERENCE (99)
✱ ALTAN AND BOULGER REFERENCE (93)
⧗ HAJDUK REFERENCE (100
⊡ GITTINS ET AL REFERENCE (95)
STRESS IN MPA
0.00
100.00
200.00
300.00
MEAN STRAIN RATE (1/SEC)
0.00
20.00
40.00
60.00
80.00
100.00
120.00

FIGURE 8

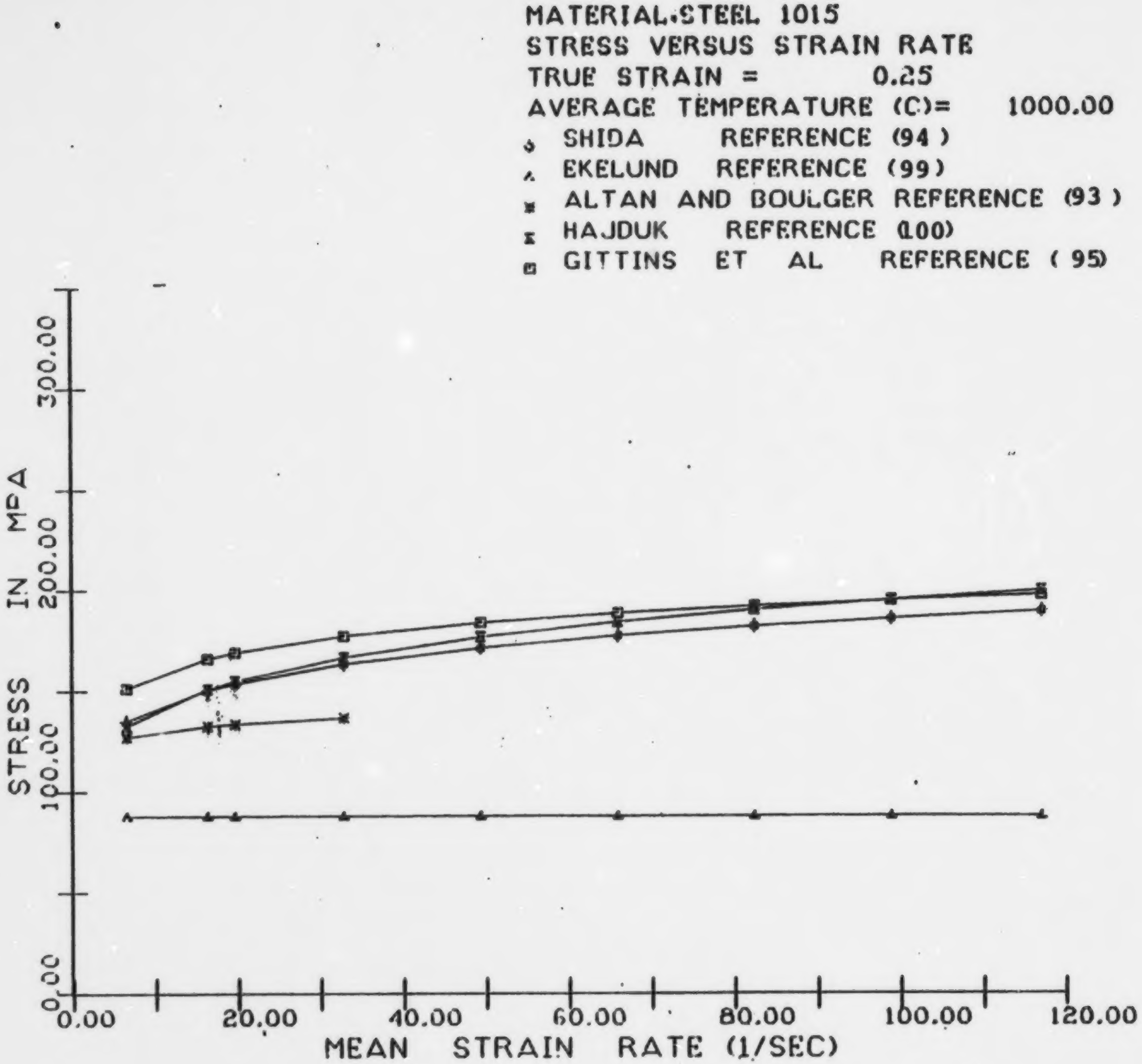
MATERIAL:STEEL 1015
STRESS VERSUS STRAIN RATE
TRUE STRAIN = 0.25
AVERAGE TEMPERATURE (C)= 1000.00
SHIDA REFERENCE (94)
EKELUND REFERENCE (99)
ALTAN AND BOULGER REFERENCE (93)
HAJDUK REFERENCE (100)
GITTINS ET AL REFERENCE (95)
STRESS IN MPA
0.00
100.00
200.00
300.00
0.00
20.00
40.00
60.00
80.00
100.00
120.00
MEAN STRAIN RATE (1/SEC)

FIGURE 9

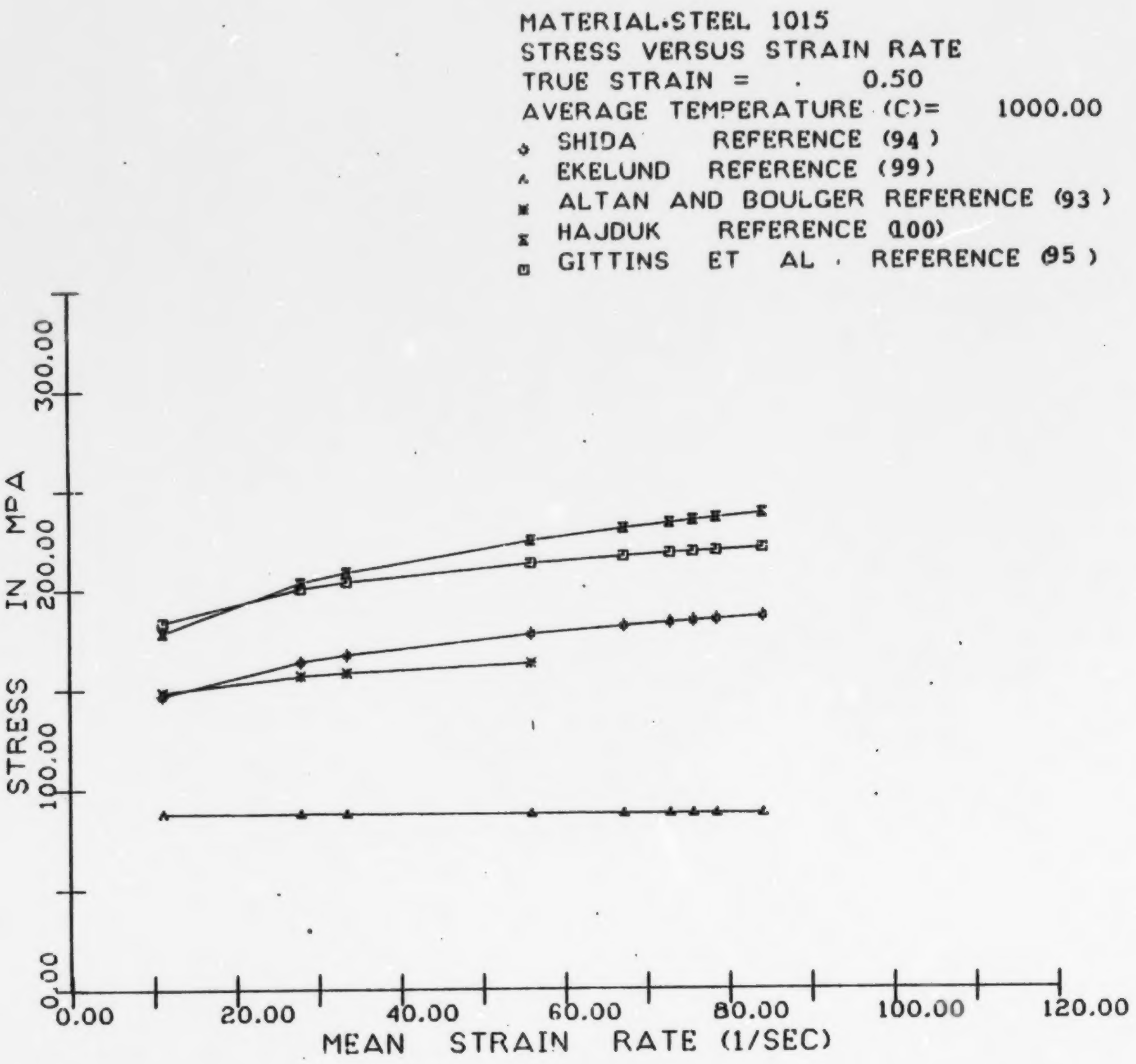
MATERIAL.STEEL 1015
STRESS VERSUS STRAIN RATE
TRUE STRAIN = . 0.50
AVERAGE TEMPERATURE (C)= 1000.00
◇ SHIDA REFERENCE (94)
△ EKELUND REFERENCE (99)
✱ ALTAN AND BOULGER REFERENCE (93)
⧗ HAJDUK REFERENCE (100)
⊡ GITTINS ET AL . REFERENCE (95)
STRESS IN MPA
0.00
100.00
200.00
300.00
0.00
20.00
40.00
60.00
80.00
100.00
120.00
MEAN STRAIN RATE (1/SEC)

FIGURE 10

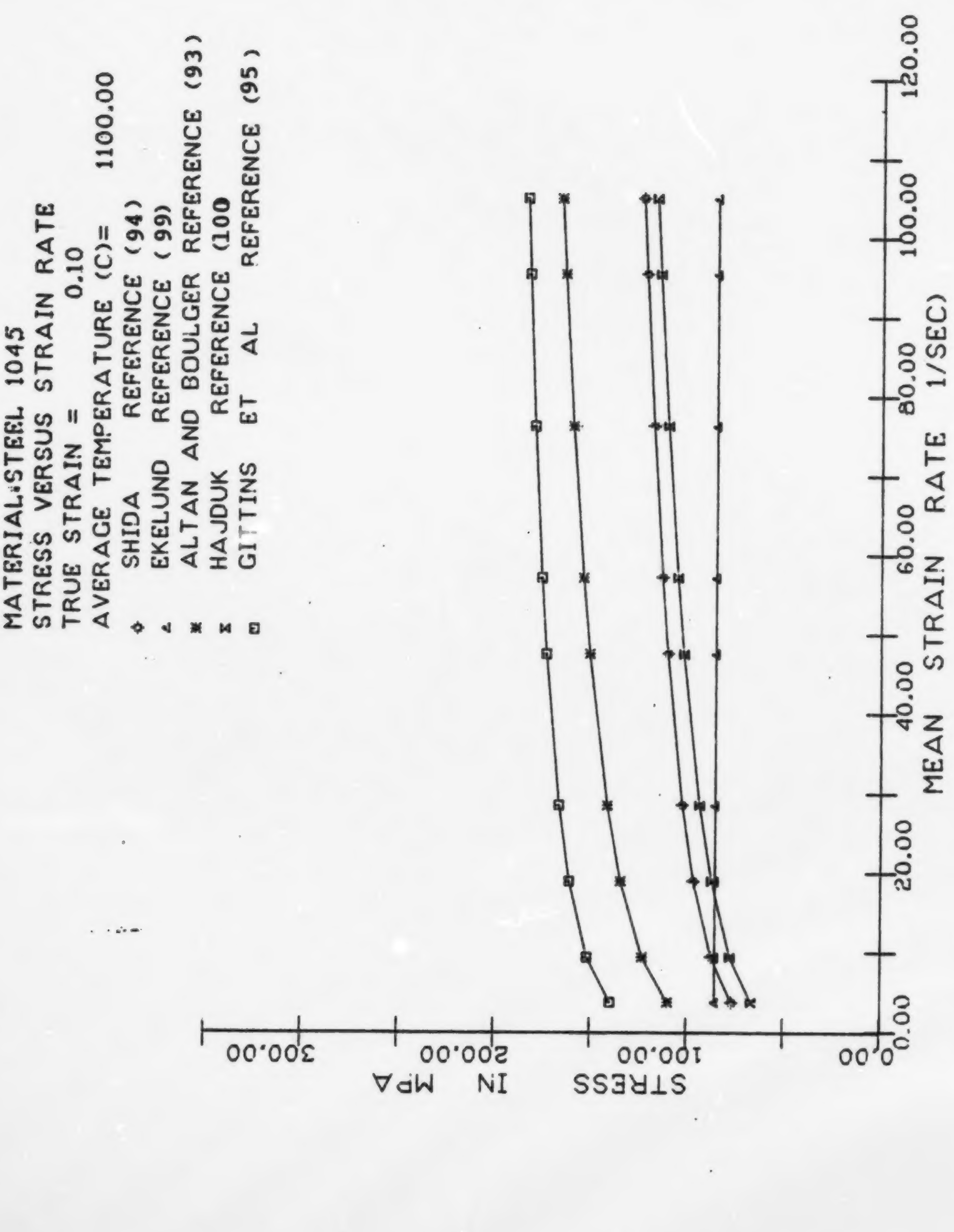
MATERIAL:STEEL 1045
STRESS VERSUS STRAIN RATE
TRUE STRAIN = 0.10
AVERAGE TEMPERATURE (C)= 1100.00
◇ SHIDA REFERENCE (94)
△ EKELUND REFERENCE (99)
✱ ALTAN AND BOULGER REFERENCE (93)
⧖ HAJDUK REFERENCE (100
□ GITTINS ET AL REFERENCE (95)
STRESS IN MPA
0.00
100.00
200.00
300.00
MEAN STRAIN RATE 1/SEC)
0.00
20.00
40.00
60.00
80.00
100.00
120.00

FIGURE 11

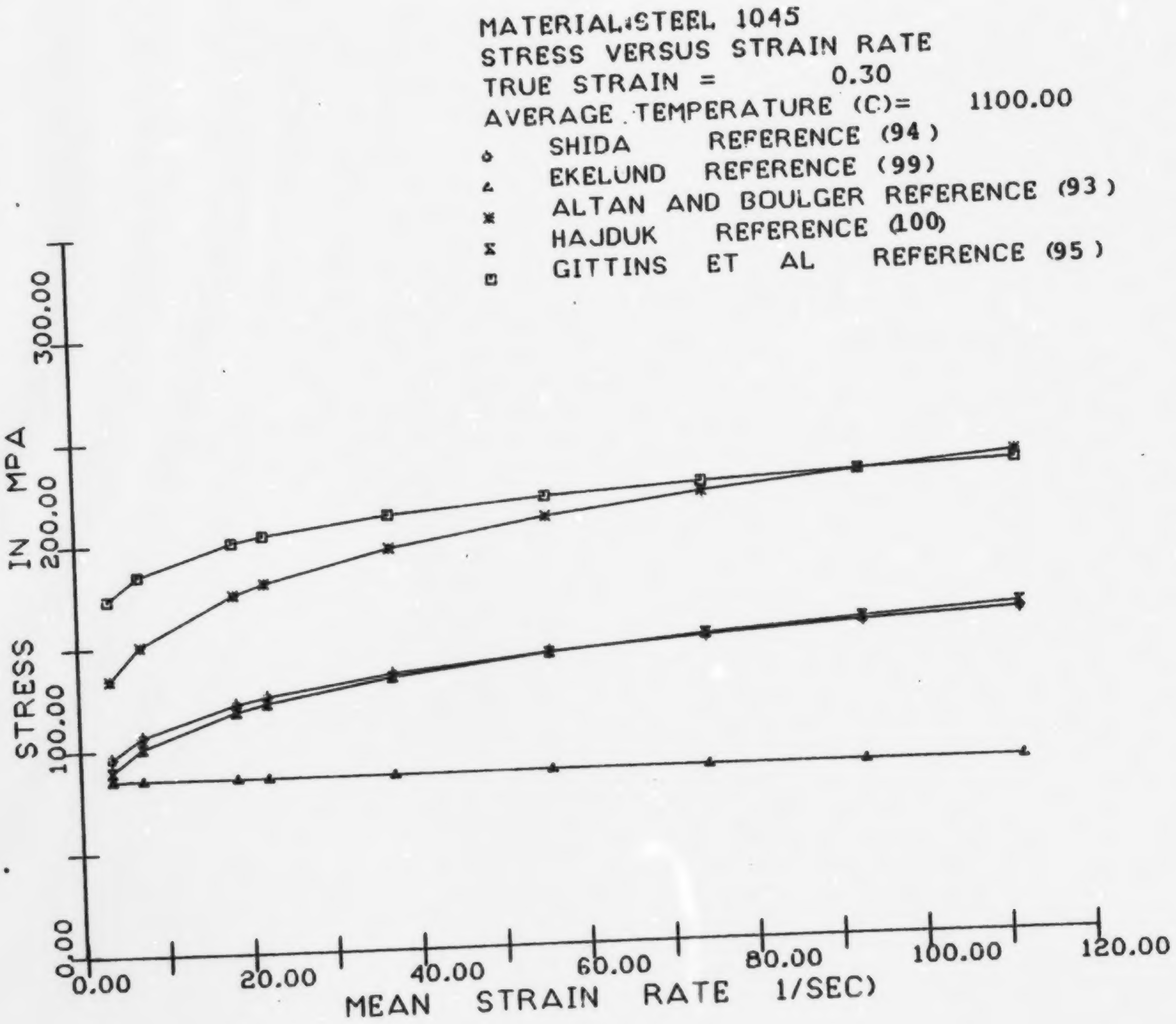
MATERIAL:STEEL 1045
STRESS VERSUS STRAIN RATE
TRUE STRAIN = 0.30
AVERAGE TEMPERATURE (C)= 1100.00
SHIDA REFERENCE (94)
EKELUND REFERENCE (99)
ALTAN AND BOULGER REFERENCE (93)
HAJDUK REFERENCE (100)
GITTINS ET AL REFERENCE (95)
STRESS IN MPA
0.00
100.00
200.00
300.00
0.00
20.00
40.00
60.00
80.00
100.00
120.00
MEAN STRAIN RATE 1/SEC)

FIGURE 12

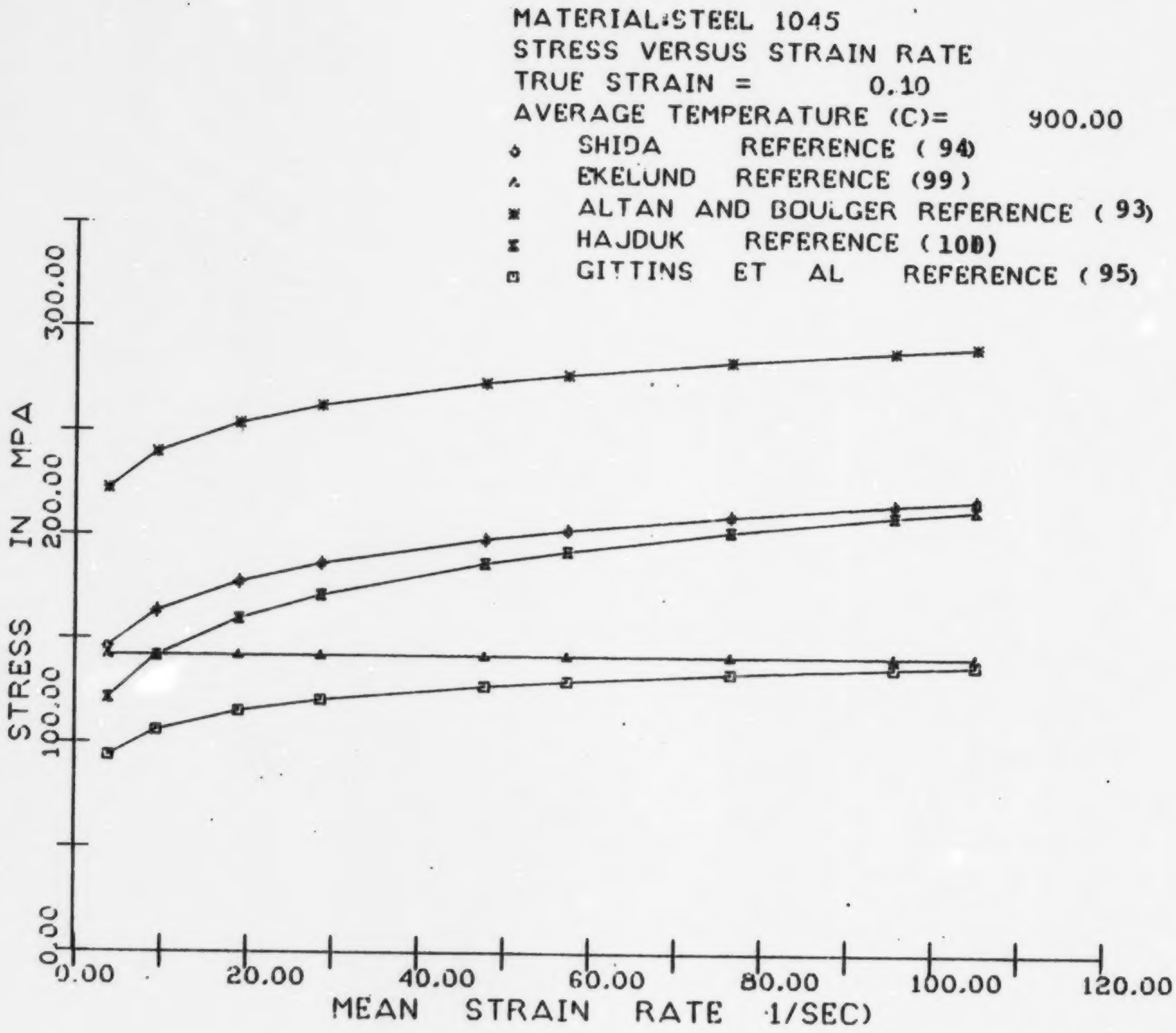
MATERIAL:STEEL 1045
STRESS VERSUS STRAIN RATE
TRUE STRAIN = 0.10
AVERAGE TEMPERATURE (C)= 900.00
◇ SHIDA REFERENCE (94)
△ EKELUND REFERENCE (99)
✱ ALTAN AND BOULGER REFERENCE (93)
⧗ HAJDUK REFERENCE (100)
□ GITTINS ET AL REFERENCE (95)
STRESS IN MPA
0.00
100.00
200.00
300.00
0.00
20.00
40.00
60.00
80.00
100.00
120.00
MEAN STRAIN RATE 1/SEC)

FIGURE 13

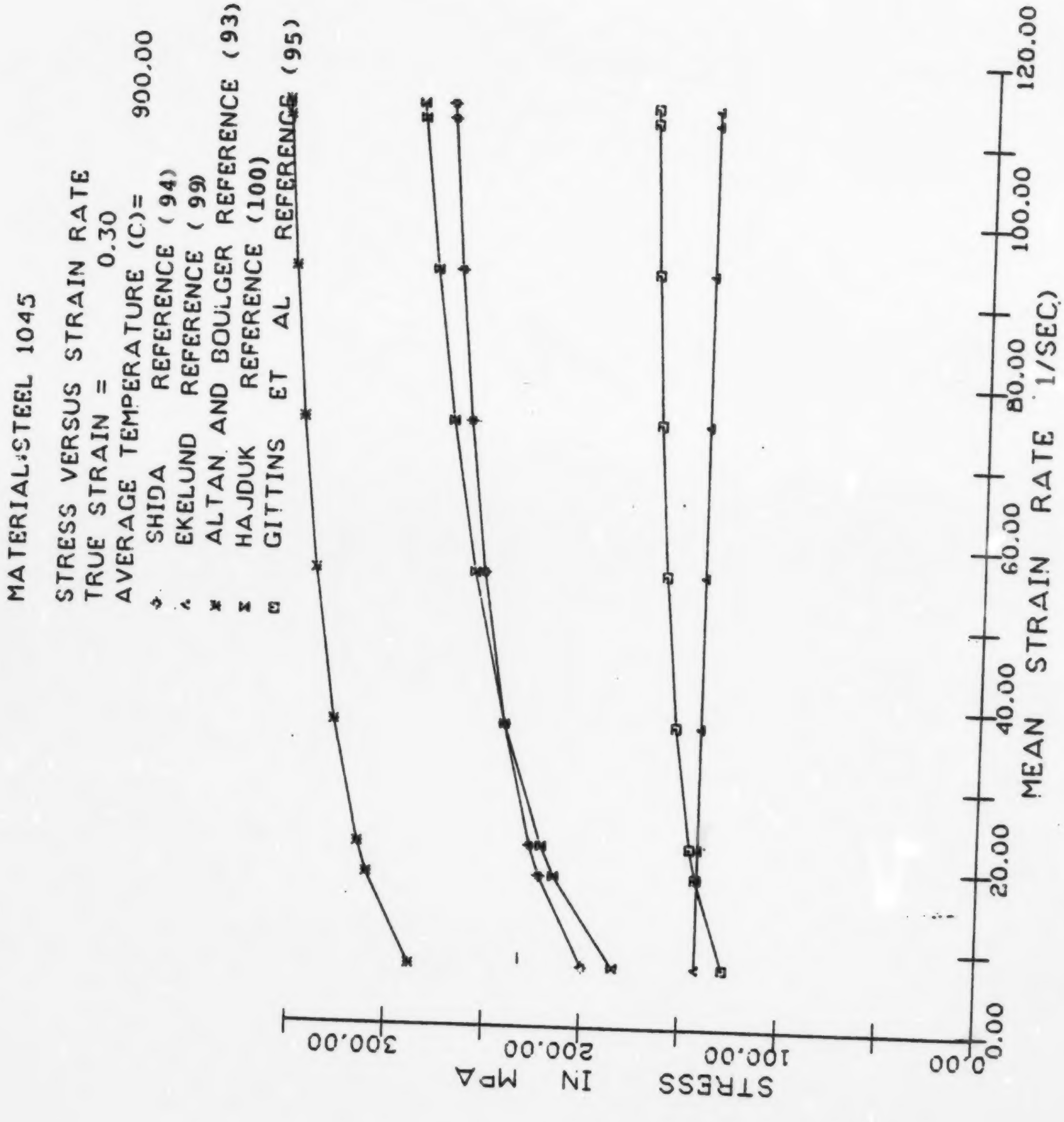
MATERIAL:STEEL 1045
STRESS VERSUS STRAIN RATE
TRUE STRAIN = 0.30
AVERAGE TEMPERATURE (C)= 900.00
SHIDA REFERENCE (94)
EKELUND REFERENCE (99)
ALTAN AND BOULGER REFERENCE (93)
HAJDUK REFERENCE (100)
GITTINS ET AL REFERENCE (95)
STRESS IN MPA
0.00
100.00
200.00
300.00
MEAN STRAIN RATE 1/SEC)
20.00
40.00
60.00
80.00
100.00
120.00

FIGURE 14

CHAPTER 7

CALCULATIONS USING FLAT ROLLING MODELS

Introduction

In this chapter the predictive capabilities of the models, developed by Orowan [27], Sims [25], Bland and Ford [131] and Roychoudhuri and Lenard [132] are compared considering hot and cold strip rolling.

Roll pressures, forces and torques - cold rolling

The calculations are performed for cold rolled AISI 1020 steel, whose uniaxial flow curve is represented by the equation

$$\sigma = 593.50\ (1 + 78.3\varepsilon)^{0.067}\ \text{MPa.}$$

The roll radius is taken as 125 mm, the ambient temperature as 20 degrees C and the roll rpm as 10.

Results: (μ = constant)

Comparative plots of the numerical predictions of roll forces, roll pressures and roll torques for AISI 1020 are presented in Figures 15 to 24.

In each case the non-dimensional roll forces and roll torques are plotted against the percentage reduction. These plots represent the first pass of the strip with a constant entry thickness of 5 mm.

Three coefficients of friction are used: 0.1, 0.3, and 0.5. In Figure 15, 17 and 19 the dimensionless roll forces versus reduction are shown.

Figures 16, 18 and 20 numerically simulate the dimensionless roll torques at various reductions.

It is observed that the force predictions of the three models are reasonably close when the coefficient of friction is not larger than 0.3. Beyond that value the differences are quite large. Similar observations are made when the torque predictions are evaluated.

Two conclusions may be drawn from these observations. First is the fact that a coefficient of friction of 0.5 is unrealistically high for cold rolling and the models "object" numerically; the second is that the roll distortion due to shearing forces is becoming a large component of the total roll flattening. This latter phenomenon then results in unrealistically large roll gap contact. The models of References [27] and [131] do not account for the growth of the contact zone; that of Reference [132] does.

Figures 21,22, 23 and 24 show the predicted roll pressure distributions at specific reductions and coefficients of friction.

In general, the predictions of [132] underestimate those of [27] and [131] when considering a low coefficient; when a higher coefficient of friction is used, Reference [132]'s results tend to be higher than those of Orowan and Bland and Ford.

Further, as a higher frictional coefficient is used, the iterative calculations converge for larger percentage reductions--see Figures 15 to 19. When a coefficient of friction of 0.5 is used only Reference [132]'s calculations converge.

The predicted roll forces by all three models are in better agreement than the roll torques. The differences between the three models in predicting the roll force and roll torque increase when the coefficient of friction increases.

In Figures 21, 22, 23 and 24, the predicted roll pressure distributions along the roll are presented. Note that in Reference [132] the roll pressure distribution due to elastic entry and elastic exit is included. This is not the case for References [127] and [131]. The latter two analyses do not calculate the roll pressures at exit and entry but rather apply compensation factors in order to obtain their constributions to the total roll force and roll torque.

In Figures 22, 23 and 24, the effect of reduction

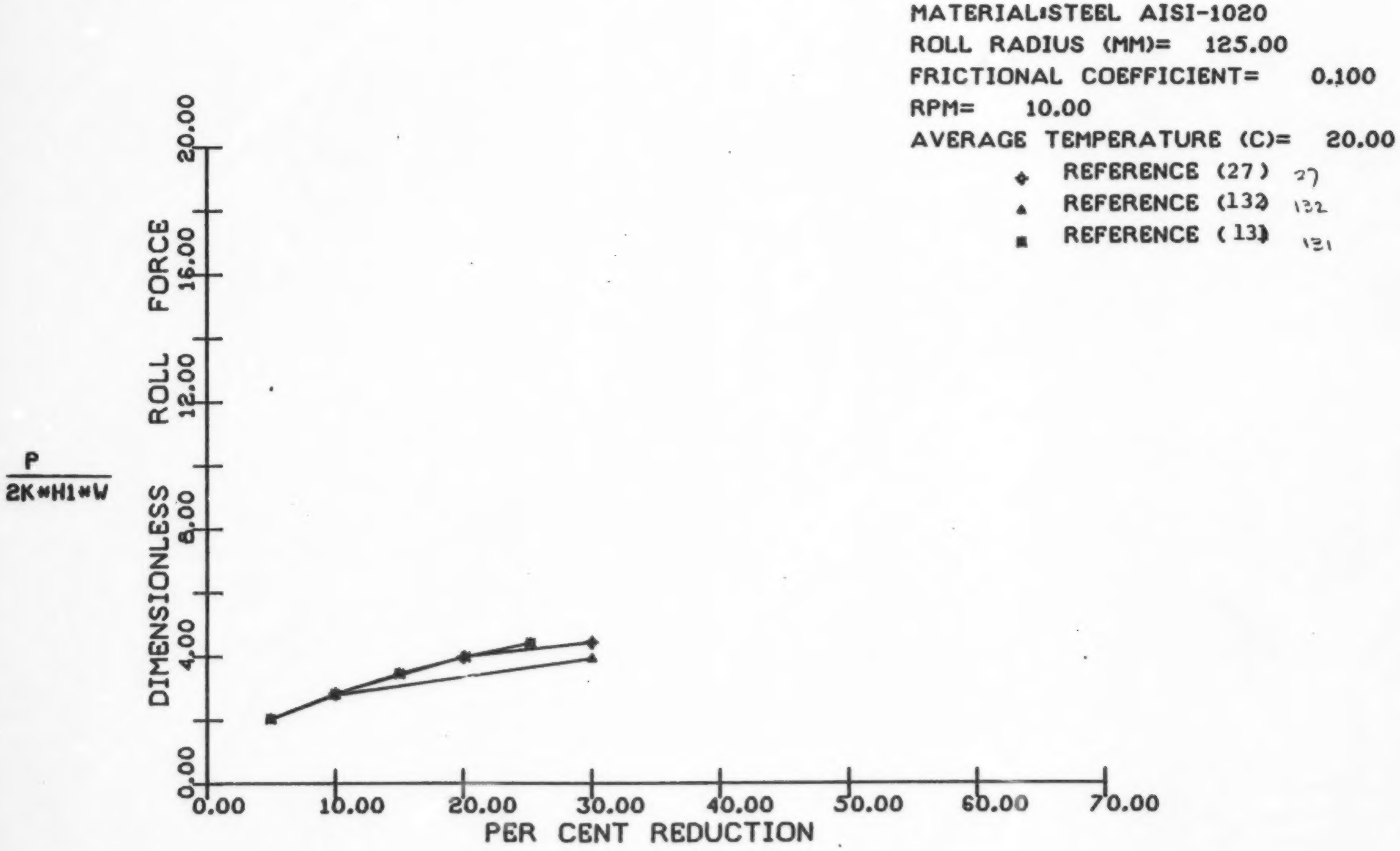
MATERIAL:STEEL AISI-1020
ROLL RADIUS (MM)= 125.00
FRICTIONAL COEFFICIENT= 0.100
RPM= 10.00
AVERAGE TEMPERATURE (C)= 20.00
◆ REFERENCE (27) 27
▲ REFERENCE (132) 132
■ REFERENCE (131) 131
P / 2K*H1*W
DIMENSIONLESS ROLL FORCE
0.00
4.00
8.00
12.00
16.00
20.00
0.00
10.00
20.00
30.00
40.00
50.00
60.00
70.00
PER CENT REDUCTION

FIGURE 15

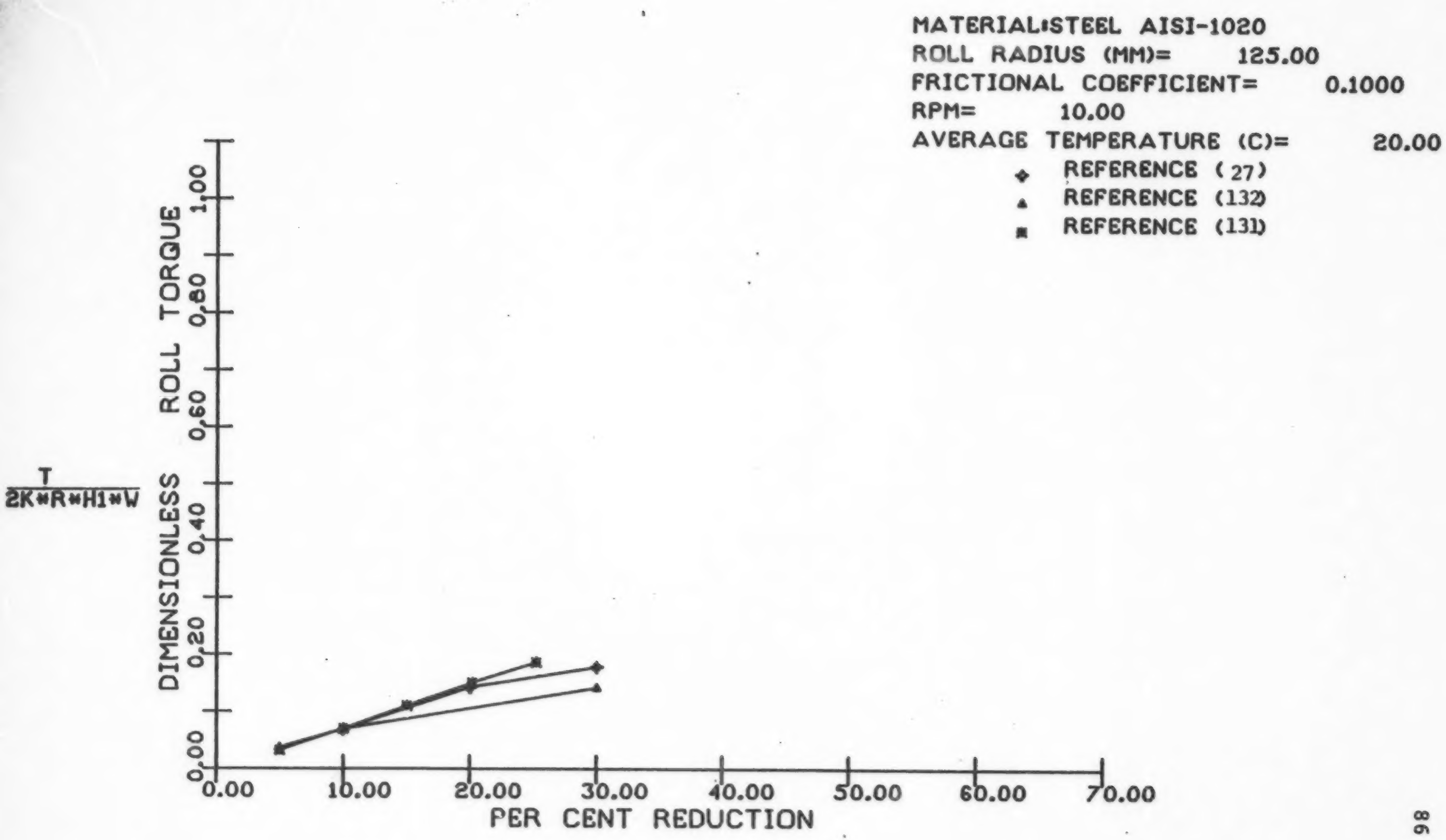
MATERIAL:STEEL AISI-1020
ROLL RADIUS (MM)= 125.00
FRICTIONAL COEFFICIENT= 0.1000
RPM= 10.00
AVERAGE TEMPERATURE (C)= 20.00
◆ REFERENCE (27)
▲ REFERENCE (132)
■ REFERENCE (131)
T / 2K*R*H1*W
DIMENSIONLESS ROLL TORQUE
0.00
0.20
0.40
0.60
0.80
1.00
0.00
10.00
20.00
30.00
40.00
50.00
60.00
70.00
PER CENT REDUCTION

FIGURE 16

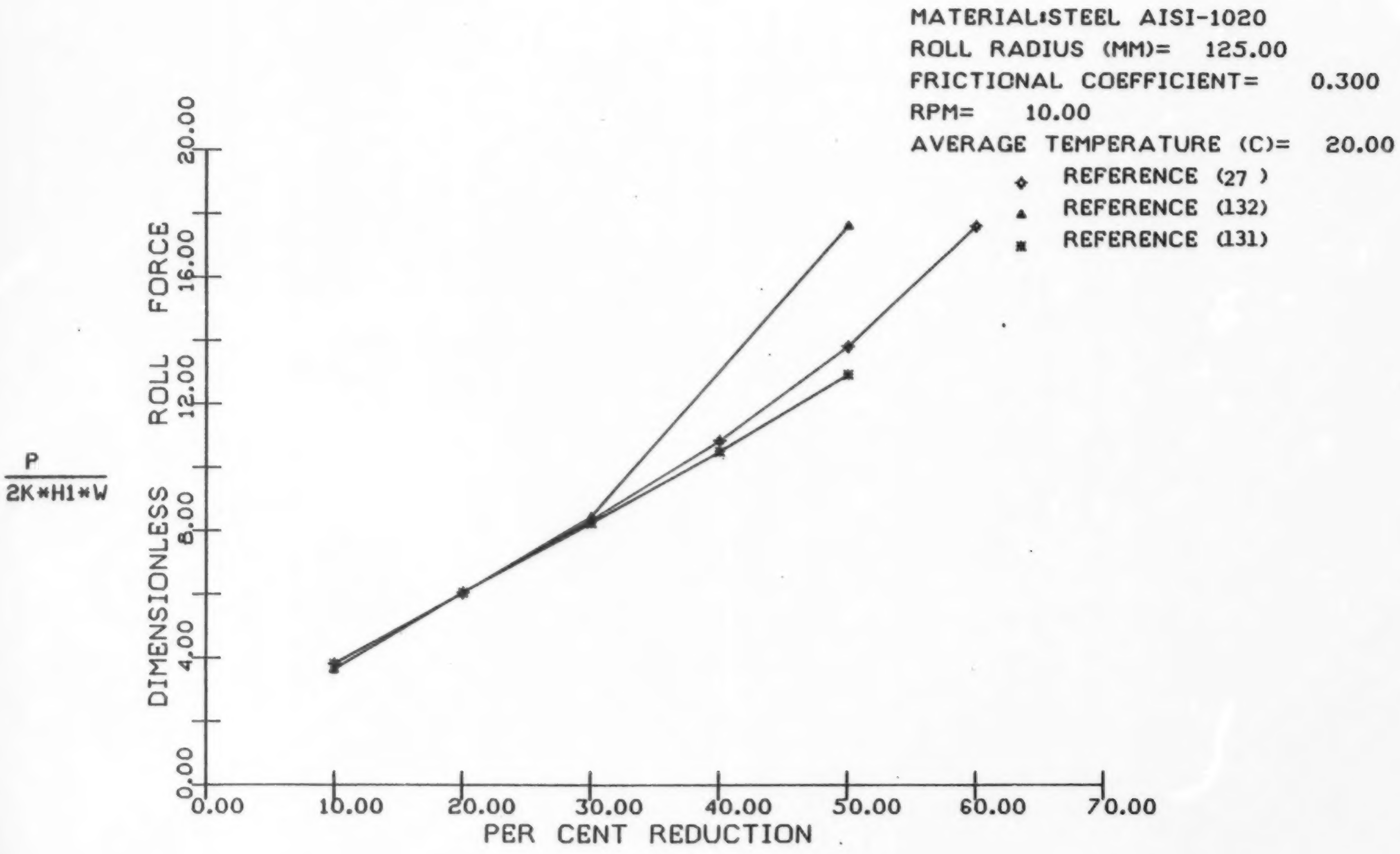
MATERIAL:STEEL AISI-1020
ROLL RADIUS (MM)= 125.00
FRICTIONAL COEFFICIENT= 0.300
RPM= 10.00
AVERAGE TEMPERATURE (C)= 20.00
◆ REFERENCE (27)
▲ REFERENCE (132)
✱ REFERENCE (131)
P / 2K*H1*W
DIMENSIONLESS ROLL FORCE
0.00
4.00
8.00
12.00
16.00
20.00
0.00
10.00
20.00
30.00
40.00
50.00
60.00
70.00
PER CENT REDUCTION

FIGURE 17

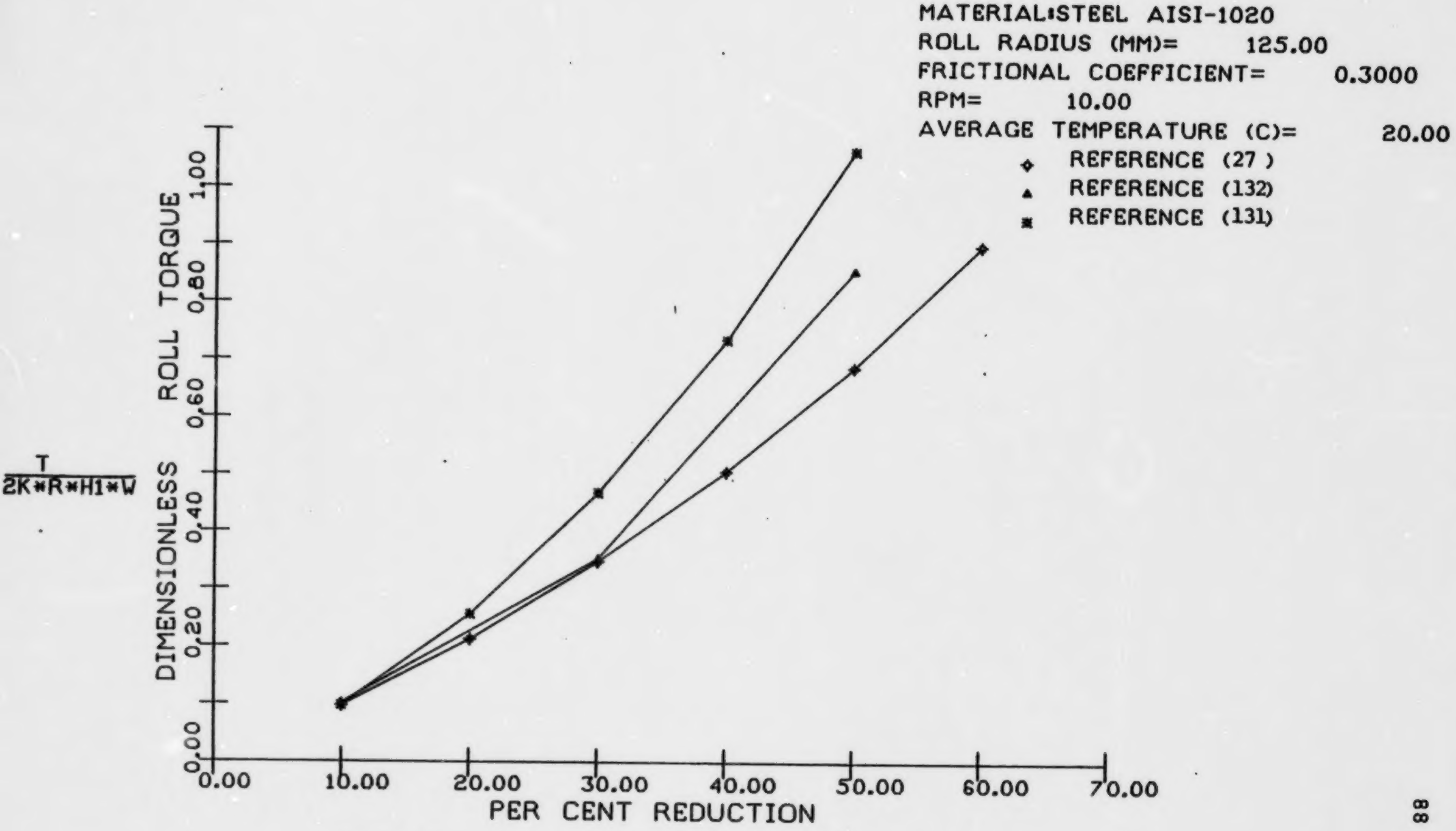
MATERIAL:STEEL AISI-1020
ROLL RADIUS (MM)= 125.00
FRICTIONAL COEFFICIENT= 0.3000
RPM= 10.00
AVERAGE TEMPERATURE (C)= 20.00
◆ REFERENCE (27)
▲ REFERENCE (132)
✱ REFERENCE (131)
$\frac{T}{2K*R*H1*W}$
DIMENSIONLESS ROLL TORQUE
0.00
0.20
0.40
0.60
0.80
1.00
0.00
10.00
20.00
30.00
40.00
50.00
60.00
70.00
PER CENT REDUCTION

FIGURE 18

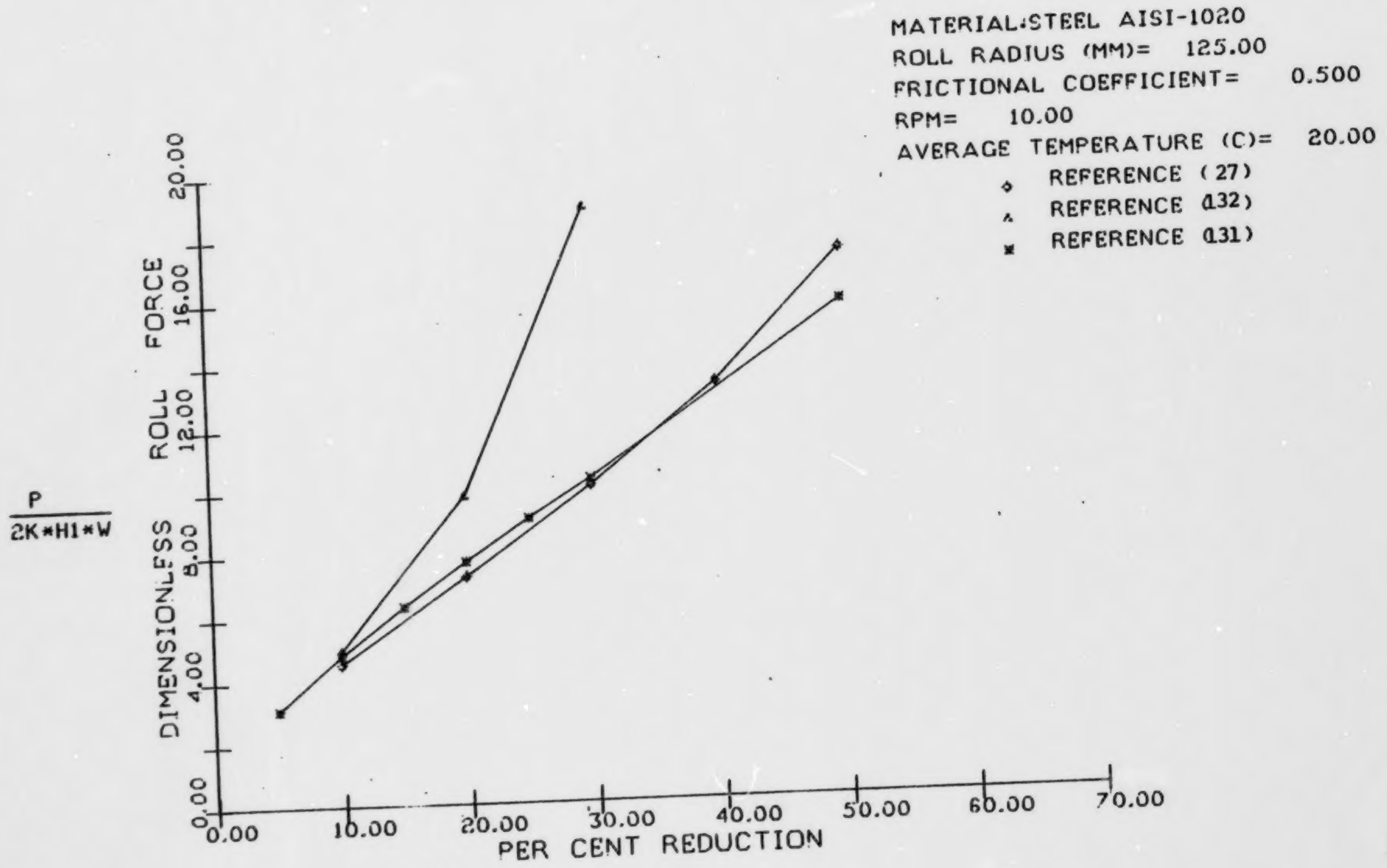
MATERIAL:STEEL AISI-1020
ROLL RADIUS (MM)= 125.00
FRICTIONAL COEFFICIENT= 0.500
RPM= 10.00
AVERAGE TEMPERATURE (C)= 20.00
◇ REFERENCE (27)
^ REFERENCE (132)
✻ REFERENCE (131)
P / 2K*H1*W
DIMENSIONLESS ROLL FORCE
0.00
4.00
8.00
12.00
16.00
20.00
0.00
10.00
20.00
30.00
40.00
50.00
60.00
70.00
PER CENT REDUCTION

FIGURE 19

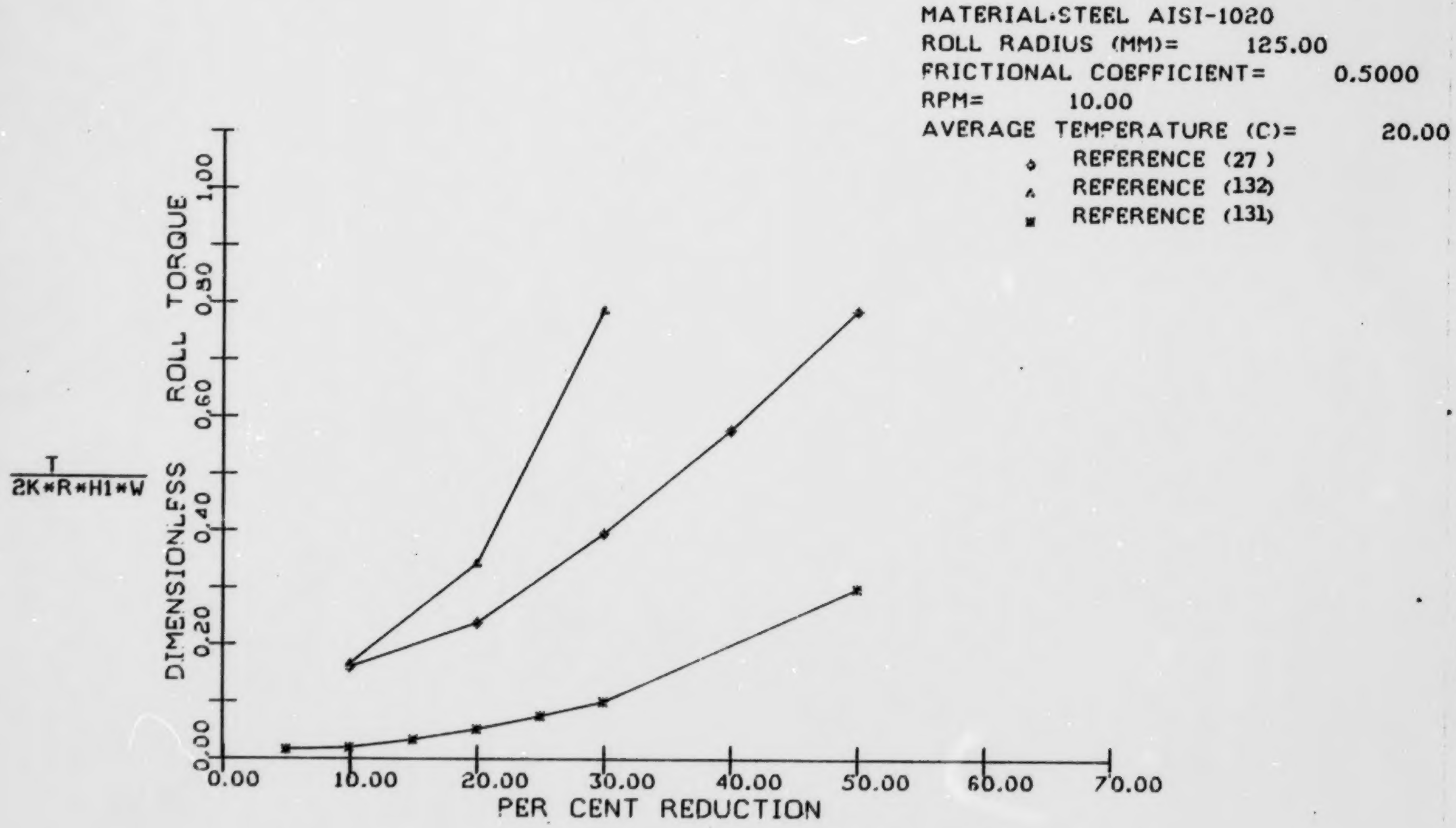
MATERIAL:STEEL AISI-1020
ROLL RADIUS (MM)= 125.00
FRICTIONAL COEFFICIENT= 0.5000
RPM= 10.00
AVERAGE TEMPERATURE (C)= 20.00
◆ REFERENCE (27)
▲ REFERENCE (132)
✱ REFERENCE (131)
T / 2K*R*H1*W
DIMENSIONLESS ROLL TORQUE
0.00
0.20
0.40
0.60
0.80
1.00
0.00
10.00
20.00
30.00
40.00
50.00
60.00
70.00
PER CENT REDUCTION

FIGURE 20

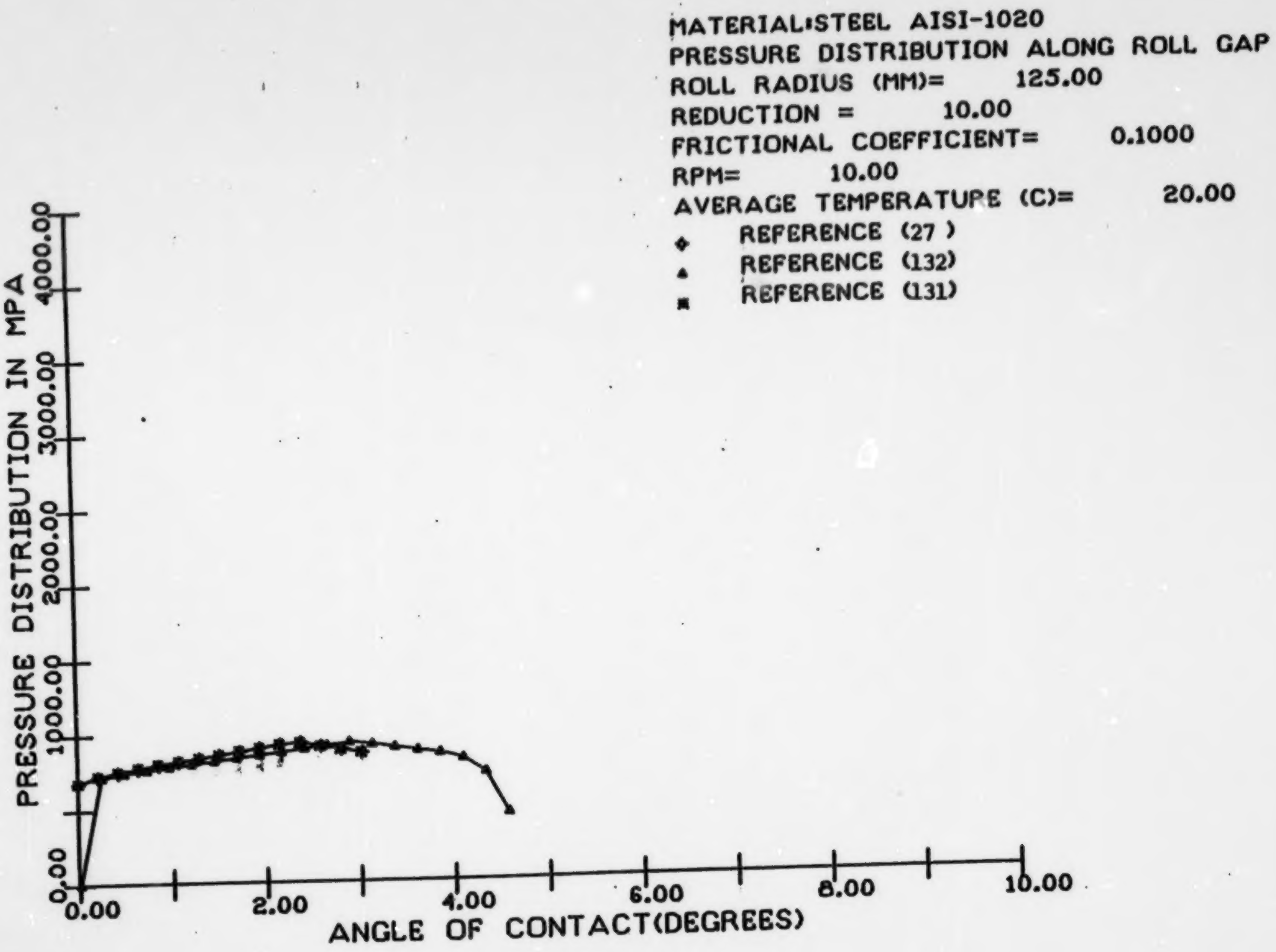
MATERIAL:STEEL AISI-1020
PRESSURE DISTRIBUTION ALONG ROLL GAP
ROLL RADIUS (MM)= 125.00
REDUCTION = 10.00
FRICTIONAL COEFFICIENT= 0.1000
RPM= 10.00
AVERAGE TEMPERATURE (C)= 20.00
◆ REFERENCE (27)
▲ REFERENCE (132)
■ REFERENCE (131)
PRESSURE DISTRIBUTION IN MPA
0.00
1000.00
2000.00
3000.00
4000.00
0.00
2.00
4.00
6.00
8.00
10.00
ANGLE OF CONTACT(DEGREES)

FIGURE 21

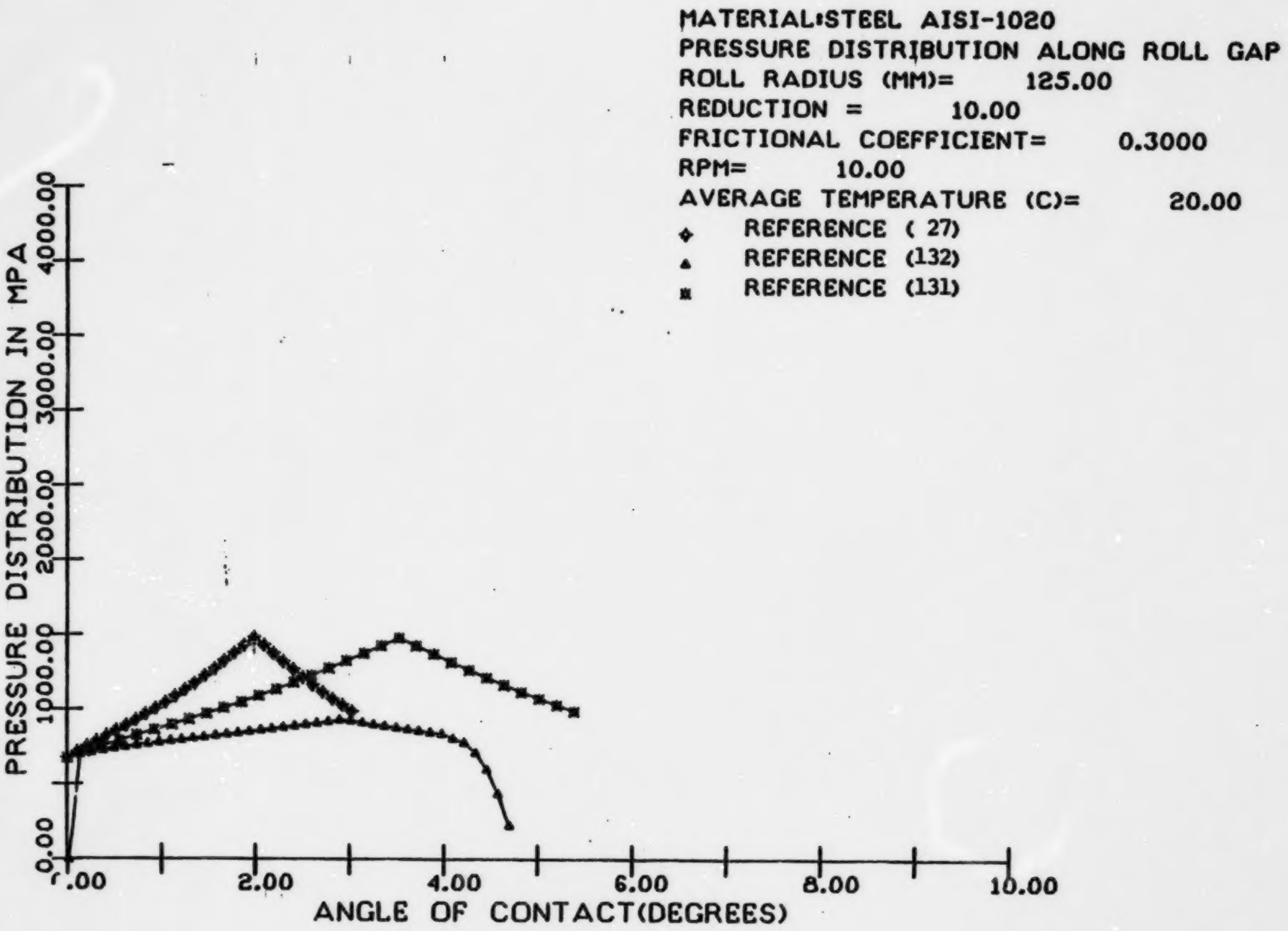
MATERIAL:STEEL AISI-1020
PRESSURE DISTRIBUTION ALONG ROLL GAP
ROLL RADIUS (MM)= 125.00
REDUCTION = 10.00
FRICTIONAL COEFFICIENT= 0.3000
RPM= 10.00
AVERAGE TEMPERATURE (C)= 20.00
◆ REFERENCE (27)
▲ REFERENCE (132)
✖ REFERENCE (131)
PRESSURE DISTRIBUTION IN MPA
0.00
1000.00
2000.00
3000.00
4000.00
.00
2.00
4.00
6.00
8.00
10.00
ANGLE OF CONTACT(DEGREES)

FIGURE 22

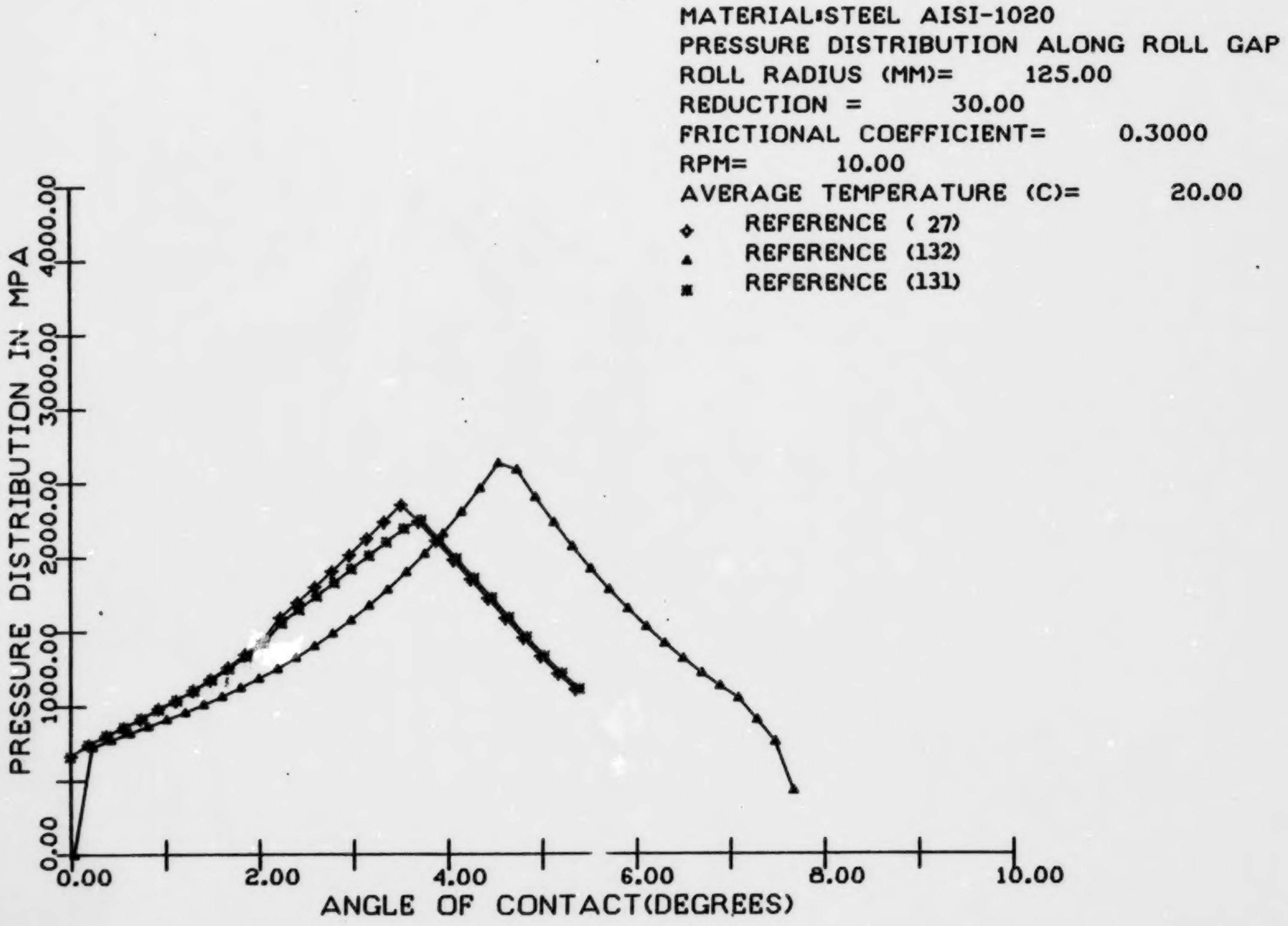
MATERIAL:STEEL AISI-1020
PRESSURE DISTRIBUTION ALONG ROLL GAP
ROLL RADIUS (MM)= 125.00
REDUCTION = 30.00
FRICTIONAL COEFFICIENT= 0.3000
RPM= 10.00
AVERAGE TEMPERATURE (C)= 20.00
◆ REFERENCE (27)
▲ REFERENCE (132)
✱ REFERENCE (131)
PRESSURE DISTRIBUTION IN MPA
0.00
1000.00
2000.00
3000.00
4000.00
0.00
2.00
4.00
6.00
8.00
10.00
ANGLE OF CONTACT(DEGREES)

FIGURE 23

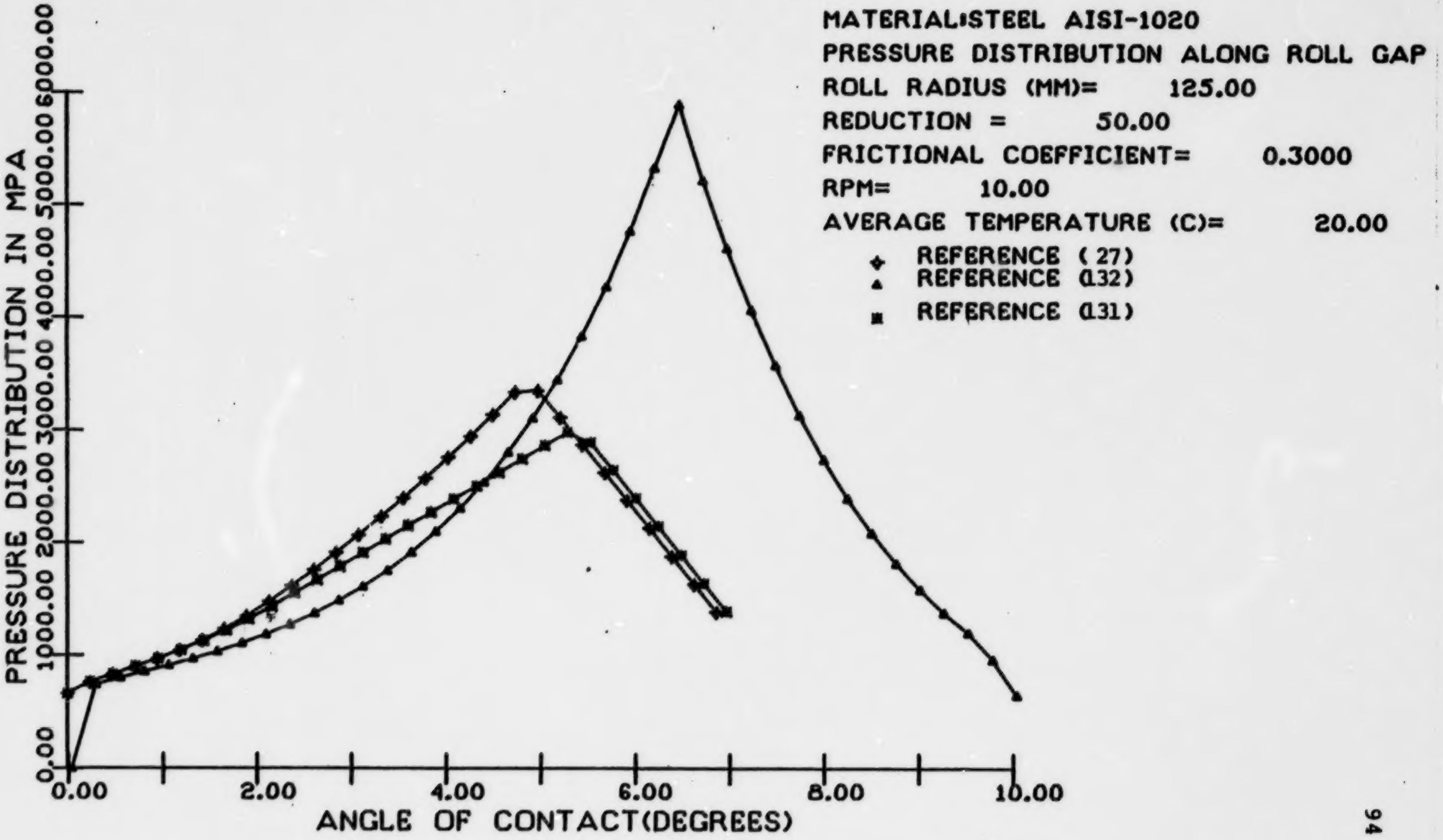
MATERIAL:STEEL AISI-1020
PRESSURE DISTRIBUTION ALONG ROLL GAP
ROLL RADIUS (MM)= 125.00
REDUCTION = 50.00
FRICTIONAL COEFFICIENT= 0.3000
RPM= 10.00
AVERAGE TEMPERATURE (C)= 20.00
✚ REFERENCE (27)
▲ REFERENCE (132)
■ REFERENCE (131)
PRESSURE DISTRIBUTION IN MPA
0.00
1000.00
2000.00
3000.00
4000.00
5000.00
6000.00
0.00
2.00
4.00
6.00
8.00
10.00
ANGLE OF CONTACT(DEGREES)

FIGURE 24

on the roll pressure is shown. It is observed that as the amount of reduction is increased, a steep pressure hill is formulated.

At low coefficients of friction, the pressure distributions of the three models tend to be similar.

Results: [$\mu = \mu(\theta)$]

This section describes the effect of the use of a coefficient of friction, varying along the roll gap, on the distribution of roll pressures in flat rolling. In previous discussions, evidence of the existence of non-constant friction stress to normal pressure ratios in the roll gap during cold rolling, was presented. As well, one of the causes of the non-convergence of traditional flat rolling calculations was identified as the friction hill which is a direct consequence of the assumption that the frictional coefficient remains constant. The effect of using a variable coefficient has also been referred to; not only do computations converge but the predictive capabilities of models may increase significantly.

Roll pressure distribution curves for various parameters are shown in Figure 25. In all of the plots, curves obtained using the traditional Amonton theory are compared to those obtained by assuming that the coefficient of friction changes algebraic sign--from positive at entry to negative at exit--somewhere along the roll gap. The location of the change--the "neutral point"--is now established by requiring that the exit boundary condition on the roll pressure be satisfied. Two curves are plotted in this fashion. Curves identified by #1 are obtained by allowing a reasonably fast change of the coefficient, while for curve #2 a somewhat smoother changeover is effected--see Figure 26.

It is observed that in both cases the roll pressure distribution changes in a significant manner. Specifically it is to be noted that the magnitudes of the peak pressures are reduced. This aids the convergence of the iterations when variable frictional coefficients are used. Figures 27 and 28 show the corresponding roll force and roll torque values.

Roll pressures, forces and torques - hot rolling

In this section, the results of calculations obtained in comparing the hot rolling theories of Orowan [27], Sims [25] and Ford and Alexander [26] are described. In performing these calculations, a low carbon steel(AISI 1020) is used and Shida's flow strength formulation [94] is employed to compute the flow strength. A two high rolling mill with 250 mm rolls is used in the study; two speeds--40 and 100 rpm--are considered and as Alexander [28] recommends, the existence of sticking friction is assumed.

Results:.

Flow curves for the AISI 1020 steel, as predicted

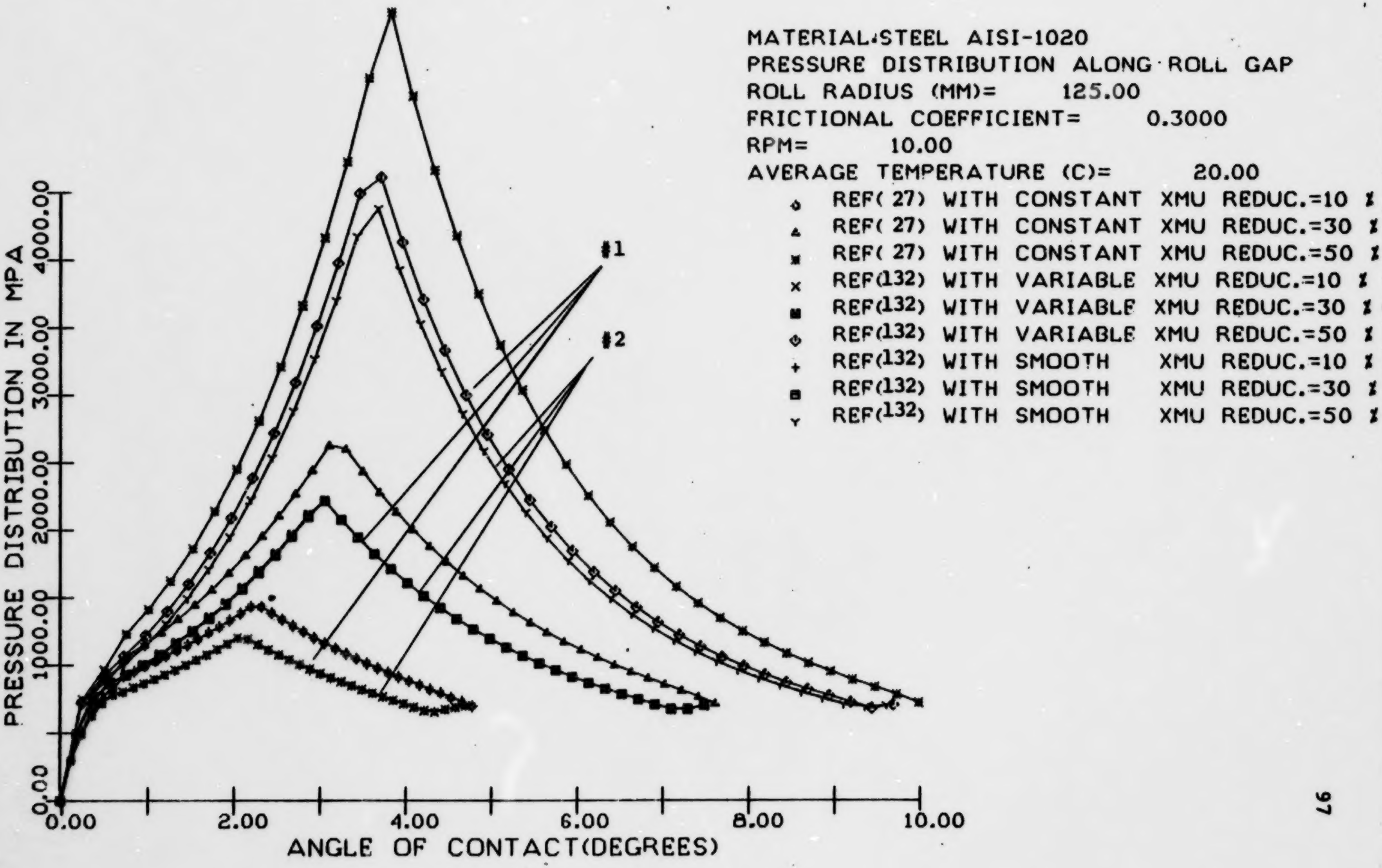
MATERIAL:STEEL AISI-1020
PRESSURE DISTRIBUTION ALONG ROLL GAP
ROLL RADIUS (MM)= 125.00
FRICTIONAL COEFFICIENT= 0.3000
RPM= 10.00
AVERAGE TEMPERATURE (C)= 20.00
REF(27) WITH CONSTANT XMU REDUC.=10 %
REF(27) WITH CONSTANT XMU REDUC.=30 %
REF(27) WITH CONSTANT XMU REDUC.=50 %
REF(132) WITH VARIABLE XMU REDUC.=10 %
REF(132) WITH VARIABLE XMU REDUC.=30 %
REF(132) WITH VARIABLE XMU REDUC.=50 %
REF(132) WITH SMOOTH XMU REDUC.=10 %
REF(132) WITH SMOOTH XMU REDUC.=30 %
REF(132) WITH SMOOTH XMU REDUC.=50 %
#1
#2
PRESSURE DISTRIBUTION IN MPA
0.00
1000.00
2000.00
3000.00
4000.00
ANGLE OF CONTACT(DEGREES)
0.00
2.00
4.00
6.00
8.00
10.00

FIGURE 25

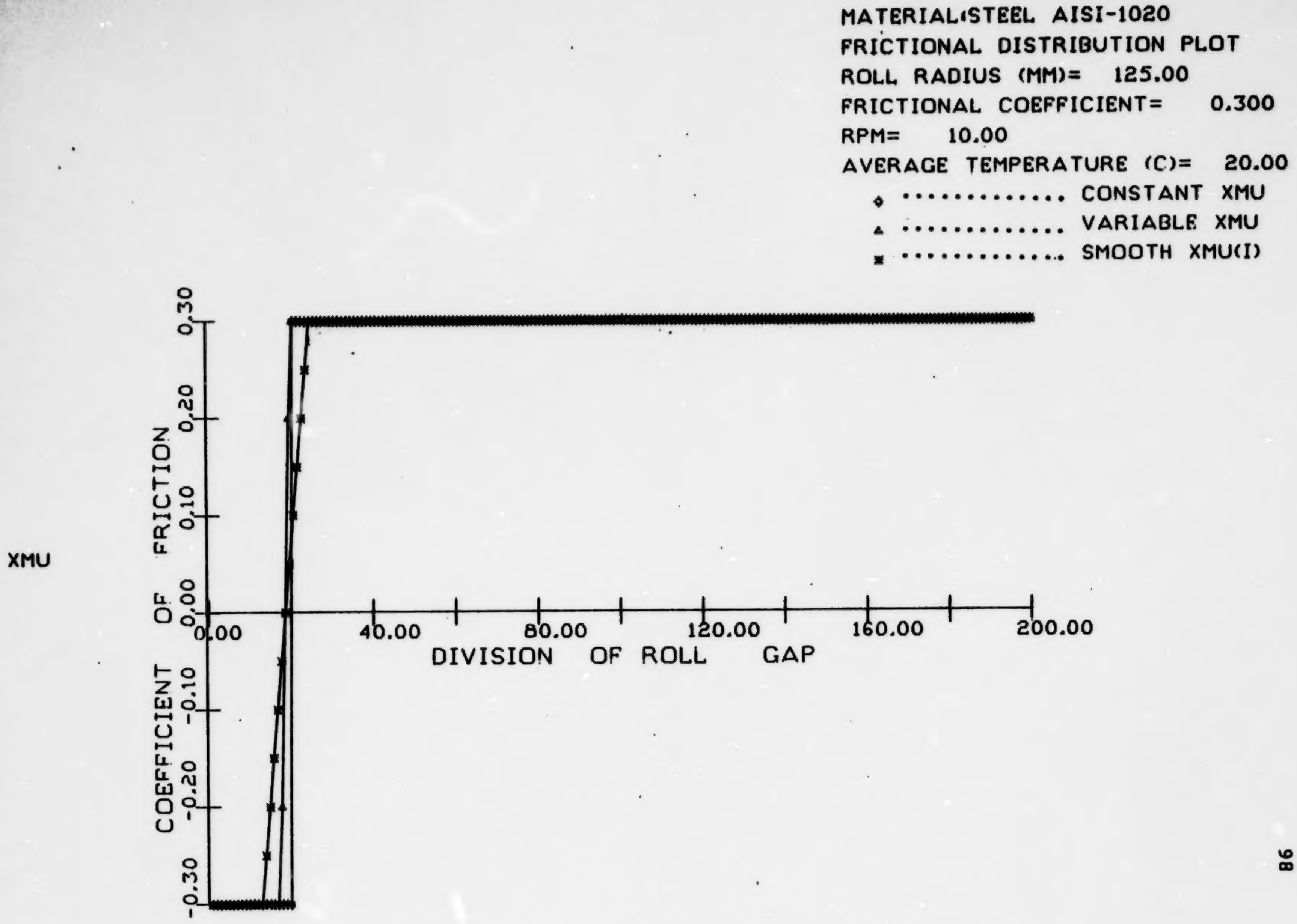
MATERIAL:STEEL AISI-1020
FRICTIONAL DISTRIBUTION PLOT
ROLL RADIUS (MM)= 125.00
FRICTIONAL COEFFICIENT= 0.300
RPM= 10.00
AVERAGE TEMPERATURE (C)= 20.00
◇ .... CONSTANT XMU
△ .... VARIABLE XMU
✱ .... SMOOTH XMU(I)
XMU
COEFFICIENT OF FRICTION
0.30
0.20
0.10
0.00
-0.10
-0.20
-0.30
0.00
40.00
80.00
120.00
160.00
200.00
DIVISION OF ROLL GAP

FIGURE 26

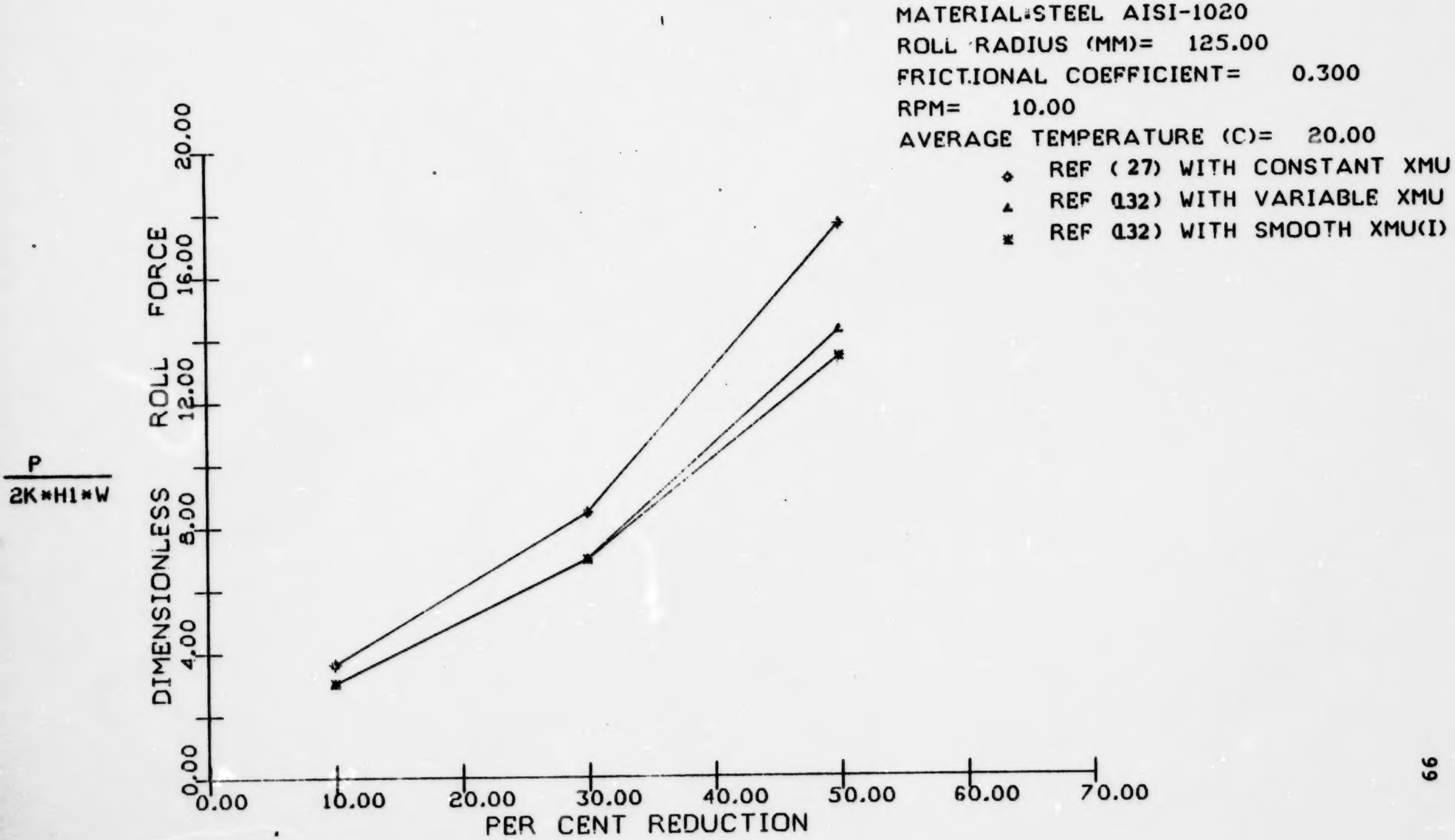
MATERIAL:STEEL AISI-1020
ROLL RADIUS (MM)= 125.00
FRICTIONAL COEFFICIENT= 0.300
RPM= 10.00
AVERAGE TEMPERATURE (C)= 20.00
◇ REF (27) WITH CONSTANT XMU
▲ REF (132) WITH VARIABLE XMU
✱ REF (132) WITH SMOOTH XMU(I)
P / 2K*H1*W
DIMENSIONLESS ROLL FORCE
0.00
4.00
8.00
12.00
16.00
20.00
0.00
10.00
20.00
30.00
40.00
50.00
60.00
70.00
PER CENT REDUCTION

FIGURE 27

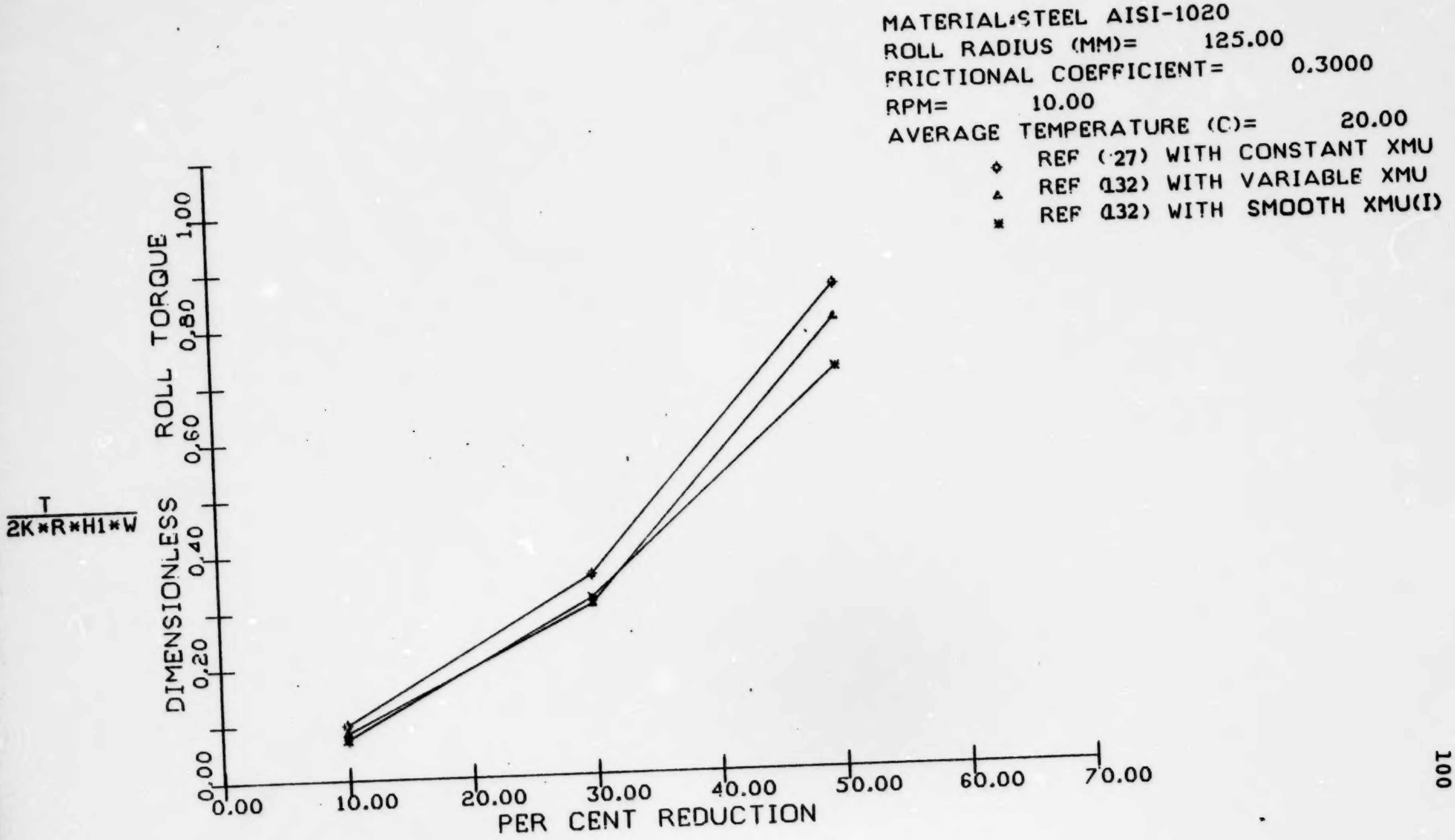
MATERIAL:STEEL AISI-1020
ROLL RADIUS (MM)= 125.00
FRICTIONAL COEFFICIENT= 0.3000
RPM= 10.00
AVERAGE TEMPERATURE (C)= 20.00
◇ REF (27) WITH CONSTANT XMU
△ REF (132) WITH VARIABLE XMU
✱ REF (132) WITH SMOOTH XMU(I)
T / 2K*R*H1*W
DIMENSIONLESS ROLL TORQUE
0.00
0.20
0.40
0.60
0.80
1.00
0.00
10.00
20.00
30.00
40.00
50.00
60.00
70.00
PER CENT REDUCTION

FIGURE 28

by Shida's formulation, are given in Figure 29--see Chapter 6. Three temperatures (880°C, 950°C and 1200°C) and two sets of strain rates (10.0/s and 50.5/s) are considered.

Typical roll pressure distributions given by Orowan's and Sims' theory are shown in Figure 30 for 880°C and for 1200°C. As in the previously considered cases of cold rolling, sharp pressure peaks, whose locations coincide with the locations of zero interfacial shear, are obtained.

Nondimensional separating forces and roll torques versus functions of % reduction, as calculated by the three theories considered are shown in Figures 31 to 38. As above, temperatures are taken to be 880°C, 950°C and 1200°C; roll rpm at 40 and 100. It is observed that the predictions of the three theories vary broadly. The largest values for both force and torque are given in the Ford and Alexander theory. The values given by Sims' and Orowan's theory are in reasonable agreement for both roll force and roll torque predictions.

Note that in the calculations the entry thickness (h_1) was taken as 5 mm. The values of the mean flow strength (2k) are given below:

Temperature (C)	Mean Flow Strength (MPA)	
880	32.5	
950	24.8	40 rpm
1200	11.5	
880	35.8	
950	27.6	100 rpm
1200	13.2	

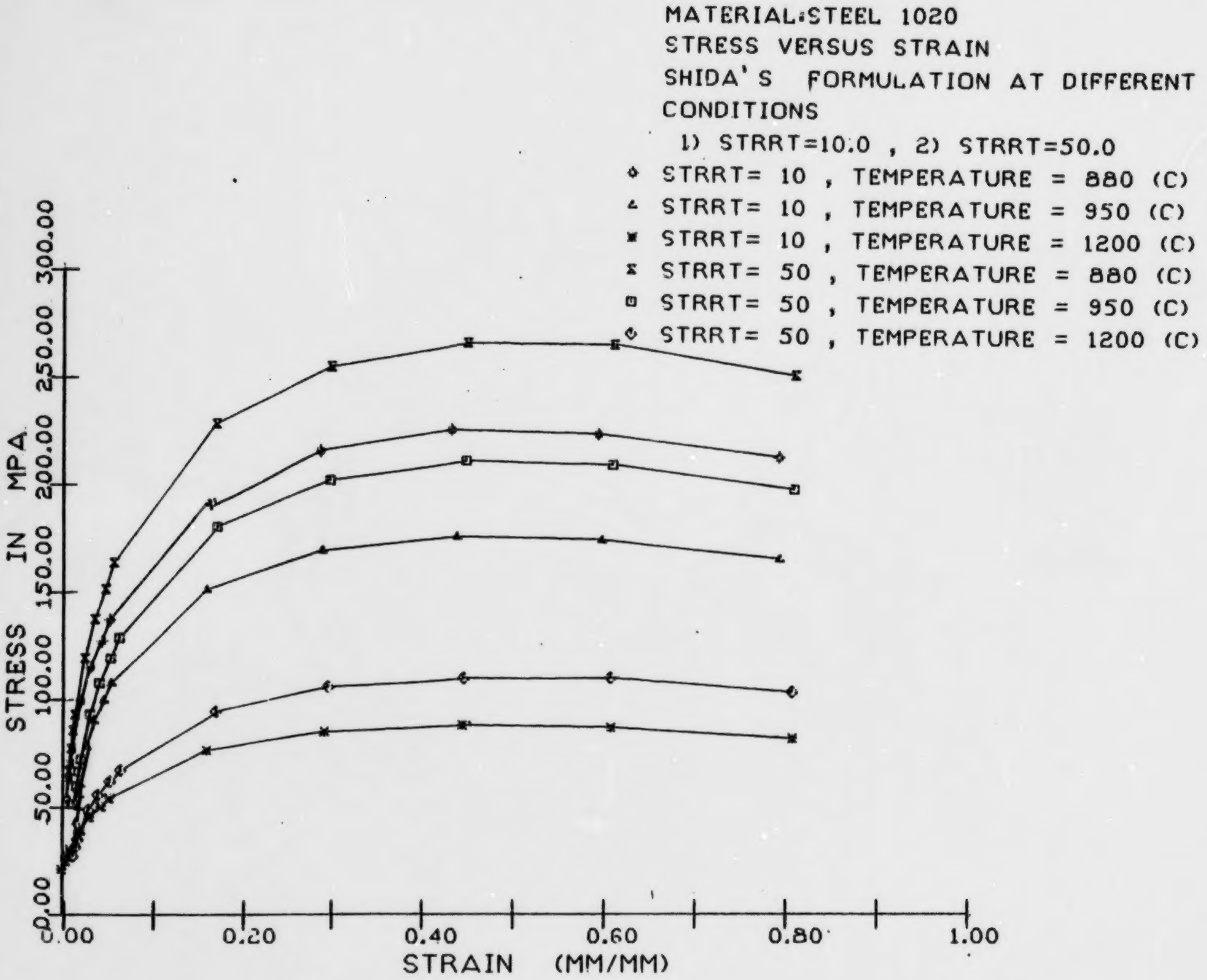
MATERIAL:STEEL 1020
STRESS VERSUS STRAIN
SHIDA'S FORMULATION AT DIFFERENT CONDITIONS
1) STRRT=10.0 , 2) STRRT=50.0
◇ STRRT= 10 , TEMPERATURE = 880 (C)
△ STRRT= 10 , TEMPERATURE = 950 (C)
✱ STRRT= 10 , TEMPERATURE = 1200 (C)
⧗ STRRT= 50 , TEMPERATURE = 880 (C)
□ STRRT= 50 , TEMPERATURE = 950 (C)
◈ STRRT= 50 , TEMPERATURE = 1200 (C)
STRESS IN MPA
0.00
50.00
100.00
150.00
200.00
250.00
300.00
0.00
0.20
0.40
0.60
0.80
1.00
STRAIN (MM/MM)

FIGURE 29

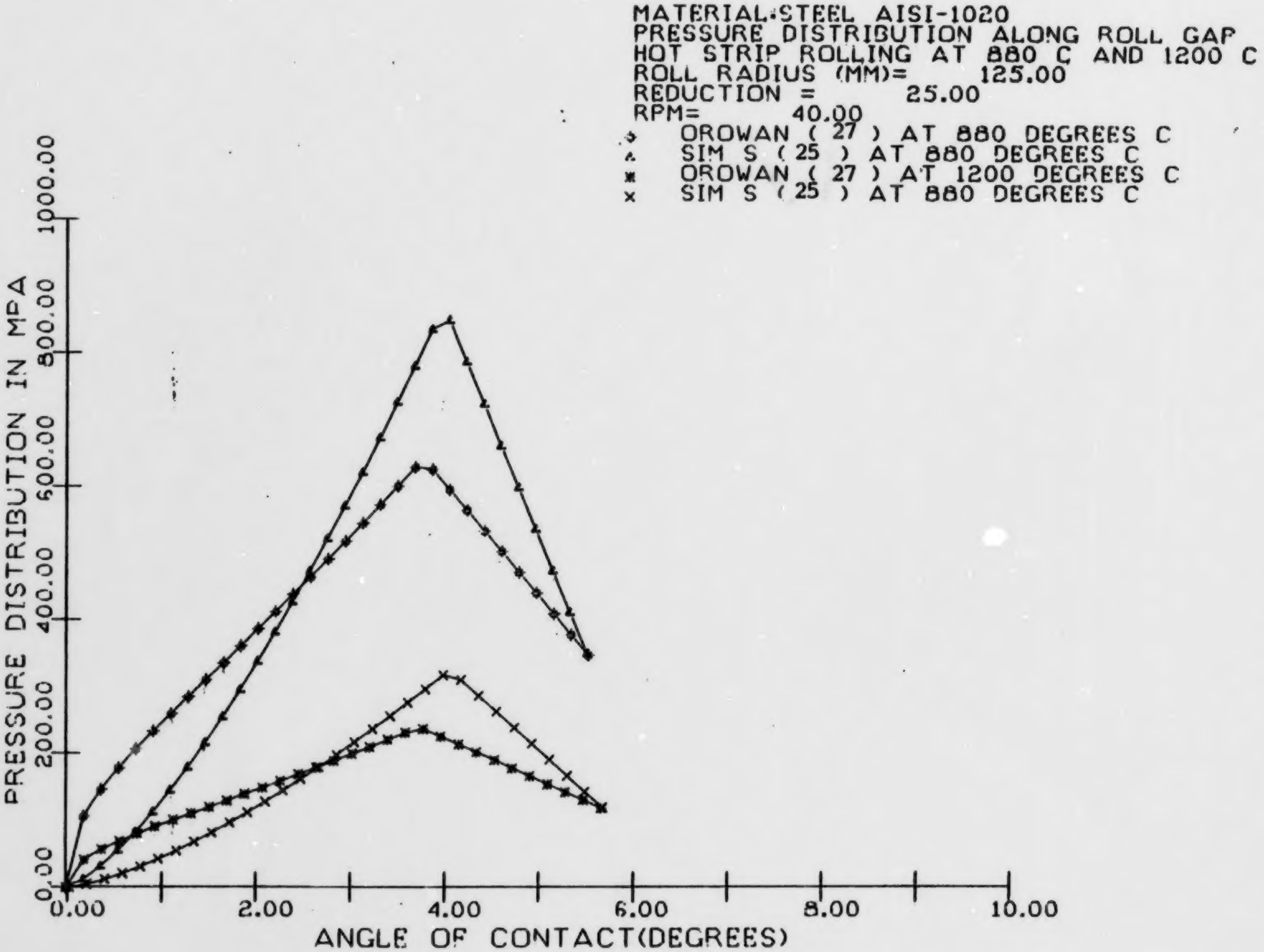
MATERIAL:STEEL AISI-1020
PRESSURE DISTRIBUTION ALONG ROLL GAP
HOT STRIP ROLLING AT 880 C AND 1200 C
ROLL RADIUS (MM)= 125.00
REDUCTION = 25.00
RPM= 40.00
◆ OROWAN (27) AT 880 DEGREES C
▲ SIM S (25) AT 880 DEGREES C
✱ OROWAN (27) AT 1200 DEGREES C
× SIM S (25) AT 880 DEGREES C
PRESSURE DISTRIBUTION IN MPA
0.00
200.00
400.00
600.00
800.00
1000.00
0.00
2.00
4.00
6.00
8.00
10.00
ANGLE OF CONTACT(DEGREES)

FIGURE 30

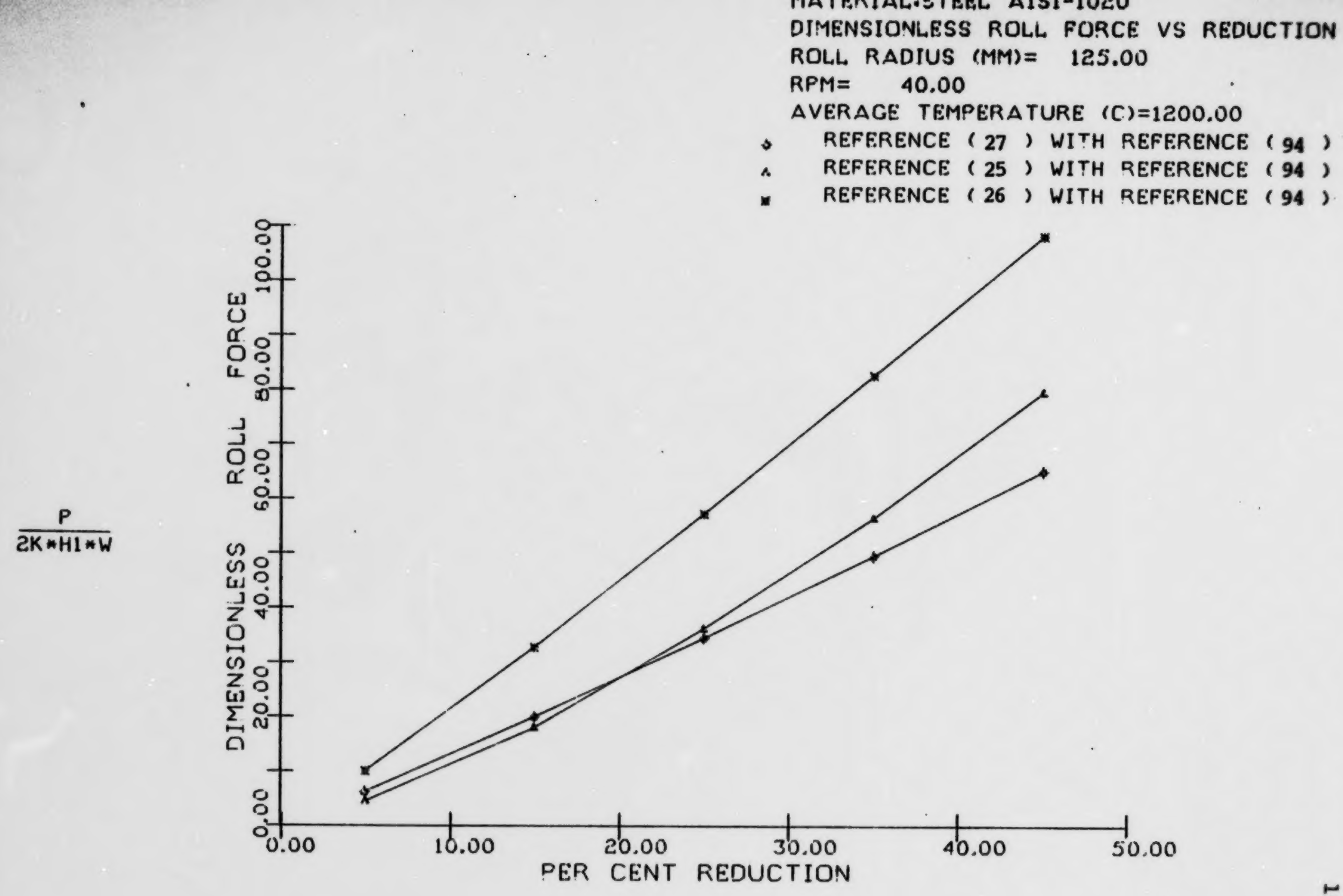
MATERIAL:STEEL AISI-1020
DIMENSIONLESS ROLL FORCE VS REDUCTION
ROLL RADIUS (MM)= 125.00
RPM= 40.00
AVERAGE TEMPERATURE (C)=1200.00
REFERENCE (27) WITH REFERENCE (94)
REFERENCE (25) WITH REFERENCE (94)
REFERENCE (26) WITH REFERENCE (94)
$\frac{P}{2K*H1*W}$
DIMENSIONLESS ROLL FORCE
0.00
20.00
40.00
60.00
80.00
100.00
0.00
10.00
20.00
30.00
40.00
50.00
PER CENT REDUCTION

FIGURE 31

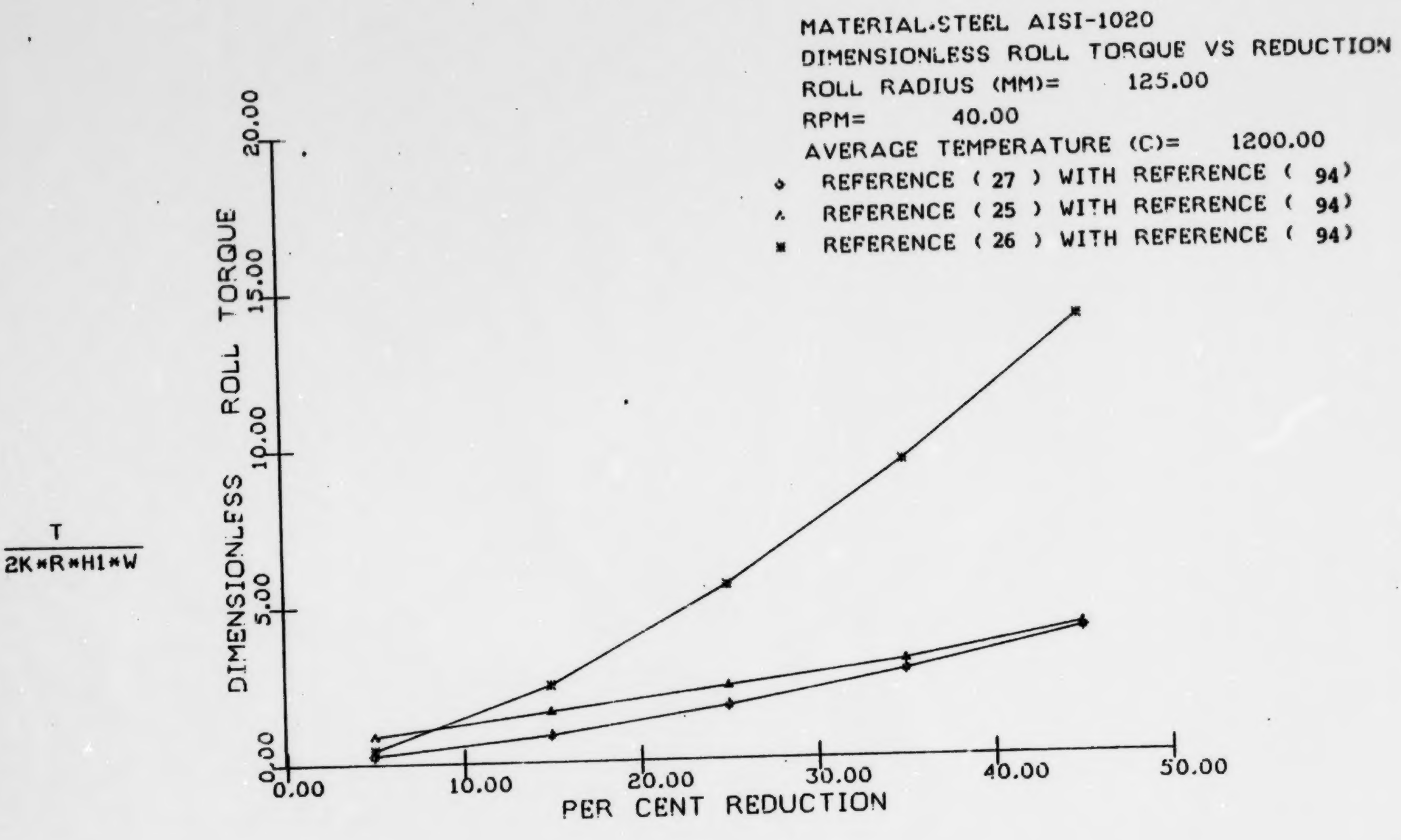
MATERIAL-STEEL AISI-1020
DIMENSIONLESS ROLL TORQUE VS REDUCTION
ROLL RADIUS (MM)= 125.00
RPM= 40.00
AVERAGE TEMPERATURE (C)= 1200.00
◆ REFERENCE (27) WITH REFERENCE (94)
▲ REFERENCE (25) WITH REFERENCE (94)
✱ REFERENCE (26) WITH REFERENCE (94)
T / 2K*R*H1*W
DIMENSIONLESS ROLL TORQUE
0.00
5.00
10.00
15.00
20.00
0.00
10.00
20.00
30.00
40.00
50.00
PER CENT REDUCTION

FIGURE 32

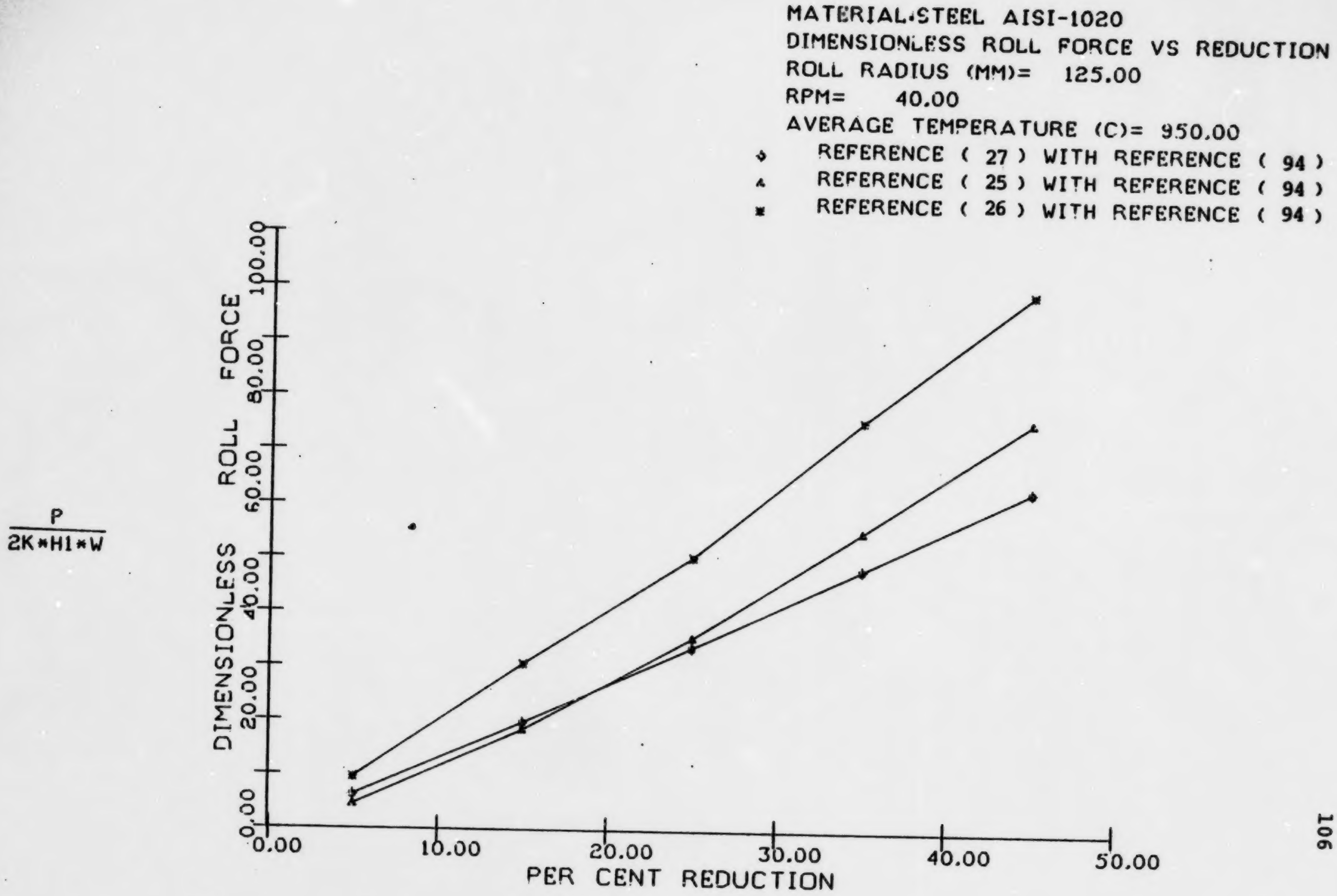
MATERIAL:STEEL AISI-1020
DIMENSIONLESS ROLL FORCE VS REDUCTION
ROLL RADIUS (MM)= 125.00
RPM= 40.00
AVERAGE TEMPERATURE (C)= 950.00
◆ REFERENCE (27) WITH REFERENCE (94)
▲ REFERENCE (25) WITH REFERENCE (94)
✱ REFERENCE (26) WITH REFERENCE (94)
$\frac{P}{2K*H1*W}$
DIMENSIONLESS ROLL FORCE
0.00
20.00
40.00
60.00
80.00
100.00
0.00
10.00
20.00
30.00
40.00
50.00
PER CENT REDUCTION

FIGURE 33

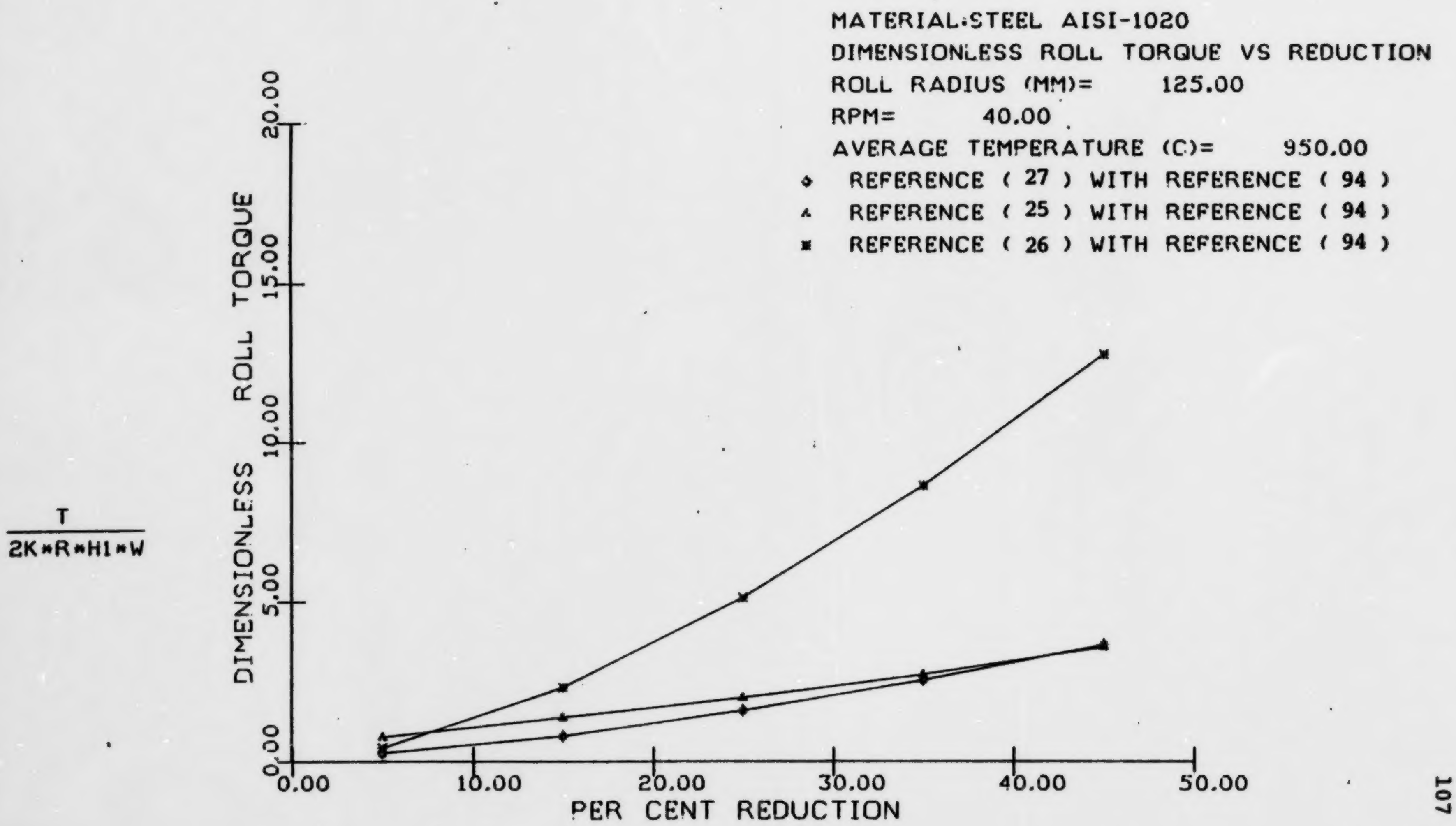
MATERIAL:STEEL AISI-1020
DIMENSIONLESS ROLL TORQUE VS REDUCTION
ROLL RADIUS (MM)= 125.00
RPM= 40.00
AVERAGE TEMPERATURE (C)= 950.00
◆ REFERENCE (27) WITH REFERENCE (94)
▲ REFERENCE (25) WITH REFERENCE (94)
✱ REFERENCE (26) WITH REFERENCE (94)
T / 2K*R*H1*W
DIMENSIONLESS ROLL TORQUE
0.00
5.00
10.00
15.00
20.00
0.00
10.00
20.00
30.00
40.00
50.00
PER CENT REDUCTION

FIGURE 34

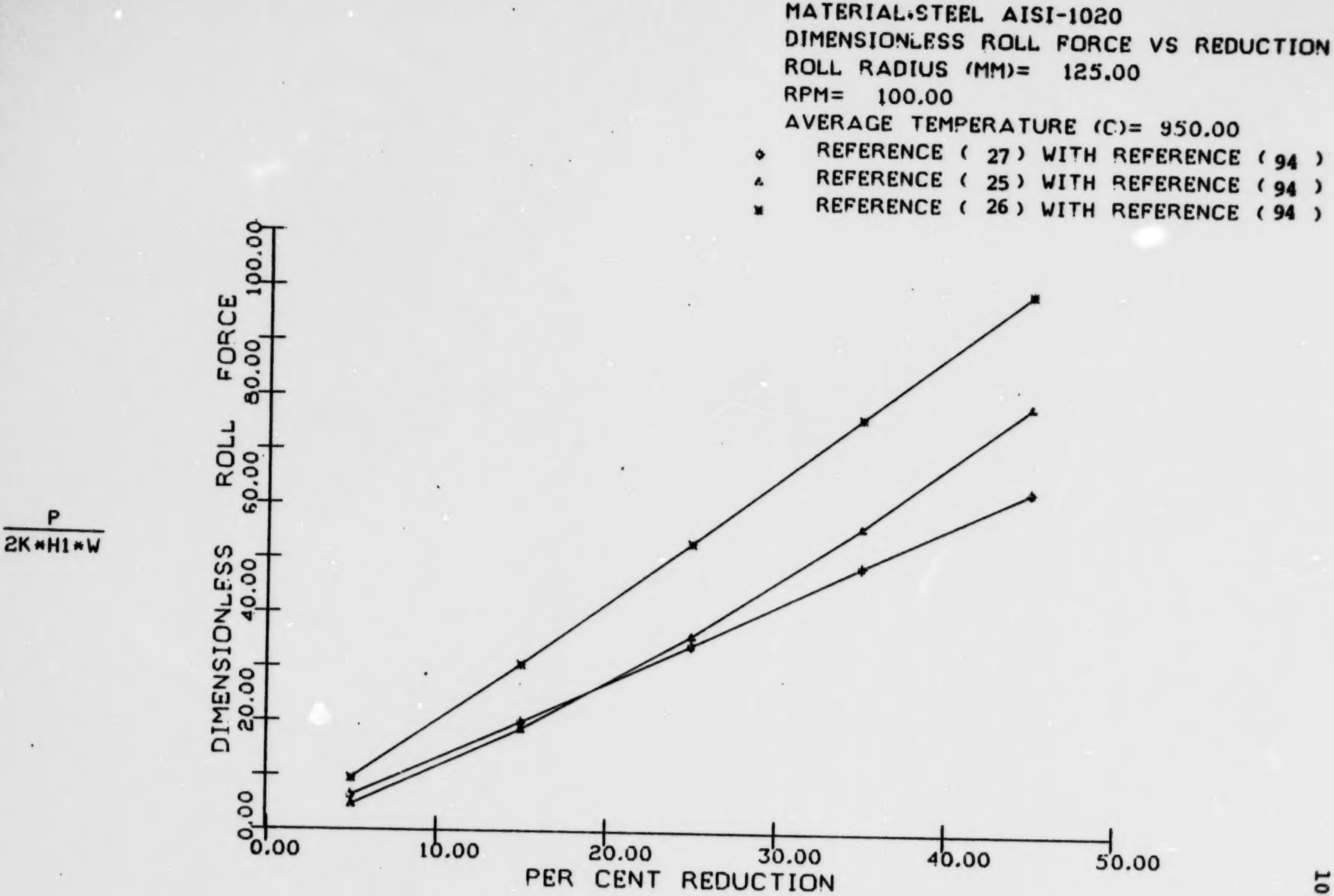
MATERIAL:STEEL AISI-1020
DIMENSIONLESS ROLL FORCE VS REDUCTION
ROLL RADIUS (MM)= 125.00
RPM= 100.00
AVERAGE TEMPERATURE (C)= 950.00
◆ REFERENCE (27) WITH REFERENCE (94)
▲ REFERENCE (25) WITH REFERENCE (94)
✱ REFERENCE (26) WITH REFERENCE (94)
$\frac{P}{2K*H1*W}$
DIMENSIONLESS ROLL FORCE
0.00
20.00
40.00
60.00
80.00
100.00
0.00
10.00
20.00
30.00
40.00
50.00
PER CENT REDUCTION

FIGURE 35

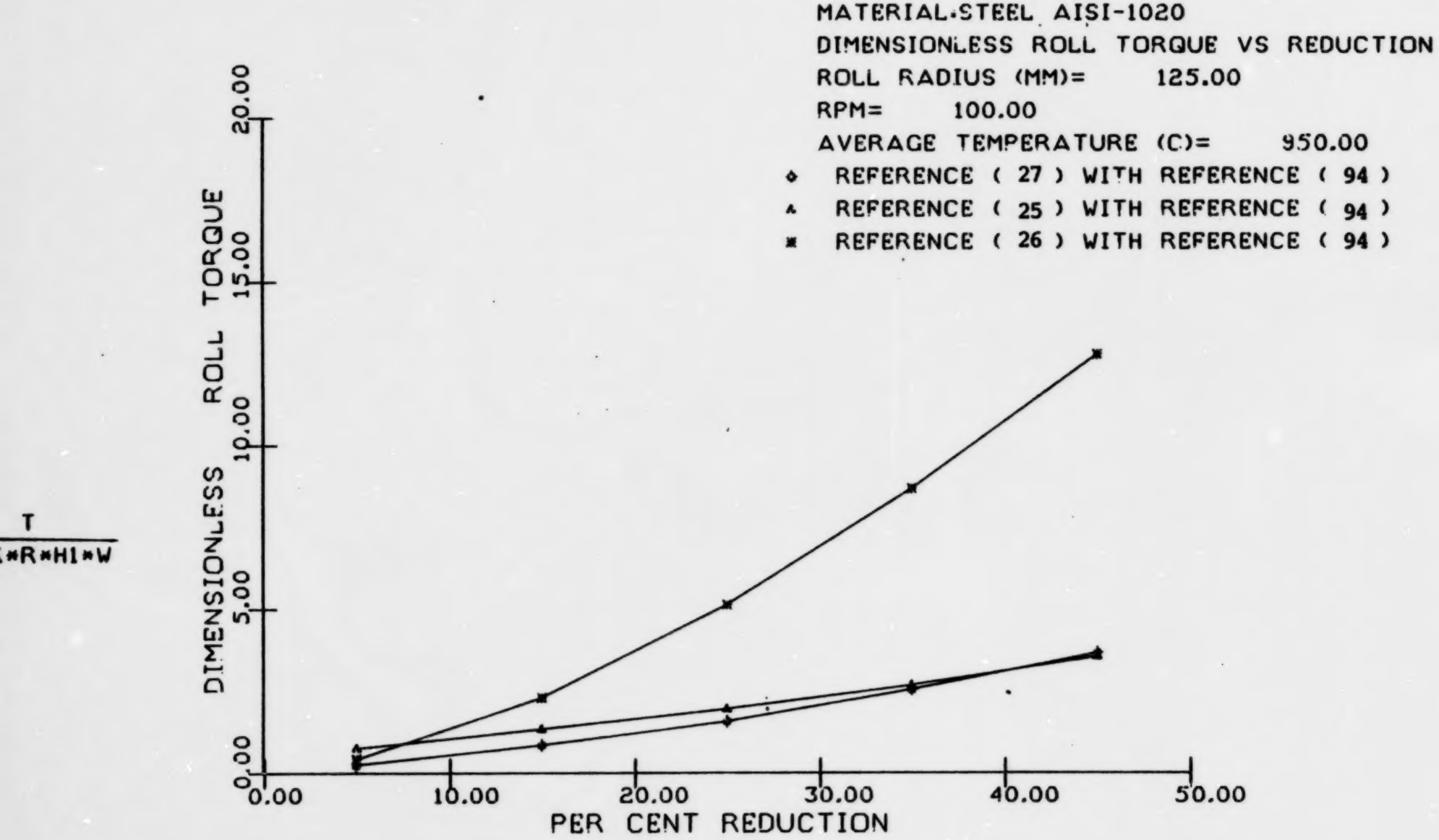
MATERIAL:STEEL AISI-1020
DIMENSIONLESS ROLL TORQUE VS REDUCTION
ROLL RADIUS (MM)= 125.00
RPM= 100.00
AVERAGE TEMPERATURE (C)= 950.00
◇ REFERENCE (27) WITH REFERENCE (94)
▵ REFERENCE (25) WITH REFERENCE (94)
✱ REFERENCE (26) WITH REFERENCE (94)
T
*R*H1*W
DIMENSIONLESS ROLL TORQUE
0.00
5.00
10.00
15.00
20.00
0.00
10.00
20.00
30.00
40.00
50.00
PER CENT REDUCTION

FIGURE 36

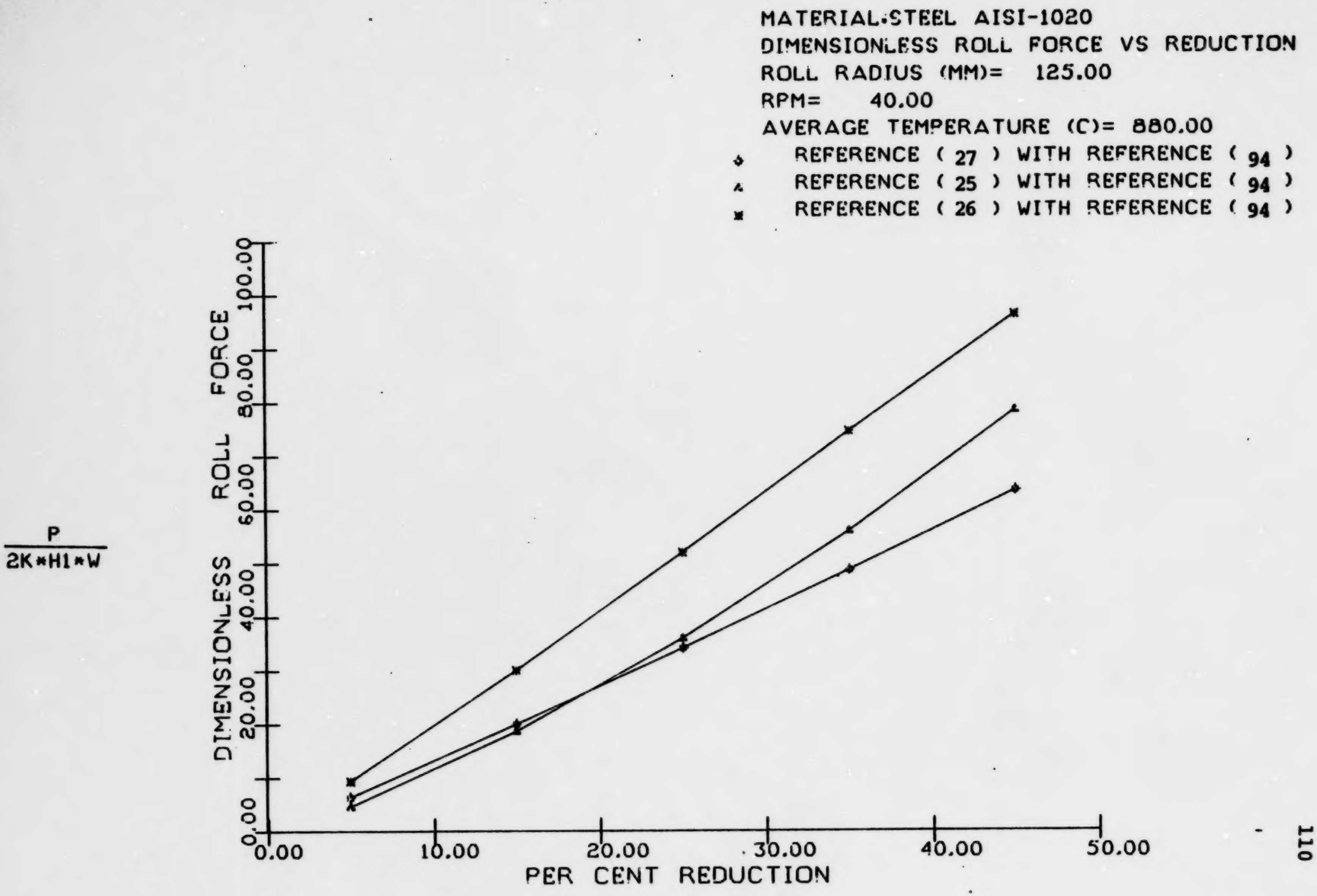
MATERIAL:STEEL AISI-1020
DIMENSIONLESS ROLL FORCE VS REDUCTION
ROLL RADIUS (MM)= 125.00
RPM= 40.00
AVERAGE TEMPERATURE (C)= 880.00
REFERENCE (27) WITH REFERENCE (94)
REFERENCE (25) WITH REFERENCE (94)
REFERENCE (26) WITH REFERENCE (94)
P / 2K*H1*W
DIMENSIONLESS ROLL FORCE
0.00
20.00
40.00
60.00
80.00
100.00
0.00
10.00
20.00
30.00
40.00
50.00
PER CENT REDUCTION

FIGURE 37

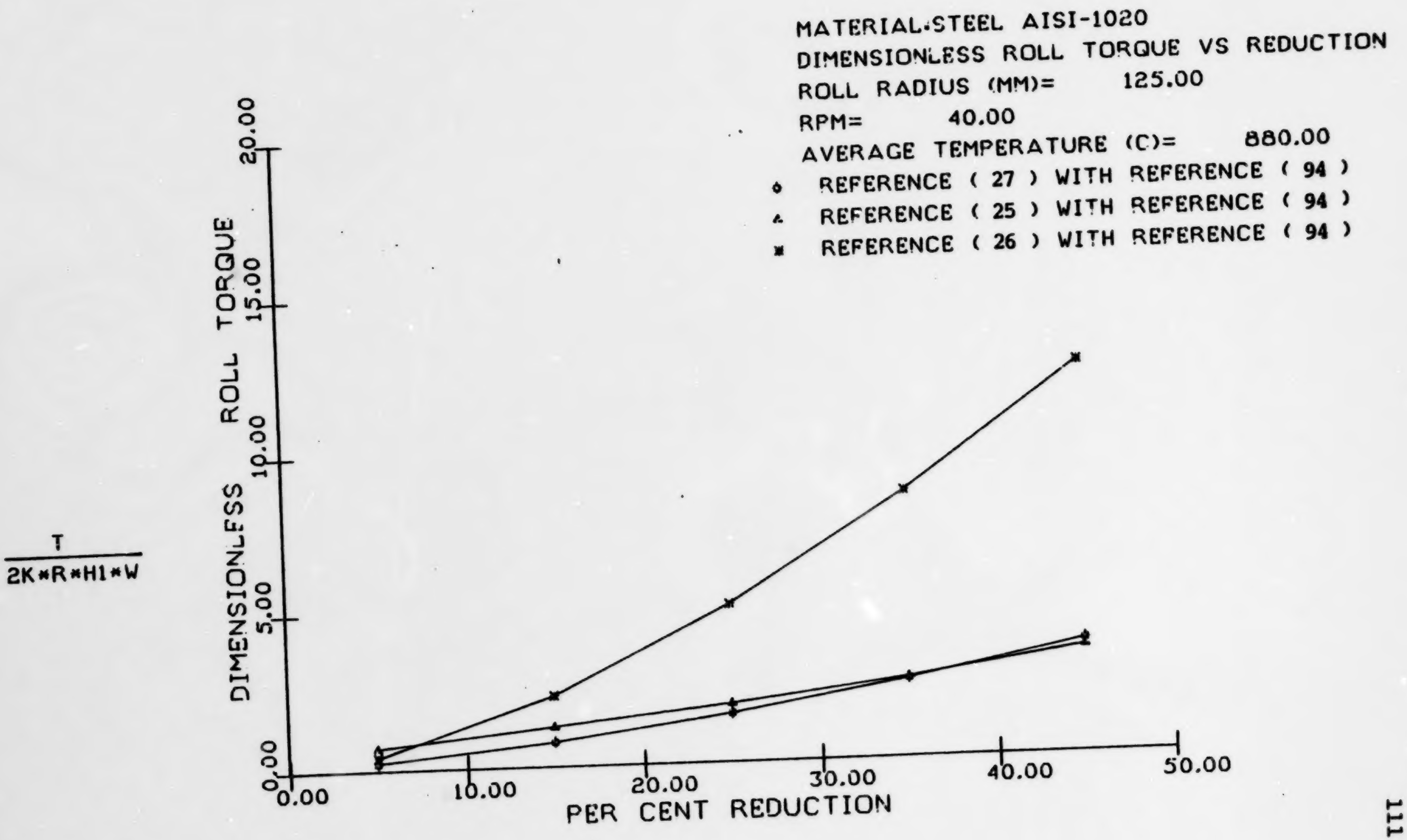
MATERIAL:STEEL AISI-1020
DIMENSIONLESS ROLL TORQUE VS REDUCTION
ROLL RADIUS (MM)= 125.00
RPM= 40.00
AVERAGE TEMPERATURE (C)= 880.00
◆ REFERENCE (27) WITH REFERENCE (94)
▲ REFERENCE (25) WITH REFERENCE (94)
✱ REFERENCE (26) WITH REFERENCE (94)
T / 2K*R*H1*W
DIMENSIONLESS ROLL TORQUE
0.00
5.00
10.00
15.00
20.00
0.00
10.00
20.00
30.00
40.00
50.00
PER CENT REDUCTION

FIGURE 38

In general, it is observed that the force predictions of Orowan are very close to that of Sims for reductions of less than 25%. Beyond that value, Orowan's predictions are below that of Sims'. Ford and Alexander's predictions are significantly higher--for both forces and torques--than Orowan's and Sims. The torque predictions of Orowan and Sims appear to be very close for all parameters.

Roll deformation

The results of calculations performed to predict the shape of a work roll under actual conditions are described in this section. Three mathematical models are employed. These are due to Orowan [27], Bland and Ford [131], and Roychoudhuri and Lenard [132]. References [27] and [131] employ Hitchcock's formula [138]; Reference [132] uses Michell's solution and Fourier expansions--see Chapter 5.

For the calculations, cold rolling of AISI 1020 steel is considered. The constitutive relations are taken as

$$\sigma = 593.50\ (1 + 78.3\,\varepsilon)^{0.067}\ \text{MPa};$$

the roll radius as 125 mm, and the entry thickness as 5 mm. The coefficient of friction and percent reduction are varied and roll countours are plotted.

Results:

Plots of deformed roll contours for the three models mentioned above are shown in Figures 39 to 46. In Figures 39 to 41, the deformed roll radius is plotted against the percentage reduction as predicted by References [27] and [131]. In Figures 42 and 43, the X and Y coordinates of the deformed roll for reductions of 10 and 30 percent are shown. In these Figures, all three models are compared. As well, the shape of a rigid roll is given. Finally, Figures 44 and 45 present the deformed X and Y contours as given by Reference [132]. Reductions of 10%, 30% and 50% are shown for a constant coefficient of friction of 0.3.

From Figures 39 to 41 it is clear that with a coefficient of friction of 0.1, the simplifying assumptions of Reference [131] do not affect the results and indeed their predicted radii are approximately the same as in [27]. However, as the coefficient of friction is increased, significant differences exist between the predictions of [27] and [131]. It should be mentioned that using Hitchcock'f formula, the deformed roll radius at low reductions is predicted to be larger than at intermediate reductions. At much higher reductions, the roll radius increases again.

A comparison of the predictions of the three cold

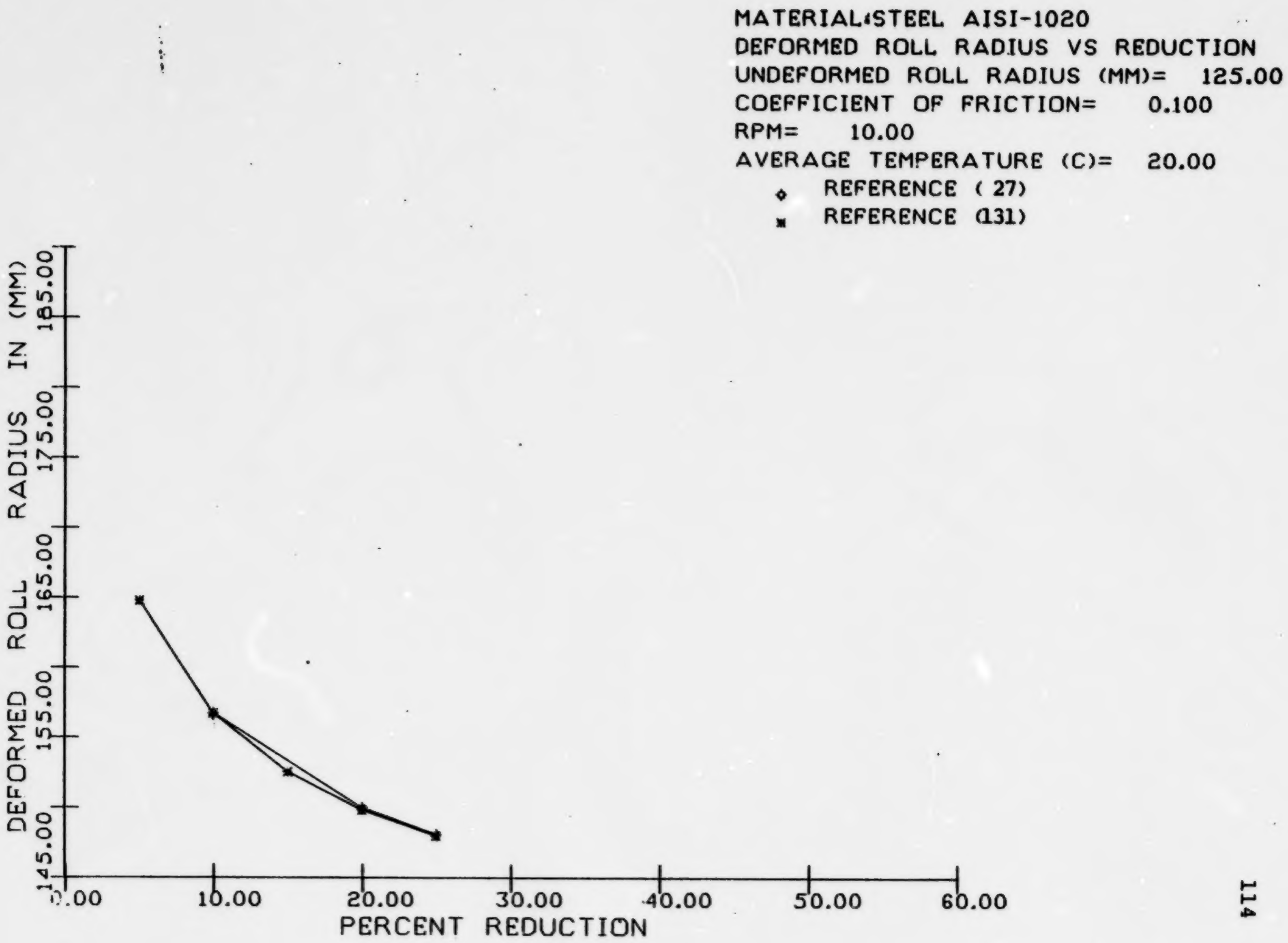
MATERIAL:STEEL AISI-1020
DEFORMED ROLL RADIUS VS REDUCTION
UNDEFORMED ROLL RADIUS (MM)= 125.00
COEFFICIENT OF FRICTION= 0.100
RPM= 10.00
AVERAGE TEMPERATURE (C)= 20.00
◇ REFERENCE (27)
✱ REFERENCE (131)
DEFORMED ROLL RADIUS IN (MM)
145.00
155.00
165.00
175.00
185.00
0.00
10.00
20.00
30.00
40.00
50.00
60.00
PERCENT REDUCTION

FIGURE 39

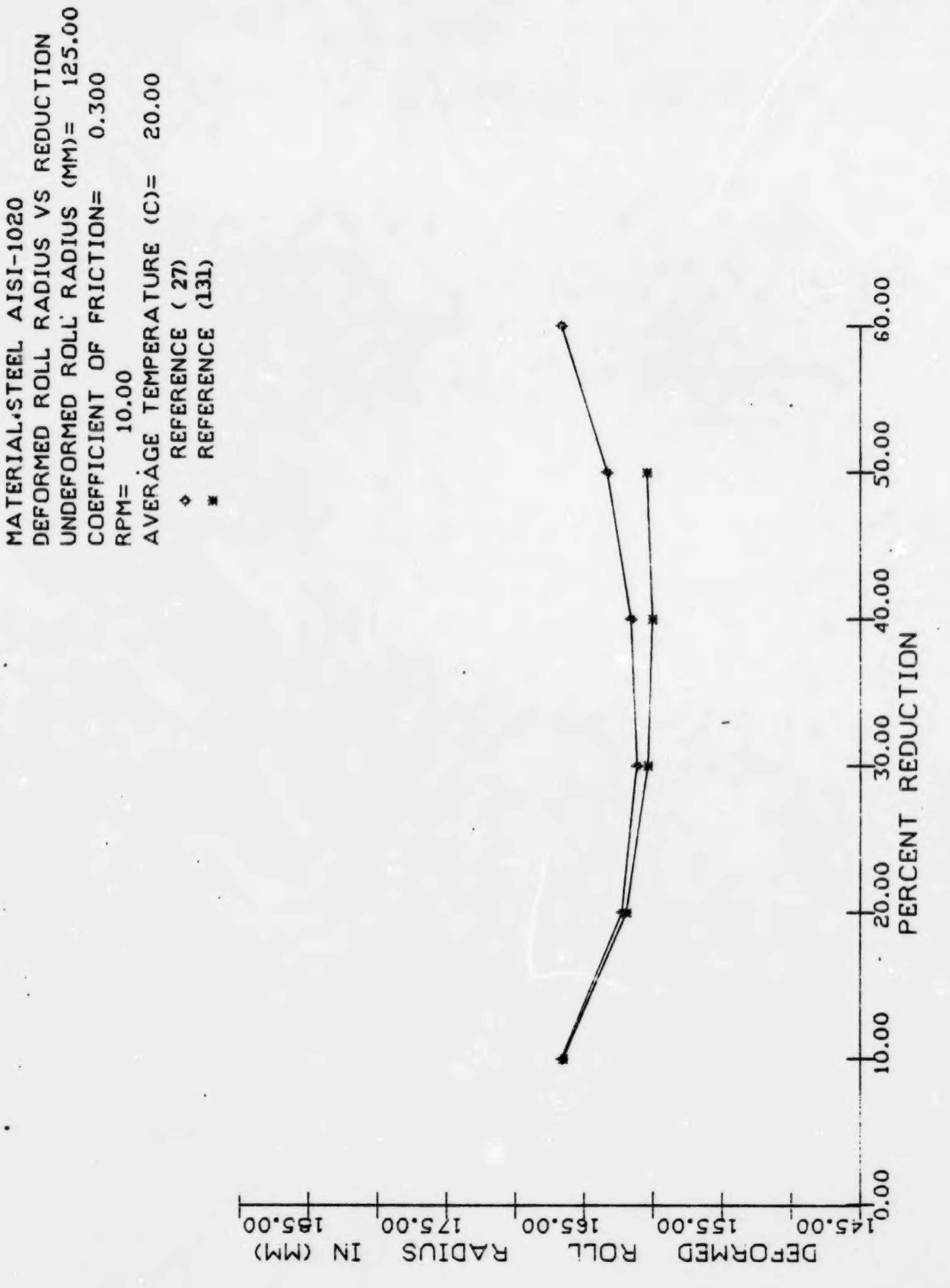
MATERIAL:STEEL AISI-1020
DEFORMED ROLL RADIUS VS REDUCTION
UNDEFORMED ROLL RADIUS (MM)= 125.00
COEFFICIENT OF FRICTION= 0.300
RPM= 10.00
AVERAGE TEMPERATURE (C)= 20.00
◆ REFERENCE (27)
✱ REFERENCE (131)
DEFORMED ROLL RADIUS IN (MM)
145.00
155.00
165.00
175.00
185.00
0.00
10.00
20.00
30.00
40.00
50.00
60.00
PERCENT REDUCTION

FIGURE 40

MATERIAL:STEEL AISI-1020
DEFORMED ROLL RADIUS VS REDUCTION
UNDEFORMED ROLL RADIUS (MM)= 125.00
COEFFICIENT OF FRICTION= 0.500
RPM= 10.00
AVERAGE TEMPERATURE (C)= 20.00
◆ REFERENCE (27)
✱ REFERENCE (31)

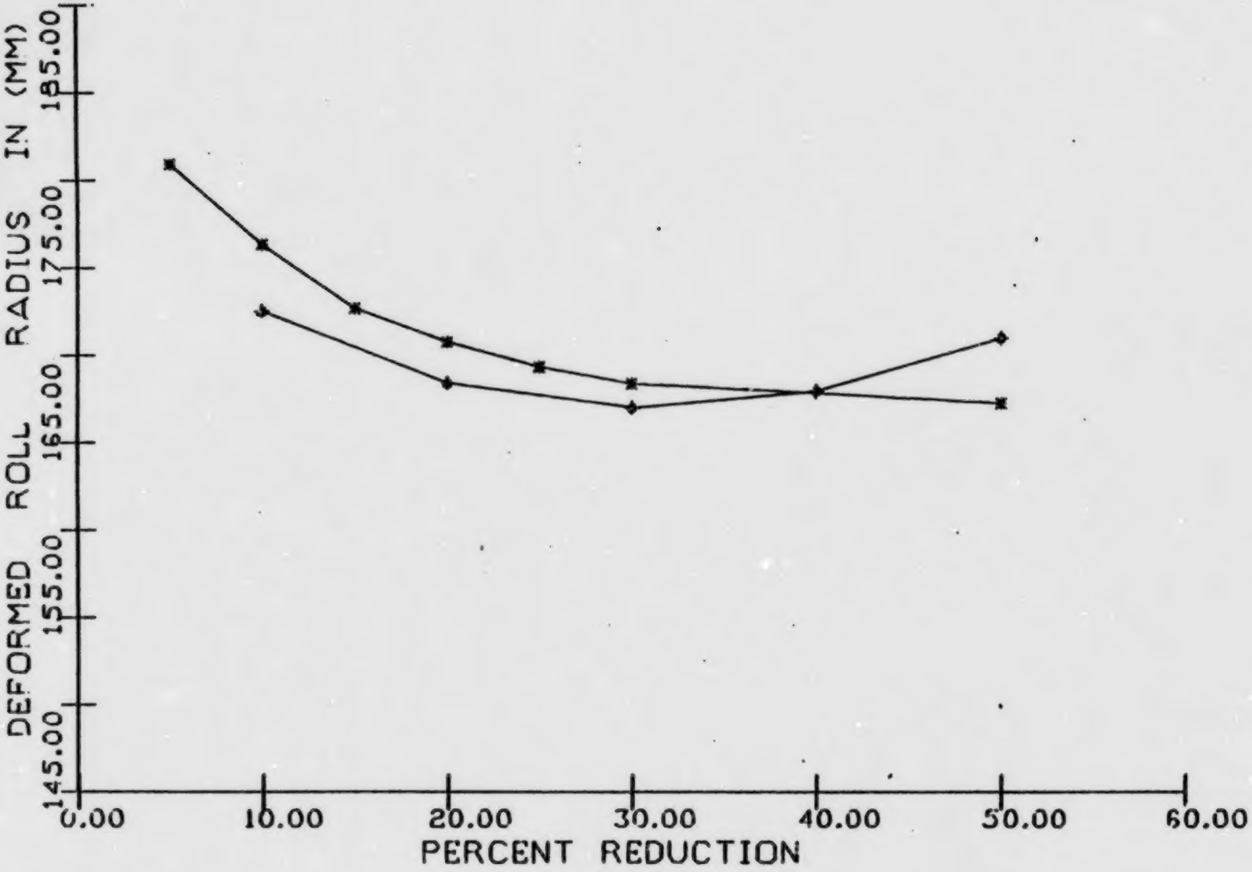

FIGURE 41

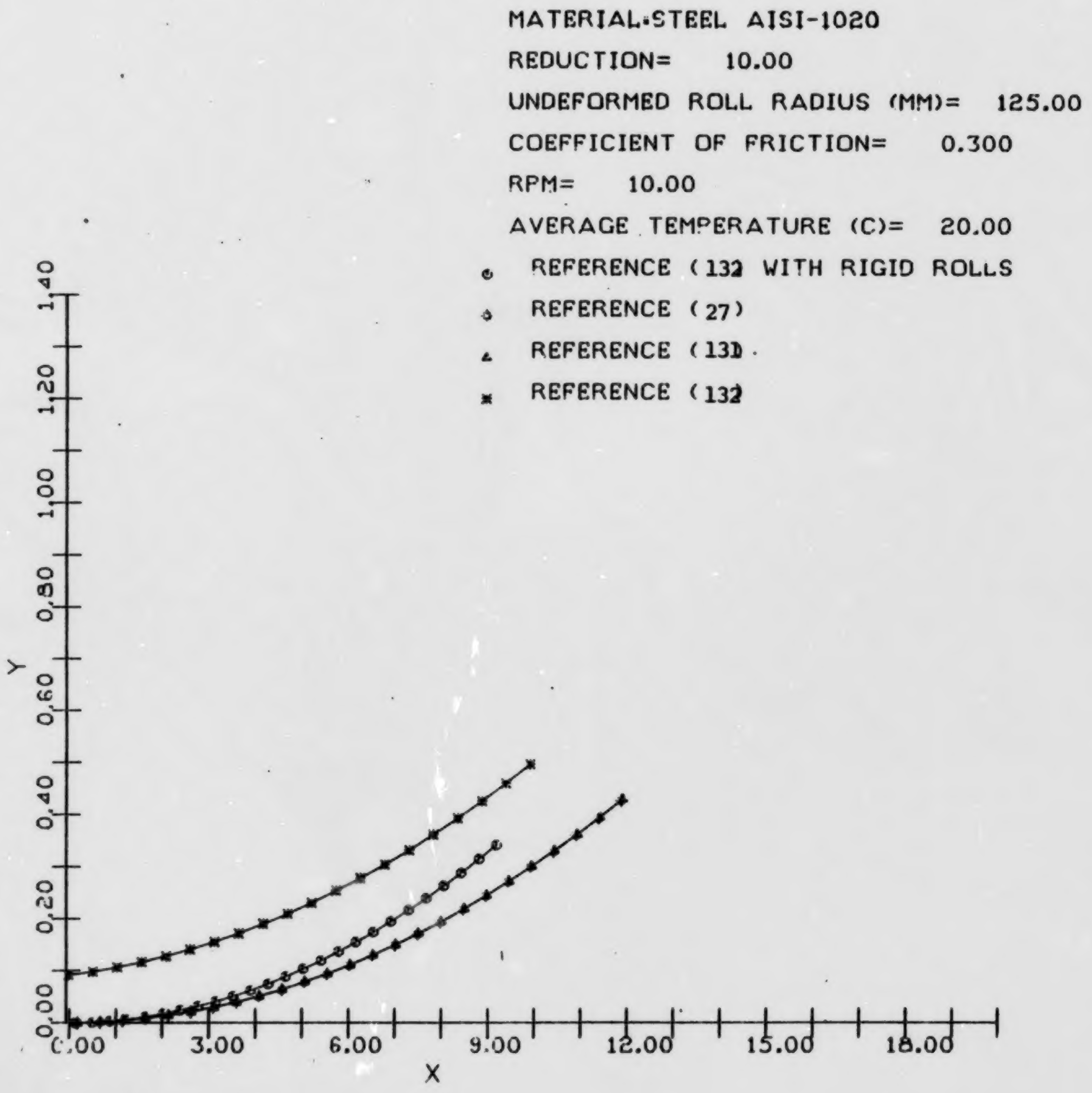
MATERIAL:STEEL AISI-1020
REDUCTION= 10.00
UNDEFORMED ROLL RADIUS (MM)= 125.00
COEFFICIENT OF FRICTION= 0.300
RPM= 10.00
AVERAGE TEMPERATURE (C)= 20.00
REFERENCE (132) WITH RIGID ROLLS
REFERENCE (27)
REFERENCE (131)
REFERENCE (132)
Y
0.00
0.20
0.40
0.60
0.80
1.00
1.20
1.40
X
0.00
3.00
6.00
9.00
12.00
15.00
18.00

FIGURE 42

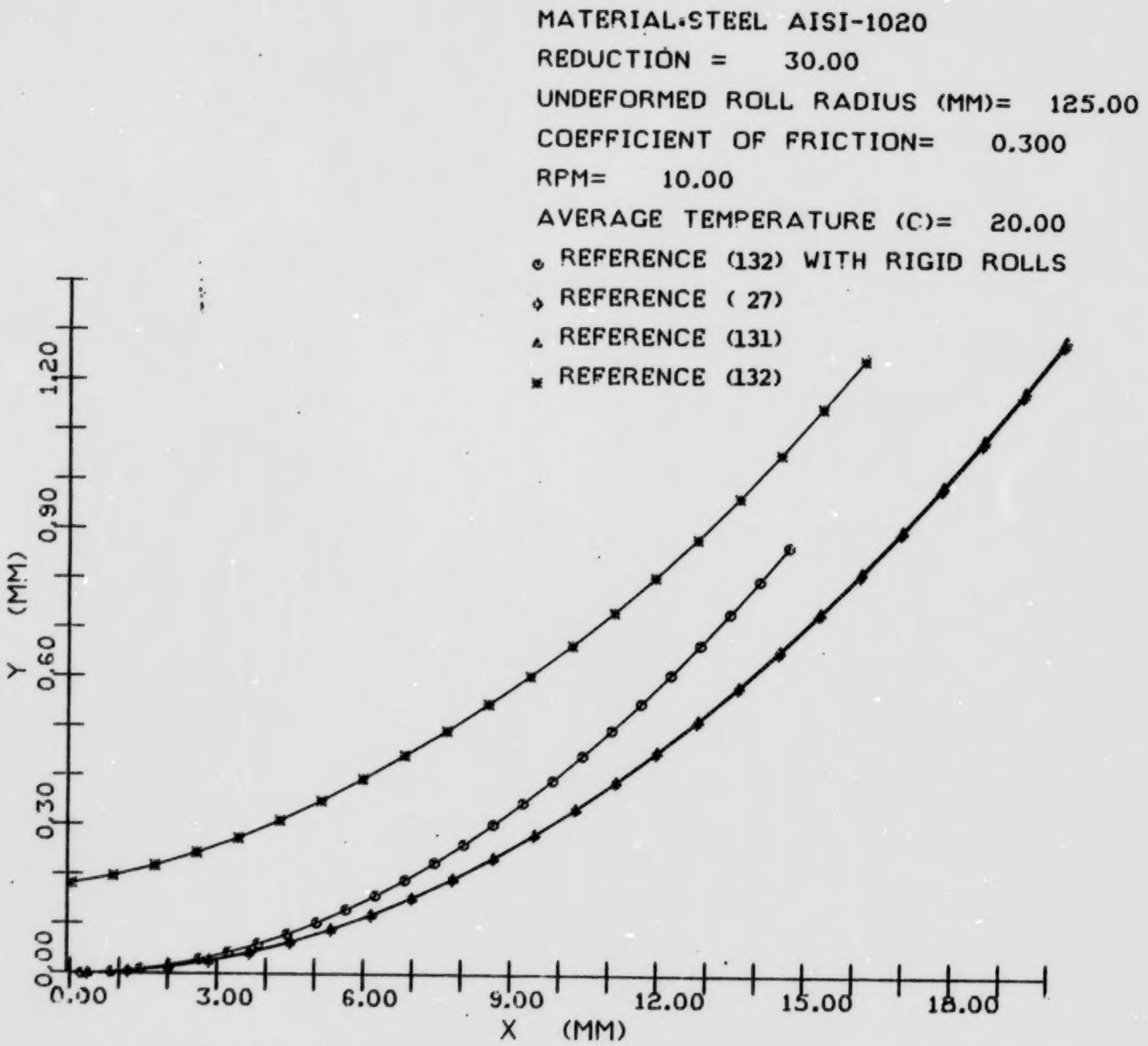
MATERIAL:STEEL AISI-1020
REDUCTION = 30.00
UNDEFORMED ROLL RADIUS (MM)= 125.00
COEFFICIENT OF FRICTION= 0.300
RPM= 10.00
AVERAGE TEMPERATURE (C)= 20.00
⊙ REFERENCE (132) WITH RIGID ROLLS
◇ REFERENCE (27)
△ REFERENCE (131)
✱ REFERENCE (132)
Y (MM)
0.00
0.30
0.60
0.90
1.20
X (MM)
0.00
3.00
6.00
9.00
12.00
15.00
18.00

FIGURE 43

rolling models under investigation is shown in Figures 42 and 43. The undeformed roll shape is also shown in the Figures. The centre of the deformed roll is taken to be the same for all of the models.

The effect of reduction on the roll contours, as predicted by Reference [132] is shown in Figures 44 .

It is observed that some indentation exists for all three reductions shown (10%, 30% and 50%). As the amount of reduction is increased, so is the magnitude of the roll indentation. It is believed that the indentation is a direct consequence of the use of unrealistic roll pressure distributions used in the models.

Further, as observed in Figure 45, where roll contours for rolls of various stiffnesses are given, for a constant coefficient of friction, use of which is responsible for the resulting indented shape, the indentation grows as the modulus of elasticity is decreasing.

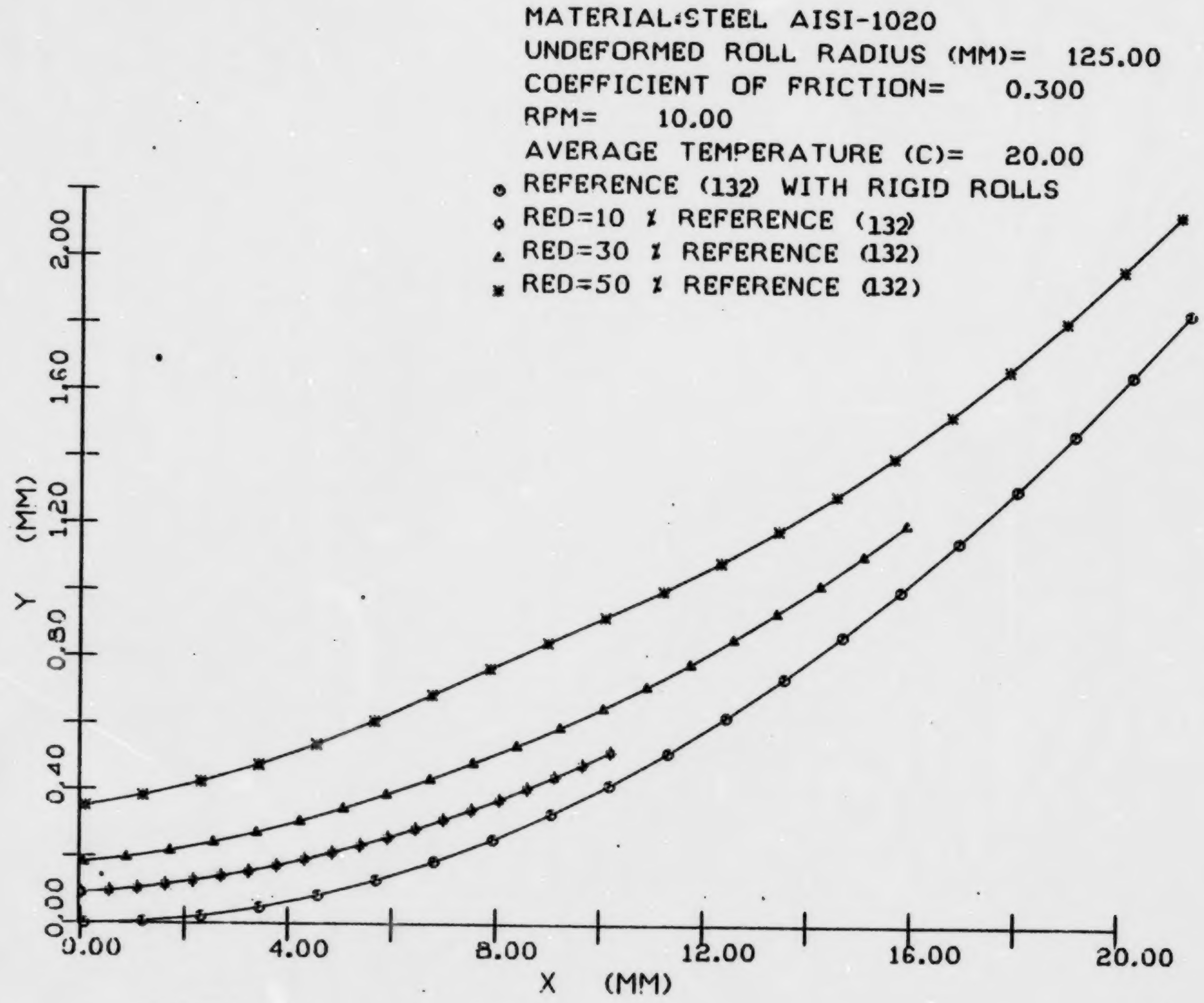
MATERIAL:STEEL AISI-1020
UNDEFORMED ROLL RADIUS (MM)= 125.00
COEFFICIENT OF FRICTION= 0.300
RPM= 10.00
AVERAGE TEMPERATURE (C)= 20.00
⊙ REFERENCE (132) WITH RIGID ROLLS
◇ RED=10 % REFERENCE (132)
▲ RED=30 % REFERENCE (132)
✱ RED=50 % REFERENCE (132)
Y (MM)
0.00
0.40
0.80
1.20
1.60
2.00
X (MM)
0.00
4.00
8.00
12.00
16.00
20.00

FIGURE 44

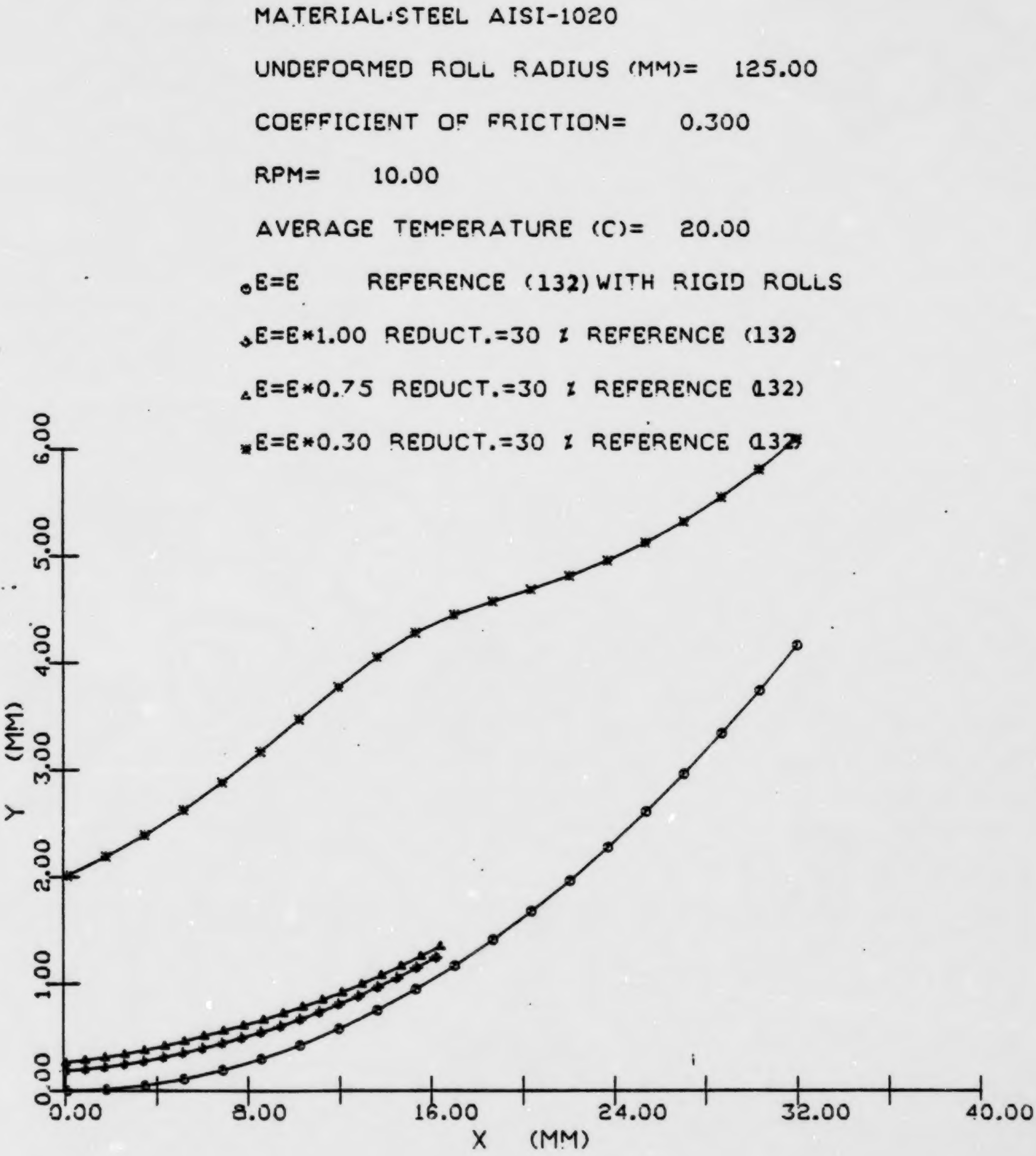
MATERIAL:STEEL AISI-1020
UNDEFORMED ROLL RADIUS (MM)= 125.00
COEFFICIENT OF FRICTION= 0.300
RPM= 10.00
AVERAGE TEMPERATURE (C)= 20.00
○ E=E REFERENCE (132) WITH RIGID ROLLS
◇ E=E*1.00 REDUCT.=30 % REFERENCE (132)
△ E=E*0.75 REDUCT.=30 % REFERENCE (132)
✱ E=E*0.30 REDUCT.=30 % REFERENCE (132)
Y (MM)
0.00
1.00
2.00
3.00
4.00
5.00
6.00
X (MM)
0.00
8.00
16.00
24.00
32.00
40.00

FIGURE 45

CHAPTER 8

EXPERIMENTAL SUBSTANTIATION OF VARIOUS FLAT ROLLING MODELS

Introduction

Mathematical models that predict separating forces and roll torques in hot strip rolling are numerous - see References [25] - [28]. Some of these models are based on analysis of the mechanics of the roll gap while others present empirical relationships, derived from the results of experiments and regression analysis. All of these techniques require a priori knowledge of probably the most important parameter; the flow strength of the material being rolled. Information regarding material behaviour at high temperatures can be found in the published literature - see References [93] to [96].

Recent advances in the rolling industry include computer control of strip mills. The computer programs that are used to control the mills must be able to predict accurately and fast separating forces and roll torques, hence they must make use of one of the above mentioned models. The choice of this model is important; it can affect the quality and quantity of the product.

In this chapter the predictive abilities of hot and cold rolling models are compared to measurements obtained in production runs as well as in a laboratory setting. In the first part four methods of calculations are compared, in a statistical manner, to roll force and mill power results; in the second, accurate flow strength data are used in Orowan's and in Roychoudhuri and Lenard's models to test their abilities in predicting laboratory data.

Statistical analysis of predictive capabilities of four mathematical models for hot, flat rolling

In this section two techniques of computations and two material flow strength formulations are tested for their ability to predict consistently and accurately separating forces and mill powers in hot strip rolling. These are referred to as Methods 1 to 4 and are listed below:

Method (1) Orowan's model [27] for the mechanics of rolling together with a modified version of Shida's flow strength formulation [94];

Method (2) Orowan's model with Ekelund's flow strength formulation [99];

Method (3) Ford and Alexander's model [26] for the mechanics of rolling together with the Shida's flow strength formulation; and

Method (4) Ford and Alexander's model with Ekelund's flow strength formulation.

Results

Materials Used

Low carbon steel and HSLA steel were used in the laboratory experiments. Their chemical compositions are given below:

	C	Mn	S	P	Si	Cr	Ni	Cu	Mo	Nb
LC	0.19	0.82	-	-	-	0.1	-	-	-	-
HSLA	0.18	1.14	0.028	0.04	0.02	0.04	0.01	0.02	0.01	0.022

The compositions of the materials used in the production runs are not revealed in here other than mention that Niobium bearing HSLA steels and low carbon steel were analysed.

Computer Times

These are given in Table 1. As expected, Method 1 is the most time consuming; Method 4 is the fastest. It is to be noted that a total of about 100 hours of computer time were used in producing the numbers that appear below.

Method	Theory Used	CPU Time (secs)	No. of Passes	No. of Statements Executed	Time/Pass (secs)
1	Orowan and Shida	1980.0	24	8×10^6	82.5
2	Orowan and Ekelund	1576.0	78	6×10^6	20.2
3	Ford, Alexander and Shida	3.35	326	51×10^3	0.010
4	Ford, Alexander and Ekelund	1.97	320	21×10^3	0.006

Table 1 Computing times for various models

Statistical evaluation

The results of the calculations are given in Tables 2, 3 and 4. Tables 2 and 3 involve data taken off industrial logs; Table 4 is concerned with data generated on a small, experimental rolling mill. In each case, the numbers given represent the percentage differences of measured and predicted values.

Table 2 shows the means and the standard deviations of the errors involving separating force calculations. Results for the first four stands of the finishing mill are given. Low carbon steel and HSLA steel are contrasted by having respective numbers placed in corresponding rows.

Table 3 repeats the above but is concerned with mill power; Table 4 gives the results of computations for the laboratory data.

Some general observations may be made. These are listed below.

a) In all of the analyses of industrial data, the variation of percent error with stand number shows a definite and identical trend. The error becomes more positive in the first through third stand and dips (i.e. becomes less positive) in the fourth stand. Note that the percentage error for both force as well as power is calculated as

$$\% \text{ Error} = \frac{\text{Measured value - Predicted value}}{\text{Measured value}}$$

from which it is evident that an increasing error percentage implies a predicted value which is decreasing with respect to the measured value. It is well known that the strain rate increases with stand number while the average temperature decreases. In fact both these factors result in an increasing value of material flow strength. But of the four computational schemes used for predicting forces and powers, the two using Ekelund's material formulation do not acknowledge any influence of strain rate. This means that although the material is actually becoming harder, the predictive techniques are not keeping track of this increase resulting in a predicted value which is decreasing with respect to the measured value. Though the other techniques using Shida's formulation as the basis for material behaviour do acknowledge a variation of predicted forces and powers with increasing strain rates, it could be argued that it is possible they do not do so sufficiently, resulting in a predicted value that is less than the actual value.

A similar argument may hold for the effect of decreasing temperatures. Though admittedly, all four models contain the temperature factor it is possible that the effect of temperature is not represented sufficiently causing the predicted forces and powers to lag behind the measured values.

In all calculations it has been assumed that a condition of sticking friction exists. A study of relevant literature reveals that in most cases of hot rolling, this is a reasonable assumption. However at the lower temperatures encountered at the fourth stand it seems likely that this assumption is no longer valid and instead the friction stress may be governed by a relation of the form

$$\tau = s \ \mu \ (s, t, v, \text{material, surface condition})$$

where τ is the frictional stress, s is the normal pressure, μ is the coefficient of friction as a function of normal pressure, temperature, velocity of sliding and contacting materials.

Assuming that this is the case it follows that at the fourth stand the numerical technique (which continues to use the sticking friction condition) will predict forces and powers that have increased with respect to the measured values. This would explain the reversed trend occurring at the fourth stand.

b) On studying the variation of standard deviation with stand number it is observed that the standard deviation is least in the second and third stands and increases in the first and fourth stands. The magnitude of the effect varies but the general trend is always the same. It is impossible to pinpoint any one reason for this effect. It could be caused by a combination of one or more of the following possibilities.

It seems reasonable to believe that the first stand which receives the strip directly from the roughing mill would receive a greater variation in strip thickness than the subsequent stands. Since the data logging device used in the industry probably reads an instantaneous value of strip thickness, a variation in the input thickness would result in a variation in the percentage error calculated for the first stand.

The difference between the inlet side looper tension and the outlet side looper tension at any stand represents the net pull on the strip. This net pull is always the largest in the first stand since the inlet side tension is always zero. The larger net pull will result in a shift of neutral point closer to one end of the arc of contact in the roll gap. This shift in the netural point may make the calculations for that stand more susceptible to variation in the frictional stress. As the friction effect varies randomly between sticking friction and coulombic friction (due to the presence of scales in the roll gap) the error in the predictions will vary.

As has been observed earlier, at the fourth stand it is likely that the nature of friction has changed. This could help explain the greater variance in the predictions at the fourth stand.

The second, third and fourth finishing mill stands operate in a temperature zone which is in the vicinity of the border between hot and cold rolling. The exact point of occurrence of this transition is not clear. However it is likely that this transition occurs close to the temperatures normally encountered at the fourth stand, i.e. conditions at the fourth stand may alternate between hot rolling and cold rolling.

The standard deviation inherent in the industry data is unknown. It is possible that the input data itself may have a variation in standard deviation from stand to stand and this may have, to a greater or lesser extent, reflected in the error readings.

		Method 1		Method 2		Method 3		Method 4	
		$\bar{F}$	σ	$\bar{F}$	σ	$\bar{F}$	σ	$\bar{F}$	σ
Stand #1	LC	15.897	9.679	4.608	12.954	-49.186	17.290	-51.305	20.067
	HSLA	19.972	12.040	-8.490	21.965	-41.388	19.170	-63.871	21.280
Stand #2	LC	26.656	6.740	13.667	9.177	-26.808	11.622	-32.969	13.725
	HSLA	25.730	9.270	-1.518	14.178	-27.733	14.015	-50.606	20.574
Stand #3	LC	45.034	6.323	34.928	8.399	7.425	10.634	1.528	15.118
	HSLA	45.220	10.359	20.642	13.689	4.085	12.393	-12.583	18.477
Stand #4	LC	41.494	9.085	30.707	11.392	4.067	15.699	-2.185	18.254
	HSLA	36.546	13.214	14.397	16.503	-3.366	18.805	-20.518	24.612

Table 2. Separating forces - industrial data

c) The mean error between the predicted value and the observed value represents the 'accuracy' of the prediction whereas the standard deviation in this error represents the 'precision' of the prediction. While the 'accuracy' determines how close the predicted value comes to the measured value, the "precision" determines the reproducibility of the result. In judging the usefuleness of a predictive technique both these factors should be taken into consideration. However it should be borne in mind that an inaccurate result can be corrected for by an additional multiplying factor, but the effect of an imprecise result can never be corrected. Hence, in any predictive technique, good accuracy is desirable and good precision essential.

d) It should be pointed out here that normally one would expect the measured values to be greater than the predicted values because the latter do not take into consideration the efficiency of the bearings and the power transmission train. Adding a factor to the predicted values to compensate for this effect would make the errors in the Ford and Alexander predictions higher (i.e. further negative). It would however help to bring the values predicted by the Orowan method closer to the actual measured values.

e) It is noted that for the laboratory data, the distinction between the Ford and Alexander technique and the Orowan formulation becomes even more pronounced; errors in force prediction reach as high as 100% and more.

		Method 1		Method 2		Method 3		Method 4	
		$\bar{P}$	σ	$\bar{P}$	σ	$\bar{P}$	σ	$\bar{P}$	σ
Stand #1	LC	2.833	12.389	-10.267	14.513	-35.797	25.039	-36.472	26.591
	HSLA	5.726	20.921	-28.993	25.939	-31.822	24.597	-51.995	25.063
Stand #2	LC	20.413	8.705	5,736	11.389	-6.094	17.152	-10.179	18.602
	HSLA	17.643	11.778	-12.865	19.846	-6.482	12.288	-25.336	15.917
Stand #3	LC	25.891	10.602	11.838	13.441	8.480	16.405	4.212	17.824
	HSLA	26.970	21.020	-6.332	20.071	9.336	13.118	-6.290	17.937
Stand #4	LC	24.940	10.787	10.535	13.747	11.067	16.625	8.847	18.976
	HSLA	17.499	23.160	-12.139	24.713	7.179	16.774	-8.168	21.551

Table 3. Mill powers - industrial data

		Method 1		Method 2		Method 3		Method 4	
		$\bar{P}$ or $\bar{F}$	σ	$\bar{P}$ or $\bar{F}$	σ	$\bar{P}$ or $\bar{F}$	σ	$\bar{P}$ or $\bar{F}$	σ
Separating force	LC	9.949	17.213	-43.564	12.486	-38.829	21.527	-101.758	23.713
	HSLA	-34.857	26.857	-57.247	17.654	-129.089	47.928	-128.097	35.448
Power	LC	15.019	18.732	-19.547	30.139	12.498	20.201	-28.101	35.626
	HSLA	6.083	14.501	-6.090	32.325	-17.137	20.270	-26.577	64.378

Table 4. Results - laboratory data

The reason for this phenomenon, it is felt, is that the Ford-Alexander technique does not consider the effect of looper tension explicitly while the Orowan technique does. In the laboratory testing, no back or front tensions have been applied on the strip. Presumably, then, the Orowan technique can adjust to a value of zero looper tension, whereas the Ford-Alexander technique cannot.

f) On the whole, for industrial data as well as for laboratory data, standard deviations for HSLA steel are higher than corresponding values for mild steel.

This is probably due to the fact that the material flow strength models used do not consider the strengthening effects of the microalloying elements in the HSLA steel, thus introducing an extra element of variability that is not allowed for in the predictive models.

g) Contrary to what may be expected, mean errors for HSLA steel are more negative than the corresponding values for mild steel. Since the material models used do not consider the strengthening effect of the microalloying elements, one would expect the predicted forces and powers to decrease with respect to the measured values, thus resulting in the error becoming more positive. This does not appear to be the case.

h) In general, it may be noted from the results both for industrial as well as laboratory data that accuracy and precision seem to go hand in hand with the relative complexity (represented by CPU time/pass) of the predictive scheme. Thus the Orowan and Shida technique appears to be the most consistently accurate followed by Orowan and Ekelund, and then Ford, Alexander and Shida and finally Ford, Alexander and Ekelund. The CPU times also follow the same pattern. However, CPU times for the two Orowan based programs are so large that those two programs can never be used for on-line control of strip mills. Another drawback with these two programs is that they have very large memory space requirements.

Predictive abilities of flat rolling models: laboratory data

Hot Rolling

A niobium bearing high strength low alloy steel is used in this portion of the project. Flow curves of the steel are obtained in constant strain rate, uniaxial compression and the data are then incorporated in two hot rolling theories. The objective is to test whether the use of accurate strength data with a superior treatment of the mechanics of rolling will enhance the accuracy over that of the traditional Orowan model.

Material properties

CHEMISTRY: The material was received in the form of hot rolled strips, from Algoma Steel Corporation Ltd. The chemical composition by weight % is given below:

C	Mn	Si	Al	P	Nb
0.09	0.90	0.02	0.04	0.008	0.02

SAMPLE PREPARATION: Cylindrical specimens of 4 mm diameter and 6 mm height were machined in a direction perpendicular to rolling in the plane of the strips.

FLOW CURVES: True stress-true strain curves of the steel, obtained in constant strain-rate compression at 950°, are shown in Figure 46 for strain rates of 0.01, 0.02, 1, 10 and 50 s^{-1}--see Reference [133]. No correction for adiabatic temperature rise was included in plotting these curves.

PRIOR SOLUTION TREATMENT: Each sample was heated to 1150° in a split, laboratory furnace, attached to the microprocessor-controlled servohydraulic testing system. The samples were held at that temperature for 20 minutes and cooled to the test temperature inside the furnace at a rate of 0.3°C/second. The specimens were then held for 5 minutes more to ensure even temperature distribution and the experiment was performed.

FRICTION CONTROL: Following the recommendation of Baragar and Crawley [134], no lubricant was used during the tests. Some, but not excessive, barreling was observed.

Hot rolling experiments

SAMPLE PREPARATION: Strips of approximately 0.25 inches

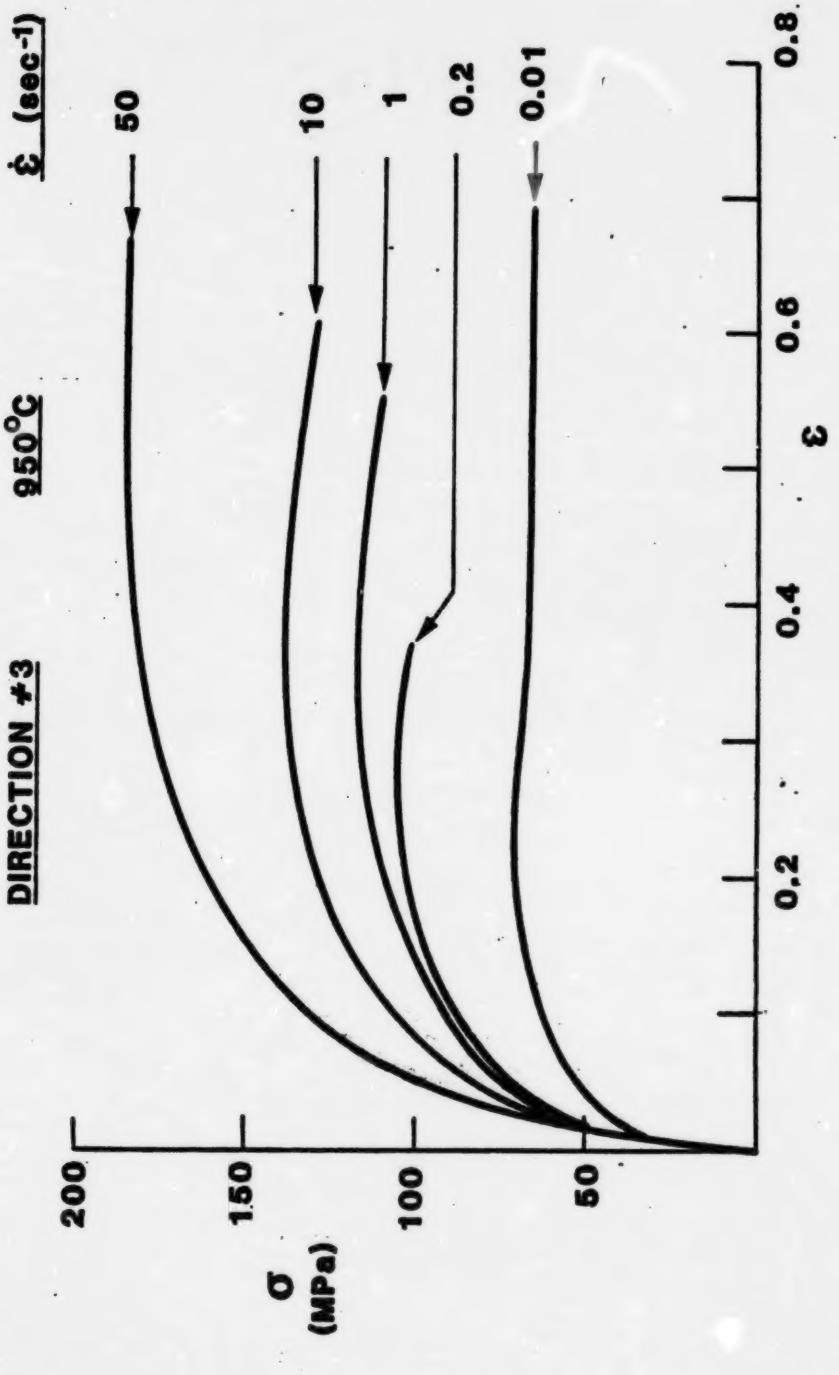

FLOW CURVES OF 0.02% NB BEARING HSLA STEEL AT 950°C

FIGURE 46

thickness, 1.5 inches width and 4 inches length were used in the hot rolling experiments. A type K (chromel-alumel) thermocouple of 1/16th of an inch diameter was embedded to a depth of 0.25 inch in the tail end of every strip.

PRIOR SOLUTION TREATMENT: Each strip was heated to 1150° in the prewarmed furnace. The temperature of the strip was monitored using the embedded thermocouples. Twenty minutes after the solution treatment temperature was reached the strip was transferrred to the rolling mill. The cooling rate during the transfer process was significantly higher than in the compression tests; approximately 30°C/second was recorded. This difference in cooling rates probably caused different degrees of precipitation hardening during hot rolling and compression.
The strip was placed in the roll gap when 950° was reached.

DATA ACQUISITION: A multichannel A/D converter and an LSI 11/23 microprocessor were used to collect roll force and roll torque data. Sampling was begun when the strip entered the roll gap. Measurements were taken at 0.005 second intervals.

ROLLING MILL: The rolling mill employed was a two-high mill with rolls having a diameter of 254 mm and an axial length of 254 mm. The roll material was AISI 4340 alloy steel, hardened to Rc = 38. These rolls were driven through universal couplings by a pair of spur gears, which in turn were driven by a variable speed D.C. motor (15 kW) via two gear reduction mechanisms. The universal couplings were attached to the rolls by means of a pair of square drive shafts. The roll bearings were precision machined journal bearings and the bearing blocks were mounted on square thread screws having a diameter of 76.2 mm. The lower bearing blocks were seated on two load cells which were seated in turn in a fixed position on the base of the mill frame.

Torque strain gauges were cemented on the spindles of the universals and the roll-gorques were monitored through two mercury-bath slip rings.

Screw-down was manually controlled by two worm-gear drives, both connected to the bearing blocks of the upper work-roll. One turn of the screw-down control resulted in a 0.025 mm change of the roll-gap. The mill frame has a total load carrying cross-sectional area of 20.6 x 10^3 mm^2 (32 $in.^2$). During the design phase this was expected to cause the mill to be fairly rigid. Mill stretch, however, has been measured to be approximately half a millimeter during 15 percent reduction of 1100-T0 aluminum strips.

Method of calculation

CONSTANT STRAIN RATE FLOW CURVES: In this approach the flow curves, developed in Reference [133], and briefly reviewed above, are used for the predictions of roll forces. The method recommended by Schey [24] is followed. First, the true stress-true strain curves, given in Figure 46, are replotted to give values of true stress and strain rate for various levels of strains--see Figure 47. Then the average strain rate/pass is calculated by the formula given in Reference [24]:

$$\dot{\varepsilon} = \frac{\Pi d n}{\sqrt{R(h_0 - h_1)}} \ln (h_0/h_1)$$

where d = roll diameter

n = revolutions/second

R = roll radius

h_o = entry thickness

h_1 = exit thickness

The average strength is read from Figure 47 for the appropriate strain level and is used as if the material were in a state of ideal plasticity.

HOT ROLLING THEORIES: Two theories are employed in the predictive type calculations. One of these is the traditional Orowan theory; the other is due to Roychoudhuri and Lenard -- the "Lenard model" [132].

RESULTS: The results of the hot rolling tests and the predictions are shown in Figures 48 - 50. A compilation of

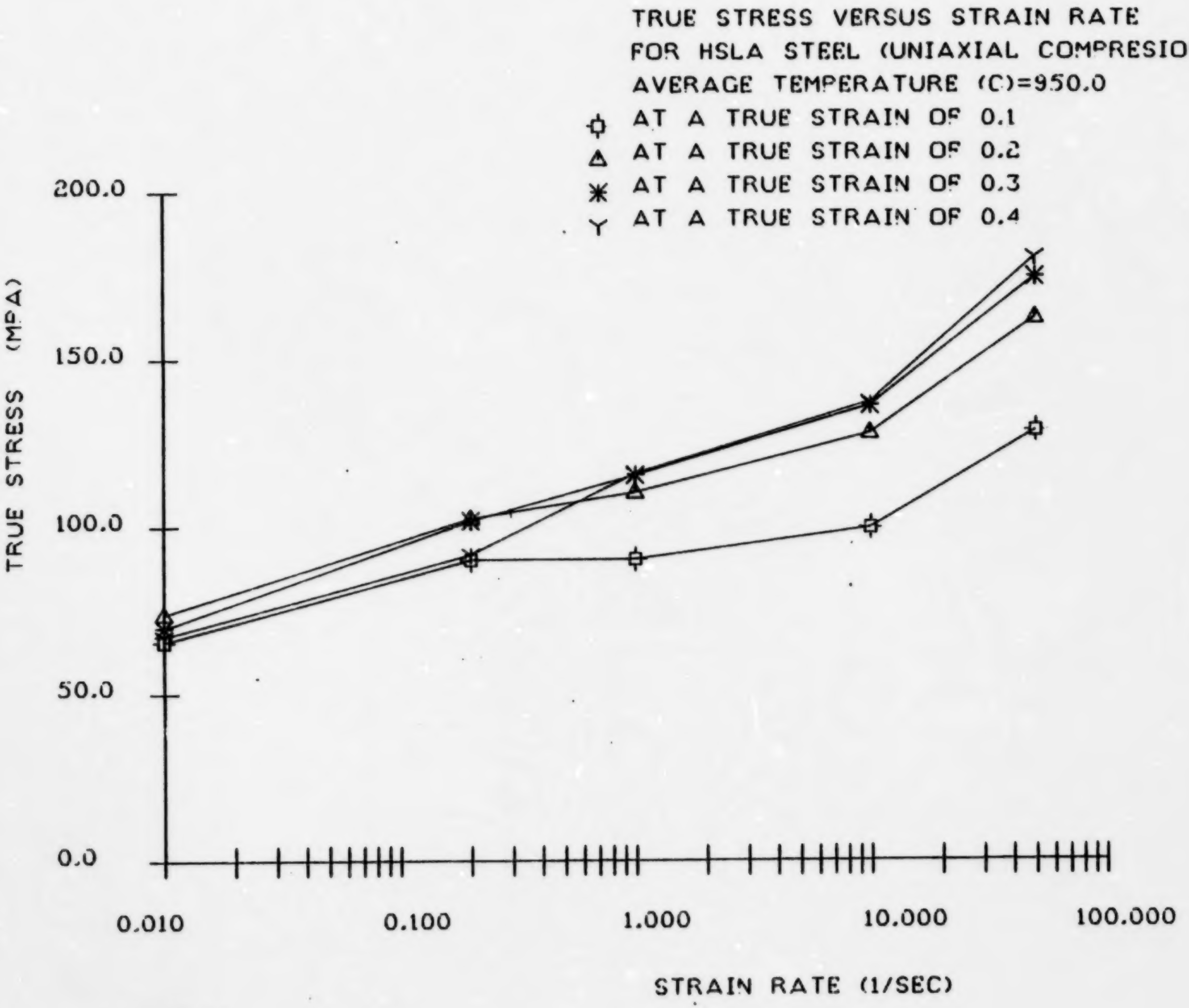
TRUE STRESS VERSUS STRAIN RATE
FOR HSLA STEEL (UNIAXIAL COMPRESION)
AVERAGE TEMPERATURE (C)=950.0
AT A TRUE STRAIN OF 0.1
AT A TRUE STRAIN OF 0.2
AT A TRUE STRAIN OF 0.3
AT A TRUE STRAIN OF 0.4
TRUE STRESS (MPA)
200.0
150.0
100.0
50.0
0.0
0.010
0.100
1.000
10.000
100.000
STRAIN RATE (1/SEC)

FIGURE 47

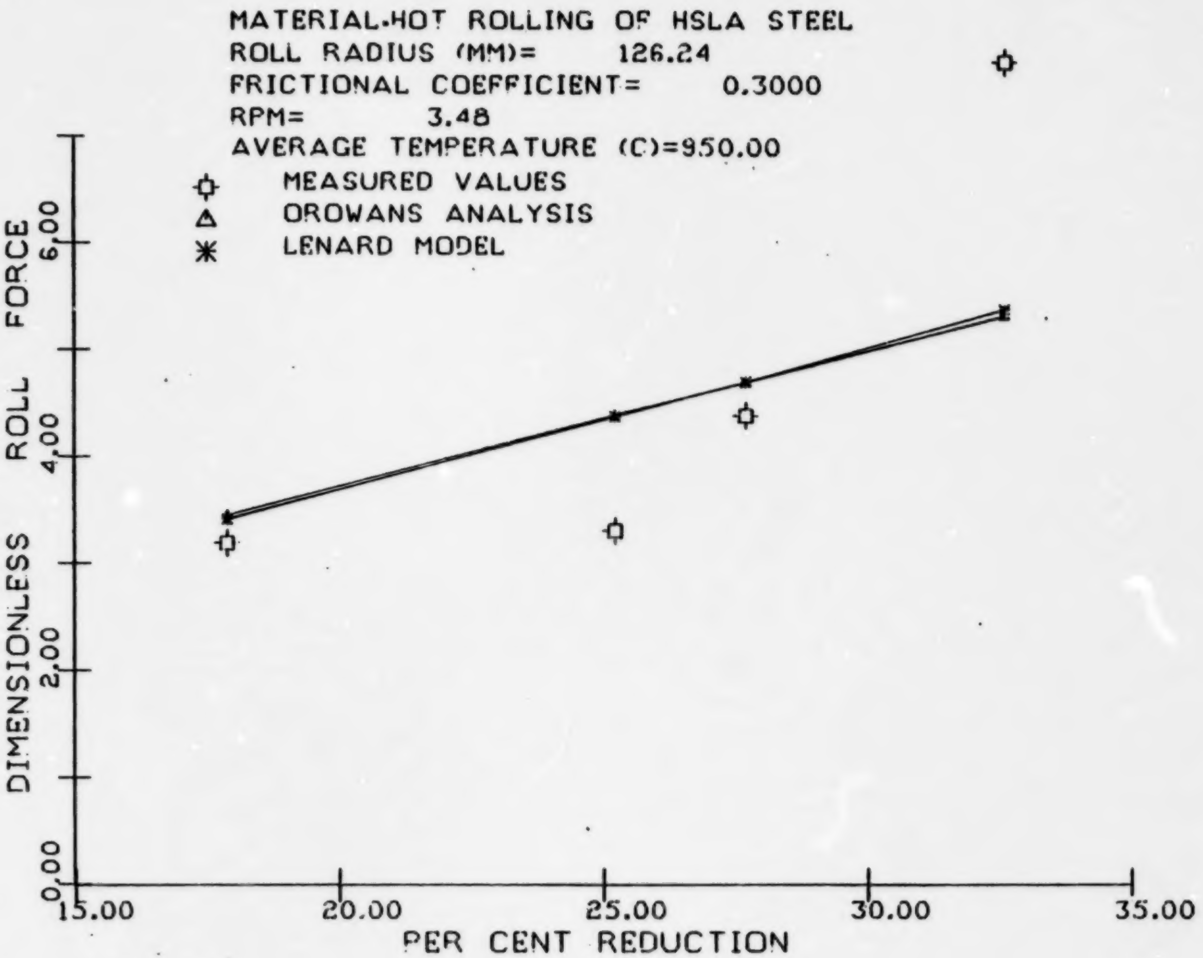
MATERIAL.HOT ROLLING OF HSLA STEEL
ROLL RADIUS (MM)= 126.24
FRICTIONAL COEFFICIENT= 0.3000
RPM= 3.48
AVERAGE TEMPERATURE (C)=950.00
MEASURED VALUES
OROWANS ANALYSIS
LENARD MODEL
DIMENSIONLESS ROLL FORCE
0.00
2.00
4.00
6.00
15.00
20.00
25.00
30.00
35.00
PER CENT REDUCTION

FIGURE 48

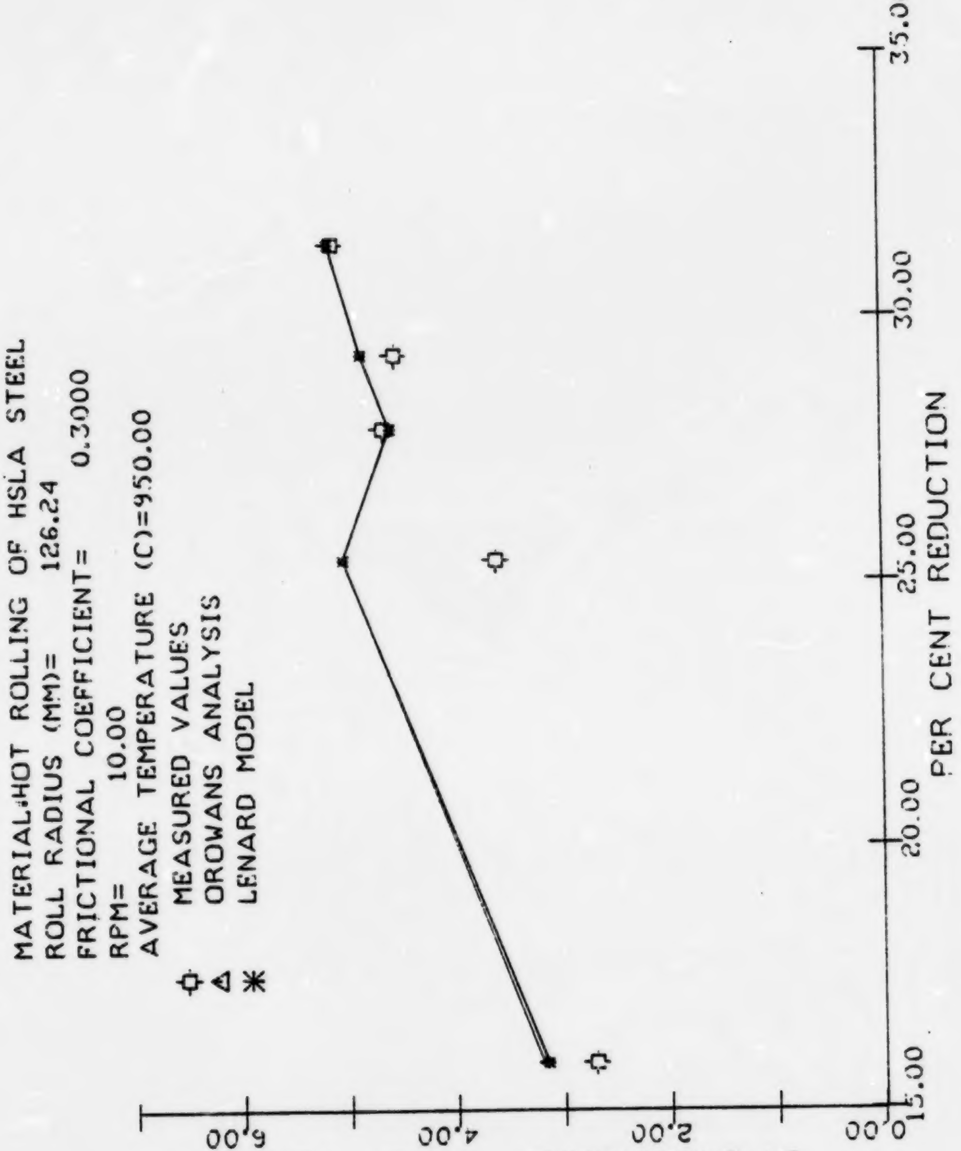
MATERIAL:HOT ROLLING OF HSLA STEEL
ROLL RADIUS (MM)= 126.24
FRICTIONAL COEFFICIENT= 0.3000
RPM= 10.00
AVERAGE TEMPERATURE (C)=950.00
MEASURED VALUES
OROWANS ANALYSIS
LENARD MODEL
DIMENSIONLESS ROLL FORCE
0.00
2.00
4.00
6.00
PER CENT REDUCTION
15.00
20.00
25.00
30.00
35.00

FIGURE 49

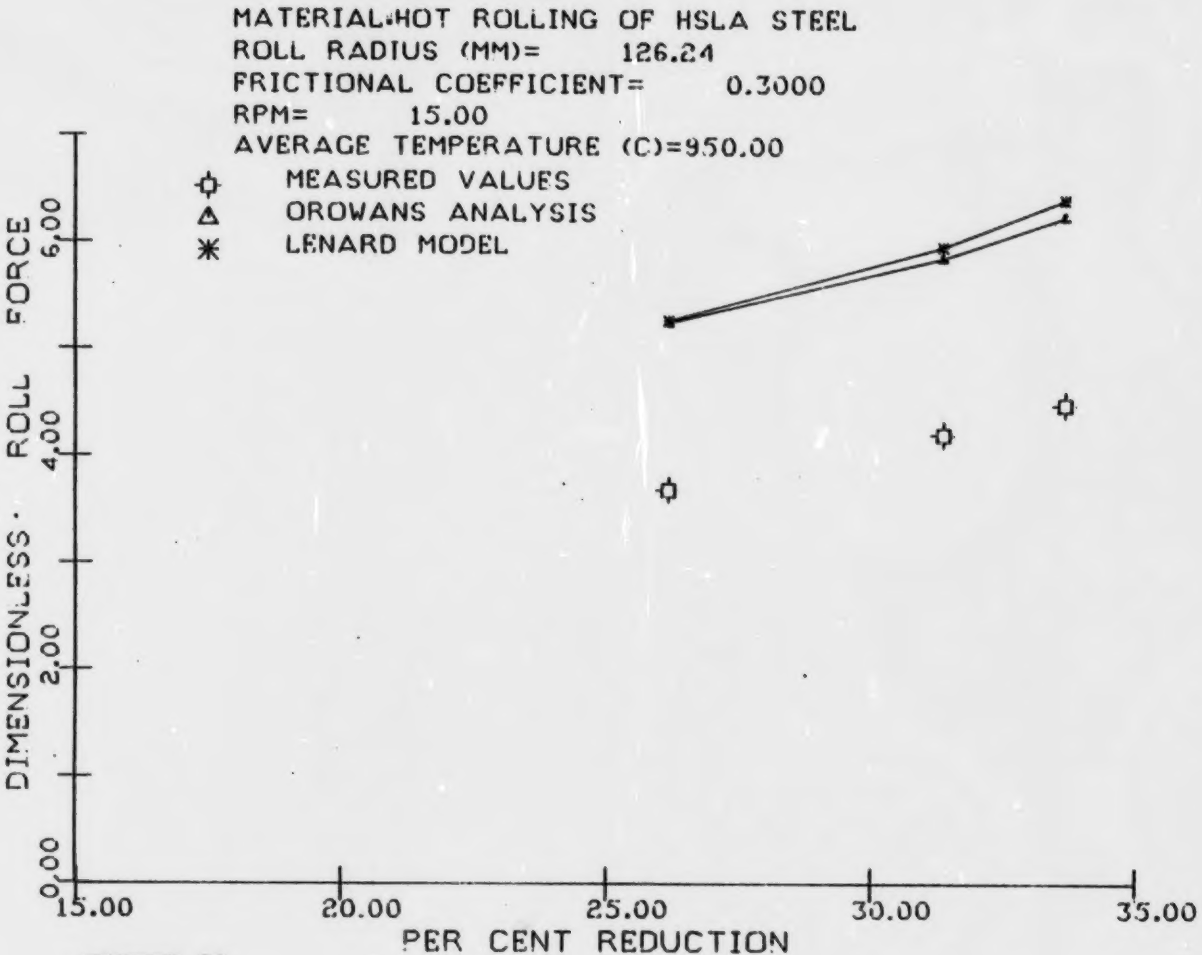
MATERIAL:HOT ROLLING OF HSLA STEEL
ROLL RADIUS (MM)= 126.24
FRICTIONAL COEFFICIENT= 0.3000
RPM= 15.00
AVERAGE TEMPERATURE (C)=950.00
MEASURED VALUES
OROWANS ANALYSIS
LENARD MODEL
DIMENSIONLESS · ROLL FORCE
0.00
2.00
4.00
6.00
15.00
20.00
25.00
30.00
35.00
PER CENT REDUCTION

FIGURE 50

all data is given in Table 5.

Figure 48 presents the measured and predicted roll force values versus % reduction at a roll rotational velocity of 3.48 rpm, corresponding roughly to an average strain rate/pass of unity.

Similar results appear in Figure 49 for 10 rpm and a strain rate of about 3 sec^{-1} and in Figure 50 for 15 rpm or $\dot{\varepsilon} = 5$ s^{-1}. In all, the measured values are indicated by the squares, Orowan's predictions by the triangles and that of the Lenard model by the stars. In all experiments, except one, both models overestimate the magnitudes of the nondimensionalized separating forces by approximately equal amounts. As well, there appears to be no significant differences in the predictions of either technique of computation. It is observed that the predictions depend very strongly on the chosen magnitude of the coefficients of friction which was taken arbitrarily as 0.3 in all of the numerical work. This is contrary to a general agreement among previous workers who believe that during hot rolling sticking friction exists. Two comments need to be considered in this respect. First, as pointed out by Murthy and Lenard [135] the sticking friction assumption may have been responsible for some discrepancies in predictive capabilities when the last few stands of a finishing mill were analyzed. As well, chilling at the roll-strip interface, when rolling thin, hot strips, must have been severe, even if the temperature at the centre was over the

YO	HO	H1	RED	ε	TEMP	F(exp)	F(Orowan)	(Lenard)
(T/IN ^{2})	(in)	(in)	(%)	(1/sec)	(C)	(DIMENSIONLESS)		
RPM = 3.48								
7.04	0.218	0.179	17.9	1.070	964	3.196	3.455	3.415
7.49	0.218	0.163	25.2	1.010	940	3.308	4.393	4.378
8.18	0.220	0.159	27.7	1.070	957	4.386	4.695	4.698
7.54	0.218	0.147	32.6	1.240	952	7.685	5.320	5.380
RPM = 10.0								
7.158	0.219	0.184	15.9	2.180	957	2.711	3.202	3.160
8.067	0.185	0.138	25.4	3.170	960	3.609	5.038	5.040
8.095	0.222	0.160	27.9	3.080	940	4.655	4.593	4.634
8.237	0.222	0.157	29.3	3.180	935	4.504	4.856	4.874
8.293	0.220	0.151	31.4	3.350	944	5.120	5.156	5.197
RPM = 15.0								
8.408	0.186	0.136	26.9	4.920	960	3.686	5.247	5.268
8.465	0.188	0.129	31.4	5.380	960	4.206	5.860	5.962
8.521	0.187	0.124	33.7	5.720	945	4.486	6.244	6.401
RPM = 33.2								
9.203	0.187	0.125	27.4	10.32	957	3.486	6.192	6.336

TABLE 5

recrystallization temperature. Hence, sticking friction probably did not exist in these experiments.*

The results of all thirteen experiments are tabulated in Table 5 along with all relevant parameters.

Note that no torque measurements were taken in this set of experiments due to malfunctioning slip rings. Because of the continuing difficulties with the "homemade" torque transducers and sliprings, they are being replaced with a pair of Lebow sensors.

The last line of Table 5 shows the results of an experiment, conducted at 33.2 rpm roll speed. It is observed that both theories, while similar in their predictions grossly over-estimate the measured separating force.

---

*A project to measure the variation of the friction stress/normal pressure ratio in hot rolling, funded by an NSERC Strategic Grant has begun at UNB.

Cold Rolling

In this section of the Report, four aluminum alloys are cold rolled to various reductions and roll forces and torques are measured using the above described data acquisition system. The flow curves of the alloys are measured in tension on an electrohydraulic Instron Universal testing system, as prescribed by ASTM standards. Nonlinear regression analysis is used to determine the constants in an equation of the form

$$\sigma = Y(1+B\varepsilon)^{n}$$

This equation is then employed in calculations of the expected roll forces and torques.

Material properties

CHEMISTRY: The chemical compositions of the materials as supplied by the vendor, Ideal Metals and Alloys Co., are given below:

	Mn	Si	Al	Fe	CU	Mg	Cr	Zn	Ti
Al 1100 - TO & H14	.05	1.0	rest		.05-0.20			.10	
Al 2024 - T3	.30-.90	.50	rest	.50	3.8 -4.9	1.2-1.8	.10	.25	.15
Al 5052 - H34	.10	.25	rest	.40	.10	2.2-2.8	.15-.35	.10	
Al 6061 - T6	.15	.40-.80	rest	.70	.15-.40	.80-1.20	.04-.35	2.5	.15

FLOW CURVES: Constitutive relations, parameters of anisotropy and Vickers hardness values have been determined and are given below:

	Yield Strength* (MPa)	Ultimate Strength* (MPa)	Hardness Vickers	r value	Constitutive Law
Al 1100 - T0			30	0.871	$\sigma = 85.00(1+96.8\varepsilon)^{0.200}$
Al 2024 - T3	275.60	420.29	143	0.946	$\sigma = 299.86(1+98.8\varepsilon)^{0.123}$
Al 5052 - H34	179.14	234.26	95	1.446	$\sigma = 199.60(1+201.8\varepsilon)^{0.097}$
Al 6061 - T6	241.15	289.38	128	0.641	$\sigma = 264.95(1+192.1\varepsilon)^{0.029}$

*Values provided by the suppliers

Cold Rolling Experiments

FRICTION: In an earlier publication, Lim and Lenard [136] and Karagiozis and Lenard [137] measured the dependence of the ratio of friction stress to normal pressure in the roll gap during cold rolling of the above mentioned aluminum alloys. Some typical results are shown in Figures 51 to 53. The use of data, giving the coefficient of friction as a variable along the roll gap has already been shown to result in superior predictive capability -- see Lenard [50]; a set of calculations from that publication is repeated below:

Material	Dimension (mm)	Reduction (%)	Roll Separating Force (MN/m) (Integrated)			Roll Torque (Nm/m) (Integrated)		
Aluminum	6.27 X 76.2	14.17	0.696	0.779	0.817	2290.7	3366.0	2383.8
Aluminum	6.27 X 76.20	34.41	1.914	1.893	1.877	9278.5	14005.8	8896.0
Copper	6.35 X 76.20	14.80	1.986	2.189	2.282	5760.2	10813.7	5439.9

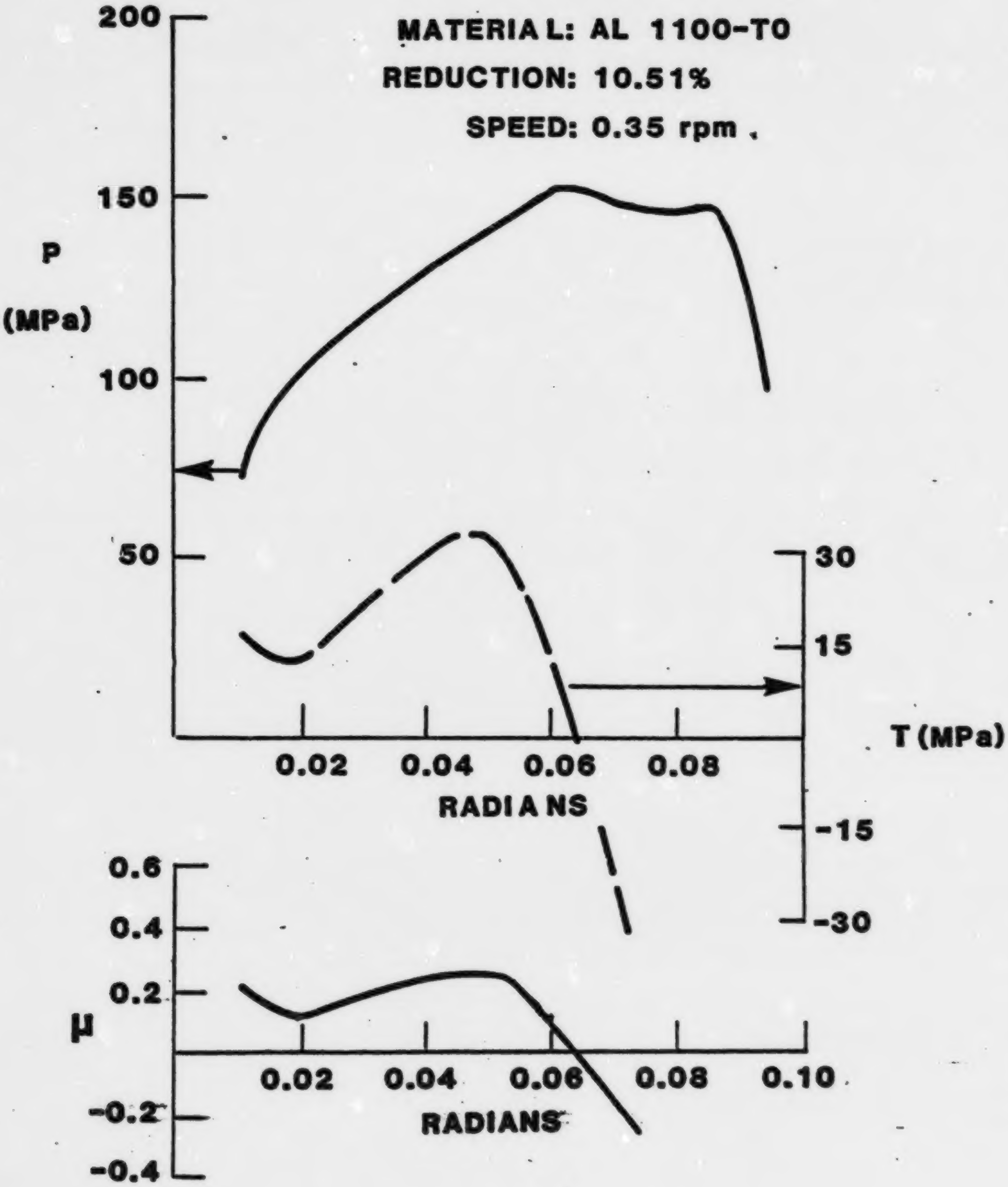
MATERIAL: AL 1100-TO
REDUCTION: 10.51%
SPEED: 0.35 rpm
P
(MPa)
200
150
100
50
30
15
-15
-30
T (MPa)
0.02
0.04
0.06
0.08
RADIANS
μ
0.6
0.4
0.2
-0.2
-0.4
0.02
0.04
0.06
0.08
0.10
RADIANS

FIGURE 51

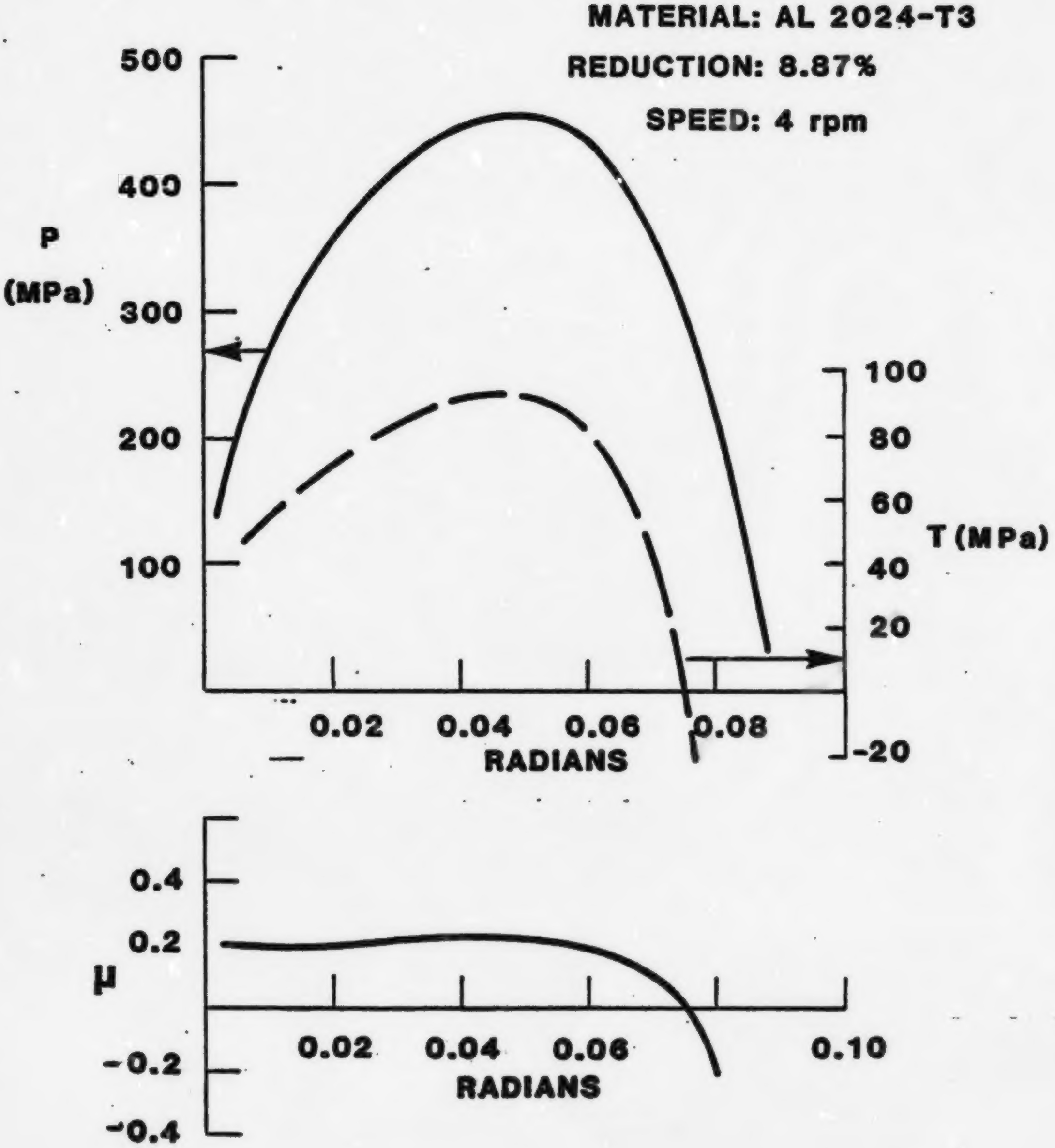
MATERIAL: AL 2024-T3
REDUCTION: 8.87%
SPEED: 4 rpm
500
400
300
200
100
P
(MPa)
100
80
60
40
20
-20
T (MPa)
0.02
0.04
0.06
0.08
RADIANS
0.4
0.2
μ
-0.2
-0.4
0.02
0.04
0.06
0.10
RADIANS

FIGURE 52

In this part of the project the data developed in [136] and [137] are used to test the predictive capabilities of Orowan's and Roychoudhuri and Lenard's models.

ROLLING MILL: A 2-high 0.75 kW Hille Experimental Rolling Mill was used throughout the program. Rotational velocity of the rolls was kept constant at 30 rpm. The roll diameter was 57.15 mm and its width 76.20 mm; the rolls were made of SAE 4340 steel, hardened and ground. Surface variations of less than 0.005 mm and out-of-roundness variations of less than 0.0075 mm were measured. No lubrication was used during the experiments. The separating forces were measured by two force transducers placed under the bearing blocks of the lower roll; roll torques were monitored by two specially designed torque transducers, mounted on both drive spindles. The torque transducers were calibrated on the mill by applying a known torque through the work roll; the reported values of torque are the sum of the means of signals obtained from the two transducers.

Method of calculations

ROLL FORCE AND TORQUE: Orowan's and Roychoudhuri and Lenard's models were used here, coupled with the flow strength and friction data given above.

The values of the average frictional coefficients are read from Figure 53, reproduced here from Reference [137]. For reductions beyond 22% linear extrapolation is used.

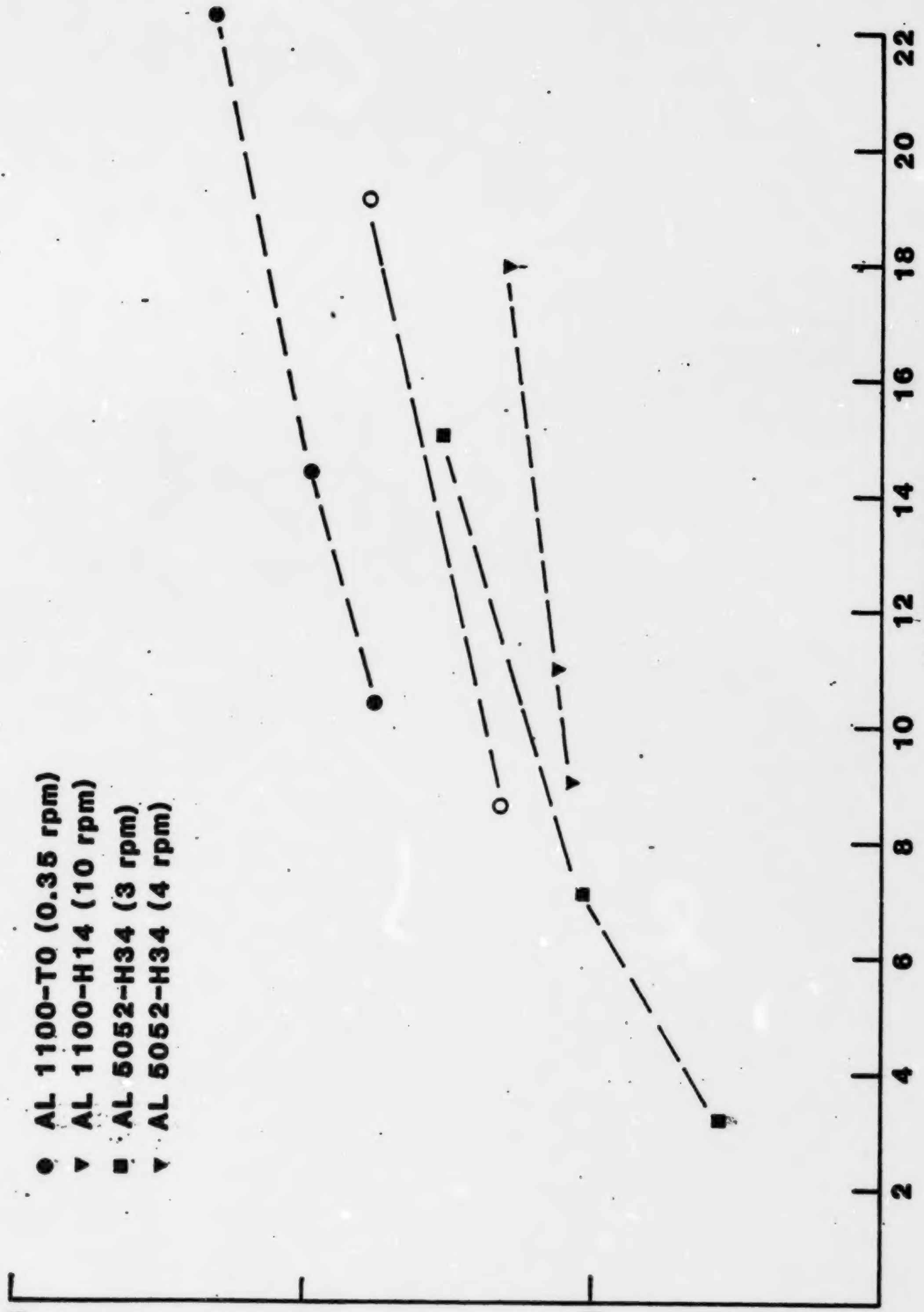
● AL 1100-TO (0.35 rpm)
▼ AL 1100-H14 (10 rpm)
■ AL 5052-H34 (3 rpm)
▼ AL 5052-H34 (4 rpm)
μ_{ave}
0.3
0.2
0.1
2
4
6
8
10
12
14
16
18
20
22
% REDUCTION

FIGURE 53

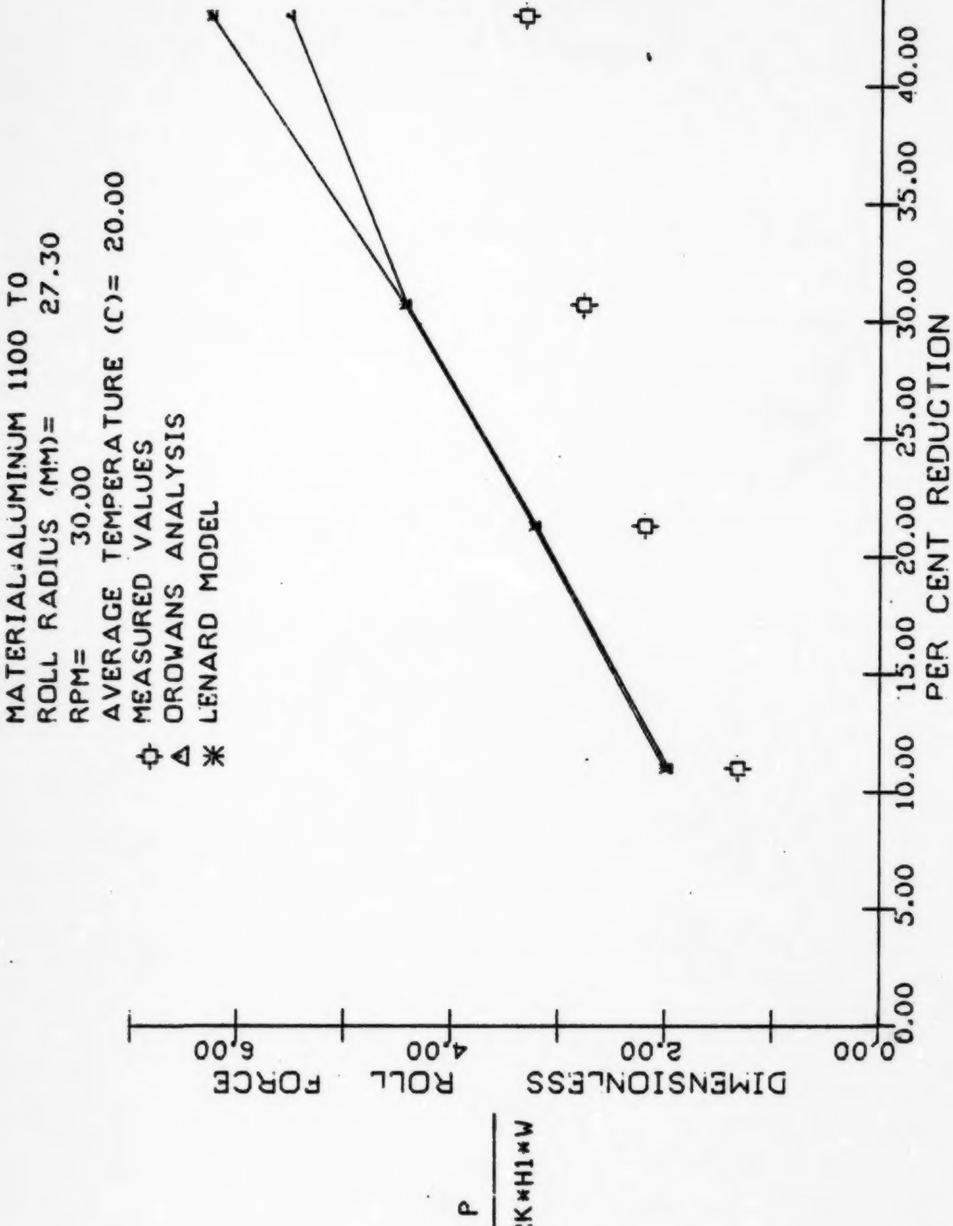
MATERIAL:ALUMINUM 1100 TO
ROLL RADIUS (MM)= 27.30
RPM= 30.00
AVERAGE TEMPERATURE (C)= 20.00
MEASURED VALUES
OROWANS ANALYSIS
LENARD MODEL
P / 2K*H1*W
DIMENSIONLESS ROLL FORCE
0.00
2.00
4.00
6.00
PER CENT REDUCTION
0.00
5.00
10.00
15.00
20.00
25.00
30.00
35.00
40.00
45.00

FIGURE 54

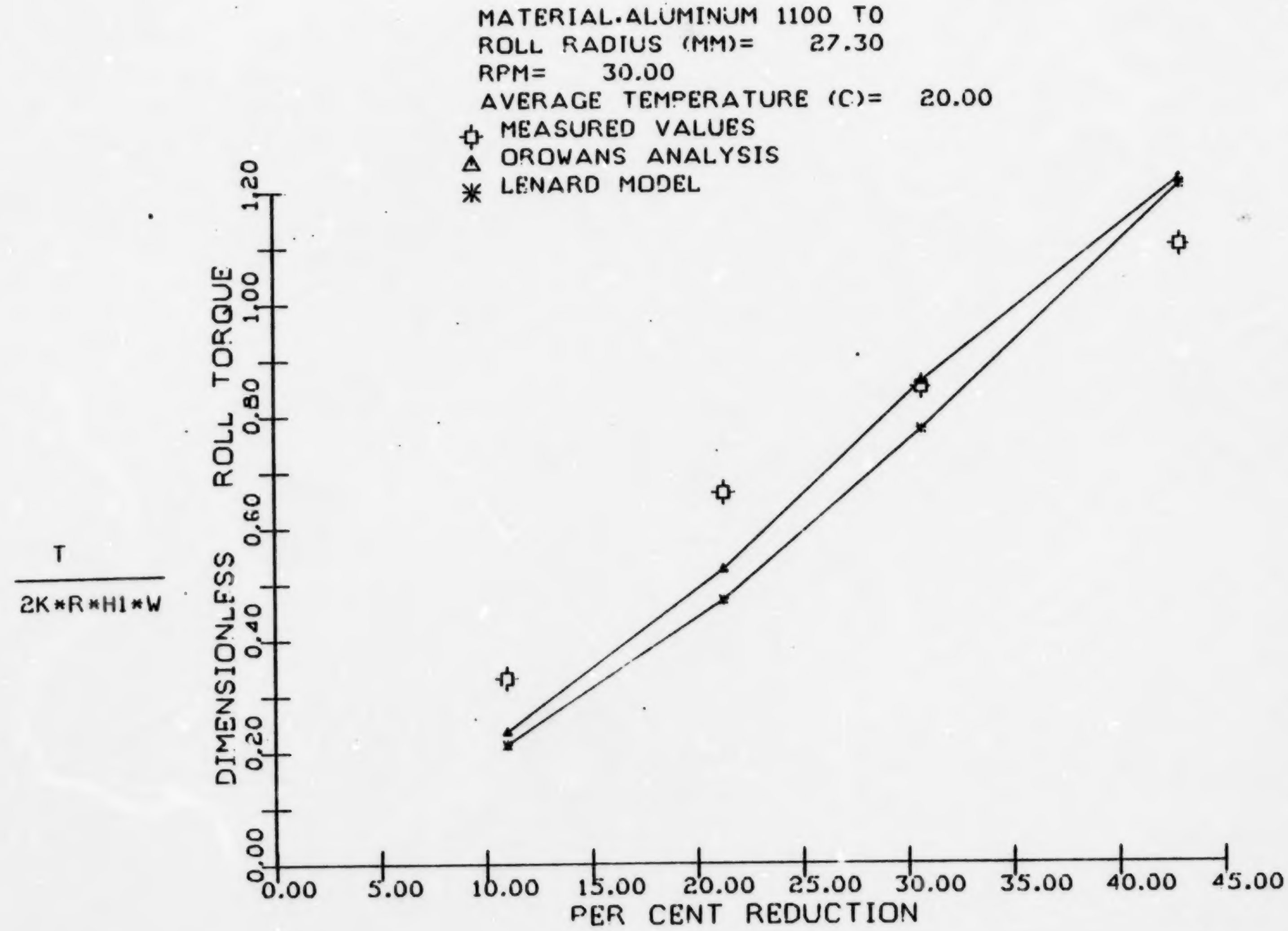
MATERIAL.ALUMINUM 1100 TO
ROLL RADIUS (MM)= 27.30
RPM= 30.00
AVERAGE TEMPERATURE (C)= 20.00
MEASURED VALUES
OROWANS ANALYSIS
LENARD MODEL
T / 2K*R*H1*W
DIMENSIONLESS ROLL TORQUE
0.00
0.20
0.40
0.60
0.80
1.00
1.20
0.00
5.00
10.00
15.00
20.00
25.00
30.00
35.00
40.00
45.00
PER CENT REDUCTION

FIGURE 55

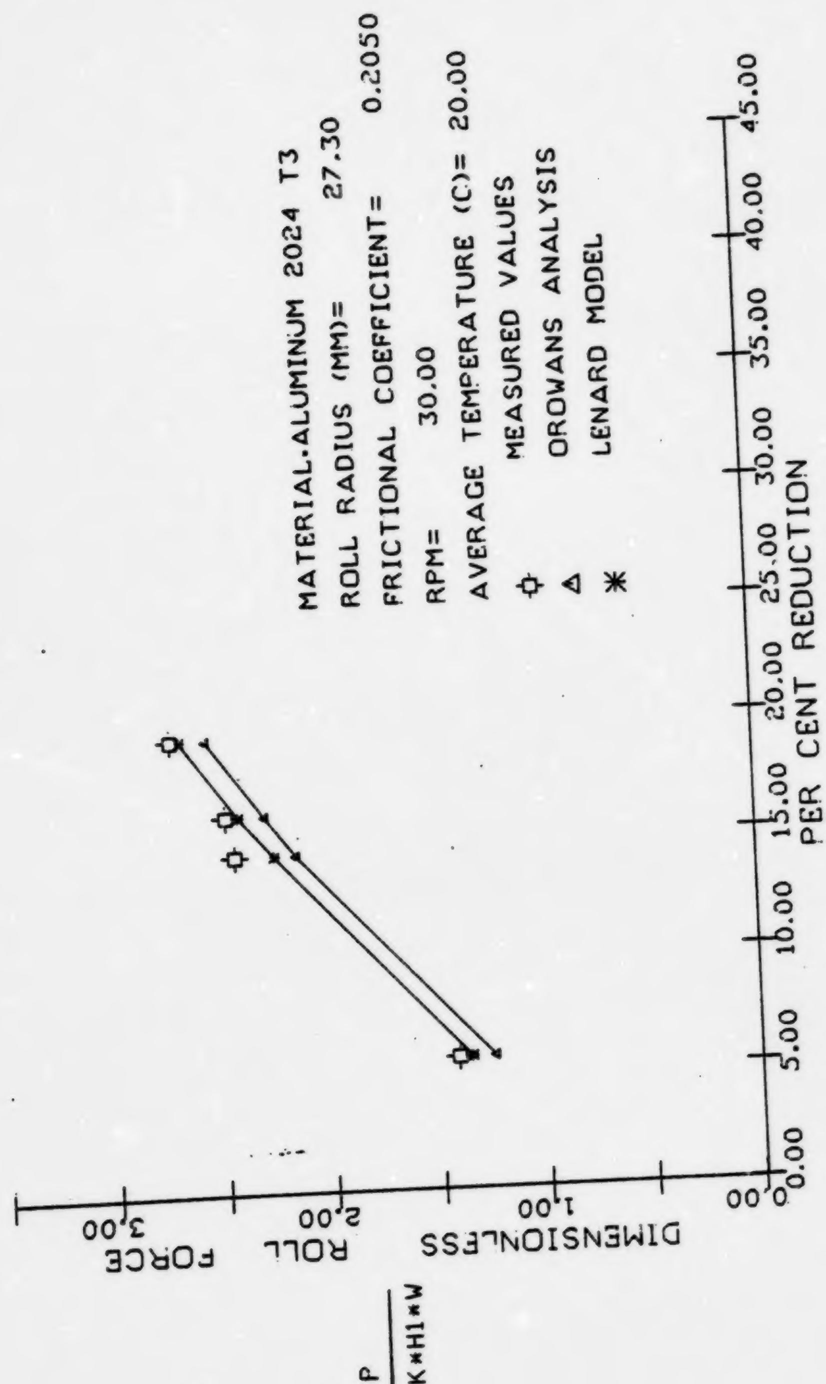
MATERIAL.ALUMINUM 2024 T3
ROLL RADIUS (MM)= 27.30
FRICTIONAL COEFFICIENT= 0.2050
RPM= 30.00
AVERAGE TEMPERATURE (C)= 20.00
MEASURED VALUES
OROWANS ANALYSIS
LENARD MODEL
DIMENSIONLESS ROLL FORCE
P / 2K*H1*W
0.00
1.00
2.00
3.00
PER CENT REDUCTION
0.00
5.00
10.00
15.00
20.00
25.00
30.00
35.00
40.00
45.00

FIGURE 56

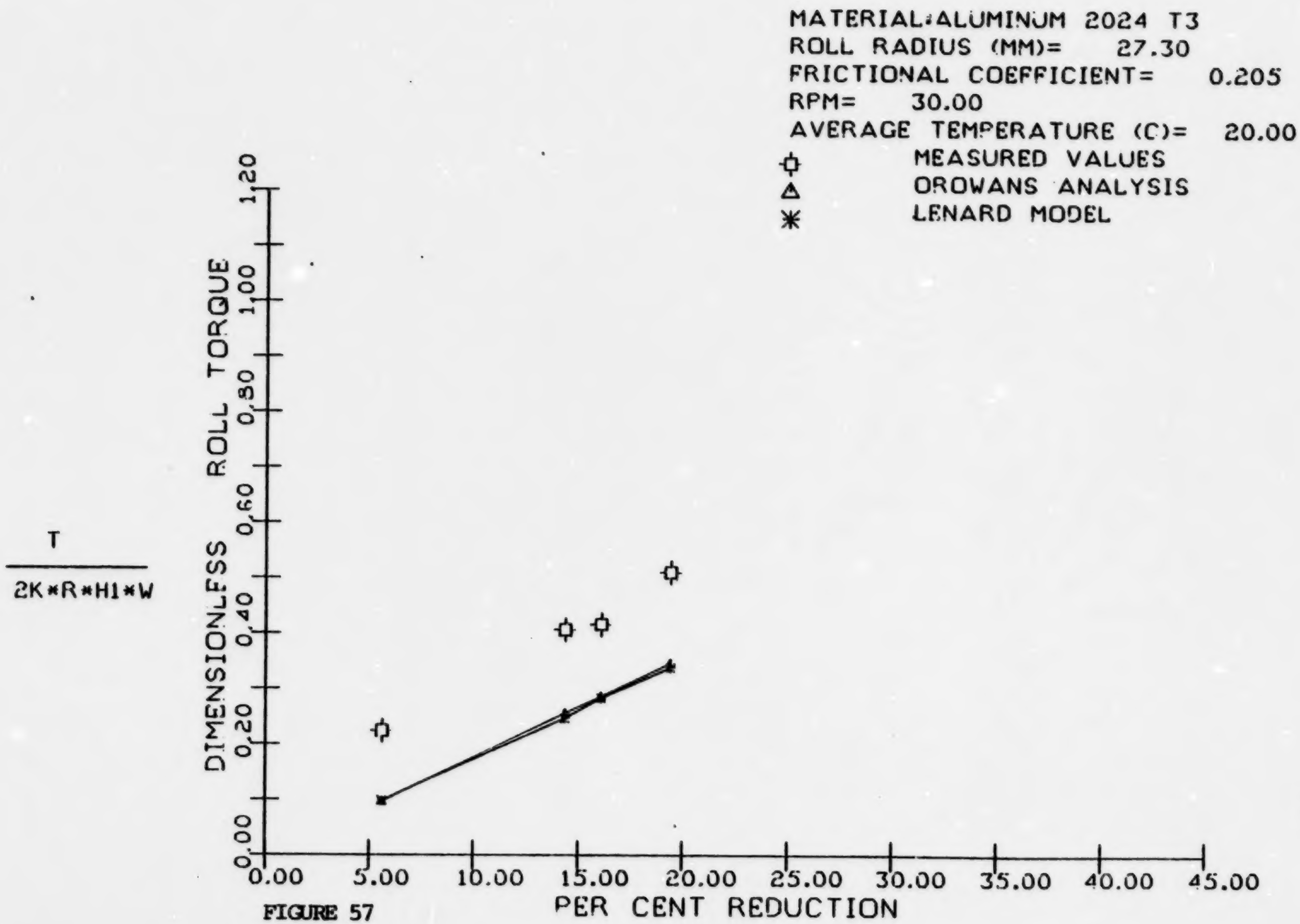
MATERIAL:ALUMINUM 2024 T3
ROLL RADIUS (MM)= 27.30
FRICTIONAL COEFFICIENT= 0.205
RPM= 30.00
AVERAGE TEMPERATURE (C)= 20.00
MEASURED VALUES
OROWANS ANALYSIS
LENARD MODEL
T / 2K*R*H1*W
DIMENSIONLESS ROLL TORQUE
0.00
0.20
0.40
0.60
0.80
1.00
1.20
0.00
5.00
10.00
15.00
20.00
25.00
30.00
35.00
40.00
45.00
PER CENT REDUCTION

FIGURE 57

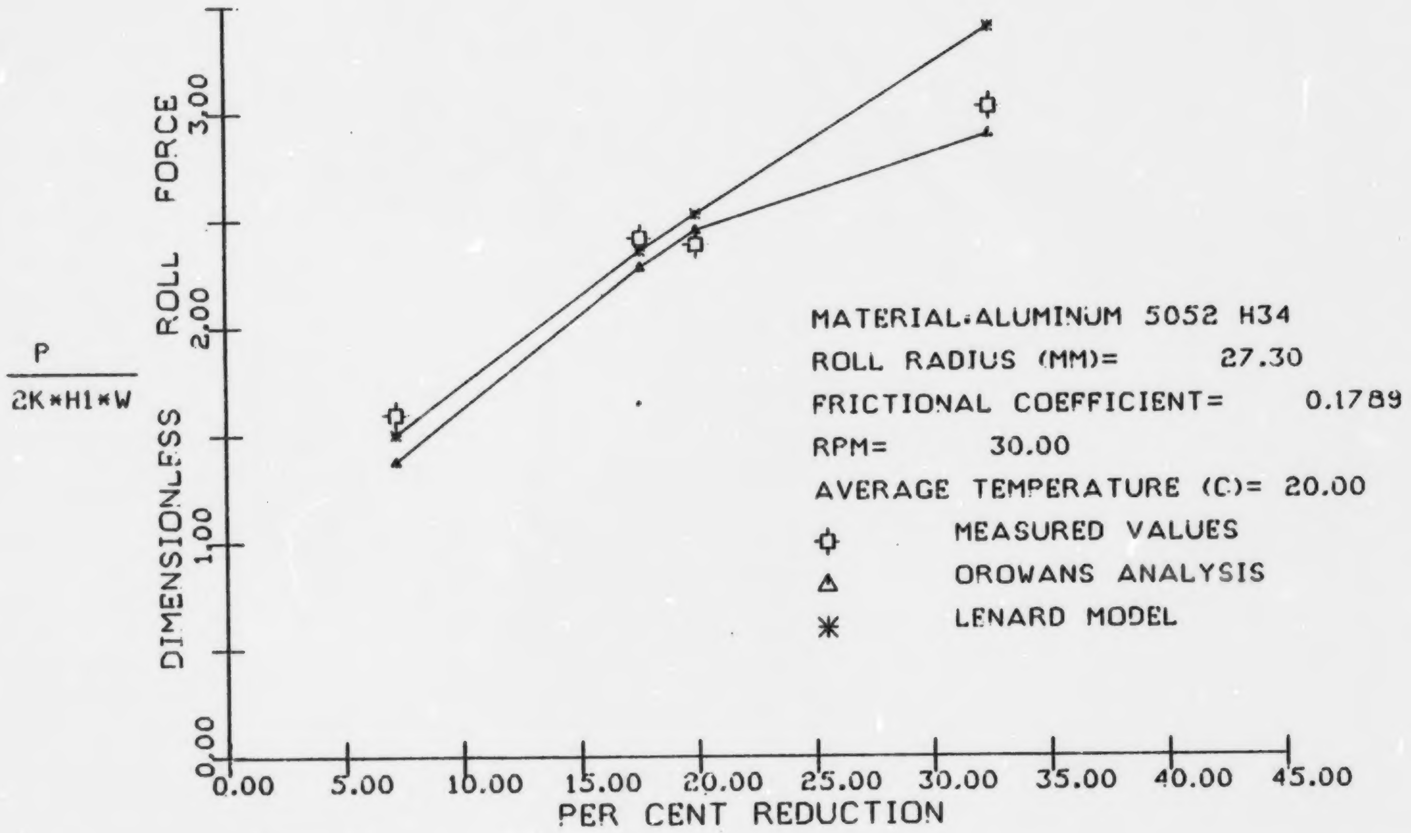
P / 2K*H1*W
DIMENSIONLESS ROLL FORCE
0.00
1.00
2.00
3.00
0.00
5.00
10.00
15.00
20.00
25.00
30.00
35.00
40.00
45.00
PER CENT REDUCTION
MATERIAL:ALUMINUM 5052 H34
ROLL RADIUS (MM)= 27.30
FRICTIONAL COEFFICIENT= 0.1789
RPM= 30.00
AVERAGE TEMPERATURE (C)= 20.00
MEASURED VALUES
△ OROWANS ANALYSIS
✳ LENARD MODEL

FIGURE 58

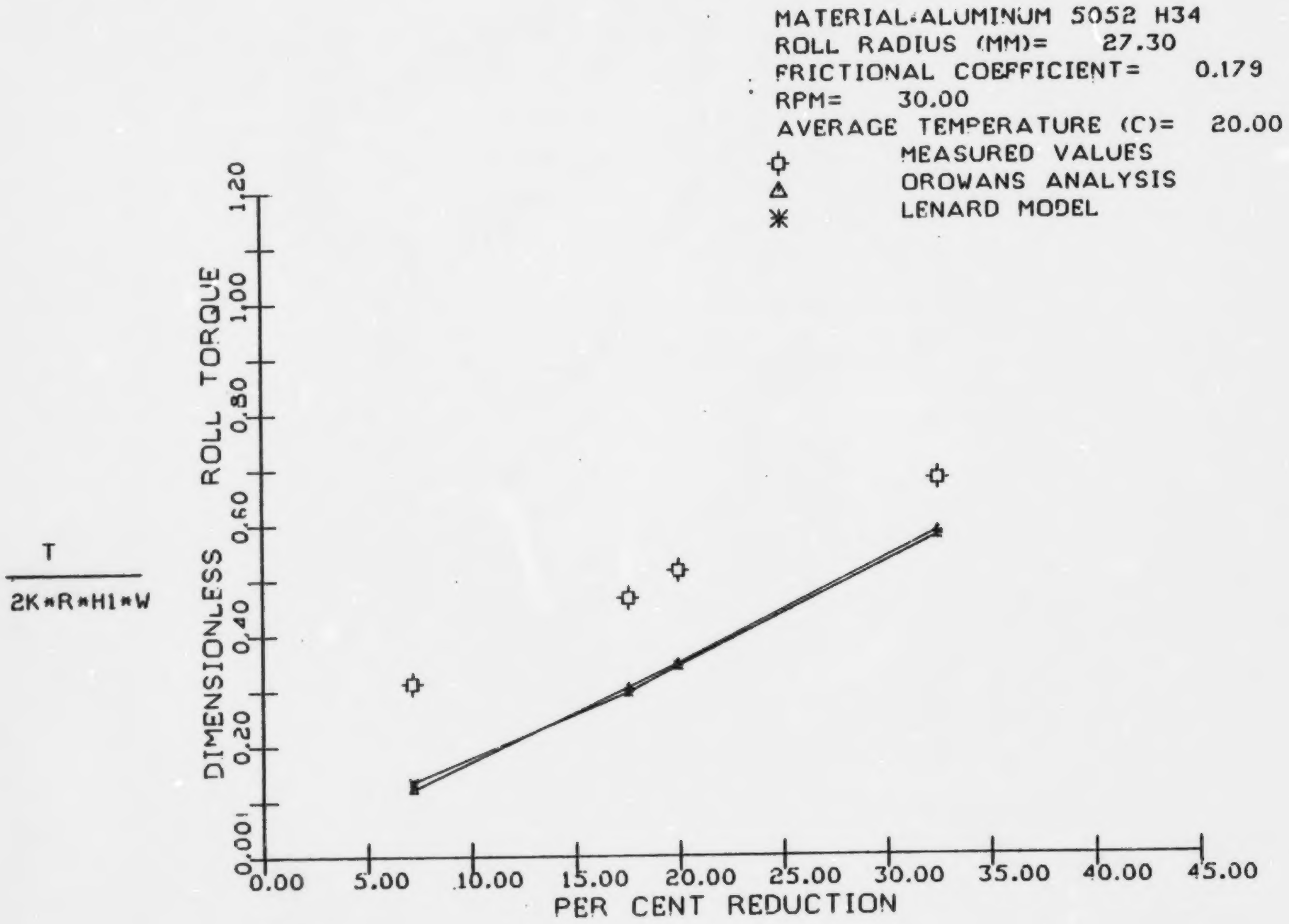
MATERIAL:ALUMINUM 5052 H34
ROLL RADIUS (MM)= 27.30
FRICTIONAL COEFFICIENT= 0.179
RPM= 30.00
AVERAGE TEMPERATURE (C)= 20.00
MEASURED VALUES
OROWANS ANALYSIS
LENARD MODEL
T / 2K*R*H1*W
DIMENSIONLESS ROLL TORQUE
0.00
0.20
0.40
0.60
0.80
1.00
1.20
0.00
5.00
10.00
15.00
20.00
25.00
30.00
35.00
40.00
45.00
PER CENT REDUCTION

FIGURE 59

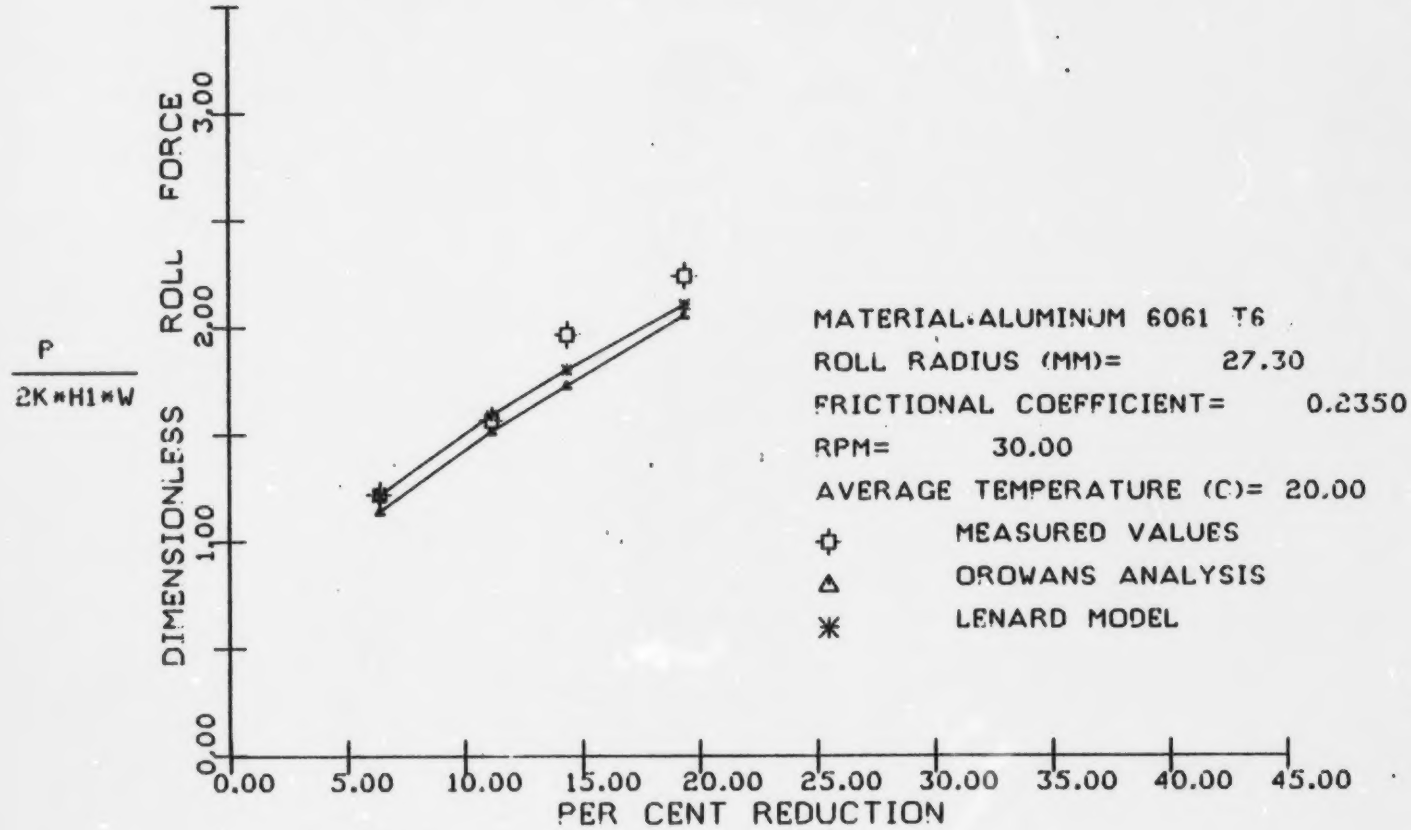
P / 2K*H1*W
DIMENSIONLESS ROLL FORCE
0.00
1.00
2.00
3.00
0.00
5.00
10.00
15.00
20.00
25.00
30.00
35.00
40.00
45.00
PER CENT REDUCTION
MATERIAL:ALUMINUM 6061 T6
ROLL RADIUS (MM)= 27.30
FRICTIONAL COEFFICIENT= 0.2350
RPM= 30.00
AVERAGE TEMPERATURE (C)= 20.00
MEASURED VALUES
OROWANS ANALYSIS
LENARD MODEL

FIGURE 60

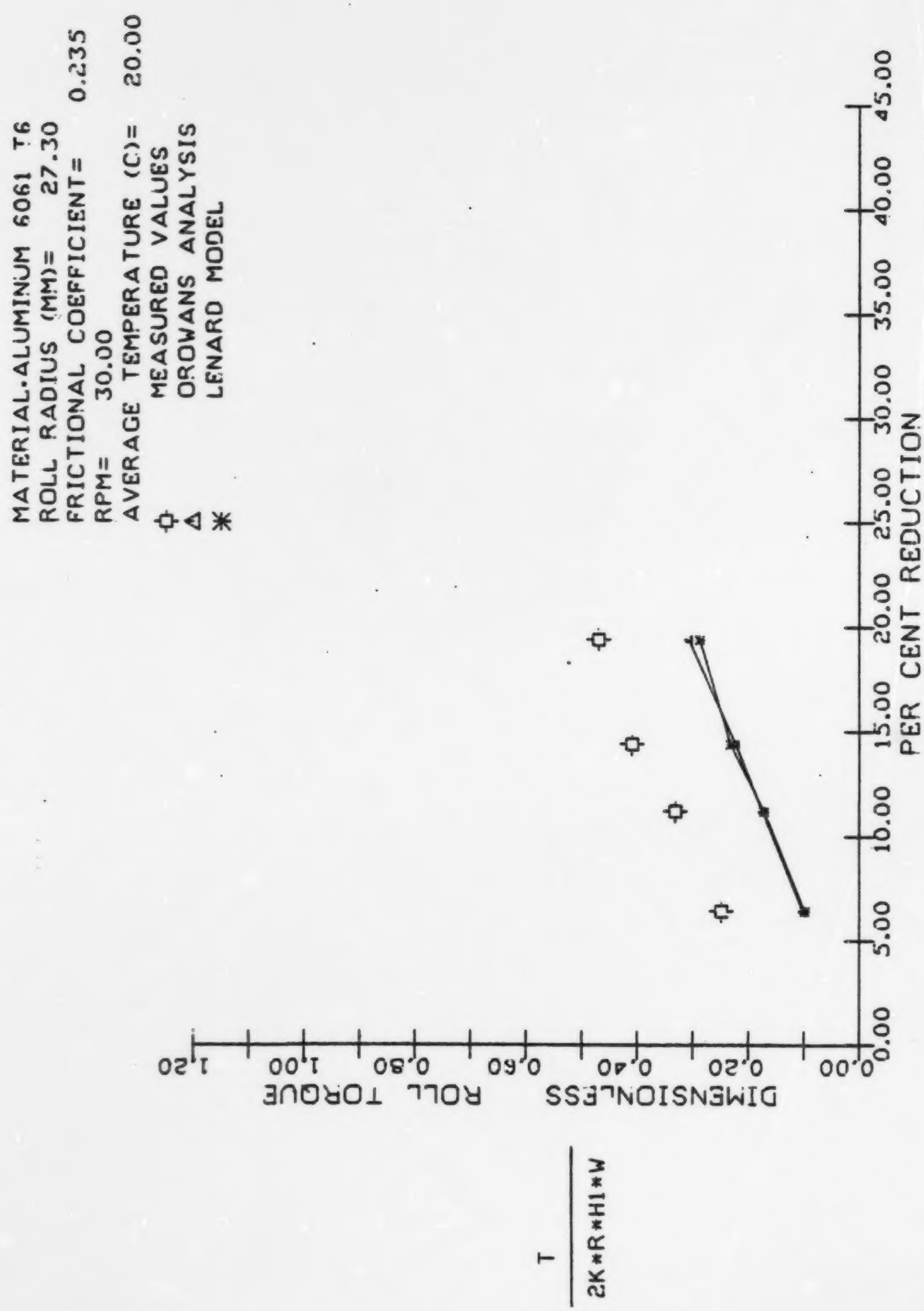
MATERIAL.ALUMINUM 6061 T6
ROLL RADIUS (MM)= 27.30
FRICTIONAL COEFFICIENT= 0.235
RPM= 30.00
AVERAGE TEMPERATURE (C)= 20.00
⌑ MEASURED VALUES
△ OROWANS ANALYSIS
✳ LENARD MODEL
T / 2K*R*HI*W
DIMENSIONLESS ROLL TORQUE
0.00
0.20
0.40
0.60
0.80
1.00
1.20
PER CENT REDUCTION
0.00
5.00
10.00
15.00
20.00
25.00
30.00
35.00
40.00
45.00

FIGURE 61

RESULTS: Measured and nondimensionalized roll force and torque values are plotted versus % reduction and the predictions of Orowan's and Lenard's models are shown in Figures 54 and 55 for Aluminum 1100-T0*, in Figures 56 and 57 for Aluminum 2024-T3, in Figures 58 and 59 for Aluminum 5052-H34 and in Figures 60 and 61 for Aluminum 6061-T6. In all, squares denote the experimental values, the triangles indicate Orowan's theory and the stars refer to the Lenard model. A general conclusion regarding all of these plots is the observation that both Orowan's and Lenard's predictions are within the "ballpark". The use of accurate flow curves and frictional coefficients affected both analyses by approximately the same amount.

The value of the more refined model becomes apparent when use is made of the detailed data developed in References [136] and [137]. Figures 62 and 63 give the measured roll pressures and the frictional coefficients as functions of the roll gap angle for 22.35% reduction of 1100-T0 Aluminum and for 7.53% reduction of 5052-H34 Aluminum. When the coefficient of friction values are digitized and included in the Lenard model, noticeable improvements in the predictive capabilities are observed. See below where the nondimensionalized roll force values are compared:

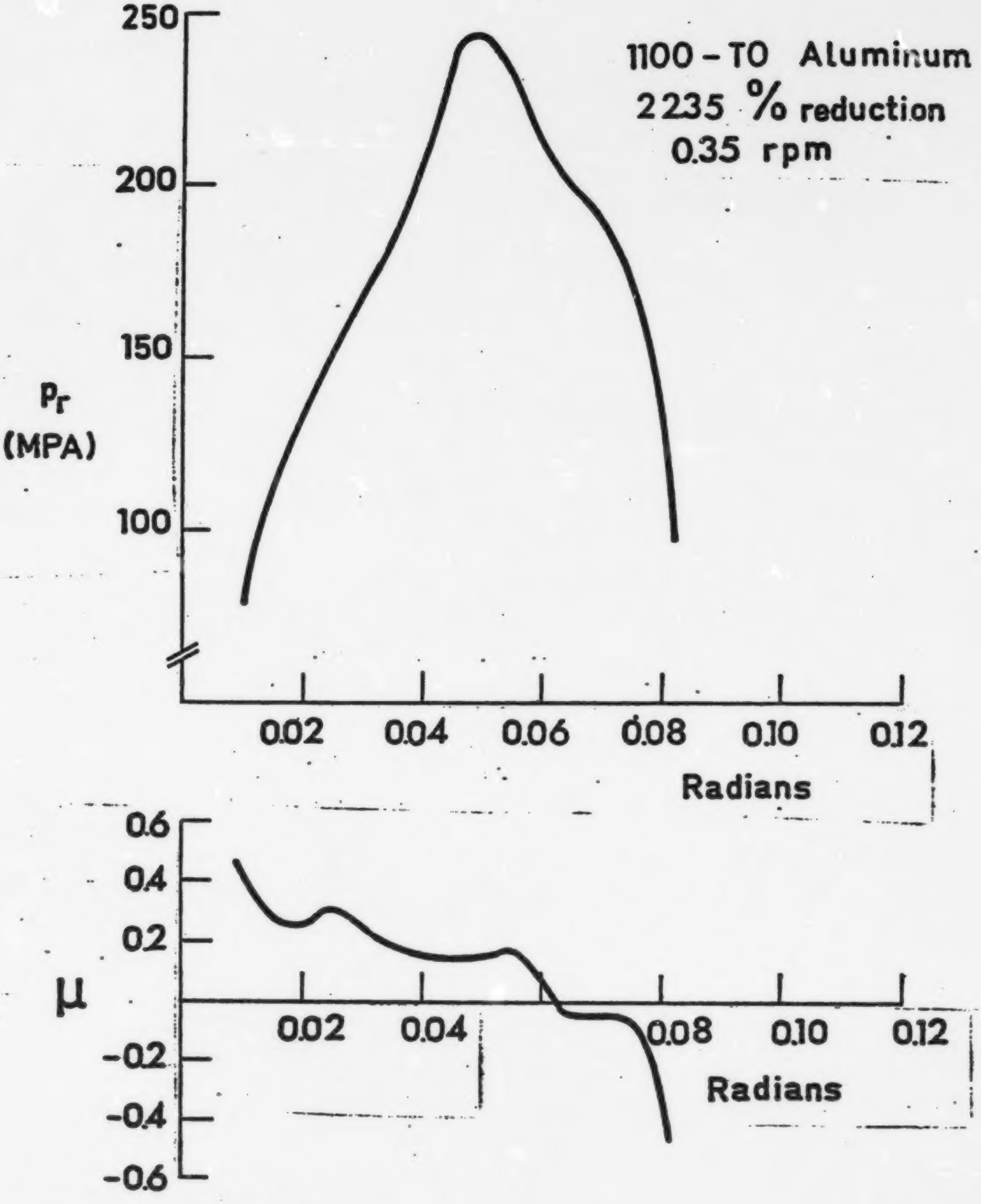
1100 - TO Aluminum
2235 % reduction
0.35 rpm
250
200
150
100
P_r
(MPA)
0.02
0.04
0.06
0.08
0.10
0.12
Radians
0.6
0.4
0.2
μ
-0.2
-0.4
-0.6
0.02
0.04
0.08
0.10
0.12
Radians

FIGURE 62

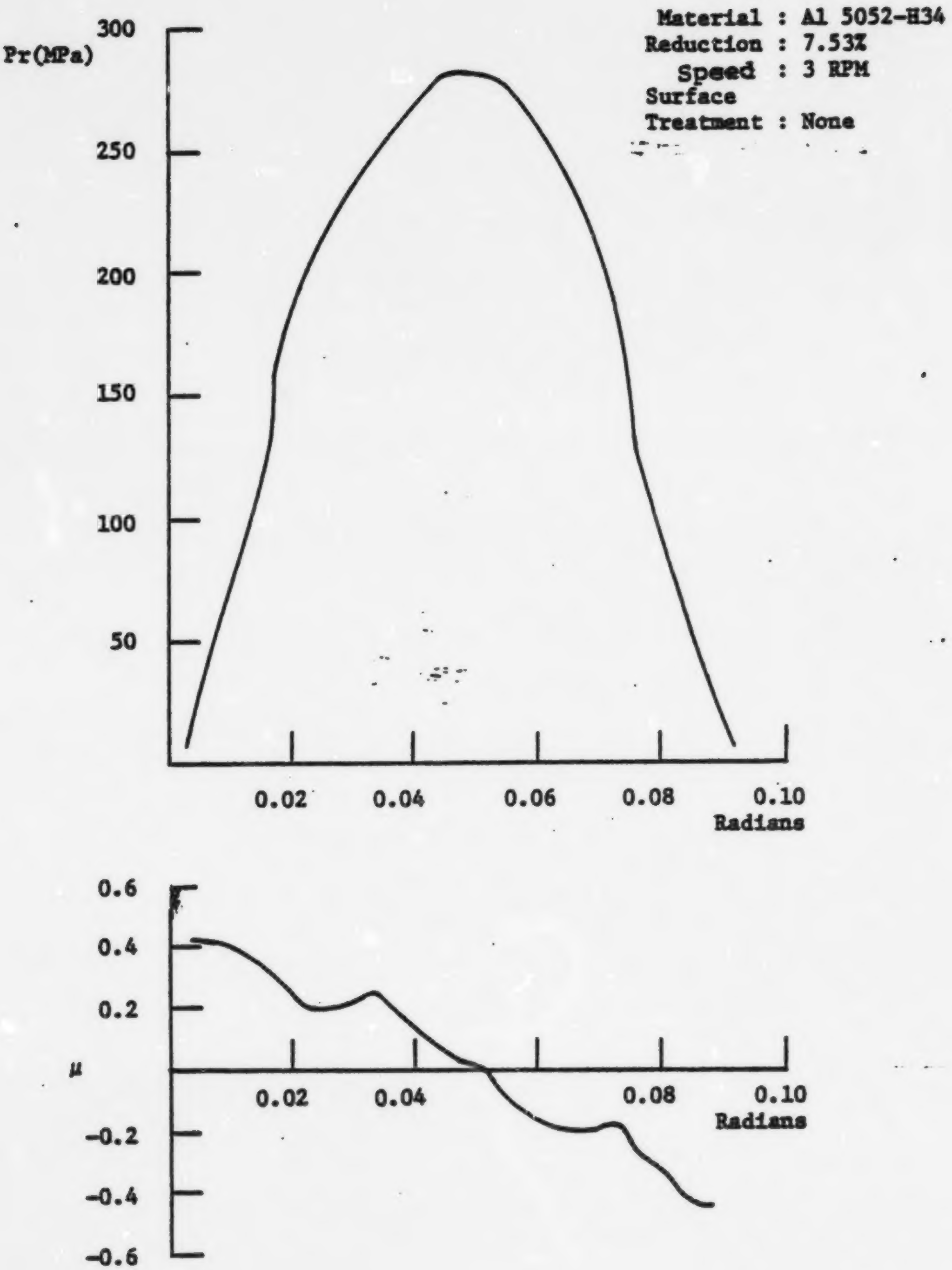
Material : Al 5052-H34
Reduction : 7.53%
Speed : 3 RPM
Surface
Treatment : None
Pr(MPa)
300
250
200
150
100
50
0.02
0.04
0.06
0.08
0.10
Radians
0.6
0.4
0.2
μ
-0.2
-0.4
-0.6
0.02
0.04
0.08
0.10
Radians

FIGURE 63

	F (exp)	F (Orowan)	F(Lenard)	F [Lenard, $\mu = \mu(\phi)$]
Al 1100-TO	2.198	3.210	3.236	2.6203
Al 50520H34	1.598	1.379	1.505	1.5934

* The coefficients of friction in Figures 54 and 55 are:
0.18 (10%); 0.22 (22%); 0.27 (31%); 0.31 (43%).

Conclusions

Since the detailed results were reviewed and discussed in the body of this chapter, only general conclusions will be given here.

In comparing the predictions of the Orowan and the Lenard models to measurements in 13 hot rolling and 16 cold rolling experiments, both models were found to be adequate. The use of accurate flow strength data did not result in enhanced predictions. The use of accurate friction data did result in better roll force predictions in two instances.

The writer believes that it is premature to extend the validity of the above conclusions any further unless a thorough statistical analysis of a large number of measurements and predictions confirms them. It is strongly felt that one-to-one comparison cannot replace an investigation of standard deviations and means of differences between measured and comsputed values.

Further, there is a significant lack of knowledge of the appropriate material model to be chosen for hot deformation of microalloyed steels. The technique used in this report is probably adequate but it should be compared to other, equally adequate methods. Some possibilities to consider include development of empirical relations--but, of course, of what form?--or the development of databanks where material parameters are stored in multidimensional arrays and are retrieved when required.*

Finally, the advantage of using a variable coefficient of friction in predictions was demonstrated in cold rolling of two aluminum alloys.

It is recommended that the predictive capabilities of the Lenard model be tested in a statistical treatment of production data, obtained in cold rolling of hard materials, with large R/h ratios. It is known that Orowan's model does not converge for $R/h \gg 1$ and $Y_o \gg 1$; it has been shown that the Lenard model does.

---

*A feasibility study along these lines is being formulated by Energy Technology Consultants, Ltd., UNB and Professors Alexander, Kaftanoglu, Lange, von Turkovich and Lenard. As well, the statistical analysis of Reference [135] is being extended with funding from an NSERC Strategic grant at UNB.

CHAPTER 9

DISCUSSION AND CONCLUSIONS

Introduction

In this chapter the information presented thus far will be reviewed in the context of the following headings:

i. Availability of the information for use in modelling;
ii. Potential of existing mathematical models for on-line control;
iii. Directions for further research.

Availability of the information for use in modelling

As pointed out above, the components of a steady state, quasi-static mathematical model for flat rolling include:

i. Equations of motion of the rolled strip;
ii. Elastic deformation of the work rolls;
iii. Material properties of the strip;
iv. Initial/boundary conditions.

In the present writer's opionion, the two most important aspects in hot rolling are the material's resistance to deformation and interfacial friction.

Other than a few empirical formulae given in Reference [99], no reliable, general information regarding friction is available. The choice of a coefficient of friction for a particular case of metal-metal or metal-lubricant-metal contact is still one of "informed guess". References [49], [51], [136] and [137] have given specific information on the values of the frictional coefficient for a few selected materials. More of that type of information would be necessary to remove μ from the status as one possible "cook factor".

The picture is even more muddy when friction in hot rolling is considered. The usual approach is to assume that sticking friction exists.In the experience of the writer, however, a coefficient of friction of 0.3 was found to give good results during hot rolling of microalloyed steels. In general, no detailed information regarding the dependence of friction on process parameters has been presented as yet.

Similar doubts regarding the availability of reliable data on the material's resistance to deformation exist.

Multitudes of publications can be found regarding hot strength of metals. Close examination of the data, however, reveals some contradictions. For example, considering AISI 1015 steel at 1200°C, subjected to a strain of 50% at a strain rate of 20 $\sec^{-1}$, Shida [94] predicts the flow strength to be 97 MPa, Altan and Boulger [93] predict 78 MPa, Cornfield and Johnson [97] give 7 MPa, while Wusatowski [99] prescribes 34 MPa. For other process parameters, the data calculated are similarly inconsistent.

When the rest of the parameters, listed in Chapter 3 are considered,some further gaps are observed.

Theories of anisotropy do not appear to be of use when modelling of cold rolling is attempted. Mill dynamics and chatter, minimum rollable thickness, material properties in the softening/steady state range, looper dynamics and heat transfer problems have not yet been combined even to give a complete formulation of the flat rolling problem.

In summary, however, the question "Should one bother to include these parameters in a 'complete' model?" is difficult to answer. The questioner would have to define the accuracy required. In light of some experimental results presented in Chapter 7, a tentative answer would have to admit that while some improvements in predictive abilities are observed when more elaborate models are used, those improvements may not warrant the extra effort needed to produce them.

Potential for on-line control

Introduction

The three main attractions of digital computers are their ability to perform calculations at very high speeds, their usefulness in data acquisition and in process control.

Calculations may be performed by using "programs"; these are sets of instructions on how and in what order certain computations are to be completed.

Data acquisition is achieved by the use of analogue to digital converters and transducers; analogue voltages generated by the transducers are transformed into a discrete set of values which are measured at certain, very short, intervals. These are then displayed and/or stored and/or manipulated.

Process control is done through digital to analogue converters--preprogrammed or calculated voltages are transformed into "continuous" signals which in turn operate stepping motors, switches, valves, etc.

It is a combination of these three functions that one makes use of in order to automate metal forming equipment.

A paragraph from the document "Research Needs in Mechanical Systems--Report of the Select Panel on Research Goals and Priorities in Mechanical Systems" [Reference [139]) needs to be quoted here:

> Major opportunities for computer integration exist in at least four major areas of mechanical systems:
>
> - First is the design and manufacture of products and systems, where the computer has the potential for integration and optimization of the entire process from conceptual design through manufacture and quality assurance to the marketplace. Only elementary steps have been taken (i.e. CAD/CAM systems) in some of the largest industries toward full integration. Major improvements in industrial productivity and product quality lie in this area.
>
> - Second is the realization of intelligent machines and products which the next generation of integrated circuits (VLSI) will make possible. Machines which have vision, touch and speech, and at least elementary powers of reasoning are included.
>
> - Third is the integration of computers with humans in ways which take best advantage of the capabilities of both; for example, coupling the conceptual and judgmental abilities of humans with the analytical, computational and memory power of computers.
>
> - Fourth is the integration of computers into the educational process at all levels from the computer-interactive textbook to the use of sophisticated interactive graphics systems in design and manufacturing systems education.

While the authors of the cited report considered the U.S.A., their conclusions are equally valid for Canada.

Computer control is indicated when the following process conditions prevail:

(1) Complex calculations and decisions are required that exceed both the operator's capabilities and his ability to react sufficiently fast.

(2) A large number of simple comparisons and decisions are required, but corrective action must be made quickly.

(3) A large amount of operating data and summarizing information is required for operational reasons.

Probably the most thorough description of computer application to hot strip rolling is present by MacAlister and Eades [140]. In their introduction they state:

> A modern high-production hot-strip mill represents an anormous capital investment. The economic climate in the developed countries penalizes inefficiently deployed capital, and more sophisticated world-wide customer requirements dictate ever-improving quality targets for strip products. It is only by the use of advanced automation techniques that these targets can be met. Computer automation, has, therefore, risen in status from being a useful addition to being an essential component for production and process control.

In general, a predictive-adaptive computer program for the control of a hot strip mill would perform the following functions:

1) When the required billet temperature in the reheat furnace is reached and the rougher is ready, the furnace doors are automatically opened and the billet slides on the skids to the conveyor.
2) Depending on the material to be rolled and the capabilities of the rougher, the roughing sequence is decided and the roughing schedule is set up, including control of edgers and watersprays.
3) Depending on the temperature of the strip exiting from the rougher, on the finishing gauge and temperature, the finishing schedule is set up and when the finishing train is ready, the sequence begins.
4) The development of temperature is monitored, its effect on the flow strength--and on the roll force and torque--is calculated, and roll gaps are changed accordingly.
5) If required, the cooling sprays are turned on before coiling.

Details of these computer schemes are closely guarded by steel companies.

Mathematical models in on-line control

It is difficult to arrive at definitive conclusions regarding the potential use of the Lenard Model for on-line control of strip mills, based on the results of 13 hot rolling and 16 cold rolling experiments. The statistical analysis, as performed in Reference [135] ought to be repeated using the model before a final recommendation could be made with confidence. The difficulties, as seen by this writer, include the following:

i. There are no established and reliable means of representing the flow curves of micro-alloyed steels.
ii. There is little understanding of the nature of friction in hot strip rolling.
iii. In an experimental rolling mill, simulation of events at the finishing mill, while possible, may be problematic.
iv. The time required for computation would be large. In Reference [135], over 100 hours of CPU time were used.

Note that as pointed out in several footnotes, work on these problems is now beginning at the Manufacturing Processes Laboratory at UNB, under funding by an NSERC Strategic grant.

Directions for future research

It is believed that understanding the following problems may lead to improved productivity of steel mills as well as to better quality products. Discussion of the items included in the list presented below is invited.

1. Representation of the material's resistance to deformation for use in metal forming analyses.
2. History dependence of flow curves in multistage deformation.
3. Evaluation of the accuracy of flow curves.
4. Friction at high temperatures.
5. Statistical analysis of predictive capabilities of the Lenard Model.
6. Comparison of the predictive capabilities of finite element models and the Lenard Model.
7. Development of databanks for use in metalforming analyses.
8. Representation of a functional form for the coefficient of friction in terms of material and process parameters.
9. Mill stretch and mill dynamics.
10. Mill chatter.
11. Temperature distribution in the rolled product during rolling.

REFERENCES

1. Backofen, W.A., Deformation Processing, Addison-Wesley, Reading, Mass., 1972.
2. Geleji, S., A Fémek Kèplèkeny alakitàsànak elmèlete, Akadèmiai Kiadò,Budapest, Hungary, 1967.
3. Hosford, W.H. and Caddell, R.M., Metalforming: Mechanics and Metallurgy, Prentice Hall Inc., Englewood Cliffs, N.J., 1983.
4. Hoffman, O., and Sachs, G., Introduction to the Theory of Plasticity for Engineers, McGraw Hill, New York, 1953.
5. Rowe, G.W., Principles of Industrial Metal Working Processes, Edward Arnold, London, England, 1977.
6. Avitzur, B., Metal Forming: Processes and Analysis, McGraw Hill, New York, 1968.
7. Hill, R., The Mathematical Theory of Plasticity, Oxford, 1967.
8. Johnson, W., Sowerby, R., Haddow, J.B., Plane Strain Slip Line Fields, Edward Arnold, London, England, 1970.
9. Owen, D.R.J., and Hinton, E., Finite Elements in Plasticity, Pineridge Press, Swansea, U.K., 1980.
10. Thompson, W., and Denmeade, K., 1st ICTP, Tokyo, 1984, p. 291.
11. Suzuki, H., Yokouchi, Y., Murata, M., and Negishi, H., 1st ICTP, Tokyo, 1984, p. 367.
12. Wenner, M.L., 1st ICTP, Tokyo, 1984, p. 654.
13. Chung, K., and Lee, D., 1st ICTP, Tokyo, 1984, p. 660.
14. Nakamachi, E., and Sowerby, R., 1st ICTP, Tokyo, 1984, p. 666.
15. Iseki, H., and Murota, T., 1st ICTP, Tokyo, 1984, p. 678.
16. Kobayashi, S., 1st ICTP, Tokyo, 1984, p. 1035.
17. Zienkiweicz, O.C., Nakazawa, S., and Vilotte, J.P., 1st ICTP, Tokyo, 1984, p. 1041.
18. Oh, S.I., Tang, J.P., and Badawy, A., 1st ICTP, Tokyo, 1984, p. 1051.
19. Kihara, J. and Ishii, K., 1st ICTP, Tokyo, 1984, p. 1059.
20. Kiefer, B.V., 1st ICTP, Tokyo, 1984, p. 1116.
21. Varita, I., Mallett, L., and Lee, E.H., 1st ICTP, Tokyo, 1984, p.1126.
22. Kirakawa, T., Fujita, F., Kamata, M., and Yamada, Y., 1st ICTP, Tokyo, 1984, p. 1132.
23. Pawelski, O., Rasp, W., and Teutsch, H., 1st ICTP, Tokyo, 1984, p. 1146.

24. Schey, J.A., Introduction to Manufacturing Processes, McGraw Hill, New York, 1977.
25. Sims, R.B., Proc. I. Mech. E., 168, 1954, p. 191.
26. Ford, H., and Alexander, J.M., Journal of the Institute of Metals, 92, 1964, p. 397.
27. Orowan, E., Proc. I. Mech. E., 150, 1943, p. 141.
28. Alexander, J.M., Proceedings of the Royal Society of London, A236, 1972, p. 535.
29. Rabinowicz, J.E., Friction and Wear of Materials, John Wiley & Sons, New York, 1965.
30. Mokhtar, M.O.A., Zaki, M., and Shawki, G.S.A., Wear, 65, 1980, p. 29.
31. Tabor, D., ASME Journal of Lubrication Technology, 103, 1981, p. 169.
32. Schey, J.A., J. Metals, 33, 1980, p. 28.
33. Plevy, T.A.H., Wear, 58, 1979, p. 1.
34. Al-Rubeye, H.S., ASME Journal of Lubrication Technology, Paper No. 79-Lub-28.
35. Koura, M.M., and Omar, M.A., Wear, 73, 1981, p. 235.
36. Kuhlmann-Wilsdorf, D., J. Metallkunde, 72, 1981, p. 832.
37. Woo, K.L., and Thomas, T.R., Wear, 58, 1979, p. 331.
38. Mokhtar, M.O.A., Wear, 72, 1981, p. 287.
39. Tabata, T., and Masaki, S., Int. J. Mech. Sci., 20, 1978, p. 505.
40. Kaftanoglu, B., Wear, 25, 1973, p. 177.
41. Ghosh, A.K., Int. J. Mech. Sci., 19, 1977, p. 457.
42. Klamecki, B.E., Wear, 63, 1980, p. 113.
43. Phan-Thien, N., ASME Journal of Applied Mechanics, 48, 1981, p. 438.
44. Nadai, A., ASME J. Appl. Mech., 61, 1939, p. A54.
45. Siebel, E., and Lueg, W., Mitt. K.W. Inst. Eisenf. 15, 1933, p. 14.
46. Underwood, L.R., The Rolling of Metals, John Wiley and Sons, New York, 1950.
47. Hsu, Y.W., Proc. NAMRC VIII, 1980, Rolla, Missouri, p. 176.
48. McPherson, D.J., Metallurgical Transactions, 5, 1974, p. 2479.
49. Al-Salehi, F.A.K., Firbank, T.C., and Lancaster, P.B., Int. J. Mech. Sci., 15, 1973, p. 693.
50. Lenard, J.G., Proceedings of COBEM 81, Brazil, 1981, p. 13.
51. Van Rooyen, G.T., and Backofen, W.A., Journal of the Iron and Steel Institute, 186, 1957, p. 235.
52. Banerji, A., and Rice, W.B., CIRP Annals, 21, 1972, p. 53.
53. Cole, I.M., and Sansome, D.H., MTDR,1968, pp. 271-286.
54. MacGregor, C.W., and Palme, R.B., ASME, J. Appl. Mech., 1948, 70, p. 297.

55. Muzalevskii, O.G., and Grishkov, A.I., Izvest. VUZ. Mashinostroenie, II, 1959, p. 82.
56. Keller, J.D., Blast Furnace and Steel Plant, 25, 1937, p. 1110.
57. Stone, M.D., Iron and Steel Engineer, 30, 1953, p. 61.
58. Tong, K., and Sachs, G., J. Mech. Phys. Solids, 6, 1957, p. 35.
59. Ford, H., and Alexander, J.M., J. Inst. Metals, 88, 1959-69, p. 193.
60. Hill, R., and Longman, I.M., Sheet Metal Industry, 28, 1951, p. 134.
61. Roberts, W.L., Iron and Steel Eng. Year Book, 1965, p. 925.
62. Huggins, P.J.G., J. Inst. Metals, 96, 1966, p. 238.
63. Kuhn, H.A. and Weinstein, A.S., ASME, Journal of Lubrication Technology, 93, 1971, p. 331.
64. Roberts, W.L., Cold Rolling of Steel, Marcel Dekker, Inc., New York, 1978.
65. Horvath, A., and Vero, B., Kohaszat, 101, 1968, p. 213.
66. Pawelski, von O., and Kadding, G., Stahl und Eisen, 87, 1967, p. 1340.
67. Yokote, Y., and Nomura, S., J. Inst. Metals, 88, 1959-60, p. 241.
68. Barrett, C.S., and Bassalski, T.B., Structure of Metals, McGraw Hill, New York, 1966.
69. Betten, J., Archiv fur das Eisenhuttenwesen, 46, No. 5, 1975, p. 317.
70. Lankford, W.T., Snyder, S.C., and Bauscher, J.A., Steel, 125, 1949, p. 82.
71. Hitchcock, J.H., Report of ASME Research Committee on Roll Neck Bearings, 1935.
72. Jortner, D., Osterle, J.F., and Zorowski, C.F., Iron and Steel Eng. Yearbook, 1958, p. 403.
73. Michell, J.H., Proc. London Math. Soc., 1900, p. 44.
74. Golten, J.W., Ph.D. Dissertation, U. of Wales, Swansea, 1969.
75. Grimble, J.J., GEC J. Science & Technology, 43, 1976, p. 3.
76. Watanabe, Y., Sakamoto, H., and Hari, H., Bulletin of the JSME, 15, 1972, p. 1041.
77. Kobasa, D., and Schultz, R.A., Iron and Steel Engng., 45, 1968, p. 97.
78. Thomsen, E.G., Shabaik, A.H., and Sohrabpour, S., ASME J. Engng. Mat. & Tech., 99, 1977, p. 252.
79. Marion, R.H., J. Testing and Evaluation, 6, 1978, pp. 3-8.
80. Nicholas, T., Exp. Mechanics, 21, 1981, p. 177.
81. McQueen, H.J., and Jonas, J., Proceedings of the Symposium of the Relation Between Theory and Practice in Metal Forming, Plenum Press, New York, 1970, p. 393.

82. Stewart, M.J., Can. Met. Quarterly,13,1974, p.503.
83. Luton, M.J.,Immarigeon,J-P., and J.J.Jonas, J. Physics, 7,1974, p. 862.
84. Douglas, J.R. and Altan, T., ASME J. Eng. Ind.,97,1975, p. 66
85. Suzuki, H. et al. U. of Tokyo Reprt, 18, 1968, p. 139.
86. Watts, A.B. and Ford, H., Proc. I.Mech. E.,81,1952, p.448.
87. Weinstein, A.S., and Matsufuji, A., Iron & Steel Inst.,45, 1968, p. 121.
88. Cook, M. and Larke, E.C., J. Inst. Metals,71,1945,p.371.
89. Gelin, J.C., Oudin, J. and Ravalard, Y., J. Mech. Work. Techn.,5,1981,p.297.
90. Ellwod. S. and Griffiths, J.L., and Parry, D.J., J.Phys. E., 15,1982,p.280.
91. Ashby, M.F. and Verral, R.A., Acta Met., 21,1973,p.149.
92. Paton, N., ASME J. Eng. Mat. and Techn., 97,1975,p.313.
93. Altan, T. and Boulger, F.W., ASME J. Eng. Ind.,95,1973,p.1009.
94. Shida, S., Hitachi Lab.,Tokyo, 1974, p.1.
95. Gittins, A., Moller, R.H. , and Everett, J.R., BHP Tech. Bull., 18, 1974, p. 2.
96. Cook, P.M., and McCrum, A.W. BISRA, 1958.
97. Cornfield, G.C., and Johnson, R.H., J. Iron and Steel Inst., 211, 1973, p. 567.
98. Sellars, C.M., and Tegart, W.J. McG., Mem. Sci., Rev. Metall, LXIII, 1966, p. 731.
99. Wusatowski, Z., Fundamentals of Rolling, Pergamon Press, Oxford, 1969.
100. Hajduk, M., Hutn. Listy, 8, 1972, p. 567.
101. Alexander, J.M., "Plasticity Today," Udine, Italy, June, 1983.
102. Monaco, G., Iron and Steel Engineer, 54, 1977, p. 35.
103. Tlusty, J., Chandra, G., Critchley, S., and Paton, D., CIRP Annals, 31, 1982, p. 195.
104. Roberts, W.L., Proc. Int. Conf. Steel Rolling, 1980, p. 1215.
105. Moller, R., and Hoggart, R., Australian Inst. Metals, 12, 1967, p. 155.
106. Pickering, F.B., Proc. Int. Conf. Technology and Applications of HSLA Steels, Philadelphia, PA, 1983.
107. Bryant, G.F., and Chiu, T.S.L., Metals Technology, 9, 1982, p. 478.
108. Bryant, G.F., and Chiu, T. S. L., Metals Technology, 9, 1982, p. 485.
109. Bryant G.F., and Heselton, M.O., Metals Technology, 9, 1982, p. 469.
110. Sheppard, T., and Wright, D.S., Metals Technology, 7, 1980, p. 274.
111. Kannel, J.W. and Dow, T.A., J. Lub. Techn., 1974, p. 611.
112. Heedman, P. and Sjostrom, A., 23rd Mechanical Working and Steel Processing Cont., Pittsburg, 1981.

113. Heedman, P., Rutqvist, S.P. and Sjostrom, J.A., Metals Technology, 8, 1981, p. 352.
114. Lee, P.W., Sims, R.B., and Wright, H., J. Iron and Steel Inst., 1963, p. 270.
115. Sigalla, A., J. Iron and Steel Inst., 186, 1957, p. 90.
116. Roberts, W., Proc. Int. Conf. on the Technology and Applications of HSLA Steels, 1983, Philadelphia, p. 33.
117. Ouchi, C., Tanaka, J., Kozasu, I., and Tsukada, K., Micon 78, Philadelphia, 1979, p. 105.
118. Fegredo, D.M., Boyd, J.D., and Stewart, M.J., Proc. Int. Conf. on the Technology and Applications of HSLA Steels, 1983, Philadelphia, p. 95.
119. Heedman, P., Sjostrom, A., and Jarl, M., Proc. Int. Conf. on the Technology and Applications of HSLA Steels, 1983, Philadelphia, p. 121.
120. Fegredo, D.M., Parsons, D.E., Pollard, W.A. and Ng-Yelim, J., Can. Met. Quart., 22, 1983, p. 385.
121. Mano, J., Kato, T., Aoyagi, N. and Kuwagata, M., Proc. Int. Conf. on the Technology and Applications of HSLA Steels, 1983, Philadelphia, p. 287.
122. Carney, D.J., Trans. ASM, 46, 1954, p. 882.
123. Farren, W.S., and Taylor, G.I., Proc. Royal Soc., A107, 1925, p. 422.
124. Cerni, S., Weinstein, A.S. and Zorowski, C.F., Iron and Steel Eng., 1963., p. 165.
125. Wilmotte, S., Mignon, J., Economopoulos, M., and Thomas, G., C.R.M. No. 36, 1973, p. 35.
126. Pavlossoglou, J., Arch. Eisenhuttenwes., 52, 1981, p. 275.
127. Bishop, J.F.W., Q.J. Mech. and Appl. Math., IX, 1956, p. 236.
128. Lahoti, G.D., Shah, S.N., & Altan, T., J. Eng. Ind., 100,1978, p.159.
129. Hollander, F.,Iron and Steel Inst.,123,1970,p.46.
130. Seredynski, F., J. Iron and Steel Inst., 1973,p.197.
131. Bland, D.R. and Ford, H., Proc. I.Mech. E.,159,1948,p.144.
132. Roychoudhury, R. and Lenard. J.G., Proc.1st. ICTP.,Tokyo, 1984, p.1138.
133. D'Orazio, L.R., Mitchell, A.B. and Lenard, J.G.,HSLA 85, Beijing, (in press).
134. Baragar, D.L., and Crawley, A.F., J. Mech. Working Techn., 9,1984,p.291.
135. Murthy, A., and Lenard. J.G., J. Eng. Mat. & Techn., 104, 1982, p.47.
136. Lim, Lai-Seng and Lenard, J.G., J. Eng. Mat.& Techn., 106, 1984, p.139.
137. Karagiozis, A.N., and Lenard, J.G., Proc. Eurotrib 55, Lyon, 1985, p.2-13.
138. Hitchcock, J.H., ASME Research Report, 1935.
139. Research Needs in Mechanical Systems, Panel Steering Committee of NSF, J. Trib., 106,1984, p.2.
140. MacAlister, A.F. and Eades, C.G., GEC J. Sci. and Techn, 44,1978,p. 123.

141. Atreya, A. and Lenard, J.G., J. Eng. Mat. & Techn.,101, 1979, p.129.
142. Saeed, U. and Lenard, J.G., J. Eng. Mat. & Techn., 102, 1980, p.223.

APPENDICES

COMPUTER PROGRAMS - Orowan
Sims
Bland & Ford
Lenard

```
C            A L E X A N D E R   M O D E L
C
C
C
C          HOT ROLLING WITH SHIDA'S FLOW STRENGTH
C
C
      COMMON H2,RD,XMU,Z,B,HO,YO,XN,Q
      COMMON C,TEMP,VS,WW,EN,RPM,R,H1
      COMMON HPW,PMN
      COMMON AA
      EXTERNAL  G1,G2,G3,G4
      DIMENSION S(2002),SPHI(2002),SEX(2002),SEN(2002),
     1TAU(2002),XK(2002),SSIN(2002),GORD(2002),TAUSIN(2002),SCOS(2002)
    1 READ (5,38) E,XNU,YO,B,XN,LC
      IF (LC.NE.0) GO TO 27
   38 FORMAT (5F14.7,1X,I1)
      READ(5,2)M,XMU,R,HO,H1,H2,T1,T2
    2 FORMAT(I4,7F9.5)
      READ(5,99) TEMP,C,WW,RPM
   99 FORMAT(4F7.2)
C
C     TEST FOR SLAB ENTRY CONDITION,TO INCREASE H2 IF NECESSARY.
C
   53 H2MIN=H1-2.0*R*(1.0-COS(ATAN(XMU)))
      IF (H2.LT.H2MIN) H2=H2MIN
      RR=(H1-H2)/H1
      Z=2.0/SQRT(3.0)
C     TEST FOR MAGNITUDE OF TENSIONS,TO DECREASE THEM IF NECESSARY
      DRAFT=H1-H2
C
C     CALCULATE FLOW STRENGTH AT ENTRY AND EXIT
C     XXKK IS GIVEN BY A SUBROUTINE
C
      E11=HO/H1
      E12=HO/H2
      X2K1=XXKK(E11)
      X2K2=XXKK(E12)
      IF(T1.GT.X2K1) T1=X2K1
      IF(T2.GT.X2K2) T2=X2K2
      J=0
      M1=M-1
      K=M/102+1
      RL=SQRT(R*DRAFT)
      HM=(2.0*H2+H1)/3.0
      WRITE(6,3)
    3 FORMAT(1H1,30X,'ALL UNITS ARE IN TONS AND INCHES.',///7X,'E',14X,
     1'XNU',11X,'YO',10X,'B',16X,'XN',7X,'XMU',5X,'R',7X,'HO',7X,'H1',5X
     2,'H2',5X,'T1',5X,'T2'/)
      WRITE(6,41)E,XNU,YO,B,XN,XMU,R,HO,H1,H2,T1,T2
   41 FORMAT(5F14.7,7F8.4)
      A=XMU*RL/HM
      X2KM=(X2K1+2.0*X2K2)/3.0-(T1+T2)/2.0
      PAP=X2KM*RL*(EXP(A)-1.0)/A
      RD=R*(1.0+0.000334*PAP/DRAFT)
      P1=PAP
      TE1=T1
      TE2=T2
   11 PHI1=ARCOS(1.0-DRAFT/(2.0*RD))
      XM=M
      DPHI=PHI1/(XM-1.0)
      PHI=PHI1
C
C     XXK REPRESENTS THE FLOW STENGTH OF THE STRIP (2K)
C     IT IS GIVEN BY A SUBROUTINE
C     DXXK REPRESENTS D(2K)/DPHI; IT IS ALSO GIVEN BY A SUBROUTINE
C
      DO32I=1,M
      XK(I)=0.5*XXK(PHI)
   32 PHI=PHI-DPHI
      S(1)=(X2K1-TE1)/(1.0+XMU*TAN(PHI1))
      IF(XMU*S(1).GT.XK(1)) S(1)=X2K1-TE1-XK(1)*TAN(PHI1)
      S(M)=X2K2-TE2
      SEX(M)=S(M)
      PHI=0.0
C     FORWARD INTEGRATION TO DETERMINE SEN(I) AND SEX(I) USING THE
C     FOURTH ORDER RUNGE KUTTA PROCESS.
      Q=1.0
      DO 12 I=1,M1
      L=M+1-I
      IF(XMU*SEX(L).LT.XK(L)) CALL RUNGE(PHI,SEX(L),DPHI,DS,G1,G2)
      IF(XMU*SEX(L).GE.XK(L)) CALL RUNGE(PHI,SEX(L),DPHI,DS,G4,G3)
      SEX(L-1)=SEX(L)+DS
   12 PHI=PHI+DPHI
      SEN(1)=S(1)
      PHI=PHI1
      Q=-1.0
      DO 13 I=1,M1
      IF(XMU*SEN(I).LT.XK(I)) CALL RUNGE(PHI,SEN(I),DPHI,DS,G1,G2)
      IF(XMU*SEN(I).GE.XK(I)) CALL RUNGE(PHI,SEN(I),DPHI,DS,G4,G3)
      SEN(I+1)=SEN(I)+DS
   13 PHI=PHI-DPHI
C     FIND S(I),BEING THE SMALLER OF SEN(I) AND SEX(I) ACROSS THE ARC.
      DO 14 I=1,M
      IF(SEX(I).LE.SEN(I))  S(I)=SEX(I)
      IF(SEN(I).LE.SEX(I)) S(I)=SEN(I)
   14 CONTINUE
C     NOW DETERMINE PHIN AND SN.
      DO 15 I=1,M1
      IF(SEX(I).GE.SEN(I).AND.SEN(I+1).GE.SEX(I+1)) GO TO 16
   15 CONTINUE
      GO TO 24
   16 X=DPHI/(1.0+(SEX(I)-SEN(I))/(SEN(I+1)-SEX(I+1)))
      XI1=I+1
      PHIN=(XM-XI1)*DPHI+X
      Y=(SEN(I+1)-SEN(I))*(1.0-X/DPHI)
      SN=SEN(I)+Y
      IN=I
C     INTEGRATE ROLL PRESSURE BY TRAPEZOIDAL RULE TO FIND THE ROLL FORCE
C     INCLUDING THE EFFECT OF THE ANGLE AND CONTRIBUTION OF THE SHEAR
C     STRESSES. FIRST FIND TAUN.
      XKN=0.5*XXK(PHIN)
      IF(XMU*SN.LT.XKN) TAUN=XMU*SN
      IF(XMU*SN.GE.XKN) TAUN=XKN
      PHI=PHI1
      DO 18 I=1,M
      ARG=PHI-0.5*PHI1
      XS=SIN(ARG)
      XC=COS(ARG)
      SPHI(I)=S(I)*PHI
      SSIN(I)=S(I)*XS
      SCOS(I)=S(I)*XC
      IF(XMU*S(I).LT.XK(I)) TAU(I)=XMU*S(I)
      IF(XMU*S(I).GE.XK(I)) TAU(I)=XK(I)
      TAUSIN(I)=TAU(I)*XS
      GORD(I)=TAU(I)*(RD-(RD-R)*XC)
   18 PHI=PHI-DPHI
      TAUNSN=TAUN*SIN(PHIN-PHI1*0.5)
      DAEN=(TAUSIN(IN)+TAUNSN)*(DPHI-X)*0.5
      DAEX=(TAUSIN(IN+1)+TAUNSN)*X*0.5
      CALL TRAPEZ(TAUSIN,DPHI, 2,IN-1,AREA)
      AREAEN=AREA+DAEN
      CALL TRAPEZ(TAUSIN,DPHI,IN+2,M-1,AREA)
      AREAEX=AREA+DAEX
      CALL SIMPSN(SCOS,DPHI,2,M-3,AREAP)
      P=RD*(AREAP+AREAEN-AREAEX)
      J1=0
      PE11=(1.0-XNU**2)*H1*(X2K1-T1)**2*SQRT(RD/DRAFT)/(4.0*E)
   44 TE1=T1-2.0*XMU*PE11/H1
      PE1=(1.0-XNU**2)*H1*(X2K1-TE1)**2*SQRT(RD/DRAFT)/(4.0*E)
      IF(ABS((PE1-PE11)).LT.1.0E-01.OR.J1.GT.10) GO TO 46
      PE11=PE1
      J1=J1+1
      GO TO 44
   46 A1=(2.0/3.0)*SQRT(RD*H2*(1.0-XNU**2)/E)
      J2=0
      PE21=A1*(X2K2-T2)**1.5
   39 TE2=T2-2.0*XMU*PE21/H2
      PE2=A1*(X2K2-TE2)**1.5
      IF(ABS((PE2-PE21)).LT.1.0E-01.OR.J2.GT.25) GO TO 40
      PE21=PE2
      J2=J2+1
      GO TO 39
   40 P=P+PE1+PE2
      DRAFTT=XNU*(1.0+XNU)*(H2*T2-H1*T1)/E
      DRAFTE=(1.0-XNU**2)*(X2K2-TE2)*H2/E
      A2=.000334/(SQRT(DRAFT+DRAFTE+DRAFTT)+SQRT(DRAFTE))**2
      RD=R*(1.0+A2*P)
      ITERATE J TIMES TO FIND COMPATIBLE P AND RD.
      IF(ABS((P-P1)).LT.1.0E-1.OR.J.GT.30) GO TO 17
      P1=P
      J=J+1
      GO TO 11
   17 GE1=XMU*R*PE1
      GE2=-XMU*R*PE2
C     INTEGRATE SHEAR STRESSES TO DETERMINE THE TORQUE APPROXIMATELY---
      DAEXT=(TAUN+TAU(IN+1))*X/2.0
      DAENT=(TAUN+TAU(IN))*(DPHI-X)/2.0
      CALL TRAPEZ(TAU,DPHI,2,IN-1,AREA)
      AREANT=AREA+DAENT
      CALL TRAPEZ(TAU,DPHI,IN+2,M-1,AREA)
      AREAXT=AREA+DAEXT
      TAP=R*RD*(AREANT-AREAXT)
      GAP=RD**2*(AREANT-AREAXT)-0.5*(RD-R)*(P*PHI1+T1*H1-T2*H2)
      CALL SIMPSN(SPHI,DPHI,2,M-3,AREAT)
      T=R*RD*AREAT+(R/2.0)*(T1*H1-T2*H2)
      G=RD**2*AREAT+(R/2.0)*(T1*H1-T2*H2)-P*(RD-R)*PHI1/2.0
C      INTEGRATE EXACT EQUATION TO FIND ACCURATE TORQUE GAC.
      GORDN=TAUN*(RD-(RD-R)*COS(PHIN-PHI1*0.5))
      DAEXG=(GORDN+GORD(IN+1))*X*0.5
      DAENG=(GORDN+GORD(IN))*(DPHI-X)*0.5
      CALL TRAPEZ(GORD,DPHI, 2,IN-1,AREA)
      AREANG=AREA+DAENG
      CALL TRAPEZ(GORD,DPHI,IN+2,M-1,AREA)
      AREAXG=AREA+DAEXG
      CALL SIMPSN(SSIN,DPHI,2,M-3,AREAG)
      GAC=RD*(RD-R)*AREAG+RD*(AREANG-AREAXG)
      GAC12=GAC+GE1+GE2
      TT=GAC12/(17.32*H1*R)
      PPP=P/(17.32*H1)
      WRITE (6,5432) P,GAC12,XMU,PPP,TT
 5432 FORMAT(/5X,'ROLL FORCE=',F15.4,' T/IN'//5X,'ROLL TORQUE='
     1,F15.4,' T IN/IN'/5X,'COEFFICIENT OF FRICTION=',F8.4,5X,2E15.8)
      WRITE (6,19) P,P1,PAP,T,TAP,J,RD,X2K1,X2K2,X2KM,G,GAP,GAC,J1,PE1,
     1TE1,GE1,J2,PE2,TE2,GE2,GAC12,PHI1,DPHI,PHIN,SN
   19 FORMAT(/2X,'P= ',F20.4,'T/IN.P1=',F12.8,'T/IN.PAP='
     1,F12.8,'T/IN.',/2X,'T=',F13.8,'T IN/IN. TAP=',F12.8,
     2'TIN/IN.J=',I2,'ITERATIONS. RD=',F12.8,'INS.'/2X,'X2K1=
     3',F12.8,'T/SQIN.X2K2=',F12.8,'T/SQIN.X2KM=',F12.8,'T/SQ
     4IN.'/2X,'G=',F20.4,'T IN/IN. GAP=',F20.4,'T IN/IN. GAC=
     5',F20.4,'T IN/IN . J1=',I2,'ITERATIONS,'/2X,'PE1=',F12.8,
     6'T/IN. TE1=',F12.8,'T/SQIN.GE1=',E15.8,'T IN/IN.J2='
     7,I2,'ITERATIONS,'/2X,'PE2=',F12.8,'T/IN.TE2=',F12.8,'T/SQ
     8IN. GE2=',E15.8,'TIN/IN. GAC12=',F20.4,'T IN/IN.'/
     9   2X,'PHI1=',F12.9,', DPHI=',E15.8,',PHIN=',F12.9,
     1', ALL IN RADIANS, SN=',F12.8,'T/SQ IN.'/)
      DO 22 I=1,M,K
      X2K=2.0*XK(I)
   22 WRITE (6,23)I,S(I),XK(I)
   23 FORMAT(I6,2F15.3)
      GO TO 26
   24 WRITE(6,25)
   25 FORMAT(/1X,'NO NEUTRAL POINT CAN BE FOUND,THEREFORE A FEASIBLE SO
     1LUTION DOES NOT EXIST FOR THESE CONDITIONS.'/)
```

```
      WRITE(6,33)
   33 FORMAT(/4X,'I',9X,'SEN T/SQ IN',8X,'SEX T/SQ IN',12X,'S T/SQ IN
     1'//)
      DO 34 I=1,M,K
   34 WRITE (6,35) I,SEN(I),SEX(I),S(I)
   35 FORMAT (I6,3F20.10)
   26 GO TO 1
   27 STOP
      END
      FUNCTION  H(PHI)
      COMMON H2,RD,XMU,Z,B,HO,YO,XN,Q
      COMMON C,TEMP,VS,WW,EN,RPM,R,H1
      COMMON HPW,PMN
      COMMON AA
      H=H2+2.0*RD*(1.0-COS(PHI))
      RETURN
      END
      FUNCTION W(PHI)
      COMMON H2,RD,XMU,Z,B,HO,YO,XN,Q
      COMMON C,TEMP,VS,WW,EN,RPM,R,H1
      COMMON HPW,PMN
      COMMON AA
      W=Z*ALOG(HO/H(PHI))
      RETURN
      END
      FUNCTION XXK(PHI)
      COMMON H2,RD,XMU,Z,B,HO,YO,XN,Q
      COMMON C,TEMP,VS,WW,EN,RPM,R,H1
      COMMON HPW,PMN,AA
      XC=COS(PHI)
      XS=SIN(PHI)
      XH=H2+2.0*RD*(1.0-XC)
      EN=0.41-0.07*C
      EE=Z*ALOG(HO/(XH))
      EF=1.3*(EE/0.2)**EN-0.3*(EE/0.2)
      TP=(TEMP+273.0)/1000.0
      TD=0.95*(C+0.41)/(C+0.32)
      IF (TP.GT.TD) GO TO 110
      GCT=30.*(C+.9)*(TP-.95*(C+.49)/(C+.42))**2+(C+.06)/(C+.09)
      SF=0.28*GCT*EXP(5.0/TD-0.01/(C+0.05))
      EM=(0.081*C-0.154)*TP+(0.207-0.019*C)+0.027/(C+0.32)
      GO TO 111
  110 SF=0.28*EXP(5.0/TP-0.01/(C+0.05))
      EM=(0.126-0.019*C)*TP+(0.075*C-0.05)
  111 RED=(HO-H2)/HO
      STRR=6.2832*RPM*SQRT(RD/HO)*ALOG(1.0/(1.0-RED))/(60.0*
     1SQRT(RED))
C     XXK=Z*SF*EF*(EE/10.0)**EM
      XXK=Z*SF*EF*(STRR/10.0)**EM
      XXK=((25.4)**2/(2240.0*0.453))*XXK
      RETURN
      END
      FUNCTION XXKK(ANGLE)
      COMMON H2,RD,XMU,Z,B,HO,YO,XN,Q
      COMMON C,TEMP,VS,WW,EN,RPM,R,H1
      COMMON HPW,PMN,AA
      XC=COS(ANGLE)
      XS=SIN(ANGLE)
      XH=H2+2.0*R*(1.0-XC)
      EN=0.41-0.07*C
      EE=Z*ALOG(ANGLE)
      EF=1.3*(EE/0.2)**EN-0.3*(EE/0.2)
      TP=(TEMP+273.0)/1000.0
      TD=0.95*(C+0.41)/(C+0.32)
      IF (TP.GT.TD) GO TO 110
      GCT=30.*(C+.9)*(TP-.95*(C+.49)/(C+.42))**2+(C+.06)/(C+.09)
      SF=0.28*GCT*EXP(5.0/TD-0.01/(C+0.05))
      EM=(0.081*C-0.154)*TP+(0.207-0.019*C)+0.027/(C+0.32)
      GO TO 111
  110 SF=0.28*EXP(5.0/TP-0.01/(C+0.05))
      EM=(0.126-0.019*C)*TP+(0.075*C-0.05)
  111 RED=(H0-H2)/H0
      STRR=6.2832*RPM*SQRT(R/H0)*ALOG(1.0/(1.0-RED))/(60.0*
     1SQRT(RED))
C     XXKK=Z*SF*EF*(EE/10.0)**EM
      XXKK=Z*SF*EF*(STRR/10.0)**EM
      XXKK=((25.4)**2/(2240.0*0.453))*XXKK
      RETURN
      END
      FUNCTION DXXK(PHI)
      COMMON H2,RD,XMU,Z,B,H0,Y0,XN,Q
      COMMON C,TEMP,VS,WW,EN,RPM,R,H1
      COMMON HPW,PMN,AA
      XC=COS(PHI)
      XS=SIN(PHI)
      XH=H2+2.0*RD*(1.0-XC)
      EN=0.41-0.07*C
      EE=Z*ALOG(H0/XH)
      IF(EE.LT.0.0001) EE=0.0001
      EF=1.3*(EE/0.2)**EN-0.3*(EE/0.2)
      TP=(TEMP+273.0)/1000.0
      TD=0.95*(C+0.41)/(C+0.32)
      IF (TP.GT.TD) GO TO 110
      GCT=30.*(C+.9)*(TP-.95*(C+.49)/(C+.42))**2+(C+.06)/(C+.09)
      SF=0.28*GCT*EXP(5.0/TD-0.01/(C+0.05))
      EM=(0.081*C-0.154)*TP+(0.207-0.019*C)+0.027/(C+0.32)
      GO TO 111
  110 SF=0.28*EXP(5.0/TP-0.01/(C+0.05))
      EM=(0.126-0.019*C)*TP+(0.075*C-0.05)
  111 RED=(H0-H2)/H0
      STRR=6.2832*RPM*SQRT(RD/H0)*ALOG(1.0/(1.0-RED))/(60.0*
     1SQRT(RED))
      DE=-2.0*Z*RD*XS/XH
      DF=1.3*EN*(0.2/EE)**(1.0-EN)*(DE/0.2)-1.5*DE
      IF(STRR.LT.0.00001) STRR=0.00001
C     DXXK=Z*SF*(DF*(EE/10.0)**EM+EF*EM*((10./EE)**(1.0-EM))*DE/10.0)
      DXXK=Z*SF*DF*(STRR/10.0)**EM
      DXXK=DXXK*(25.4**2)/(2240.0*0.453)
      RETURN
      END
      FUNCTION G1(PHI)
      COMMON H2,RD,XMU,Z,B,HO,YO,XN,Q
      COMMON C,TEMP,VS,WW,EN,RPM,R,H1
      COMMON HPW,PMN
      COMMON AA
      XS=SIN(PHI)
      XC=COS(PHI)
      XH=H2+2.0*RD*(1.0-XC)
      G1=Q*XMU*(2.0*RD/XH+1.0/XC)/(XC-XMU*XS*Q)
      RETURN
      END
      FUNCTION  G2(PHI)
      COMMON H2,RD,XMU,Z,B,HO,YO,XN,Q
      COMMON C,TEMP,VS,WW,EN,RPM,R,H1
      COMMON HPW,PMN
      COMMON AA
      XS=SIN(PHI)
      XC=COS(PHI)
      XH=H2+2.0*RD*(1.0-XC)
      G2=(2.0*RD*XXK(PHI)*XS/XH+DXXK(PHI))/(1.0-XMU*Q*XS/XC)
      RETURN
      END
      FUNCTION G3(PHI)
      COMMON H2,RD,XMU,Z,B,HO,YO,XN,Q
      COMMON C,TEMP,VS,WW,EN,RPM,R,H1
      COMMON HPW,PMN
      COMMON AA
      XS=SIN(PHI)
      XC=COS(PHI)
      XH=H2+2.0*RD*(1.0-XC)
      G3=XXK(PHI)*(2.0*RD*XS*(1.0+Q*0.5*XS/XC)/XH+Q*RD*XC/XH+0.5*Q/XC**2
     1)+(1.0+0.5*Q*XS/XC)*DXXK(PHI)
      RETURN
      END
      FUNCTION G4(PHI)
      COMMON H2,RD,XMU,Z,B,HO,YO,XN,Q
      COMMON C,TEMP,VS,WW,EN,RPM,R,H1
      COMMON HPW,PMN
      COMMON AA
      G4=0.0
      RETURN
      END
      SUBROUTINE TRAPEZ(Y,DX,N1,N2,A)
      DIMENSION Y(1)
      SUM=0.0
      DO 1 I=N1,N2
    1 SUM=SUM+Y(I)
      A=(DX/2.0)*(Y(N1-1)+2.0*SUM+Y(N2+1))
      RETURN
      END
      SUBROUTINE SIMPSN(Y,DX,N1,N2,A)
      DIMENSION Y(1)
      ODD=0.0
      EVEN=0.0
      DO 1 I=N1,N2,2
      EVEN=EVEN+Y(I)
    1 ODD=ODD+Y(I+1)
      A=(DX/3.0)*(Y(N1-1)+4.0*(EVEN+Y(N2+2))+2.0*ODD+Y(N2+3))
      RETURN
      END
      SUBROUTINE RUNGE (X,Y,DX,DY,FA,FB)
      COMMON H2,RD,XMU,Z,B,HO,YO,XN,Q
      COMMON C,TEMP,VS,WW,EN,RPM,R,H1
      COMMON HPW,PMN
      COMMON AA
      F0=FA(X)*Y+FB(X)
      A=FA(X+0.5*Q*DX)
      CC=FB(X+0.5*Q*DX)
      F1=A*(Y+0.5*Q*DX*F0)+CC
      F2=A*(Y+0.5*Q*DX*F1)+CC
      F3=FA(X+Q*DX)*(Y+Q*DX*F2)+FB(X+Q*DX)
      DY=DX*(F0+2.0*(F1+F2)+F3)*Q/6.0
      RETURN
      END
$ENTRY
013396.000000000000.280000000038.490000000078.300310000000.0670000 0
1501000.80000004.92120000.19690000.19690000.18720000.00000000.00000
0950.000000.200050.000040.00
  4500.000000000000.300000000012.170000000096.800000000000.2000000 5
```

```
C
C     S I M ' S   H O T   R O L L I N G   M O D E L
C
C
C
C  THIS USES SHIDAS FLOW STRESS FORMULATION WITH THE MEAN STRAIN RATE
C
C
C
      COMMON H2,RD,XMU,Z,B,HO,YO,XN,Q
      COMMON C,TEMP,VS,WW,EN,R,H1
      COMMON HPW,PMN
      COMMON AA,PHIDOT,RPM,PHI1
C     COMMON TEMP1,C1,RPM
      INTEGER IXLBL(50) , IYLBL(50),N,ZZ,K11,II
      INTEGER IXLBL1(50) , IYLBL1(50)
      INTEGER IXLBL2(50) , IYLBL2(50)
      REAL X1(2250),Y1(2250),SP1(2250),TRQ1(2250),RPM
      REAL AA1(2250),FP1(2250),REDUCT(52)
      REAL DIFF,TEMP,XMU1,ACHIL,REDUC
      EXTERNAL  G1,G2,G3,G4
      DIMENSION S(2002),SPHI(2002),SEX(2002),SEN(2002),
     1TAU(2002),XK(2002),SSIN(2002),GORD(2002),TAUSIN(2002),SCOS(2002)
    1 READ (5,38) E,XNU,YO,B,XN,LC
      IF (LC.NE.0) GO TO 27
   38 FORMAT (5F14.7,1X,I1)
      READ(5,2)M,XMU,R,HO,H1,H2,T1,T2
    2 FORMAT(I4,7F9.5)
C
C     TEST FOR SLAB ENTRY CONDITION,TO INCREASE H2 IF NECESSARY.
C
      DIFF=0.0
C
      K11=5
      RPM =40.0
      C=0.2
      PHIDOT=RPM/(2.*3.145*60.)
      TEMP=950.0
      TEMP1=TEMP
      XMU1=XMU
      REDUC =0.0
      II=25
C
C
C         THIS IS TO USE FOR VARIOUS REDUCTIONS
C
       DO 711 ZZ=1,K11
C
       DIFF=0.0
C
C         OBSERVE THAT THE INCREMENT AT EXIT STRIP
```

```
      IF(ZZ.EQ.1)GO TO 686
      H2=H2-0.02
686   REDUCT(ZZ)=((H1-H2)/H0)*100.
      ACHIL=REDUCT(ZZ)
   53 H2MIN=H1-2.0*R*(1.0-COS(ATAN(XMU)))
      IF (H2.LT.H2MIN) H2=H2MIN
      RR=(H1-H2)/H1
      Z=2.0/SQRT(3.0)
C     TEST FOR MAGNITUDE OF TENSIONS,TO DECREASE THEM IF NECESSARY
      DRAFT=H1-H2
C
C     CALCULATE FLOW STRENGTH AT ENTRY AND EXIT
C     XXKK IS GIVEN BY A SUBROUTINE
C
      WRITE(6,*)H0,H1,H2
      RD=R
      PHI1=ARCOS(1.0-DRAFT/(2.0*RD))
      E11=H0/H1
      E12=H0/H2
      WRITE(6,*)E11,E12
      X2K1=XXKK(E11)
      X2K2=XXKK(E12)
      IF(T1.GT.X2K1) T1=X2K1
      IF(T2.GT.X2K2) T2=X2K2
      J=0
      M1=M-1
      K=M/102+1
      RL=SQRT(R*DRAFT)
      HM=(2.0*H2+H1)/3.0
      WRITE(6,3)
    3 FORMAT(1H1,30X,'ALL UNITS ARE IN TONS AND INCHES.',///7X,'E',14X,
     1'XNU',11X,'Y0',10X,'B',16X,'XN',7X,'XMU',5X,'R',7X,'H0',7X,'H1',5X
     2,'H2',5X,'T1',5X,'T2'/)
      WRITE(6,41)E,XNU,Y0,B,XN,XMU,R,H0,H1,H2,T1,T2
   41 FORMAT(5F14.7,7F8.4)
      A=XMU*RL/HM
      X2KM=(X2K1+2.0*X2K2)/3.0-(T1+T2)/2.0
      PAP=X2KM*RL*(EXP(A)-1.0)/A
      RD=R*(1.0+0.000334*PAP/DRAFT)
      P1=PAP
      TE1=T1
      TE2=T2
   11 PHI1=ARCOS(1.0-DRAFT/(2.0*RD))
      XM=M
      DPHI=PHI1/(XM-1.0)
      PHI=PHI1
C
C     XXK REPRESENTS THE FLOW STENGTH OF THE STRIP (2K)
C     IT IS GIVEN BY A SUBROUTINE
C     DXXK REPRESENTS D(2K)/DPHI; IT IS ALSO GIVEN BY A SUBROUTINE

      DO32I=1,M
      XK(I)=0.5*XXK(PHI)
   32 PHI=PHI-DPHI
      S(1)=(X2K1-TE1)/(1.0+XMU*TAN(PHI1))
      IF(XMU*S(1).GT.XK(1)) S(1)=X2K1-TE1-XK(1)*TAN(PHI1)
      S(M)=X2K2-TE2
      SEX(M)=S(M)
      PHI=0.0
C     FORWARD INTEGRATION TO DETERMINE SEN(I) AND SEX(I) USING THE
C     FOURTH ORDER RUNGE KUTTA PROCESS.
      Q=1.0
      DO 12 I=1,M1
      L=M+1-I
C
C
C     IF(XMU*SEX(L).LT.XK(L)) CALL RUNGE(PHI,SEX(L),DPHI,DS,G1,G2)
C     IF(XMU*SEX(L).GE.XK(L)) CALL RUNGE(PHI,SEX(L),DPHI,DS,G4,G3)
      CALL RUNGE(PHI,SEX(L),DPHI,DS,G4,G3)
      SEX(L-1)=SEX(L)+DS
   12 PHI=PHI+DPHI
      SEN(1)=S(1)
      PHI=PHI1
      Q=-1.0
      DO 13 I=1,M1
C
C          THIS IS ALSO CHANGED FOR SIMS FORMULATION
C
C     IF(XMU*SEN(I).LT.XK(I)) CALL RUNGE(PHI,SEN(I),DPHI,DS,G1,G2)
      IF(XMU*SEN(I).GE.XK(I)) CALL RUNGE(PHI,SEN(I),DPHI,DS,G4,G3)
      CALL RUNGE(PHI,SEN(I),DPHI,DS,G4,G3)
      SEN(I+1)=SEN(I)+DS
   13 PHI=PHI-DPHI
C     FIND S(I),BEING THE SMALLER OF SEN(I) AND SEX(I) ACROSS THE ARC.
      DO 14 I=1,M
      IF(SEX(I).LE.SEN(I))  S(I)=SEX(I)
      IF(SEN(I).LE.SEX(I)) S(I)=SEN(I)
      FP1(I)=S(I)
   14 CONTINUE
C     NOW DETERMINE PHIN AND SN.
      DO 15 I=1,M1
      IF(SEX(I).GE.SEN(I).AND.SEN(I+1).GE.SEX(I+1)) GO TO 16
   15 CONTINUE
      GO TO 24
   16 X=DPHI/(1.0+(SEX(I)-SEN(I))/(SEN(I+1)-SEX(I+1)))
      XI1=I+1
      PHIN=(XM-XI1)*DPHI+X
      Y=(SEN(I+1)-SEN(I))*(1.0-X/DPHI)
      SN=SEN(I)+Y
      IN=I
C     INTEGRATE ROLL PRESSURE BY TRAPEZOIDAL RULE TO FIND THE ROLL FORCE
C     INCLUDING THE EFFECT OF THE ANGLE AND CONTRIBUTION OF THE SHEAR
C     STRESSES. FIRST FIND TAUN.
      XKN=0.5*XXK(PHIN)
      IF(XMU*SN.LT.XKN) TAUN=XMU*SN
      IF(XMU*SN.GE.XKN) TAUN=XKN
      PHI=PHI1
      DO 18 I=1,M
      ARG=PHI-0.5*PHI1
      XS=SIN(ARG)
      XC=COS(ARG)
      SPHI(I)=S(I)*PHI
      SSIN(I)=S(I)*XS
      SCOS(I)=S(I)*XC
      IF(XMU*S(I).LT.XK(I)) TAU(I)=XMU*S(I)
      IF(XMU*S(I).GE.XK(I)) TAU(I)=XK(I)
      TAUSIN(I)=TAU(I)*XS
      GORD(I)=TAU(I)*(RD-(RD-R)*XC)
   18 PHI=PHI-DPHI
      TAUNSN=TAUN*SIN(PHIN-PHI1*0.5)
      DAEN=(TAUSIN(IN)+TAUNSN)*(DPHI-X)*0.5
      DAEX=(TAUSIN(IN+1)+TAUNSN)*X*0.5
      CALL TRAPEZ(TAUSIN,DPHI, 2,IN-1,AREA)
      AREAEN=AREA+DAEN
      CALL TRAPEZ(TAUSIN,DPHI,IN+2,M-1,AREA)
      AREAEX=AREA+DAEX
      CALL SIMPSN(SCOS,DPHI,2,M-3,AREAP)
      P=RD*(AREAP+AREAEN-AREAEX)
      J1=0
      PE11=(1.0-XNU**2)*H1*(X2K1-T1)**2*SQRT(RD/DRAFT)/(4.0*E)
   44 TE1=T1-2.0*XMU*PE11/H1
      PE1=(1.0-XNU**2)*H1*(X2K1-TE1)**2*SQRT(RD/DRAFT)/(4.0*E)
C     DIKO MOU STATEMENT
      IF(PE1.EQ.0.) GO TO 46
      WRITE(6,888)PE11,PE1,TE1
  888 FORMAT('0',2X,'PE11',F15.5,3X,'PE1',F15.5,'TE1',F15.5)
      IF(ABS((PE1-PE11)/PE1).LT.1.0E-06.OR.J1.GT.10) GO TO 46
      PE11=PE1
      J1=J1+1
      GO TO 44
   46 A1=(2.0/3.0)*SQRT(RD*H2*(1.0-XNU**2)/E)
      J2=0
      PE21=A1*(X2K2-T2)**1.5
   39 TE2=T2-2.0*XMU*PE21/H2
      PE2=A1*(X2K2-TE2)**1.5
      IF(ABS((PE2-PE21)/PE2).LT.1.0E-06.OR.J2.GT.25) GO TO 40
      PE21=PE2
      J2=J2+1
      GO TO 39
   40 P=P+PE1+PE2
      DRAFTT=XNU*(1.0+XNU)*(H2*T2-H1*T1)/E
      DRAFTE=(1.0-XNU**2)*(X2K2-TE2)*H2/E
      A2=.000334/(SQRT(DRAFT+DRAFTE+DRAFTT)+SQRT(DRAFTE))**2
      RD=R*(1.0+A2*P)
C     ITERATE J TIMES TO FIND COMPATIBLE P AND RD.
      IF(ABS((P-P1)/P1).LT.1.0E-6.OR.J.GT.30) GO TO 17
      P1=P
      J=J+1
      GO TO 11
   17 GE1=XMU*R*PE1
      GE2=-XMU*R*PE2
      DO 666 I=1,M
      DIFF=DIFF+(DPHI)*360./(2.*3.141592)
      AA1(I)=DIFF
666   CONTINUE
C
C
C     INTEGRATE SHEAR STRESSES TO DETERMINE THE TORQUE APPROXIMATELY---
      DAEXT=(TAUN+TAU(IN+1))*X/2.0
      DAENT=(TAUN+TAU(IN))*(DPHI-X)/2.0
      CALL TRAPEZ(TAU,DPHI,2,IN-1,AREA)
      AREANT=AREA+DAENT
      CALL TRAPEZ(TAU,DPHI,IN+2,M-1,AREA)
      AREAXT=AREA+DAEXT
      TAP=R*RD*(AREANT-AREAXT)
      GAP=RD**2*(AREANT-AREAXT)-0.5*(RD-R)*(P*PHI1+T1*H1-T2*H2)
      CALL SIMPSN(SPHI,DPHI,2,M-3,AREAT)
      T=R*RD*AREAT+(R/2.0)*(T1*H1-T2*H2)
      G=RD**2*AREAT+(R/2.0)*(T1*H1-T2*H2)-P*(RD-R)*PHI1/2.0
C      INTEGRATE EXACT EQUATION TO FIND ACCURATE TORQUE GAC.
      GORDN=TAUN*(RD-(RD-R)*COS(PHIN-PHI1*0.5))
      DAEXG=(GORDN+GORD(IN+1))*X*0.5
      DAENG=(GORDN+GORD(IN))*(DPHI-X)*0.5
      CALL TRAPEZ(GORD,DPHI, 2,IN-1,AREA)
      AREANG=AREA+DAENG
      CALL TRAPEZ(GORD,DPHI,IN+2,M-1,AREA)
      AREAXG=AREA+DAEXG
      CALL SIMPSN(SSIN,DPHI,2,M-3,AREAG)
      GAC=RD*(RD-R)*AREAG+RD*(AREANG-AREAXG)
      GAC12=GAC+GE1+GE2
      TT=GAC12/(17.32*H1*R)
      PPP=P/(17.32*H1)
      SP1(ZZ)=P
      TRQ1(ZZ)=GAC12
      WRITE (6,5432) P,GAC12,XMU,PPP,TT
 5432 FORMAT(/5X,'ROLL FORCE=',F15.4,' T/IN'//5X,'ROLL TORQUE='
     1,F15.4,' T IN/IN'/5X,'COEFFICIENT OF FRICTION=',F8.4,5X,2E15.8)
      WRITE (6,19) P,P1,PAP,T,TAP,J,RD,X2K1,X2K2,X2KM,G,GAP,GAC,J1,PE1,
     1TE1,GE1,J2,PE2,TE2,GE2,GAC12,PHI1,DPHI,PHIN,SN
   19 FORMAT(/2X,'P= ',F20.4,'T/IN.P1=',F12.8,'T/IN.PAP='
     1,F12.8,'T/IN.',/2X,'T=',F13.8,'T IN/IN. TAP=',F12.8,
     2'TIN/IN.J=',I2,'ITERATIONS. RD=',F12.8,'INS.'/2X,'X2K1=
     3',F12.8,'T/SQIN.X2K2=',F12.8,'T/SQIN.X2KM=',F12.8,'T/SQ
     4IN.'/2X,'G=',F20.4,'T IN/IN. GAP=',F20.4,'T IN/IN. GAC=
     5',F20.4,'T IN/IN . J1=',I2,'ITERATIONS,'/2X,'PE1=',F12.8,
     6'T/IN. TE1=',F12.8,'T/SQIN.GE1=',E15.8,'T IN/IN.J2='
     7,I2,'ITERATIONS,'/2X,'PE2=',F12.8,'T/IN.TE2=',F12.8,'T/SQ
     8IN. GE2=',E15.8,'TIN/IN. GAC12=',F20.4,'T IN/IN.'/
     9   2X,'PHI1=',F12.9,', DPHI=',E15.8,',PHIN=',F12.9,
     1', ALL IN RADIANS. SN=',F12.8,'T/SQ IN.'/)
      DO 914 I=1,M,10
      WRITE(6,444)FP1(I),AA1(I)
  +4  FORMAT('0',2X,'ROLL PRESSURE=',F10.5,'ANGLE =',5X,F10.5)
914   CONTINUE
```

```
   1  CONTINUE
      GO TO 26
  24  WRITE(6,25)
  25  FORMAT(/1X,'NO NEUTRAL POINT CAN BE FOUND,THEREFORE A FEASIBLE SO
     1LUTION DOES NOT EXIST FOR THESE CONDITIONS.'/)
      WRITE(6,33)
  33  FORMAT(/4X,'I',9X,'SEN T/SQ IN',8X,'SEX T/SQ IN',12X,'S T/SQ IN
     1'//)
      DO 34 I=1,M,K
  34  WRITE (6,35) I,SEN(I),SEX(I),S(I)
  35  FORMAT (I6,3F20.10)
  26  GO TO 1
  27  STOP
      END
      FUNCTION  H(PHI)
      COMMON H2,RD,XMU,Z,B,HO,YO,XN,Q
      COMMON C,TEMP,VS,WW,EN,R,H1
      COMMON HPW,PMN
      COMMON AA,PHIDOT,RPM
      H=H2+RD*(PHI)**2
      RETURN
      END
      FUNCTION W(PHI)
      COMMON H2,RD,XMU,Z,B,HO,YO,XN,Q
      COMMON C,TEMP,VS,WW,EN,R,H1
      COMMON HPW,PMN
      COMMON AA,PHIDOT,RPM
      W=Z*ALOG(HO/H(PHI))
      RETURN
      END
      FUNCTION XXK(PHI)
      COMMON H2,RD,XMU,Z,B,HO,YO,XN,Q
      COMMON C,TEMP,VS,WW,EN,R,H1
      COMMON HPW,PMN
      COMMON AA,PHIDOT,RPM
      EN=0.41-0.07*C
      EN=ABS(EN)
      AA=1.3/(0.2**EN)
      TP=(TEMP+273.0)/1000.0
      TD=0.95*(C+0.41)/(C+0.32)
      IF(TP.GT.TD) GO TO 110
      GCT=30.0*(C+0.9)*(TP-0.95*(C+0.49)/(C+0.42))**2+(C+.06)/(C+.09)
      SF=0.28*GCT*EXP(5.0/TD-0.01/(C+0.05))
      EM=(0.081*C-0.154)*TP+(0.207-0.019*C)+0.027/(C+0.32)
      EM=ABS(EM)
      GO TO 111
 110  SF=0.28*EXP(5.0/TP-0.01/(C+0.05))
      EM=(0.126-0.019*C)*TP+(0.075*C-0.05)
      EM=ABS(EM)
      XC=COS(PHI)
      XS=SIN(PHI)
      XH=H2+RD*(PHI**2)
      EE=Z*ALOG(HO/XH)
      EE=ABS(EE)
      BCO=SQRT((HO-H2)/HO)
      BCO1=SQRT((RD/HO))
      BCO2=ALOG(1./(1.-((HO-H2)/HO)))
      STRRT=((2.*3.14*RPM/(60.*BCO))*BCO1*BCO2)
      STRRT=ABS(STRRT)
111   XXK=(Z*SF/(10.0**EM))*(AA*EE**EN-1.5*EE)*(STRRT**EM)
      XXK=((25.4)**2/(2240.0*0.453))*XXK
      RETURN
      END
      FUNCTION XXKK(ANGLE)
      COMMON H2,RD,XMU,Z,B,HO,YO,XN,Q
      COMMON C,TEMP,VS,WW,EN,R,H1
      COMMON HPW,PMN
      COMMON AA,PHIDOT,RPM
      EN=0.41-0.07*C
      AA=1.3/(0.2**EN)
      TP=(TEMP+273.0)/1000.0
      TD=0.95*(C+0.41)/(C+0.32)
      IF(TP.GT.TD) GO TO 120
      GCT=30.0*(C+0.9)*(TP-0.95*(C+0.49)/(C+0.42))**2+(C+.06)/(C+.09)
      SF=0.28*GCT*EXP(5.0/TD-0.01/(C+0.05))
      EM=(0.081*C-0.154)*TP+(0.207-0.019*C)+0.027/(C+0.32)
      EM=ABS(EM)
      GO TO 121
  120 SF=0.28*EXP(5.0/TP-0.01/(C+0.05))
      EM=(0.126-0.019*C)*TP+(0.075*C-0.05)
      EM=ABS(EM)
      BCO=SQRT((HO-H2)/HO)
      BCO1=SQRT((RD/HO))
      BCO2=ALOG(1./(1.-((HO-H2)/HO)))
      STRRT=((2.*3.14*RPM/(60.*BCO))*BCO1*BCO2)
  121 XXKK=Z*SF*((1.3/0.2**EN)*(Z*ALOG(ANGLE))**EN-1.5*Z*ALOG(ANGLE))
     1*(STRRT/10.0)**EM
 3333 XXKK=((25.4)**2/(2240.0*0.453))*XXKK
      RETURN
      END
      FUNCTION DXXK(PHI)
      COMMON H2,RD,XMU,Z,B,HO,YO,XN,Q
      COMMON C,TEMP,VS,WW,EN,R,H1
      COMMON HPW,PMN
      COMMON AA,PHIDOT,RPM
      EN=0.41-0.07*C
      AA=1.3/(0.2**EN)
      TP=(TEMP+273.0)/1000.0
      TD=0.95*(C+0.41)/(C+0.32)
      IF(TP.GT.TD) GO TO 130
      GCT=30.0*(C+0.9)*(TP-0.95*(C+0.49)/(C+0.42))**2+(C+.06)/(C+.09)
      SF=0.28*GCT*EXP(5.0/TD-0.01/(C+0.05))
      EM=(0.081*C-0.154)*TP+(0.207-0.019*C)+0.027/(C+0.32)
      EM=ABS(EM)
      GO TO 131
  130 SF=0.28*EXP(5.0/TP-0.01/(C+0.05))
      EM=(0.126-0.019*C)*TP+(0.075*C-0.05)
      EM=ABS(EM)
  131 XC=COS(PHI)
      XS=SIN(PHI)
      XH=H2+RD*(PHI**2)
      EE=Z*ALOG(HO/XH)
      IF(EE.LT.0.0001) EE=0.0001
      BCO=SQRT((HO-H2)/HO)
      BCO1=SQRT((RD/HO))
      BCO2=ALOG(1./(1.-((HO-H2)/HO)))
      STRRT=(((2.*3.14*RPM/(60.*BCO))*BCO1*BCO2)/10.)**EM
      B1=-1.3*EN*(0.2/EE)**(1-EN)
      B2=((2.*RD*SIN(PHI))/H(PHI))*Z/0.2
      B3=1.5*Z*2.*RD*SIN(PHI)/H(PHI)
      B4=SF*Z*(STRRT)
      DXXK=(B1*B2+B3)*B4
      DXXK=((25.4)**2/(2240.0*0.453))*DXXK
  300 RETURN
      END
      FUNCTION G1(PHI)
      COMMON H2,RD,XMU,Z,B,HO,YO,XN,Q
      COMMON C,TEMP,VS,WW,EN,R,H1
      COMMON HPW,PMN
      COMMON AA,PHIDOT,RPM
      XS=SIN(PHI)
      XC=COS(PHI)
      XH=H2+RD*(PHI**2)
      G1=0.0
      RETURN
      END
      FUNCTION  G2(PHI)
      COMMON H2,RD,XMU,Z,B,HO,YO,XN,Q
      COMMON C,TEMP,VS,WW,EN,R,H1
      COMMON HPW,PMN
      COMMON AA,PHIDOT,RPM
      XS=SIN(PHI)
      XC=COS(PHI)
      XH=H2+RD*(PHI**2)
      G2=0.0
      RETURN
      END
      FUNCTION G3(PHI)
      COMMON H2,RD,XMU,Z,B,HO,YO,XN,Q
      COMMON C,TEMP,VS,WW,EN,R,H1
      COMMON HPW,PMN
      COMMON AA,PHIDOT,RPM
      XS=SIN(PHI)
      XC=COS(PHI)
      XH=H2+RD*(PHI**2)
      G3=(4.*XXK(PHI)*RD*PHI+Q*2.*XXK(PHI)*RD)/H(PHI)
      RETURN
      END
      FUNCTION G4(PHI)
      COMMON H2,RD,XMU,Z,B,HO,YO,XN,Q
      COMMON C,TEMP,VS,WW,EN,R,H1
      COMMON HPW,PMN
      COMMON AA,PHIDOT,RPM
      G4=0.0
      RETURN
      END
      SUBROUTINE TRAPEZ(Y,DX,N1,N2,A)
      DIMENSION Y(1)
      SUM=0.0
      DO 1 I=N1,N2
    1 SUM=SUM+Y(I)
      A=(DX/2.0)*(Y(N1-1)+2.0*SUM+Y(N2+1))
      RETURN
      END
      SUBROUTINE SIMPSN(Y,DX,N1,N2,A)
      DIMENSION Y(1)
      ODD=0.0
      EVEN=0.0
      DO 1 I=N1,N2,2
      EVEN=EVEN+Y(I)
    1 ODD=ODD+Y(I+1)
      A=(DX/3.0)*(Y(N1-1)+4.0*(EVEN+Y(N2+2))+2.0*ODD+Y(N2+3))
      RETURN
      END
      SUBROUTINE RUNGE (X,Y,DX,DY,FA,FB)
      COMMON H2,RD,XMU,Z,B,HO,YO,XN,Q
      COMMON C,TEMP,VS,WW,EN,R,H1
      COMMON HPW,PMN
      COMMON AA,PHIDOT,RPM
      F0=FA(X)*Y+FB(X)
      A=FA(X+0.5*Q*DX)
      CC=FB(X+0.5*Q*DX)
      F1=A*(Y+0.5*Q*DX*F0)+CC
      F2=A*(Y+0.5*Q*DX*F1)+CC
      F3=FA(X+Q*DX)*(Y+Q*DX*F2)+FB(X+Q*DX)
      DY=DX*(F0+2.0*(F1+F2)+F3)*Q/6.0
      RETURN
      END
$ENTRY
013396.000000 000000.280000 000001.374000 000078.300000 000000.0670000 0
1501 00.80000 04.92120 00.19690 00.19690 0.187200 0.00000  0.00000
004500.000000000000.300000000012.170000000096.800000000000.2000000 5
```

```
C         B L A N D    AND    F O R D    M O D E L
C
C                    COLD ROLLING
C
      COMMON H2,RD,XMU,Z,B,HO,YO,XN,Q
      COMMON C,TEMP,VS,WW,EN,RPM,R,H1
      COMMON HPW,PMN
      COMMON AA
      INTEGER N,ZZ,K11,II
      REAL X1(2250),Y1(2250),SP1(2250),TRQ1(2250),RPM
      REAL AA1(2250),FP1(2250),REDUCT(52)
      REAL DIFF,TEMP,XMU1,ACHIL,REDUC
      EXTERNAL  G1,G2,G3,G4
      DIMENSION S(2002),SPHI(2002),SEX(2002),SEN(2002),
     1TAU(2002),XK(2002),SSIN(2002),GORD(2002),TAUSIN(2002),SCOS(2002)
C
    1 READ (5,38) E,XNU,YO,B,XN,LC
      IF (LC.NE.0) GO TO 27
   38 FORMAT (5F14.7,1X,I1)
      READ(5,2)M,XMU,R,HO,H1,H2,T1,T2
    2 FORMAT(I4,7F9.5)
C
C     TEST FOR SLAB ENTRY CONDITION,TO INCREASE H2 IF NECESSARY.
C
      DIFF=0.0
C
      K11=5
      RPM =10.0
      TEMP=20.0
      XMU1=XMU
      REDUC =0.0
      II=25
C
C
C        THIS IS TO USE FOR VARIOUS REDUCTIONS
C              OF    ACHILLES
C
       DO 711 ZZ=1,K11
C
       DIFF=0.0
C
C        OBSERVE THAT THE INCREMENT AT EXIT STRIP
C
       IF(ZZ.EQ.1)GO TO 686
       H2=H2-0.01
C      REDUC=REDUC+10.0
C      REDUCT(ZZ)=REDUC
686    REDUCT(ZZ)=((H1-H2)/HO)*100.
C      H2 = (H1*100.-H1*REDUC)/100.
       ACHIL=REDUCT(ZZ)
   53 H2MIN=H1-2.0*R*(1.0-COS(ATAN(XMU)))
      IF (H2.LT.H2MIN) H2=H2MIN
      RR=(H1-H2)/H1
      Z=2.0/SQRT(3.0)
C     TEST FOR MAGNITUDE OF TENSIONS,TO DECREASE THEM IF NECESSARY
      DRAFT=H1-H2
C
C     CALCULATE FLOW STRENGTH AT ENTRY AND EXIT
C     XXKK IS GIVEN BY A SUBROUTINE
C
      WRITE(6,*)H0,H1,H2
      E11=H0/H1
      E12=H0/H2
C     WRITE(6,*)E11,E12
      X2K1=XXKK(E11)
      X2K2=XXKK(E12)
      IF(T1.GT.X2K1) T1=X2K1
      IF(T2.GT.X2K2) T2=X2K2
      J=0
      M1=M-1
      K=M/102+1
      RL=SQRT(R*DRAFT)
      HM=(2.0*H2+H1)/3.0
      WRITE(6,3)
    3 FORMAT(1H1,30X,'ALL UNITS ARE IN TONS AND INCHES.',///7X,'E',14X,
     1'XNU',11X,'Y0',10X,'B',16X,'XN',7X,'XMU',5X,'R',7X,'H0',7X,'H1',5X
     2,'H2',5X,'T1',5X,'T2'/)
      WRITE(6,41)E,XNU,Y0,B,XN,XMU,R,H0,H1,H2,T1,T2
   41 FORMAT(5F14.7,7F8.4)
      A=XMU*RL/HM
      X2KM=(X2K1+2.0*X2K2)/3.0-(T1+T2)/2.0
      PAP=X2KM*RL*(EXP(A)-1.0)/A
      RD=R*(1.0+0.000334*PAP/DRAFT)
      P1=PAP
      TE1=T1
      TE2=T2
   11 PHI1=ACOS(1.0-DRAFT/(2.0*RD))
      XM=M
      DPHI=PHI1/(XM-1.0)
      PHI=PHI1
C
C     XXK REPRESENTS THE FLOW STENGTH OF THE STRIP (2K)
C     IT IS GIVEN BY A SUBROUTINE
C     DXXK REPRESENTS D(2K)/DPHI; IT IS ALSO GIVEN BY A SUBROUTINE
C
      DO32I=1,M
      XK(I)=0.5*XXK(PHI)
   32 PHI=PHI-DPHI
      S(1)=(X2K1-TE1)/(1.0+XMU*TAN(PHI1))
      IF(XMU*S(1).GT.XK(1)) S(1)=X2K1-TE1-XK(1)*TAN(PHI1)
      S(M)=X2K2-TE2
      SEX(M)=S(M)
      PHI=0.0
      FORWARD INTEGRATION TO DETERMINE SEN(I) AND SEX(I) USING THE
      FOURTH ORDER RUNGE KUTTA PROCESS.
      Q=1.0
      DO 12 I=1,M1
      L=M+1-I
      IF(XMU*SEX(L).LT.XK(L)) CALL RUNGE(PHI,SEX(L),DPHI,DS,G1,G2)
C     IF(XMU*SEX(L).GE.XK(L)) CALL RUNGE(PHI,SEX(L),DPHI,DS,G4,G3)
C
C
CC                  EDO BALE TO   2*K* SEX(I)
C
C
      SEX(L-1)=SEX(L)+DS
   12 PHI=PHI+DPHI
      SEN(1)=S(1)
      PHI=PHI1
      Q=-1.0
      DO 13 I=1,M1
      IF(XMU*SEN(I).LT.XK(I)) CALL RUNGE(PHI,SEN(I),DPHI,DS,G1,G2)
C     IF(XMU*SEN(I).GE.XK(I)) CALL RUNGE(PHI,SEN(I),DPHI,DS,G4,G3)
      SEN(I+1)=SEN(I)+DS
   13 PHI=PHI-DPHI
C     FIND S(I),BEING THE SMALLER OF SEN(I) AND SEX(I) ACROSS THE ARC.
C
C
      DO 14 I=1,M
      IF(SEX(I).LE.SEN(I))  S(I)=SEX(I)
      IF(SEN(I).LE.SEX(I)) S(I)=SEN(I)
      FP1(I)=S(I)
   14 CONTINUE
C     NOW DETERMINE PHIN AND SN.
      DO 15 I=1,M1
      IF(SEX(I).GE.SEN(I).AND.SEN(I+1).GE.SEX(I+1)) GO TO 16
   15 CONTINUE
      GO TO 24
   16 X=DPHI/(1.0+(SEX(I)-SEN(I))/(SEN(I+1)-SEX(I+1)))
      XI1=I+1
      PHIN=(XM-XI1)*DPHI+X
      Y=(SEN(I+1)-SEN(I))*(1.0-X/DPHI)
      SN=SEN(I)+Y
      IN=I
C     INTEGRATE ROLL PRESSURE BY TRAPEZOIDAL RULE TO FIND THE ROLL FORCE
C     INCLUDING THE EFFECT OF THE ANGLE AND CONTRIBUTION OF THE SHEAR
C     STRESSES. FIRST FIND TAUN.
      XKN=0.5*XXK(PHIN)
      IF(XMU*SN.LT.XKN) TAUN=XMU*SN
      IF(XMU*SN.GE.XKN) TAUN=XKN
      PHI=PHI1
      DO 18 I=1,M
      ARG=PHI-0.5*PHI1
      XS=SIN(ARG)
      XC=COS(ARG)
      SPHI(I)=S(I)*PHI
      SSIN(I)=S(I)*XS
      SCOS(I)=S(I)*XC
      IF(XMU*S(I).LT.XK(I)) TAU(I)=XMU*S(I)
      IF(XMU*S(I).GE.XK(I)) TAU(I)=XK(I)
      TAUSIN(I)=TAU(I)*XS
      GORD(I)=TAU(I)*(RD-(RD-R)*XC)
   18 PHI=PHI-DPHI
      TAUNSN=TAUN*SIN(PHIN-PHI1*0.5)
      DAEN=(TAUSIN(IN)+TAUNSN)*(DPHI-X)*0.5
      DAEX=(TAUSIN(IN+1)+TAUNSN)*X*0.5
      CALL TRAPEZ(TAUSIN,DPHI, 2,IN-1,AREA)
      AREAEN=AREA+DAEN
      CALL TRAPEZ(TAUSIN,DPHI,IN+2,M-1,AREA)
      AREAEX=AREA+DAEX
      CALL SIMPSN(SCOS,DPHI,2,M-3,AREAP)
      P=RD*(AREAP+AREAEN-AREAEX)
      J1=0
      PE11=(1.0-XNU**2)*H1*(X2K1-T1)**2*SQRT(RD/DRAFT)/(4.0*E)
   44 TE1=T1-2.0*XMU*PE11/H1
      PE1=(1.0-XNU**2)*H1*(X2K1-TE1)**2*SQRT(RD/DRAFT)/(4.0*E)
      IF(ABS((PE1-PE11)/PE1).LT.1.0E-06.OR.J1.GT.10) GO TO 46
      PE11=PE1
      J1=J1+1
      GO TO 44
   46 A1=(2.0/3.0)*SQRT(RD*H2*(1.0-XNU**2)/E)
      J2=0
      PE21=A1*(X2K2-T2)**1.5
   39 TE2=T2-2.0*XMU*PE21/H2
      PE2=A1*(X2K2-TE2)**1.5
      IF(ABS((PE2-PE21)/PE2).LT.1.0E-06.OR.J2.GT.25) GO TO 40
      PE21=PE2
      J2=J2+1
      GO TO 39
   40 P=P+PE1+PE2
      DRAFTT=XNU*(1.0+XNU)*(H2*T2-H1*T1)/E
      DRAFTE=(1.0-XNU**2)*(X2K2-TE2)*H2/E
      A2=.000334/(SQRT(DRAFT+DRAFTE+DRAFTT)+SQRT(DRAFTE))**2
      RD=R*(1.0+A2*P)
C     ITERATE J TIMES TO FIND COMPATIBLE P AND RD.
      IF(ABS((P-P1)/P1).LT.1.0E-6.OR.J.GT.30) GO TO 17
      P1=P
      J=J+1
      GO TO 11
   17 GE1=XMU*R*PE1
      GE2=-XMU*R*PE2
C
C        THIS IS FOR PLOTTING X-ANGLE DIRECTION
C
      DO 666 I=1,M
      DIFF=DIFF+(DPHI)*360./(2.*3.141592)
      AA1(I)=DIFF
666   CONTINUE
C
C
C     INTEGRATE SHEAR STRESSES TO DETERMINE THE TORQUE APPROXIMATELY---
      DAEXT=(TAUN+TAU(IN+1))*X/2.0
      DAENT=(TAUN+TAU(IN))*(DPHI-X)/2.0
      CALL TRAPEZ(TAU,DPHI,2,IN-1,AREA)
      AREANT=AREA+DAENT
      CALL TRAPEZ(TAU,DPHI,IN+2,M-1,AREA)
      AREAXT=AREA+DAEXT
      TAP=R*RD*(AREANT-AREAXT)
      GAP=RD**2*(AREANT-AREAXT)-0.5*(RD-R)*(P*PHI1+T1*H1-T2*H2)
      CALL SIMPSN(SPHI,DPHI,2,M-3,AREAT)
      T=R*RD*AREAT+(R/2.0)*(T1*H1-T2*H2)
      G=RD**2*AREAT+(R/2.0)*(T1*H1-T2*H2)-P*(RD-R)*PHI1/2.0
C      INTEGRATE EXACT EQUATION TO FIND ACCURATE TORQUE GAC.
      GORDN=TAUN*(RD-(RD-R)*COS(PHIN-PHI1*0.5))
      DAEXG=(GORDN+GORD(IN+1))*X*0.5
      DAENG=(GORDN+GORD(IN))*(DPHI-X)*0.5
      CALL TRAPEZ(GORD,DPHI, 2,IN-1,AREA)
      AREANG=AREA+DAENG
      CALL TRAPEZ(GORD,DPHI,IN+2,M-1,AREA)
      AREAXG=AREA+DAEXG
      CALL SIMPSN(SSIN,DPHI,2,M-3,AREAG)
      GAC=RD*(RD-R)*AREAG+RD*(AREANG-AREAXG)
      GAC12=GAC+GE1+GE2
      TT=GAC12/(17.32*H1*R)
      PPP=P/(17.32*H1)
      SP1(ZZ)=P
      TRQ1(ZZ)=GAC12
      WRITE (6,5432) P,GAC12,XMU,PPP,TT
 5432 FORMAT(/5X,'ROLL FORCE=',F15.4,' T/IN'//5X,'ROLL TORQUE='
     1,F15.4,' T IN/IN'/5X,'COEFFICIENT OF FRICTION=',F8.4,5X,2E15.8)
      WRITE (6,19) P,P1,PAP,T,TAP,J,RD,X2K1,X2K2,X2KM,G,GAP,GAC,J1,PE1,
     1TE1,GE1,J2,PE2,TE2,GE2,GAC12,PHI1,DPHI,PHIN,SN
   19 FORMAT(/2X,'P= ',F20.4,'T/IN.P1=',F12.8,'T/IN.PAP='
     1,F12.8,'T/IN.',/2X,'T=',F13.8,'T IN/IN. TAP=',F12.8,
     2'TIN/IN.J=',I2,'ITERATIONS. RD=',F12.8,'INS.'/2X,'X2K1=
     3',F12.8,'T/SQIN.X2K2=',F12.8,'T/SQIN.X2KM=',F12.8,'T/SQ
     4IN.'/2X,'G=',F20.4,'T IN/IN. GAP=',F20.4,'T IN/IN. GAC=
     5',F20.4,'T IN/IN . J1=',I2,'ITERATIONS.'/2X,'PE1=',F12.8,
     6'T/IN. TE1=',F12.8,'T/SQIN.GE1=',E15.8,'T IN/IN.J2='
     7,I2,'ITERATIONS,'/2X,'PE2=',F12.8,'T/IN.TE2=',F12.8,'T/SQ
     8IN. GE2=',E15.8,'TIN/IN. GAC12=',F20.4,'T IN/IN.'/
     9   2X,'PHI1=',F12.9,', DPHI=',E15.8,',PHIN=',F12.9,
     1', ALL IN RADIANS. SN=',F12.8,'T/SQ IN.'/)
      DO 914 I=1,M,10
      WRITE(6,444)FP1(I),AA1(I)
444   FORMAT('0',2X,'ROLL PRESSURE=',F10.5,'ANGLE =',5X,F10.5)
914   CONTINUE
      CALL PPLOT(AA1,FP1,M,IXLBL,IYLBL,R,ACHIL,XMU1,TEMP,RPM,II)
711   CONTINUE
      CALL PPLOT1(REDUCT,SP1,K11,IXLBL1,IYLBL1,R,RPM,XMU1,
     &TEMP,II,H1,Y0)
      CALL PPLOT2(REDUCT,TRQ1,K11,IXLBL2,IYLBL2,R,RPM,XMU1,
     &TEMP,II,H1,Y0)
      GO TO 26
   24 WRITE(6,25)
   25 FORMAT(/1X,'NO NEUTRAL POINT CAN BE FOUND,THEREFORE A FEASIBLE SO
     1LUTION DOES NOT EXIST FOR THESE CONDITIONS.'/)
      WRITE(6,33)
 33 FORMAT(/4X,'I',9X,'SEN T/SQ IN',8X,'SEX T/SQ IN',12X,'S T/SQ IN
   1'//)
    DO 34 I=1,M,K
 34 WRITE (6,35) I,SEN(I),SEX(I),S(I)
 35 FORMAT (I6,3F20.10)
 26 GO TO 1
 27 STOP
    END
    FUNCTION  H(PHI)
    COMMON H2,RD,XMU,Z,B,HO,YO,XN,Q
    COMMON C,TEMP,VS,WW,EN,RPM,R,H1
    COMMON HPW,PMN
    COMMON AA
C
    H=H2+RD*(PHI**2)
C
    RETURN
    END
    FUNCTION W(PHI)
    COMMON H2,RD,XMU,Z,B,HO,YO,XN,Q
    COMMON C,TEMP,VS,WW,EN,RPM,R,H1
    COMMON HPW,PMN
    COMMON AA
    W=Z*ALOG(HO/H(PHI))
    RETURN
    END
    FUNCTION XXK(PHI)
    COMMON H2,RD,XMU,Z,B,HO,YO,XN,Q
    COMMON C,TEMP,VS,WW,EN,RPM,R,H1
    COMMON HPW,PMN,AA
    XXK=Z*YO*(1.0+Z*B*ALOG(HO/H(PHI)))**XN
    RETURN
    END
    FUNCTION XXKK(ANGLE)
    COMMON H2,RD,XMU,Z,B,HO,YO,XN,Q
    COMMON C,TEMP,VS,WW,EN,RPM,R,H1
    COMMON HPW,PMN,AA
    XXKK=Z*YO*(1.0+Z*B*ALOG(ANGLE))**XN
    RETURN
    END
    FUNCTION DXXK(PHI)
    COMMON H2,RD,XMU,Z,B,HO,YO,XN,Q
    COMMON C,TEMP,VS,WW,EN,RPM,R,H1
    COMMON HPW,PMN,AA
    XS=SIN(PHI)
    DXXK=(-2.0*Z**2)*YO*XN*B*RD*XS/(((1.0+Z*B*ALOG(HO/H(PHI)))**(1.0
   1-XN))*(H(PHI)))
    RETURN
    END
    FUNCTION G1(PHI)
    COMMON H2,RD,XMU,Z,B,HO,YO,XN,Q
    COMMON C,TEMP,VS,WW,EN,RPM,R,H1
    COMMON HPW,PMN
    COMMON AA
```

```
      XS=SIN(PHI)
      XC=COS(PHI)
      XH=H2+RD*(PHI**2)
      G1=((1/XXK(PHI))*DXXK(PHI)+2.0*RD/XH*(PHI+Q*XMU))
      RETURN
      END
      FUNCTION  G2(PHI)
      COMMON H2,RD,XMU,Z,B,HO,YO,XN,Q
      COMMON C,TEMP,VS,WW,EN,RPM,R,H1
      COMMON HPW,PMN
      COMMON AA
C     XS=SIN(PHI)
C     XC=COS(PHI)
C     XH=H2+2.0*RD*(1.0-XC)
      G2=0.0
      RETURN
      END
      FUNCTION G3(PHI)
      COMMON H2,RD,XMU,Z,B,HO,YO,XN,Q
      COMMON C,TEMP,VS,WW,EN,RPM,R,H1
      COMMON HPW,PMN
      COMMON AA
      XS=SIN(PHI)
      XC=COS(PHI)
      XH=H2+RD*(PHI**2)
      G3=XXK(PHI)*(2.0*RD*XS*(1.0+Q*0.5*XS/XC)/XH+Q*RD*XC/XH+0.5*Q/XC**2
     1)+(1.0+0.5*Q*XS/XC)*DXXK(PHI)
      RETURN
      END
      FUNCTION G4(PHI)
      COMMON H2,RD,XMU,Z,B,HO,YO,XN,Q
      COMMON C,TEMP,VS,WW,EN,RPM,R,H1
      COMMON HPW,PMN
      COMMON AA
      G4=0.0
      RETURN
      END
      SUBROUTINE TRAPEZ(Y,DX,N1,N2,A)
      DIMENSION Y(1)
      SUM=0.0
      DO 1 I=N1,N2
    1 SUM=SUM+Y(I)
      A=(DX/2.0)*(Y(N1-1)+2.0*SUM+Y(N2+1))
      RETURN
      END
      SUBROUTINE SIMPSN(Y,DX,N1,N2,A)
      DIMENSION Y(1)
      ODD=0.0
      EVEN=0.0
      DO 1 I=N1,N2,2
      EVEN=EVEN+Y(I)
    1 ODD=ODD+Y(I+1)
      A=(DX/3.0)*(Y(N1-1)+4.0*(EVEN+Y(N2+2))+2.0*ODD+Y(N2+3))
      RETURN
      END
      SUBROUTINE RUNGE (X,Y,DX,DY,FA,FB)
      COMMON H2,RD,XMU,Z,B,HO,YO,XN,Q
      COMMON C,TEMP,VS,WW,EN,RPM,R,H1
      COMMON HPW,PMN
      COMMON AA
      FO=FA(X)*Y+FB(X)
      A=FA(X+0.5*Q*DX)
      CC=FB(X+0.5*Q*DX)
      F1=A*(Y+0.5*Q*DX*FO)+CC
      F2=A*(Y+0.5*Q*DX*F1)+CC
      F3=FA(X+Q*DX)*(Y+Q*DX*F2)+FB(X+Q*DX)
      DY=DX*(FO+2.0*(F1+F2)+F3)*Q/6.0
      RETURN
      END
013396.000000 000000.280000 000038.429000 000078.300000 000000.0670000 0
1501 00.50000 04.92120 00.19690 00.196900 0.1872000 0.0000000 000.00000
004500.0000000000000.3000000000012.1700000000096.8000000000000.2000000 5
```

```
      ******************************************************************
C     *  CALCULATION OF ROLL PRESSURE DISTRIBUTION, SEPARATING FORCE,  *
C     *  TORQUE & THE ARC LENGTH OF CONTACT; TAKING INTO ACCOUNT THE   *
C     *    ROLL DEFORMATION COMPUTED FROM MICHELL'S SOLUTION OF THE    *
C     *  BIHARMONIC EQUATION BY REPRESENTING THE LOAD DISTRIBUTION IN *
C     *     THE FORM OF A FOURIER SERIES FOR  A  FOUR  HIGH  MILL.     *
C     *       ELASTIC ENTRY AND EXIT CONTRIBUTION IS INCLUDED.         *
C     *................................................................*
C     *  PROCEDURE:- THE LOAD DISTRIBUTION IS FIRST CALCULATED TAKING *
C     *    AN UNDEFORMED ROLL AND USING THIS THE ROLL DEFORMATION IS   *
C     *        COMPUTED, WHICH IS THEN USED TO FIND THE NEW LOAD       *
C     *  DISTRIBUTION IN AN ITERATIVE MANNER TILL THE ROLL SEPARATING *
C     *          FORCE REACHES WITHIN THE ACCURACY REQUIRED.           *
C     *................................................................*
C     *  NOTE:1)IN THE FOLLOWING CALCULATION THE ROLL GAP IS ADJUSTED *
C     *         AFTER EACH ITERATION SO AS TO ACCOMODATE FOR THE ROLL *
C     *         DEFORMATION AND KEEP EXIT STRIP THICKNESS CONSTANT.    *
C     *       2)COULOMB  FRICTION  BETWEEN  THE ROLLS  AND THE  STRIP *
C     *         EXITS  THROUGHOUT  THE  ROLL  GAP.                     *
C     ******************************************************************
C
      IMPLICIT REAL*8 (A-H,O-Z)
C
      DIMENSION XA(500),XB(500),X(500),Y(500),HH(500),
     1          SEX(500),SEN(500),PEN(500),PEX(500),
     2          SENTRX(500),SENTRY(500),SEXTRX(500),SEXTRY(500),XK(500),
     3          URD(500),FP(500),FQ(500),A(500),
     4          PBAF(500),PBBF(500),QBA(500),QBB(500),RBA(500),RBB(500),
     2          PBA(500),PBB(500),BU(500),BL(500),AU(500),AL(500)
C
      REAL DIFF,AA(250),AA1(250),X1R(250),Y1R(250),XX(250),YY(250)
      COMMON CO,DUI,DLI,XNU,ER,RB,SUMU(500),SUML(500),L
C
C  .........INPUT PARAMETERS...........
C
C  NOTE:- M      REPRESENTS THE # OF POINTS ON THE ARC OF CONTACT
C         L      REPRESENTS THE # OF TERMS OF THE FOURIER SERIES
C
C  OUTPUT UNITS WILL CORRESPOND TO INPUT UNITS. ANY UNITS CAN BE USED
C
C  BEFORE RUNNING THE PROGRAM CHECK THE YIELD STRESS EQUATIONS IN
C  LINES # 84, 85, 135, 257 AND MAKE NECESSARY CHANGES IN INPUT VALUES.
C
              M      =200
              L      =200
              PI     =3.141592653589793
              XMU    =0.3000
              II    =5
C
C         .........ROLL........
C             ER     =210.0D03
              ER     =207.0D03
              XNU    =0.28
              RB     =(4.97000)*25.4
```

```
C        ........STRIP.......
              ES   =206840.00
              SNU  =0.30
              YO   =116.50
              BB   =00.00
              XN   =0.000
              HA   =(0.2180)*25.4
              HU   =(0.2180)*25.4
              HO   =(0.1470)*25.4
              AENTR=1219.0*HU
              AEXIT=1219.0*HO
C
C ......NOTE: T1 & T2 ARE STRESSES AND NOT FORCES.
C
              T1   =0.0/AENTR
              T2   =0.0/AEXIT
C
C  PART 1:
C  *******
C  THE NORMAL AND SHEAR LOAD DISTRIBUTION ON THE ROLL SURFACE IS
C  CALCULATED FROM A KNOWN GAUGE PROFILE
C                   .........................
C
C....TEST FOR TENSION STRESSES. IF REQUIRED DECREASE T1 & T2
C
      Z=2.0/DSQRT(3D00)
C     Z=1.0
      YK1=Z*YO*(1.0+BB*DLOG(HA/HU))**XN
      YK2=Z*YO*(1.0+BB*DLOG(HA/HO))**XN
      IF(T1.GT.YK1) T1=YK1
      IF(T2.GT.YK2) T2=YK2
C
C....TEST FOR SLAB ENTRY CONDITIONS. IF FRICTION IS LOW, PRINT MESSAGE
C
      H33=HO/(1.0+(1.0-SNU**2)*YK2/ES)
      H3MIN=HU-2.0*RB*(1.0-DCOS(DATAN(XMU)))
      IF(H33.GT.H3MIN) GO TO 100
      WRITE(6,110)
 110  FORMAT(//,12X,'*** ENTRY THRUST REQUIRED TO INITIATE ROLLING ***')
 100  CONTINUE
C
      RR=((HU-HO)/HU)*100.0
C
C....PRINT OUT ALL THE INPUT DATA WITH CORRECTIONS IF MADE
C
      WRITE(6,120)
  120 FORMAT(//16X,'INITIAL INPUT PARAMETERS WITH CORRECTIONS')
      WRITE(6,130) HU,HO,T1,T2
  130 FORMAT (//5X,'HU=',F10.7,5X,'HO=',F10.7,
     *        5X,'T1=',F14.7,5X,'T2=',F14.7)
      WRITE(6,140) RR
  140 FORMAT(//25X,'REDUCTION RATIO=',F6.2,'%')
C
```

```
C...CALCULATE AND PRINT OUT THE ARC LENGTH OF CONTACT, PHI1 & PHI2,
C      ROLL GAP H3 AND REDUCTION RATIO RR, FOR EACH ITERATION
C
C   DETERMINATION OF H1, H4 & H3 CORRECTED FOR PROPER STRESSES
C
      H11=HU*(1.0-SNU*(1.0+SNU)*T1/ES)
      H1BYHU=H11/HU
  142 H1=HU*(1.0-SNU*(1.0+SNU)*T1*H1BYHU/ES)
      H1BYHU=H1/HU
      IF((H1-H11).LT.1D-9) GO TO 141
      H11=H1
      GO TO 142
  141 CONTINUE
C
      H44=HO*(1.0-SNU*(1.0+SNU)*T2/ES)
      H4BYHO=H44/HO
  144 H4=HO*(1.0-SNU*(1.0+SNU)*T2*H4BYHO/ES)
      H4BYHO=H4/HO
      IF((H4-H44).LT.1D-9) GO TO 143
      H44=H4
      GO TO 144
  143 CONTINUE
C
      LMNK=1
C
  160 YK3=Z*YO*(1.0+BB*DLOG(HA/H33))**XN
      H3=HO/(1.0+(1.0-SNU**2)*YK3/ES)
      IF((H33-H3).LT.1D-9) GO TO 150
      H33=H3
      GO TO 160
  150 CONTINUE
      D=RB+H3/2.0
      DI=D
      DRAFT1=H1-H3
      DRAFT4=H4-H3
      PHI1=+DARCOS(1.0-DRAFT1/(2.0*RB))
      PHI4=-DARCOS(1.0-DRAFT4/(2.0*RB))
C
      SPF=0.0
C
 1000 CONTINUE
C
      IF(LMNK.EQ.1) GO TO 170
C
      N=1
      PHI3=0.0
      DELH3=UR(PHI3)
  180 PHI3=-0.0001*N
      DELH33=RB*(1.0-DCOS(PHI3))+UR(PHI3)*DCOS(PHI3)
      IF(DELH3.LT.DELH33) GO TO 190
      DELH3=DELH33
      N=N+1
      GO TO 180
  190 CONTINUE
```

```
      D=DI-DELH3
      RGAP=H3-2.0*DELH3
      DRAFT1=H1-RGAP
      DRAFT4=H4-RGAP
      PHI1=+DARCOS(1.0-DRAFT1/(2.0*RB))
      PHI4=-DARCOS(1.0-DRAFT4/(2.0*RB))
C
      U1=UR(PHI1)
      PHI1=PHI1-U1/((RB-U1)*DTAN(PHI1))
  200 PHI11=PHI1-0.0005
      U1=UR(PHI11)
      H11=2.0*(RB-(RB-U1)*DCOS(PHI11))+RGAP
      PHI1=PHI11
      IF(H11.LE.H1) GO TO 210
      GO TO 200
  210 PH1=PHI1*180.0/PI
C
      U4=UR(PHI4)
      PHI4=PHI4-U4/((RB-U4)*DTAN(PHI4))
  230 PHI44=PHI4+0.0005
      U4=UR(PHI44)
      H44=2.0*(RB-(RB-U4)*DCOS(PHI44))+RGAP
      PHI4=PHI44
      IF(H44.LE.H4) GO TO 220
      GO TO 230
  220 PH4=PHI4*180.0/PI

      PHI=PH1-PH4
      ARCL=(RB-U1)*DSIN(PHI1)-(RB-U4)*DSIN(PHI4)
C
      WRITE(6,240) LMNK-1
  240 FORMAT(//30X,'ITERATION #',I2)
      WRITE(6,250) PHI1,PH1,PHI4,PH4,PHI,ARCL,RGAP
  250 FORMAT(//,20X,'PHI1=',F8.5,' RADS =',F8.4,' DEGS',
     *       //,20X,'PHI4=',F8.5,' RADS =',F8.4,' DEGS',
     *       //,20X,'ANGLE  OF  CONTACT =',F8.4,' DEGS',
     *       //,20X,'ARC LENGTH OF CONTACT =',F10.6,
     *       //,20X,'ROLLGAP ADJUSTED TO (H3)=',F8.5,//)
C
      GO TO 280
C
  170 CONTINUE
      PH1=PHI1*180.0/PI
      PH4=PHI4*180.0/PI
      PHI=PH1-PH4
      ARCL=RB*(DSIN(PHI1)-DSIN(PHI4))
      WRITE(6,290) PHI1,PH1,PHI4,PH4,PHI,ARCL,H3
  290 FORMAT(//,20X,'PHI1=',F8.5,' RADS =',F8.4,' DEGS',
     *       //,20X,'PHI4=',F8.5,' RADS =',F8.4,' DEGS',
     *       //,20X,'ANGLE  OF  CONTACT =',F8.4,' DEGS',
     *       //,20X,'ARC LENGTH OF CONTACT =',F10.6,
     *       //,20X,'INITIAL ROLL GAP (H3) =',F10.7,//)
C
C....DIVIDE ARC OF CONTACT INTO (M-1) EQUAL DIVISIONS AND CALCULATE THE
```

```
       CORRESPONDING VALUES OF THE ANGLE & (X,Y) LOCATION ON THE SURFACE
       OF THE ROLL
C
      DO 300 I=1,M,1
      A(I)=PHI4+(PHI1-PHI4)*FLOAT(I-1)/FLOAT(M-1)
      URD(I)=0.0
      X(I)=+RB*DSIN(A(I))
      Y(I)=-RB*DCOS(A(I))
  300 CONTINUE
      DTHETA=A(2)-A(1)
C
      GO TO 310
C
  280 CONTINUE
      DO 320 I=1,M,1
      A(I)=PHI4+(PHI1-PHI4)*FLOAT(I-1)/FLOAT(M-1)
      URD(I)=UR(A(I))
      X(I)=+(RB-URD(I))*DSIN(A(I))
      Y(I)=-(RB-URD(I))*DCOS(A(I))
  320 CONTINUE
      DTHETA=A(2)-A(1)
C
  310 CONTINUE
C
C....CALCULATE THE LOAD DISTRIBUTION ON THE ROLL SURFACE

           THIS IS MINE FOR COMPARISION REASONS ONLY
C
      ABC=YK3-T2
C
C
      SEN(M)=0.0
      SEX(1)=0.0
      PEN(M)=-T1
      PEX(1)=-T2
      SENTRY(M)=0.0
      SEXTRY(1)=0.0
      SENTRX(M)=0.0
      SEXTRX(1)=0.0
C
C    GAUGE PROFILE PARAMETERS  & YIELD STRENGTH FOR EACH SLAB
C
      J=M-1
      DO 330 I=1,J,1
      XB(M-I)=(Y(M-I)-Y(M-I+1))/(X(M-I)-X(M-I+1))
      XA(M-I)=Y(M-I)-X(M-I)*XB(M-I)
      XK(M-I)=Z*YO*(1.0+BB*DLOG(HA/(2.0*D+Y(M-I)+Y(M-I+1))))**XN
      HH(M-I)=2.0*D+Y(M-I)+Y(M-I+1)
C     WRITE (6,700) I,HH(M-I)
C 700 FORMAT(20X,I5,10X,F15.5)
  330 CONTINUE

               ELASTIC  ENTRY
C
```

```
      DO 340 I=1,J,1
      E1=1.0-SNU*(XB(M-I)-XMU)/(XB(M-I)*(1.0-SNU)*(XMU*XB(M-I)+1.0))
      E2=-ES*(XB(M-I)-XMU)/(XB(M-I)*E1*(1.0-SNU**2)*(XMU*XB(M-I)+1.0))
      E3=XB(M-I)*X(M+1-I)+XA(M-I)+D
      E4=XB(M-I)*X(M-I)+XA(M-I)+D
      E5=E2*HU*E1/(2.0*(E1-1.0))
C
      PEN(M-I)=E2-E5/E4+(PEN(M+1-I)-E2)*(E3/E4)**E1+E5*(E3/E4)**E1/E3
      SEN(M-I)=-ES*(2.0*E4-HU)/(2.0*(1.0-SNU**2)*E4*(XMU*XB(M-I)+1.0))
     *            +SNU*PEN(M-I)/((1.0-SNU)*(XMU*XB(M-I)+1.0))
C
      SENTRY(M-I)=SEN(M-I)*(XMU*XB(M-I)+1.0)
      SENTRX(M-I)=SEN(M-I)*(XMU-XB(M-I))
C
      YS=SEN(M-I)*(1.0+XB(M-I)*XMU)-PEN(M-I)
      IJ=I
      IF(YS.GT.XK(M-I)) GO TO 350
  340 CONTINUE
C
  350 CONTINUE
C
C                 PLASTIC  ENTRY
C
      DO 360 I=IJ,J,1
      IF(DABS(XB(M-I)).LT.1D-9) GO TO 370

      A1=XB(M-I)*(1.0+XMU*XB(M-I))/(XMU*(1.0+XB(M-I)**2))
      A2=1.0/A1
      A3=(XA(M-I)+D+XB(M-I)*X(M+1-I))/(XA(M-I)+D+XB(M-I)*X(M-I))
C
      PEN(M-I)=(PEN(M+1-I)+XK(M-I)*(1.0-A1))*(A3**A2)+XK(M-I)*(A1-1.0)
      SEN(M-I)=(PEN(M-I)+XK(M-I))/(1.0+XB(M-I)*XMU)
C
      SENTRY(M-I)=SEN(M-I)*(XMU*XB(M-I)+1.0)
      SENTRX(M-I)=SEN(M-I)*(XMU-XB(M-I))
C
      GO TO 380
  370 PEN(M-I)=(PEN(M+1-I)+XK(M-I))*
     *         (EXP((XMU*(X(M+1-I)-X(M-I)))/(XA(M-I)+D)))-XK(M-I)
      SEN(M-I)=PEN(M-I)+XK(M-I)
C
      SENTRY(M-I)=SEN(M-I)
      SENTRX(M-I)=SEN(M-I)*XMU
  380 CONTINUE
C
  360 CONTINUE
C
C                 ELASTIC  EXIT
C
      DO 390 I=1,J,1
      F1=1.0+SNU*(XB(I)+XMU)/(XB(I)*(1.0-SNU)*(XMU*XB(I)-1.0))
      F2=+ES*(XB(I)+XMU)/(XB(I)*F1*(1.0-SNU**2)*(XMU*XB(I)-1.0))
      F3=XB(I)*X(I)+XA(I)+D
      F4=XB(I)*X(I+1)+XA(I)+D
      F5=F2*HO*F1/(2.0*(F1-1.0))

      PEX(I+1)=F2-F5/F4+(PEX(I)-F2)*(F3/F4)**F1+F5*(F3/F4)**F1/F3
      SEX(I+1)=+ES*(2.0*F4-HO)/(2.0*(1.0-SNU**2)*F4*(XMU*XB(I)-1.0))
     *             -SNU*PEX(I+1)/((1.0-SNU)*(XMU*XB(I)-1.0))
C
      SEXTRY(I+1)=+SEX(I+1)*(1.0-XMU*XB(I))
      SEXTRX(I+1)=-SEX(I+1)*(XB(I)+XMU)
C
      BIG=SEXTRY(I+1)
      IK=I+1
      IF(XB(I).GT.0.0) GO TO 400
  390 CONTINUE
C
  400 CONTINUE
C
C                    PLASTIC  EXIT
C
      DO 410 I=IK,J,1
      IF(DABS(XB(I)).LT.1D-9) GO TO 420
C
      B1=XB(I)*(1.0-XMU*XB(I))/(XMU*(1.0+XB(I)**2))
      B2=1.0/B1
      B3=(XA(I)+D+XB(I)*X(I+1))/(XA(I)+D+XB(I)*X(I))
C
      PEX(I+1)=(PEX(I)+XK(I)*(1.0+B1))*(B3**B2)-XK(I)*(B1+1.0)
      SEX(I+1)=(PEX(I+1)+XK(I))/(1.0-XB(I)*XMU)
C
      SEXTRY(I+1)=+SEX(I+1)*(1.0-XMU*XB(I))
      SEXTRX(I+1)=-SEX(I+1)*(XB(I)+XMU)
C
      GO TO 430
  420 PEX(I+1)=(PEX(I)+XK(I))*
     *             (EXP((XMU*(X(I+1)-X(I)))/(XA(I)+D)))-XK(I)
      SEX(I+1)=PEX(I+1)+XK(I)
C
      SEXTRY(I+1)=+SEX(I+1)
      SEXTRX(I+1)=-SEX(I+1)*XMU
  430 CONTINUE
C
  410 CONTINUE
C
      DIFF=0.0
      DO 440 I=1,M,1
      DIFF=DIFF+PHI/M
      AA(I)=DIFF
      IF(SEN(I).LT.SEX(I)) GO TO 450
      IF(I.NE.IK) GO TO 451
C     WRITE(6,452)
  451 FP(I)=-SEX(I)
      FQ(I)=-XMU*SEX(I)
      SENTRX(I)=SEXTRX(I)
      SENTRY(I)=SEXTRY(I)
      GP=RB*(1.0-DCOS(A(I)))+URD(I)*DCOS(A(I))
      GO TO 460
  450 IF(I.NE.(M-IJ+1)) GO TO 453
      WRITE(6,452)
  453 FP(I)=-SEN(I)
      FQ(I)=+XMU*SEN(I)
      SENTRX(I)=SENTRX(I)
      SENTRY(I)=SENTRY(I)
      GP=RB*(1.0-DCOS(A(I)))+URD(I)*DCOS(A(I))
  452 FORMAT(20X,'.....ELASTIC  PLASTIC  INTERFACE.....')
  460 WRITE(6,470) I,FP(I),URD(I),GP
  470 FORMAT(5X,'I=',I3,2X,'FP=',F14.2,2X,'URD=',F9.6,2X,
     *        2X,'GAUGE PROFILE=',F9.6)
  440 CONTINUE
      DO 441 I=1,M
      FP(I)=-FP(I)
      WRITE(6,911)AA(I),FP(I)
911   FORMAT('0',2X,F10.5,10X,F10.5)
      FP(I)=-FP(I)
441   CONTINUE
C
C....CALCULATE THE ROLL SEPARATING FORCE IN THE VERTICAL DIRECTION
C
      SP=0.0
      SPTY=0.0
      SPTX=0.0
      DO 480 I=1,J,1
      SPP=0.5*(SENTRY(I)+SENTRY(I+1))*(X(I+1)-X(I))
      SPPTX=0.25*(SENTRX(I)+SENTRX(I+1))*(X(I+1)-X(I))*(Y(I+1)+Y(I))
      SPPTY=0.5*SPP*(X(I+1)+X(I))
      SP=SP+SPP
      SPTX=SPTX+SPPTX
      SPTY=SPTY+SPPTY
  480 CONTINUE
      TRQ=SPTY-SPTX
      DSP=SP/(YO*HU)
      DTRQ=TRQ/(YO*RB*HU)
      WRITE(6,490) SP,DSP,TRQ,DTRQ
  490 FORMAT(//5X,'VERTICAL SEP FORCE=',F14.3,2X,'FORCE(DIMLESS)=',
     1F8.5,2X,'ROLL TORQUE=',F14.3,2X,'TORQUE(DIMLESS)=',F8.5)
C
      IF(DABS((SP-SPF)/SP).LT.0.01) GO TO 650
      SPF=SP
C
      LMNK=LMNK+1
C
C  PART 2:
C  *******
C  THE ROLL DEFORMATION IS COMPUTED FROM THE NORMAL AND SHEAR LOAD
C  DISTRIBUTION ON THE ROLL SURFACE CALCULATED IN PART 1
C                  .........................
C
C...CALCULATE THE COEFFICIENTS OF THE FOURIER SERIES FOR THE NORMAL
C      AND SHEAR LOAD DISTRIBUTION
C
```

```
      A(1)=A(1)+DTHETA/4.0
      A(M)=A(M)-DTHETA/4.0
C
      PBAFO=0.0
      DO 500 I=1,M,1
      PBAFO=PBAFO+FP(I)
  500 CONTINUE
      PBAFO=PBAFO*DTHETA/(2*PI)
C
      DO 520 I=1,L,1
      PBAF(I)=0.0
      DO 530 J=1,M,1
      PBAF(I)=PBAF(I)+FP(J)*DCOS(A(J)*I)
  530 CONTINUE
      PBAF(I)=PBAF(I)*DTHETA/PI
C
      PBBF(I)=0.0
      DO 540 J=1,M,1
      PBBF(I)=PBBF(I)+FP(J)*DSIN(A(J)*I)
  540 CONTINUE
      PBBF(I)=PBBF(I)*DTHETA/PI
C
      QBA(I)=0.0
      DO 550 J=1,M,1
      QBA(I)=QBA(I)+FQ(J)*DCOS(A(J)*I)
  550 CONTINUE
      QBA(I)=QBA(I)*DTHETA/PI
C
      QBB(I)=0.0
      DO 560 J=1,M,1
      QBB(I)=QBB(I)+FQ(J)*DSIN(A(J)*I)
  560 CONTINUE
      QBB(I)=QBB(I)*DTHETA/PI
  520 CONTINUE
C
      RPY=-PI*RB*PBAF(1)
      RPX=+PI*RB*PBBF(1)
C
      RQY=+PI*RB*QBB(1)
      RQX=+PI*RB*QBA(1)
C
      RX=RPX+RQX
C
      RY=RPY+RQY
C
      R=DSQRT(RX**2+RY**2)
C
      SHI=-DATAN(RX/RY)
C
      XL=3.2*DSQRT(R*RB*(1.0-XNU)**2/ER)
C
       ZETA=0.5*XL/RB

      RAMP=R*ZETA*((PI/(2*ZETA))**2-1)/(RB*PI*DCOS(ZETA))
      RBAO=-2.0*RAMP*ZETA/(PI**2)
C
      PBAO=PBAFO+RBAO
C
      DO 570 I=1,L,1
      RBA(I)=-RAMP*((DCOS(I*(-PI+SHI+ZETA))
     *       +DCOS(I*(-PI+SHI-ZETA)))/(PI/(2*ZETA)+I)+
     *       (DCOS(I*(-PI+SHI+ZETA))
     *       +DCOS(I*(-PI+SHI-ZETA)))/(PI/(2*ZETA)-I))/(2*PI)
C
      RBB(I)=-RAMP*((DSIN(I*(-PI+SHI+ZETA))
     *       +DSIN(I*(-PI+SHI-ZETA)))/(PI/(2*ZETA)+I)+
     *       (DSIN(I*(-PI+SHI+ZETA))
     *       +DSIN(I*(-PI+SHI-ZETA)))/(PI/(2*ZETA)-I))/(2*PI)
C
      PBA(I)=PBAF(I)+RBA(I)
C
      PBB(I)=PBBF(I)+RBB(I)
  570 CONTINUE
C
      DO 580 I=2,L,1
      BU(I)=(PBB(I)-QBA(I))/(2*(I+1))
C
      BL(I)=(PBA(I)+QBB(I))/(2*(I+1))
C
      AU(I)=-(I*PBB(I)-(I-2)*QBA(I))/(2*I*(I-1))
C
      AL(I)=-(I*PBA(I)+(I-2)*QBB(I))/(2*I*(I-1))
C
      SUMU(I)=AU(I)*I*(1+XNU)*RB+
     *          BU(I)*((I-2)*(1-XNU**2)+(I+2)*XNU*(1+XNU))*RB
C
      SUML(I)=AL(I)*I*(1+XNU)*RB+
     *          BL(I)*((I-2)*(1-XNU**2)+(I+2)*XNU*(1+XNU))*RB
  580 CONTINUE
C
      RYY=-PI*RB*RBA(1)
      RXX=+PI*RB*RBB(1)
C
      WRITE(6,590) R,XL,SHI
      WRITE(6,600) RX,RXX
      WRITE(6,610) RY,RYY
  590 FORMAT(//,8X,'RESULTANT=',F14.2,3X,'XL=',F14.8,3X,'SHI=',F6.3)
  600 FORMAT(/,16X,'RX=',F14.3,6X,'RXX=',F14.3)
  610 FORMAT(/,16X,'RY=',F14.3,6X,'RYY=',F14.3)
C
      CO=0.5*PBAO
C
      DUI =-0.5*QBA(1)
      DUII=+0.5*PBB(1)

      DLI =+0.5*PBA(1)
      DLII=+0.5*QBB(1)
      WRITE(6,620) DUI,DUII
      WRITE(6,630) DLI,DLII
      WRITE(6,640)
  620 FORMAT(/,15X,'DUI=',F14.3,5X,'DUII=',F14.3)
  630 FORMAT(/,15X,'DLI=',F14.3,5X,'DLII=',F14.3)
  640 FORMAT(//,14X,'*********************///*********************',//)
C
      GO TO 1000
  650 CONTINUE
C
C  I HAVE ADDED THIS TO PROGRAM
C ********************* I HAVE ADDED THIS TO PROGRAM ********
C  I HAVE ADDED THIS TO PROGRAM
       DO 556  I=1,M,1
        AA1(I)=AA(I)*2.*PI/360.0
        X1R(I)=+(RB-URD(I))*SIN(AA1(I))
        Y1R(I)=(RB-URD(I))*COS(AA1(I))
        YY(I)=RB*COS(AA1(I))
        XX(I)=RB*SIN(AA1(I))
        WRITE(6,117)X1R(I),Y1R(I),YY(I),XX(I)
117     FORMAT('0',1X,F10.5,3X,F10.5,3X,F10.5,3X,F10.5)
556     CONTINUE
       DIFFER=ABC-BIG
       WRITE(6,1176)ABC,BIG,DIFFER
 176   FORMAT('0',4X,'ABC=',F10.3,4X,'BIG=',F10.3,4X,'DIFFER=',F10.3)
      STOP
      END
C
C....THE FOLLOWING SUBPROGRAMME CALCULATES THE RADIAL DEFORMATION AS
C      THE FUNCTION OF THE ANGLE
C
      FUNCTION UR(A)
C
      IMPLICIT REAL*8 (A-H,O-Z)
C
      COMMON CO,DUI,DLI,XNU,ER,RB,SUMU(500),SUML(500),L
C
C      ..........FOR  PLANE  STRAIN..........
C
          UR=(2*CO*(1-XNU-2*XNU**2)+
     *       DUI*(1-3*XNU-4*XNU**2)*DSIN(A)+
     *       DLI*(1-3*XNU-4*XNU**2)*DCOS(A))*RB
C
      DO 801 I=2,L,1
          UR=UR-SUMU(I)*DSIN(I*A)-SUML(I)*DCOS(I*A)
  801 CONTINUE
C
          UR=-UR/ER
      RETURN
      END
```